

BINDING SERVICES
Tel +44 (0)29 2087 4949
Fax +44 (0)29 20371921
e-mail bindery@cardiff.ac.uk

**STUDIES OF LOWER EMBRYOPHYTE SPORE
WALLS WITH PARTICULAR REFERENCE TO
THE PERISPORE**

Susannah Emily Margaret Moore

**Submitted in partial fulfilment of the requirements
for the degree of Ph.D.**

Cardiff University

November 2005

UMI Number: U584809

All rights reserved

INFORMATION TO ALL USERS

The quality of this reproduction is dependent upon the quality of the copy submitted.

In the unlikely event that the author did not send a complete manuscript and there are missing pages, these will be noted. Also, if material had to be removed, a note will indicate the deletion.



UMI U584809

Published by ProQuest LLC 2013. Copyright in the Dissertation held by the Author.
Microform Edition © ProQuest LLC.

All rights reserved. This work is protected against
unauthorized copying under Title 17, United States Code.



ProQuest LLC
789 East Eisenhower Parkway
P.O. Box 1346
Ann Arbor, MI 48106-1346

Abstract

This study of lower embryophyte spore walls concentrates on the outermost layer, the perispore. The focus of this investigation has been to elucidate the evolution, function and chemistry of the perispore. Lack of knowledge of these aspects of the perispore has resulted in conflicting views which are considered herein.

A review documenting the first occurrence of the perispore and its evolution suggests that the first perispore-like layer probably occurs in *Cooksonia pertoni* (Silurian) and *Uskiella spargens* (Devonian). It is also considered that perispore envelopes surrounding cryptospores might constitute the inception of the perispore, dating back even further to the Ordovician. It is proposed that the perispore is an ancestral feature that was lost in certain plant groups but retained in some Trimerophytopsida and Progymnospermopsida. The perispore is now a feature of most extant lower embryophytes. The first true perispore is identified in the basal Upper Devonian species *Rhacophyton ceratangium*.

This work suggests that the perispore is comparable to the plant cuticle in aspects such as chemistry, ultrastructure, and most importantly, the function. The perispore is believed to act as a defence mechanism against pathogenic attack and UV radiation but also provides mechanical support. Silica is thought to either form a discrete layer on some lower embryophyte spores or to be integral with sporopollenin. Additional spore wall stability seems to be the main function of silica. No correlation between the presence of silica in pteridophyte fronds and spores was established.

This investigation also comprises the report and analysis of siliceous cubic crystals occurring on *Selaginella myosurus* megaspores. Although their chemical and crystallographic properties could not be fully elucidated, it is suggested that these cubic crystals are a new mineral, formed by an unknown bio-mineralization process occurring in plants.

A number of different analytical chemistry techniques were applied in order to elucidate perispore components and the chemical nature of sporopollenin. This study has demonstrated that with current techniques it is difficult to isolate and analyse the perispore and that previously reported data were misinterpreted. It is hypothesised that common plasticizers were wrongly described as sporopollenin compounds. The application of matrix-assisted laser desorption ionisation time-of-flight mass spectrometry (MALDI-ToF MS) to sporopollenin research is introduced.

On the basis of the results presented herein, a revised definition for the term *perispore* is offered.

DECLARATION

This work has not previously been accepted in substance for any degree and is not being concurrently submitted in candidature for any degree.

Signed *Sisamuh Hore* (Candidate)

Date 16 04 2006

Statement 1

This thesis is the result of my own investigations, except where otherwise stated. Other sources are acknowledged by footnotes giving explicit references. A bibliography is appended.

Signed *Sisamuh Hore* (Candidate)

Date 16 04 2006

Statement 2

I hereby give consent for my thesis, if accepted, to be available for photocopying and for inter-library loan, and for the title and summary to be made available to outside organisations.

Signed *Sisamuh Hore* (Candidate)

Date 16 04 2006

Acknowledgements

Three years I thoroughly enjoyed! I am very grateful for having been given this unique opportunity and the research studentship from the School of Earth, Ocean and Planetary Sciences, without which this thesis would not have been possible. It was you *Dianne Edwards*, who gave me this chance and trusted me. My sincere thanks for your guidance and advice. *Alan Hemsley*, you provided excellent supervision, humour and trust, challenged me and gave me the odd kicking when necessary. Your input and fruitful discussions, *Steve Blackmore*, were stimulating and mind broadening. Thanks to *Jenny Pike* for pastoral moments – there weren't many but your help was much appreciated.

Day to day research life is impossible without dedicated and enthusiastic members of staff: *Lindsey Axe*, *Peter Fisher*, *Tony Oldroyd*, *Derek John*, *Andrew Wiltshire*, *Gwen Pettigrew*, *Vera Walters*, *Liz Diaz*, *Jo Woolven*, *Christine Williams*, *Debbie Skene*, *Sharon Phillips*, *Sue Thomas* – your assistance and help on various occasions was invaluable!

Scientific work on the enigmatic cubic crystals (*chapter 3.5*) would not have been possible without CCLRC Daresbury Laboratories granting three days of synchrotron radiation source (beam time) at stations 9.8 and 11.1 (Grant Number 44304). Special thanks for their enthusiasm and support goes to *Fariba Bahrami* and *John Warren* (Daresbury) and also to *Norman Fry* (Cardiff) and *Hiroaki Ohfuji* (Cardiff/Japan) for never losing their interest in “cute cubes”. Most of the analytical chemistry was carried out in the School of Chemistry (Cardiff). Thank you *Thomas Wirth* and *Andrew French* for adopting me into your research group and for giving me access to the facilities. I am grateful for access to the NMR spectrometer by *Peter Griffiths* (Cardiff). *Ed Dudley* (Swansea) kindly undertook MALDI-ToF MS analysis (*chapter 4*). *Mike Turner's* (Cardiff) and *Anthony Hann's* (Cardiff) help with TEM sectioning was much appreciated, so was *Lyndon Tuck's* support at the Botanic Research Gardens, Cardiff. I would also like to acknowledge the access to comparative material at The Royal Botanic Gardens, Kew, made possible by *Peter Edwards*.

Thanks to *Lesley Chems*, *Simon Wakefield*, *Ian Butler* and *Chris Berry* for numerous helpful and cheerful moments.

Christian Baars, *Susan Hammond*, *Hiroaki Ohfuji*, *Alan Channing* (plus *Caggs* and *Ffion*), and *James Wheeley*: sharing an office with you was great fun! Thanks for your support, keeping me sane and bringing a smile back on my face! “... and to her very great surprise, Mr. Darcy, and Mr. Darcy only, entered the room.” (Jane Austen, from *Pride and Prejudice*).

Thanks to my former housemates for sociable times, my friends in Cardiff and Kent for taking my mind off work and my friends back in Germany for keeping in touch despite busy times.

My family: *Ralf*, *Margrit*, *Christian* und *Thomas* – den allerherzlichsten Dank für Eure Unterstützung und Anteilnahme aus der Ferne. *Vic* and *Jacquie*, for encouragement from over the big pond. Thank you, *Margaret* and *Wolfgang* for watching over me. *Rita* and *Bernd* - I would not be here without your understanding, help and love. I hope that one day I can give all of this back to my own children. I love you dearly.

My parents

To see a world in a grain of sand
And a heaven in a wild flower
Hold infinity in the palm of your hand
And eternity in an hour

William Blake 1757-1827
from Auguries of Innocence

Table of Contents

Abstract	i
Declaration	ii
Acknowledgements	iii
Table of Contents	iv
List of Figures	x
List of Tables	xiv
List of Abbreviations	xviii
1 Introduction	1
1.1 Background to the present study	1
1.2 Aims	4
1.3 Systematics	5
1.4 Definitions and terminology	12
1.4.1 The definition of perispore:	
its origin and modifications through time	12
1.4.1.1 Russow 1872	12
1.4.1.2 Hannig 1911	13
1.4.1.3 Bower 1923	14
1.4.1.4 Jackson 1928	14
1.4.1.5 Erdtman 1943/1952	15
1.4.1.6 Kremp 1965	16
1.4.1.7 Tryon and Lugardon 1990	16
1.4.1.8 Punt <i>et al.</i> 1994	16
1.4.1.9 Crum 2001	17
1.4.1.10 Moore 2005, herein	17
1.4.2 Terminology	17
1.5 The occurrence of the perine/ perispore	19
1.5.1 In bryophytes	19
1.5.2 In pteridophytes	21

1.6	The role of the tapetum in perispore development	34
1.7	Chemical components and ultrastructure of the perispore and other sporoderm layers	40
1.7.1	Sporopollenin: the chemistry	40
1.7.2	β-lectins, polysaccharides and lipids	43
1.7.3	Silica	47
1.7.4	Colloidal structures	47
2	Material and Methods	50
2.1	Sources of material	50
2.1.1	Extant pteridophytes, bryophytes and a gymnosperm	50
2.1.2	List of living species investigated	50
2.1.3	Fossil spore material	52
2.2	Morphological descriptions of extant bryophyte spores, pteridophyte (mega-)spores and gymnosperm pollen	52
2.3	Microscopy techniques	60
2.3.1	Light microscopy (LM)	60
2.3.1.1	Staining for callose with aniline blue	60
2.3.2	Scanning electron microscopy (SEM)	61
2.3.3	Transmission electron microscopy (TEM)	62
2.3.4	Energy dispersive x-ray analysis (EDX)	63
2.4	Silica in pteridophyte spores, rachises and pinnae/pinnules	64
2.5	Chemical treatments	66
2.5.1	Treatment with 1% KMnO_4 solution	66
2.5.2	Treatment with MMNO	66
2.5.3	Soxhlet extractions with DCM	66
2.6	Analytical Chemistry	67
2.6.1	NMR and GC-MS	68
2.6.2	MALDI-ToF MS	70

2.7 Crystallography of cubic crystals forming on	
 <i>Selaginella myosurus</i> Sw. Alston megaspores	73
2.7.1 Isolation of crystals	73
2.7.2 X-Ray Diffraction by Debye-Scherrer camera	73
2.7.3 Synchrotron beam high flux XRD	74
2.7.4 IR (Infrared) microspectrometry	74
2.7.5 IR microspectrometry with	
synchrotron radiation source (SRS)	75
2.8 Self-assembly experiments	76
3 Mineral content in bryophyte and pteridophyte spore walls	77
3.1 Silica in <i>Selaginella</i> megaspore walls	77
3.2 An unknown siliceous bio-mineral forming on	
<i>Selaginella myosurus</i> Sw. Alston megaspores	77
3.2.1 Results	78
3.2.1.1 SEM documentation combined with	
energy dispersive x-ray analysis (EDX)	78
3.2.1.2 TEM documentation combined with	
energy dispersive x-ray analysis (EDX)	82
3.2.1.3 X-ray diffraction by Debye-Scherrer camera	84
3.2.1.4 Synchrotron beam high flux XRD	85
3.2.1.5 IR microspectrometry	86
3.2.1.6 IR microspectrometry with	
synchrotron radiation source (SRS)	87
3.2.2 Discussion	89
3.3 Mineral content in pteridophyte spore walls	96
3.3.1 Results	97
3.3.1.1 Blechnaceae	98
3.3.1.2 Davalliaceae	101

3.3.1.3	Dryopteridaceae	104
3.3.1.4	Osmundaceae	112
3.3.1.5	Polypodiaceae	113
3.3.1.6	Psilotaceae	114
3.3.1.7	Pteridaceae	116
3.3.1.8	Schizaeaceae	121
3.3.1.9	Thelypteridaceae	123
3.3.2	Discussion	128
3.4	Mineral content in pteridophyte fronds	141
3.4.1	Results	141
3.4.1.1	Polypodiaceae	142
3.4.1.2	Osmundaceae	144
3.4.1.3	Pteridaceae	149
3.4.1.4	Schizaeaceae	151
3.4.1.5	Thelypteridaceae	154
3.4.2	Discussion	157
3.5	Mineral content in bryophyte spore walls	164
3.5.1	Results	164
3.5.1.1	Funariaceae	165
3.5.1.2	Meesiaceae	166
3.5.1.3	Bryaceae	167
3.5.1.4	Brachytheciaceae	169
3.5.2	Discussion	170
4	New insights into sporopollenin research from MALDI-ToF MS, NMR and GC-MS: mass spectrometry techniques applied to palynology	176
4.1	Results	176
4.1.1	MALDI-ToF MS	176

4.1.2 GC-MS and ¹ H NMR	178
4.1.3 Chemical treatments	182
4.2 Discussion	189
4.2.1 MALDI-ToF MS	189
4.2.2 GC-MS and ¹ H NMR	190
4.2.3 Chemical treatments	191
5 <i>Osmunda regalis</i> L. spores:	
a modern analogue for certain Early Devonian spores?	196
5.1 Results	198
5.1.1 <i>Osmunda regalis</i> L. spores	198
5.1.2 Fossil spores	203
5.2 Discussion	205
6 Perispore and the Fossil Record - A Review	211
6.1 Introduction	211
6.2 Perispore and the fossil record	212
6.2.1 Silurian (Přídolí)	213
6.2.2 Devonian (Lochkovian/Pragian)	213
6.2.3 Carboniferous	216
6.2.4 Permian	219
6.2.5 Jurassic	220
6.2.6 Cretaceous/Tertiary	221
6.3.6.1 Salviniaceae	222
6.3 Considerations	224

7	Discussion – lower embryophte spore walls in perspective	
	with particular focus on the perispore	229
	7.1 Evolutionary aspects of spore wall layers	229
	7.1.1 Bryophyta	229
	7.1.2 Pteridophytina	231
	7.1.3 Progymnospermopsida	235
	7.1.4 Mesozoic megaspores	236
	7.1.5 Synthesis	237
	7.2 Functions and Chemistry	241
	7.2.1 Fossil evidence	243
	7.2.2 Composition	243
	7.2.3 Ultrastructural aspects	244
	7.2.4 Permeability	246
	7.2.5 Defence mechanisms	247
	7.2.6 Other functions	252
8	Conclusions	259
	8.1 Evolutionary aspects of lower embryophyte spore wall layers	259
	8.2 Functions and Chemistry	260
	8.3 Non specific conclusions	262
9	References	264
Appendix	1 Moore <i>et al.</i> in press a (GRANA)	
	2 Moore <i>et al.</i> in press b (PROTOPLASMA)	
	3 NMR spectrum	

List of Figures

1 Introduction

- 1.1 Fern life cycle
- 1.2 General spore wall terminology
- 1.3 Modified spore wall terminology
- 1.4 Latest phylogeny of vascular plants
- 1.5 Phylogramme depicting relationships for lower vascular plants
- 1.6 Phylogramme depicting relationships for ferns
- 1.7 Phylogramme depicting relationships for higher ferns
- 1.8 Phylogenetic relationship of the monilophyte tree
- 1.9 Key for tapetum subtypes
- 1.10 Origin of sporopollenin in Euphyta

2 Material and Methods

- 2.1 Scheme of a GC-MS
- 2.2 The principle of MALDI-TOF MS
- 2.3 Apparatus used for purifying sporopollenin
- 2.4 Schematic sketch of a Debye Scherrer powder camera

Chapter 3

- 3.1 *Selaginella myosurus* megaspore with cubic crystals
- 3.2 Crystal growth on the inner wall of the sporangium
of *Selaginella myosurus*
- 3.3 Thin section of the complete *Selaginella myosurus* megaspore
- 3.4 TEM sections through *Selaginella myosurus* crystals and spore matrix
- 3.5 EDX analysis of *Selaginella myosurus* crystals
- 3.6 Debye Scherrer camera film and ring pattern
- 3.7 FT-IR spectrum of *Selaginella myosurus* spore matrix and crystal cubes
- 3.8 Synchrotron beam FT-IR spectra I of *Selaginella myosurus* crystals
- 3.9 Synchrotron beam FT-IR spectra II of *Selaginella myosurus* crystals

-
- 3.10 SEM documentation of *Selaginella myosurus* megaspore
 - 3.11 SEM and EDX of *Blechnum occidentale* spores
 - 3.12 SEM and EDX of *Doodia aspera* spores
 - 3.13 SEM and EDX of *Davallia mariesii* spores
 - 3.14 SEM and EDX of *Nephrolepis hirsutula* spores
 - 3.15 SEM and EDX of *Cyrtomium falcatum* spores
 - 3.16 SEM and EDX of *Cyrtomium fortunei* spores
 - 3.17 SEM and EDX of *Diplazium proliferum* spores
 - 3.18 SEM and EDX of *Dryopteris erythrosora* spores
 - 3.19 SEM and EDX of *Dryopteris stewardii* spores
 - 3.20 SEM and EDX of *Hypodematium fauriei* spores
 - 3.21 SEM and EDX of *Lastreopsis microsora* spores
 - 3.22 SEM and EDX of *Rumohra adiantiformis* spores
 - 3.23 SEM and EDX of *Osmunda regalis* spores
 - 3.24 SEM and EDX of *Phlebodium aureum* spores
 - 3.25 SEM and EDX of *Psilotum nudum* spores
 - 3.26 SEM and EDX of *Pellaea calomelanos* spores
 - 3.27 SEM and EDX of *Pellaea rotundifolia* spores
 - 3.28 SEM and EDX of *Pteris cretica* spores
 - 3.29 SEM and EDX of *Pteris longifolia* spores
 - 3.30 SEM and EDX of *Anemia tomentosa* spores
 - 3.31 SEM and EDX of *Macrothelypteris torresiana* spores
 - 3.32 SEM and EDX of *Oreopteris limbosperma* spores
 - 3.33 SEM and EDX of *Phegopteris decursive-pinnata* spores
 - 3.34 SEM and EDX of *Thelypteris japonica* spores
 - 3.35 Three evolutionary levels of wall structure in fern spores
 - 3.36 Occurrence of silica in bryophyte and pteridophyte spore walls
 - 3.37 SEM and TEM of siliceous needles on *Selaginella* megaspore
 - 3.38 SEM and EDX of *Phlebodium aureum*
 - 3.39 SEM and EDX of *Osmunda regalis* rachis
 - 3.40 SEM and EDX of *Osmunda regalis* pinnule
 - 3.41 SEM and EDX of *Pellaea rotundifolia* rachis and pinna
 - 3.42 SEM and EDX of rachis of *Anemia tomentosa*
 - 3.43 SEM and EDX of rachis of *Phegopteris decursive-pinnata*

- 3.44 SEM and EDX of *Funaria hygrometrica* spores
- 3.45 SEM and EDX of *Leptobryum pyriforme* spores
- 3.46 SEM and EDX of *Bryum capillare* spores
- 3.47 SEM and EDX of *Brachythecium velutinum* spores
- 3.48 Isoprenoid synthesis in plants
- 3.49 Phylogenetic tree of mosses

Chapter 4

- 4.1 MALDI-ToF MS spectra of spore powder of *Selaginella pallescens* and *Lycopodium clavatum*
- 4.2 GC-MS spectra of *Pinus sylvestris* and *Selaginella pallescens*
- 4.3 Chemical structure of 2,6-bis(1,1-dimethylethyl)-4-methyl phenol (BHT)
- 4.4 Chemical structure of 1,2 benzenedicarboxylic acid, diisooctyl ester (Phthalic acid-diisooctyl ester) and 1,2 benzenedicarboxylic acid, butyl 2-ethylhexyl ester
- 4.5 Three identical ^1H NMR spectra obtained from experiments
- 4.6 SEM pictures of *Pellaea calomelanos* and *Pellaea rotundifolia*
- 4.7 SEM pictures of *Blechnum gibbum* and *Lycopodium clavatum*
- 4.8 SEM pictures of *Selaginella pallescens* before and after treatment with MMNO
- 4.9 SEM of *Lycopodium clavatum* and *Pinus sylvestris* before and after treatment with MMNO
- 4.10 ^1H NMR spectra of MMNO treated *Selaginella pallescens* megaspores *Lycopodium clavatum* spores and *Pinus sylvestris* pollen
- 4.11 ^1H and ^{13}C NMR spectra of DCM extracted *Selaginella pallescens* megaspores, microspores and leaves as well as *Lycopodium clavatum* spores

Chapter 5

- 5.1 SEM documentation of immature spores and a sporangium of *Osmunda regalis*
- 5.2 SEM documentation of almost mature spores of *Osmunda regalis*

- 5.3 Blue auto-fluorescent immature *Osmunda regalis* spores
- 5.4 SEM documentation of mature spores of *Osmunda regalis*
- 5.5 SEM documentation of an Early Devonian spore cluster
- 5.6 SEM documentation of *Osmunda regalis* clusters

7 Discussion

- 7.1 Phylogeny of major groups of tracheophytes and their taxonomic relationships
- 7.2 Phylogeny of major groups of tracheophytes and their taxonomic relationships with speculation on potential loss of perispore character
- 7.3 Lamellate features in sporopollenin, suberin and cutin

List of Tables

1 Introduction

- 1.1 Summary of pteridophyte and bryophyte sporoderm terminology
- 1.2 Comparison of *Selaginella* and *Isoetes* megaspore walls
- 1.3 Synopsis of perine characters in *Grimma* (bryophyte)

2 Material and Methods

- 2.1 List of extant species investigated in this study
- 2.2 List of species studied for presence of silica in spores, rachises and pinnae / pinnules
- 2.3 Summary of spore wall extractions

Chapter 3

- 3.1 A synopsis of methods carried out to investigate the unknown bio-mineral
- 3.2 *Selaginella myosurus* megaspores studied by various authors
- 3.3 Summary of chapter 3.3
- 3.4 EDX results of *Blechnum occidentale*
- 3.5 EDX results of *Doodia aspera*
- 3.6 EDX results of *Davallia mariesii*
- 3.7 EDX results of *Nephrolepis hirsutula*
- 3.8 EDX results of *Cyrtomium falcatum*
- 3.9 EDX results of *Cyrtomium fortunei*
- 3.10 EDX results of *Diplazium poliferum*
- 3.11 EDX results of *Dryopteris erythrosora*
- 3.12 EDX results of *Dryopteris stewardii*
- 3.13 EDX results of *Hypodematium fauriei*
- 3.14 EDX results of *Lastreopsis microsora*
- 3.15 EDX results of *Rumohra adiantiformis*
- 3.16 EDX results of *Osmunda regalis*
- 3.17 EDX results of *Phlebodium aureum*

-
- 3.18 EDX results of *Psilotum nudum*
 - 3.19 EDX results of *Pellaea calomelanos*
 - 3.20 EDX results of *Pellaea rotundifolia* I
 - 3.21 EDX results of *Pellaea rotundifolia* II
 - 3.22 EDX results of *Pteris cretica*
 - 3.23 EDX results of *Pteris longifolia*
 - 3.24 EDX results of *Anemia tomentosa* I
 - 3.25 EDX results of *Anemia tomentosa* II
 - 3.26 EDX results of *Anemia tomentosa* III
 - 3.27 EDX results of *Macrothelypteris torresiana*
 - 3.28 EDX results of *Oreopteris limbosperma*
 - 3.29 EDX results of *Phegopteris decursive-pinnata* I
 - 3.30 EDX results of *Phegopteris decursive-pinnata* II
 - 3.31 EDX results of *Thelypteris japonica*
 - 3.32 Distribution of nutrient elements (in atomic %) in spore walls
 - 3.33 Distribution of nutrient elements plotted against fern systematics
 - 3.34 Summary of *chapter 3.4*
 - 3.35 EDX results of epidermis of *Phlebodium aureum*
 - 3.36 EDX results of parenchyma of *Phlebodium aureum*
 - 3.37 EDX results of vascular bundle of *Phlebodium aureum*
 - 3.38 EDX results of central parenchyma of *Phlebodium aureum*
 - 3.39 EDX results of hypodermis of *Osmunda regalis*
 - 3.40 EDX results of parenchyma of *Osmunda regalis*
 - 3.41 EDX results of vascular bundle of *Osmunda regalis*
 - 3.42 EDX results of vascular bundle of *Osmunda regalis*
 - 3.43 EDX results of axial part of the epidermis of *Osmunda regalis*
 - 3.44 EDX results of mesophyll of *Osmunda regalis*
 - 3.45 EDX results of epidermis of *Osmunda regalis*
 - 3.46 EDX results of hypodermis of *Pellaea rotundifolia*
 - 3.47 EDX results of vascular bundle of *Pellaea rotundifolia*
 - 3.48 EDX results of epidermis of a pinna of *Pellaea rotundifolia*
 - 3.49 EDX results of vein of *Pellaea rotundifolia*
 - 3.50 EDX results of hypodermis of *Anemia tomentosa*
 - 3.51 EDX results of parenchyma of *Anemia tomentosa*

-
- 3.52 EDX results of vascular bundle of *Anemia tomentosa*
- 3.53 EDX results of axial part of epidermis of *Anemia tomentosa*
- 3.54 EDX results of abaxial part of the epidermis of *Anemia tomentosa*
- 3.55 EDX results of epidermis and adjacent hypodermis
of *Phegopteris decursive-pinnata*
- 3.56 EDX results of parenchyma of *Phegopteris decursive-pinnata*
- 3.57 EDX results of vascular bundle of *Phegopteris decursive-pinnata*
- 3.58 EDX results of abaxial part of the epidermis
of *Phegopteris decursive-pinnata*
- 3.59 EDX results of axial part of the epidermis
of *Phegopteris decursive-pinnata*
- 3.60 EDX results of hair on the pinnule of *Phegopteris decursive-pinnata*
- 3.61 Plant nutrients and their functions
- 3.62 Summary of chapter 3.5
- 3.63 EDX results of spore cluster of *Funaria hygrometrica*
- 3.64 EDX results of spore cluster of *Leptobryum pyriforme*
- 3.65 EDX results of spore cluster of *Bryum capillare*
- 3.66 EDX results of spore cluster of *Brachythecium velutinum*
- 3.67 Secondary compounds in bryophytes

Chapter 4

- 4.1 Summary of *chapter 4*

Chapter 5

- 5.1 Summary of *chapter 5*

Chapter 6

- 6.1 Summarising the occurrence of the perispore in the fossil record (Silurian-Jurassic)
- 6.2 Summarising the occurrence of the perispore in the fossil record (Cretaceous/Tertiary).

6.3 International Stratigraphic Chart 2004 ©

7 Discussion

7.1 Comparison of features of cuticle and perispore

List of Abbreviations

BSE	Backscattered Electron Detector
CDCl_3	Deuterated Chloroform
DCM	Dichloromethane
EDX	Energy Dispersive X-ray
ESEM	Environmental Scanning Electron Microscope
Et_2O	Diethyl Ether
GC-MS	Gas Chromatography Mass Spectrometry
GSED	Gaseous Secondary Electron
HCl	Hydrochloric Acid
HF	Hydrofluoric Acid
HNO_3	Nitric Acid
IR	Infrared
KBr	Potassium Bromide
KMnO_4	Potassium Permanganate
LC	Lead Citrate
LM	Light Microscopy
MALDI-ToF	Matrix Assisted Laser Desorption/Ionisation Time of Flight
MMNO	N-Methylmorpholine N-Oxide Monohydrate
MS	Mass Spectrometry
NaHCO_3	Sodium Bicarbonate
NMR	Nuclear Magnetic Resonance
PAS	Periodic Acid Schiff's test
RIS	Receptor-Independent Sporopollenin
SAED	Selected Area Electron Diffraction
SE	Secondary Electron
SEM	Scanning Electron Microscope
SRS	Synchrotron Radiation Source
TEM	Transmission Electron Microscope
TIFF	Tagged Image File Format
TMS	Tetramethylsilane
UA	Uranyl Acetate
XRD	X-ray Diffraction

1 Introduction

1.1 Background to this study

The life cycle of a fern consists of two alternating generations, the diploid sporophyte and the haploid gametophyte. The sporophyte bears the sporangia, which produce haploid spores resulting from meiosis. It is the sporangia that give rise to the gametophyte generation. The gametophyte germinates from a spore, continues to grow through cell mitosis, and in ferns is independent from the sporophyte since it can undertake photosynthesis. Eventually, a prothallium will form which hosts the male antheridia and the female archegonia. After fertilization a diploid zygote will form, from which a new sporophytic generation will grow mitotically. With the development of sporangia and haploid spores the life cycle is completed (figure 1.1).

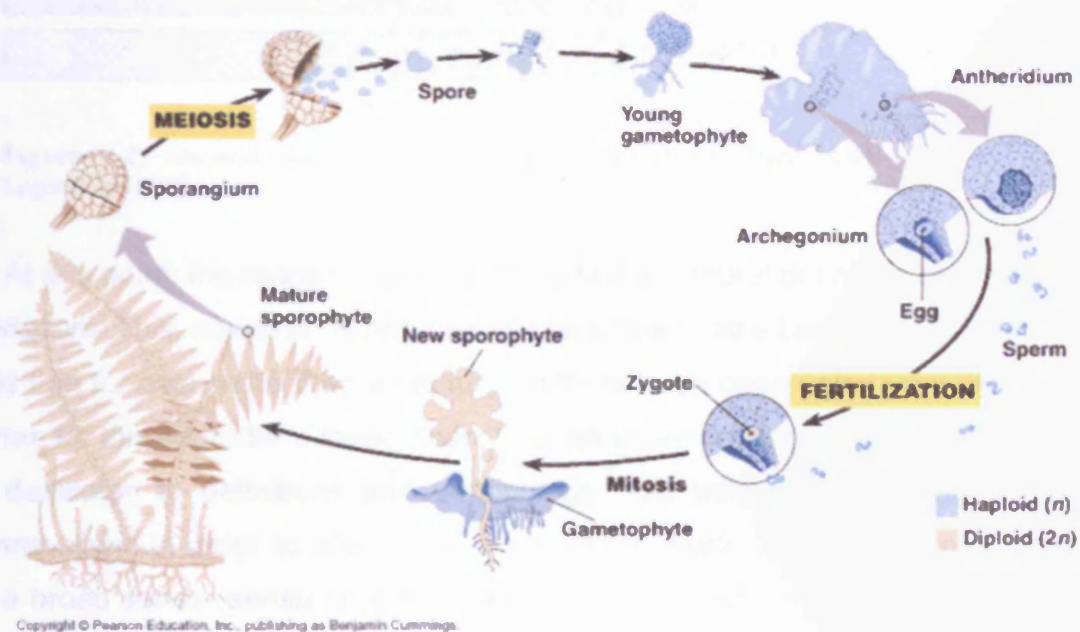


Figure 1.1: Life cycle of an isosporous fern (copyright by Pearson Education Inc.), showing the haploid gametophyte and the diploid sporophyte generations.

The three principle life histories of extant vascular plants are free-sporing homospory, free-sporing heterospory and the seed habit. For the origin of heterospory many different evolutionary concepts have been offered and this question is still under discussion (Bateman & DiMichele 1994). Among pteridophytes many orders evolved of which four heterosporous groups

remain: Salviniales and Marsileales as well as the Isoetales and Selaginellales. Except for the Selaginellales, all other orders in which heterospory occurs today are mainly aquatic or grow in seasonally wet habitats. The remaining orders of the living pteridophytes are all homosporous.

The main focus of this study is on the first haploid generation of the fern life-cycle: the spores. Their walls commonly comprise (from the outer to the inner): a perispore, an (outer, middle, inner) exospore, and an endospore (figure 1.2).

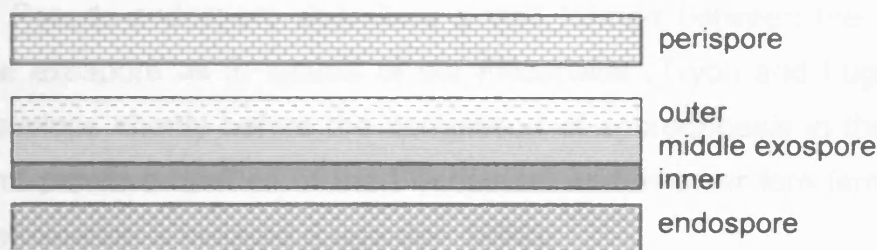


Figure 1.2: General spore wall terminology (based on Tryon and Lugardon 1990).

At this point, the reader might expect to find a general definition of the term *perispore*. This, however, is not a simple task due to little being known about it and that for over more than a century, authors have been using very different terms for this sporoderm layer. Therefore, an entire section of this introduction is dedicated to definitions and terminology (see below *1.4 Definitions and terminology*) in order to offer some clarification. I will use the term *perispore* in a broad sense (*sensu lato*) throughout this study, unless specified by 'true' perispore, representing the term in the strict sense (*sensu stricto*).

The terms "inner", "middle" and "outer" (exospore) generally have a strictly topographical value (Parkinson 1991). The exospore is defined by Tryon and Lugardon (1990) as the main sporoderm wall consisting of sporopollenin, including the aperture and is homologous to the exine of pollen. The same authors define the endospore as the inner pectocellulose wall of the sporoderm adjacent to the protoplasmic membrane, and it is considered homologous to the intine.

In some cases the terminology above is slightly modified (figure 1.3). The episore, for example, is defined (Tryon and Lugardon 1990) as the sporopollenin wall external to the exospore in the heterosporous Filicopsida and the Equisetopsida. Its formation coincides with that of the last stages of exospore development and consists of sporopollenin analogous to that of the outer exospore (Lugardon 1990).

The para-exospore is the wall external to the exospore formed of material similar to the exospore, but initiated before and largely detached from the exospore in microspores of *Isoetes* and some of *Selaginella* (Tryon and Lugardon 1990).

Pseudo-endospore describes a wall formed between the endospore and the exospore as in spores of the Filicopsida (Tryon and Lugardon 1990). It develops shortly before the completion of sporogenesis in the Equisetaceae and primitive families of the Filicopsida, and in other fern families only when germination is initiated (Lugardon 1990).

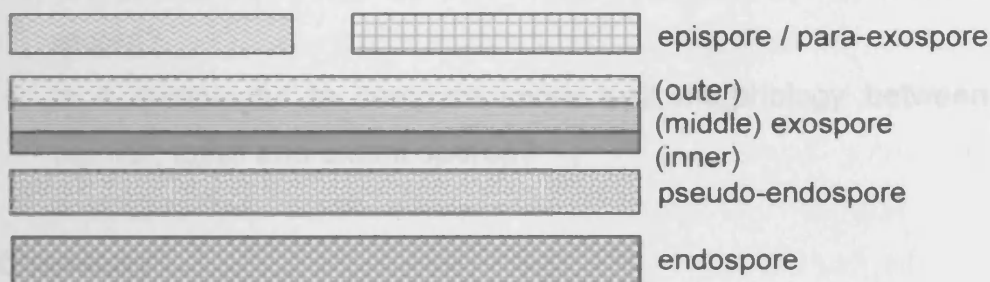


Figure 1.3: Terminology for certain spore walls occurring in pteridophytes (based on Tryon and Lugardon 1990).

The perispore is often present in isospores but can also be found in micro- or megaspore of heterosporous species (for a detailed description of the occurrence of the perispore in pteridophytes see *section 1.5* below). As the title of this project suggests, the perispore of pteridophytes has been described as enigmatic and overlooked by scientists for many decades, if not for a whole century. This is because until now, not much was known about its evolution, function and chemistry.

1.2 Aims

A perispore has been described for many pteridophyte spores as has a perine layer for numerous bryophyte species. The literature, however, does not provide exhaustive answers on its evolutionary origin, its chemical nature in extant species, and its possible function. Although several authors investigated some of these aspects (for references see individual chapters), to date and to my knowledge, no comprehensive study incorporating these aspects has been published. The only aspect that has been studied in detail is the development of the perispore and the role of the tapetum in sporogenesis (please see *section 1.6*).

The aim of this study is to provide new insights into features of the perispore and to attempt to answer questions on evolution, chemistry and function, as follows:

Evolution

- Is it possible to establish the first evidence of a perispore in the fossil record?
- Is it meaningful to compare spore wall morphology between spore mimics, fossil and extant spores?

Chemistry

- What is the chemical nature of the perispore and sporopollenin, respectively? For this approach several analytical techniques such as chemical extractions, ^{13}C and ^1H NMR and GC-MS will be used, together with less common techniques like MALDI-TOF.
- The occurrence of silica in spore walls is well described for genera like *Selaginella* and *Isoetes* but has so far not been studied in detail in other pteridophyte families or even bryophytes. Is the presence of silica in spore walls limited to lycopsids or is it much more widely distributed among pteridophytes and bryophytes? Is there a correlation between the presence of silica in spore walls and fronds that bear the parent sporangia?

- A separate study will be made in order to analyse cubic crystals, which seem to occur naturally on megaspores of *Selaginella myosurus* Sw. Alston. Although their presence on these megaspores has been known for quite a while, their true nature has yet to be demonstrated. Their chemical and crystallographic nature will be studied.

Function

- What is the function of the perispore?
- Which other spore wall components, like phenolics or lectins for example, might be linked to certain functions?

1.3 Systematics

In recent years advances in the techniques of molecular systematics have helped to generate revised phylogenies across the plant kingdom. The most significant publications are summarised and presented herein.

A study carried out in 2001 by Pryer and co-workers, revealed phylogenetic relationships among all major lineages of vascular plants gained from a maximum-likelihood analysis of combined chloroplast *rbcL*, *atpB*, *rps4* and nuclear small-subunit rDNA data set. One of the results shows that lycophytes are a monophyletic clade, as are seed plants and a clade including equisetophytes (horsetails), psilotophytes (whisk ferns) and all eusporangiate and leptosporangiate ferns (terminology *sensu* Pryer *et al.* 2001). Moreover, the study showed that horsetails as well as ferns are the closest living relatives to seed plants.

A comprehensive phylogeny of pteridophytes has so far only been published by Stevenson and Loconte (1996). With 111 taxa studied, their work is a well-established source for pteridophyte systematic classification. The reader is referred to the original publication for details; the most relevant phylogrammes are shown below (Figures 1.4 - 1.8).

More recently, Pryer *et al.* (2004) published on the phylogeny and evolution of ferns, focussing on the early leptosporangiate divergence. They sequenced over 5000 base pairs from plastid and nuclear genomes of 62 fern taxa. This

study revealed that, firstly, the Osmundaceae are sister to the rest of the leptosporangiate ferns. Secondly, Dipteridaceae, Matoniaceae, Gleicheniaceae and Hymenophyllaceae are possibly monophyletic. Thirdly, schizaeoid ferns are sister to a large clade, also referred to as “core leptosporangiates”, comprising heterosporous ferns, tree ferns and polypods. The phylogenetic relationships of the monilophyte tree (*sensu* Kenrick and Crane (1997), cited by Pryer *et al.* 2004)) are presented in figure 1.8.

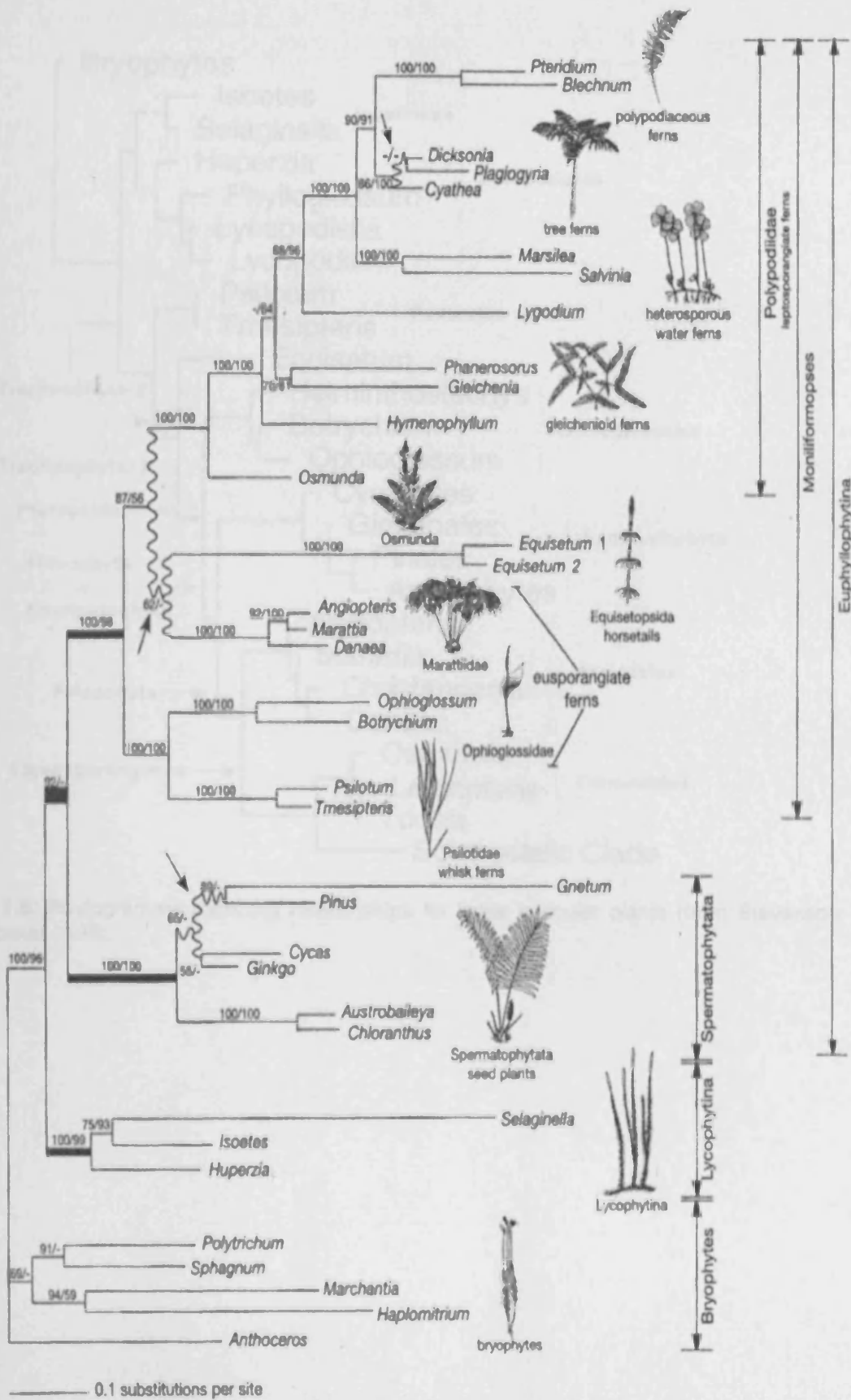


Figure 1.4: From Pryer et al. (2001) Latest phylogeny of vascular plants.

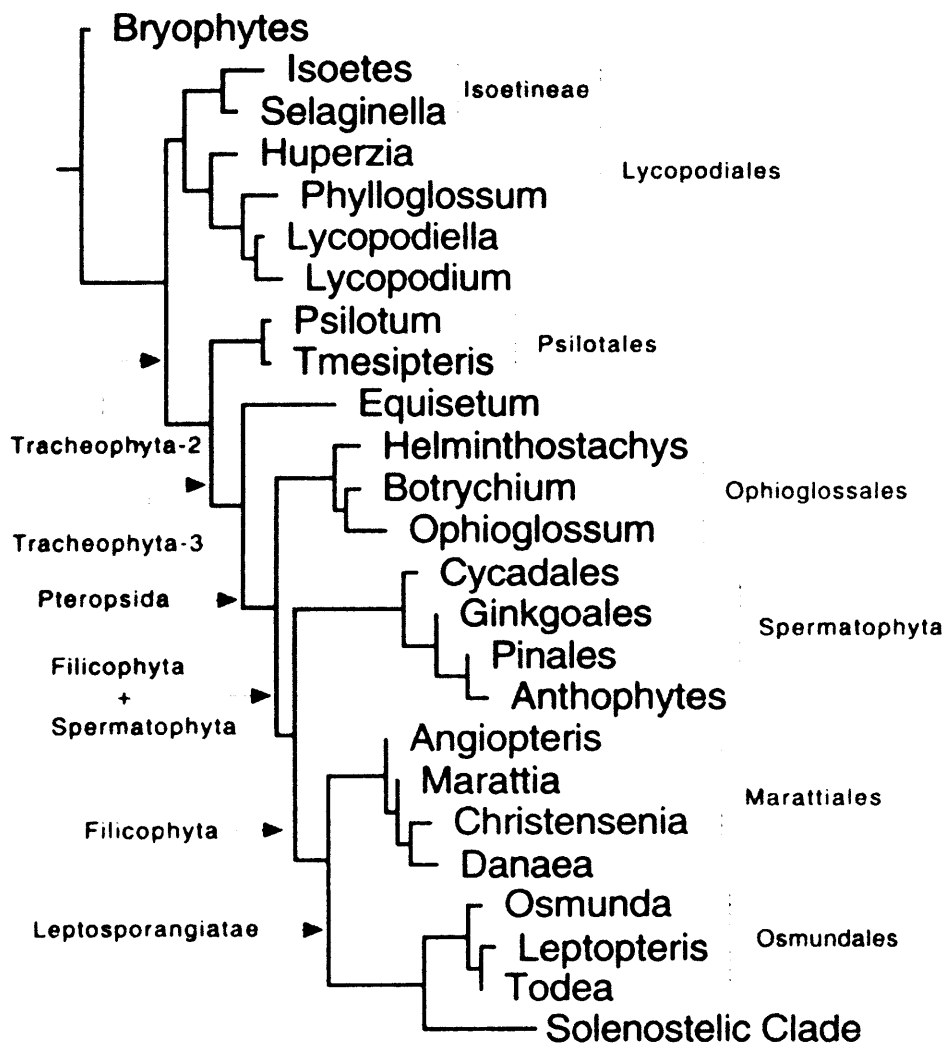


Figure 1.5: Phylogramme depicting relationships for lower vascular plants (from Stevenson and Loconte 1996).

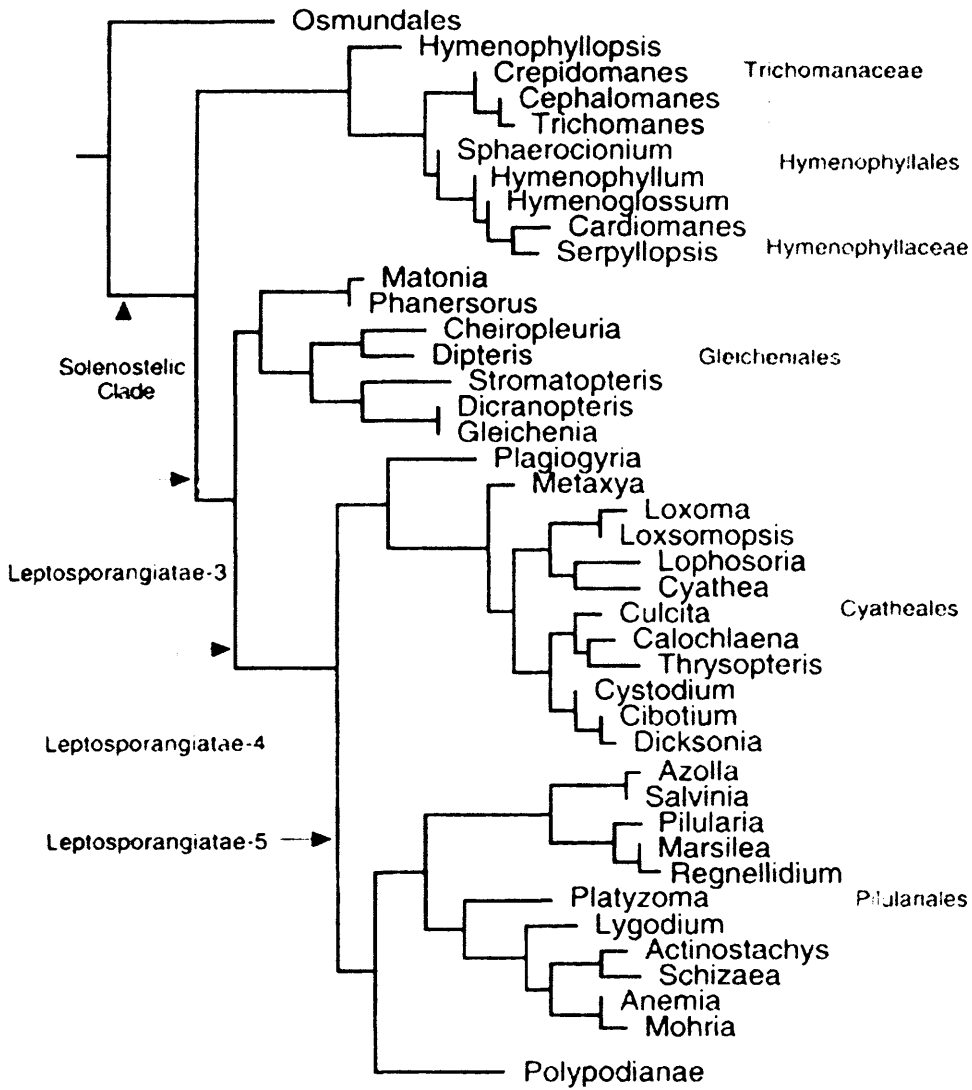


Figure 1.6: Phylogramme depicting relationships for lower ferns (from Stevenson and Loconte 1996).

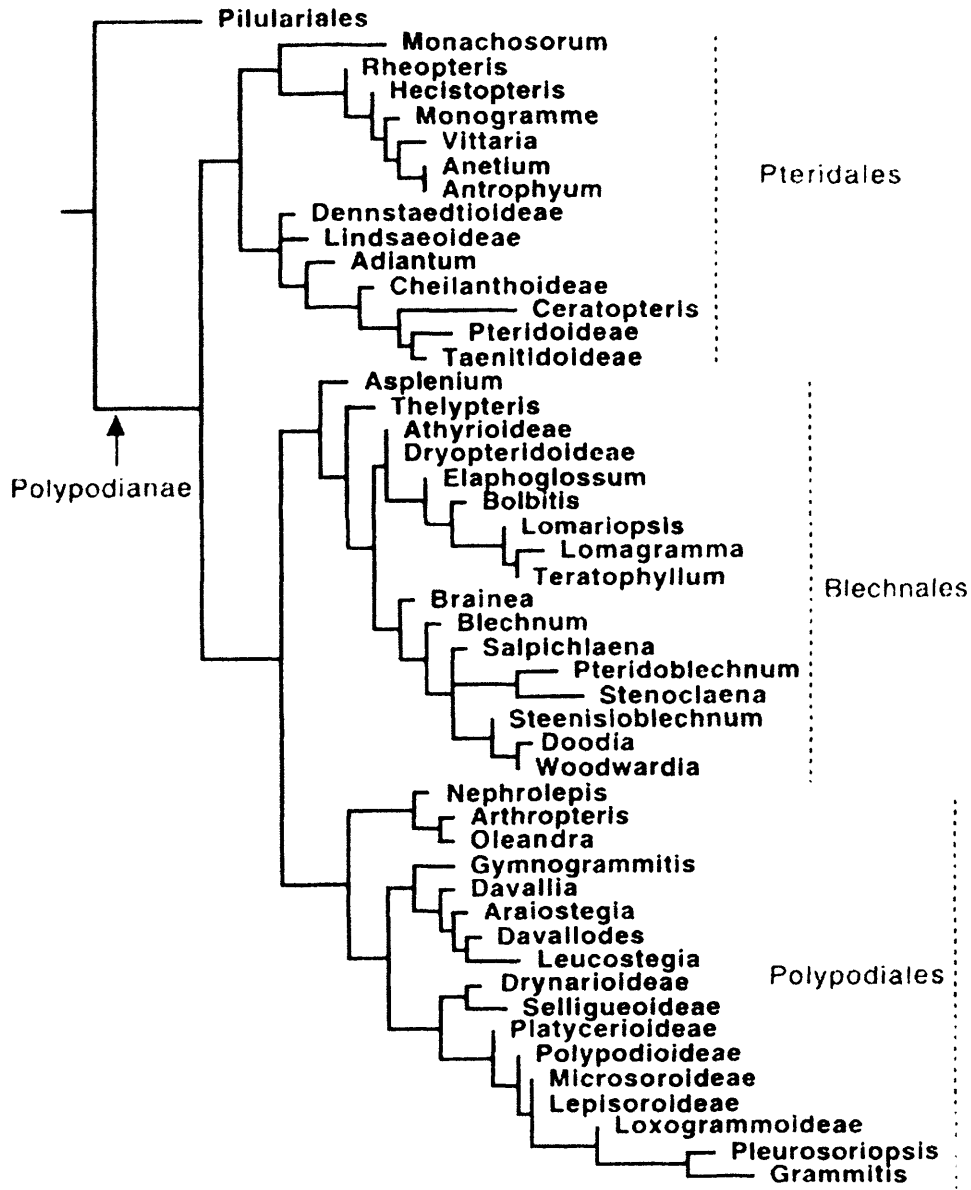


Figure 1.7: Phylogramme depicting relationships for higher ferns (from Stevenson and Loconte 1996).

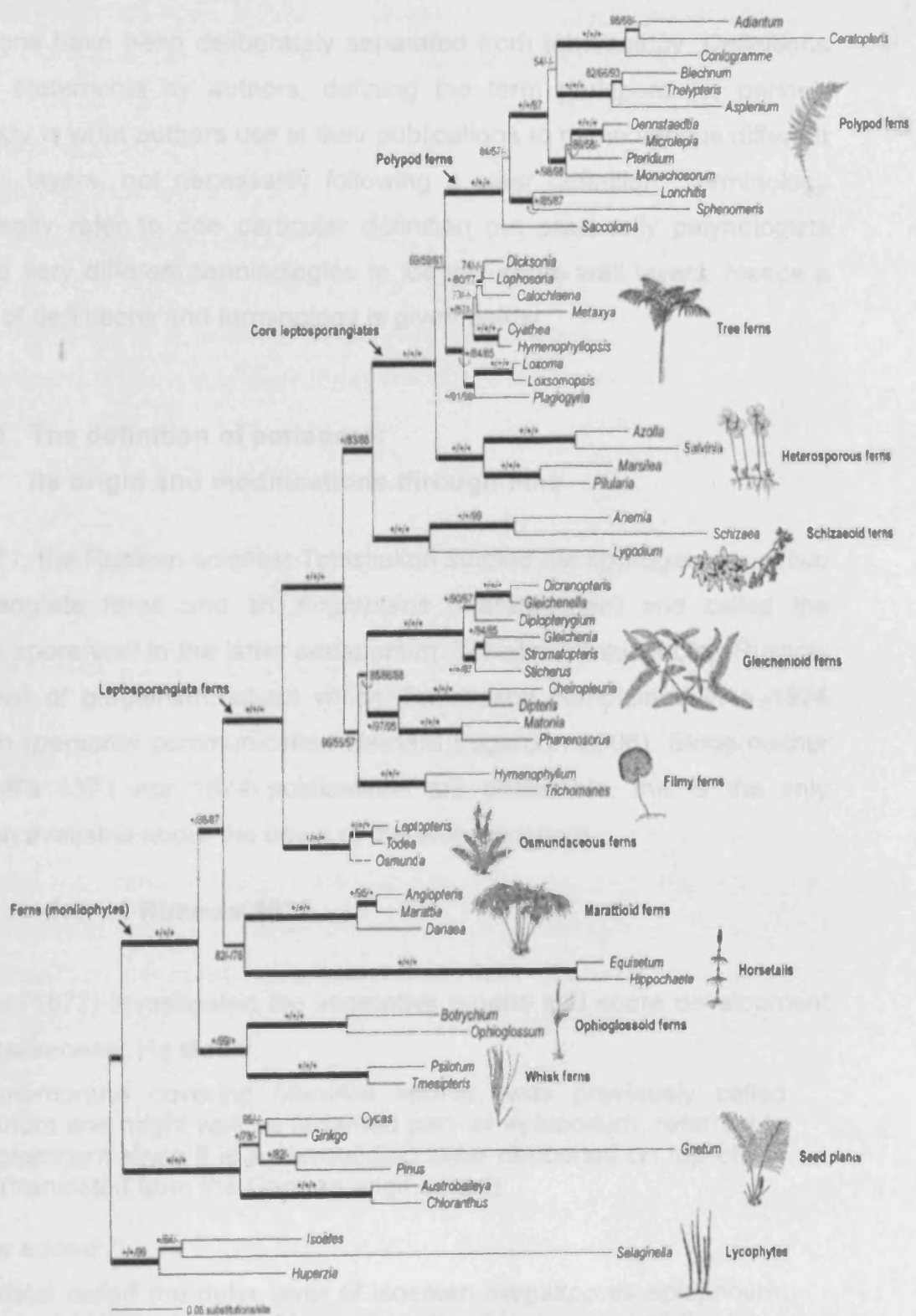


Figure 1.8: Phylogenetic relationships of the monilophyte tree from (Pryer et al. 2004), based on the Bayesian analysis of four genes (plastid *rbcl*, *atpB*, *rps4* and nuclear 18s rDNA).

1.4 Definitions and terminology

Definitions have been deliberately separated from terminology. Definitions are clear statements by authors, defining the term perispore (or perine). Terminology is what authors use in their publications to name various different spore wall layers, not necessarily following a clear definition. Terminology should ideally refer to one particular definition but practically palynologists have used very different terminologies to identify spore wall layers. Hence a summary of definitions and terminology is given below.

1.4.1 The definition of perispore: its origin and modifications through time

In 1871, the Russian scientist Tchistiakoff studied the sporogenesis of two leptosporangiate ferns and an *Angiopteris* (Marattiaceae) and called the outermost spore wall in the latter *perisporium*. Tchistiakoff suspected Russow (see below) of plagiarism, about which Tchistiakoff complained in a 1874 publication (personal communication Bernard Lugardon 2006). Since neither Tchistiakoff's 1871 nor 1874 publications are obtainable, this is the only information available about the origin of the term *perispore*.

1.4.1.1 Russow 1872

Russow (1872) investigated the vegetative organs and spore development in the Marsileaceae. He stated:

"The membrane covering *Marsilea* spores, was previously called exosporium and might well be renamed peri- or episporium, referring to its development since it is a surrounding layer deposited on top of the spore" (translated from the German original text).

Russow added:

"Hofmeister called the outer layer of isoetean megaspores episporium. Up to now I have not been able to study the development of the latter myself and therefore do not know if there is a reason for not calling this particular layer exosporium."

Even at this early stage in research a difference between perispores among pteridophytes was already recognised but using an inconsistent terminology. Lycopoid mega- and microspores are only one example: the wall external to the exospore in microspores of *Isoetes* and some *Selaginella* is called paraexospore (Kremp 1965; Tryon and Lugardon 1990). Today some authors refer to the outer layer of the megaspores of the heterosporous genera *Selaginella* and *Isoetes* as (outer/inner) exospore, which is often characterised by a siliceous content (Tryon and Lugardon 1978; Taylor 1989, 1993). In heterosporous water ferns *Salvinia* and *Marsilea* as well as *Azolla* and *Pilularia*, the outer spore layer is referred to as episporium.

1.4.1.2 Hannig 1911

Another article published in German, the title of which translates as: "The occurrence of perispores in Filicidae and their systematic implications", was one of the first to integrate the developmental aspect of perispore. In his study Hannig closely investigated the development of the perispore in *Aspidium trifoliatum*, which he called a "Sackperispor" which could be translated as "envelope". The latter originated from a tissue of the spore vacuole. Whereas the envelope tightly surrounds the spore in an early stage of development it later on loosely surrounds the exospore and grows by forming folds. He noted that the presence of a periplasmodium does not necessarily result in the development of a perispore, stating that families like the Lycopodiaceae, Ophioglossaceae and pollen of both gymnosperms and angiosperms have a periplasmodial stage but no perispore. From comprehensive TEM studies made in past decades it is known that spores of the Lycopodiaceae and Ophioglossaceae do have a perispore (Lugardon 1969, 1972). Hannig also mentioned that in some species, the perispore clearly seems to be derived from the periplasmodium and that therefore the occurrence of a perispore has systematic or phylogenetic implications. Since observations with the light microscope were limited and TEM was not available in Hannig's time, many pteridophyte families were considered to lack a perispore. Today, its presence is known in all of the families mentioned above.

1.4.1.3 Bower 1923

In his chapter "The Spore-Producing Organs" of *The Ferns* (1923) Bower commented on the perispore, which is listed under the heading "The Tapetum". He considered it to be the result of a deposition of the plasmodial tapetum on the exospore, which again shows the influence of developmental studies in general, and on the following definition in particular (Bower 1923):

"The plasmodium intrudes between the separating spore-mother-cells, forming a rich nutritive medium, which is absorbed in the more primitive ferns into the developing spores; but in certain advanced types it may in part remain as a deposit on the outside of the wall, and is called the *perispore*."

In glossaries, like that of Kremp (1965), this definition is attributed to Bower (1935), however, it was first published in *The Ferns* (1923) and repeated in the 1935 edition of the book *Primitive Land Plants* (Bower 1935).

Bower also classified ferns into two groups according to the presence of a perispore stating that no perispore is found in primitive groups like the eusporangiate ferns, Osmundaceae, Schizaeaceae, Hymenophyllaceae, Cyatheaceae, Davalliaceae or in *Ceratopteris*. Even in 1980, spores of the families of Polypodiaceae, Pteridaceae, Gleicheniaceae, Plagiogyriaceae, Vittariaceae as well as the earlier mentioned Osmundaceae and Davalliaceae were considered as "non-perinous" (Devi 1980; terminology *sensu* Devi). The comprehensive studies of Tryon and Lugardon (1990) indicate that all of the taxa mentioned above possess a perispore.

1.4.1.4 Jackson 1928

The Glossary of Botanic Terms, (Jackson 1928) defined *perispore* as:

- (1) the membrane or case surrounding a spore
- (2) the mother cell of spores in algae
- (3) equivalent to the perigynium, the involucre of the female inflorescence in bryophytes and
- (4) all incrustation containing much silica, outside the exospore of *Isoetes* (Jackson 1928).

The latter again stresses the difference in perispore material in the heterosporous Lycophytina, as observed earlier by Hofmeister/Russow.

Perinium is outlined as the outermost of the three coats of a fern spore (epispore), consequently, for Jackson, *epispore* and *perinium* are synonyms.

Perine he defines as the outermost layer of sculpturing in pollen. In order to differentiate the terminology of pteridophytes from that of angiosperms, he considered also *perisporinium* as the outermost membrane of pollen (ibid.). Based on Jackson's terminology, *perispore*, *perinium* and *epispore* can be treated as synonyms referring to the outermost coat of fern spores, whereas both the terms *perine* and *perisporinium* should be used in connection with pollen, a view which is also supported by a 1994 definition (Punt *et al.* 1994).

1.4.1.5 Erdtman 1943/1952

In his book on pollen analysis, published in 1943, Erdtman included a glossary defining *perinium* as "perine; the outermost layer, outside of exine, in certain spores". The term *perisporium* refers back to *perine* and is therefore considered as a synonym (Erdtman 1943). Later (1947) he observed that the occurrence of a perispore may be related to only certain taxa and thus is not always present (Gastony 1974). Five years later (Erdtman 1952) he revised his definition by stating:

"In the spores of certain plants (e.g. mosses, ferns), however, it (the sclerine) also comprises an outer layer, perine. The presence of this layer seems to be due to the activity of a periplasmodium with perinogenous properties. The physico-chemical qualities of the perine differ more or less from those of the exine. It is, however, still impossible, particularly when dealing with pollen grains, to decide - without undertaking cytological investigations - whether a certain layer or sporoderm element is exinous or perinous. As long as this cannot be definitely proved 'perine' can be classified under the same noncommittal heading - 'sculptine' - as the outer, sculptured part of exine."

As a result, the neutral term *sculptine*, instead of *perispore* or *perine*, was introduced by Erdman for the outermost layer when nothing else is known about its chemistry or development (Erdtman 1952).

In stating that it is sometimes very difficult to judge if a spore has a perispore or not, Erdtman made an important observation, which explains why

perispore can be regarded as an overlooked feature in pteridophyte reproductive biology.

1.4.1.6 Kremp 1965

In his *Morphological Encyclopaedia of Palynology*, Kremp (1965) provided a collection of definitions summarising many of those mentioned so far. He listed the three terms *perine*, *perinium* and *perisporium* but did not give any new or further evidence on development, function or chemistry of perispore. However, he comprehensively discussed the occurrence of perispore in Carboniferous megaspores (*Triangulati*). Unfortunately, Kremp failed to cite the articles he discussed in his reference list and it was not possible to trace all of them back to the original source. Hence these articles were not included into this review.

1.4.1.7 Tryon and Lugardon 1990

Their definition of *perispore* is: "A wall external to the exospore, derived from the tapetum, is resistant to acetolysis, and may form a large part of the sporoderm, as in spores of most derived Filicopsida." The synonym *perine* is also given. The glossary at the end of the book again lists the term *perispore* with the following entry: "The outer wall of the sporoderm consisting of material distinct from the exospore sporopollenin, and formed later than the exospore, as in the homosporous Filicopsida; = perine."

1.4.1.8 Punt *et al.* 1994

Perine is defined as "A sporoderm layer that is not always acetolysis resistant and is situated around the exine of many spores." (Punt *et al.* 1994), emphasised that the term *perine* should be used in conjunction with *sexine* and *nexine*, whereas *perispore* should be used with *exo-* and *endospore*. *Perispore*, *perine* and *perinium* are considered as synonyms, the latter being a latinised form of the term *perine*. These three terms are referred back to Erdtman 1943 (*perine*), Jackson 1928 (*perinium*) and Russow 1872

(perispore). This 1994 reference is the most recent definition in the literature. The fact that it is “not always acetolysis resistant” hints at its chemistry, which might differ within families, genera or even species of pteridophytes.

1.4.1.9 Crum 2001

Crum (2001) defines the *perine* in bryophytes as: a coating of material of sporophytic origin deposited on the outer surface of some bryophyte spores and lacking in liverworts and hornworts. It is noteworthy that throughout bryophyte spore wall literature the term *perine* is applied, which stands in contrast to the inconsistent terminology used in pteridophyte spores.

1.4.1.10 Moore 2005, herein

Due to differences in the perispore between the Lycopsidea and the non-lycopsidea pteridophytes (terminology *sensu* Kenrick and Crane 1997), which have so far not been included in any definition, I suggest the following modifications to Tryon and Lugardon's (1990) definition and that of Punt *et al.* (1994):

A wall external to, and in some cases integral with the exospore (e.g. Selaginellaceae megaspores), derived from the tapetum and not always acetolysis resistant. Whereas the perispore in the Lycopsidea is siliceous, the true perispore of the non-lycopsidea pteridophytes may or may not contain silica.

1.4.2 Terminology

The use of terminology is less straightforward than that of definitions. A summary of terms used for pteridophyte and bryophyte sporoderm layers is presented in table 1.1 below. Lycopsidea spore wall terminology is kept separately from pteridophyte terminology and is shown in table 1.2. This is mainly due to the fact that the terminology used by several authors for lycopsidea megaspore walls is inconsistent and has led to much confusion.

This becomes clear when studying both tables in the light of the definitions presented above. Over more than a decade, a number of scientists established different definitions, also introducing various new terms for sporoderm layers. The more scientists published in pteridophyte palynology, the more terms emerged, resulting in what I would call the “ultimate terminology chaos”, as seen in lycophytes.

Reference	Pteridophyte sporoderm layers			
Moore (2005), herein	perispore		exospore	endospore
Punt <i>et al.</i> (1994)	perine perispore		exospore	endospore
Tryon & Lugardon (1978)	silica layer (for lycopsid megaspores) perispore (for isospores)	outer exospore	inner exospore	endospore
Erdtman (1952)	perine sculptine	sexine	nexine exine	intine
Erdtman (1943)	perineum perine perisporium	sexine	nexine exine	intine
Bower (1923)	perispore		exospore	
Jackson (1928)	perispore perinium episporium perine perisporinium			
Hannig (1911)	perispore		exospore	endospore
Russow (1872)	perisporium or episporium		exosporium	endosporium
Reference	Bryophyte sporoderm layers			
Crum (2001)	perine	exine	exine	intine

Table 1.1: A summary of pteridophyte and bryophyte sporoderm terminology used by different authors.

Terminology	<i>Selaginella</i> megaspore	<i>Isoetes</i> megaspore	Terminology
siliceous coating ¹ outer sclerine ² sification ⁴	silica ³ perispore ⁵		silica cover ⁶
outer exospore ^{1,3} middle sclerine ² perine ⁴ exospore ⁵			outer zone of exospore ⁶ outer exospore layer ⁷
inner sclerine ² inner exospore ³ exine ⁴ mesospore, exospore ⁵			unnamed siliceous stratum belonging to the outer exospore layer
inner separable layer ¹ inner compact stratum ³			inner zone of exospore ⁶ inner exospore layer ⁷
intine ^{1,4} endospore ^{2,3,5}			inner separable layer ⁷
cytoplasm ³			endospore ^{7,6}
			lumen ⁷
¹ Taylor (1989) ² Minaki (1984) ³ Tryon & Lugardon (1978, 1990) ⁴ Kempf (1970) ⁵ Stainier (1965, 1967) ⁶ Macluf <i>et al.</i> (2003) ⁷ Taylor (1992, 1993)			

Table 1.2: Comparison of *Selaginella* and *Isoetes* megaspore walls suggesting homology (see Moore *et al.* (in press a) for details), including commonly used sporoderm terminologies by various authors.

1.5 The occurrence of the perine/perispore

1.5.1 In bryophytes

The literature on bryophyte spore ultrastructure is less comprehensive than that of pteridophytes. There also seems to have been broader study of bryophyte spores by SEM rather than TEM. This is probably because SEM studies are more straightforward, requiring less sample preparation. Those articles documenting spore ultrastructure concentrate preferentially on one particular family, genus or even species instead of providing a wider, comparative picture including, for example, different families. There is, however, enough evidence in the literature to say that ultrastructure differs in mosses and liverworts and that the three major moss groups, namely the Sphagnopsida, Andreaeopsida and Bryopsida, have their own characteristic spore wall structure (Brown and Lemmon 1990; Estébanez *et al.* 1997). For a comprehensive synopsis on bryophyte spores the reader is referred to Morgensen (1983), whose work covers spore morphology and ultrastructure, dispersal patterns, spore mass and features of life strategies as well as lines of specialization. Unlike the following section on the perispore in pteridophytes, which is structured systematically, the present section summarises the literature according to the number of species investigated. This means that studies on single species are listed first, followed by investigations on different genera and families. This brief review is not intended to cover all of the literature published on bryophyte spore ultrastructure but for the interested reader, a range of further studies are cited herein.

Sphagnum lescurii Sull. is described by Brown *et al.* (1982) with a unique spore ultrastructure among the Bryophyta. The spores consist of a two-layered exine: an inner, lamellate and a thick homogenous outer layer, which was only described for *S. lescurii* as in other mosses the exine is made of a single layer. Whereas the thick, homogenous exine gives rise to primary surface sculpturing, the perine forms the secondary surface ornamentation. The authors assumed that the perine is of exogenous origin and that by the

time perine formation is completed, the spore cytoplasm is metabolically dormant.

A series of studies focused on the sporogenous lineage in *Timmiella barbuloides* (Brid.) Moenk, Pottiales, (Gambardella *et al.* 1993a, 1993b, 1994). It is the 1994 publication that discussed spore ultrastructure and the development of the tapetum. The authors concluded that a secretory tapetum is responsible for perine formation, which is deposited as a thin, homogenous, opaque outmost layer. Gambardella *et al.* (1994) referred to a number of other investigations on tapetal development and sporogenesis. All species mentioned in these studies are shown to have a perine: *Funaria* (Jarvis 1974), *Fissidens* (Mueller 1974), *Cinclidium* (Morgensen 1978), *Amblystegium* (Brown and Lemmon 1985) and *Archidium* (Brown and Lemmon 1984).

A recent publication by Renzaglia and Vaughn (2000) summarised the anatomy, development and classification of hornworts. Their work also included a number of TEM pictures of the spores of *Notothylas temperata*, on which a “perine-like layer” (*sensu* Renzaglia and Vaughn) can be seen. The authors emphasised that this outmost layer, which they described as a thin dark band of fibrous material, is not a true perine, which by definition derives from the inner sporangial wall. The “perine-like layer” seen in *Notothylas temperata* is derived from deposition of residue of the sporocyte wall and the intrasporal septum and thus is not a true perine. The perine in bryophytes is defined as “a coating of material of sporophytic origin” (Crum 2001).

The ultrastructure of six *Grimmia* species was studied by Estébanez *et al.* (1997). The species investigated comprised *Grimmia descipiens*, *G. elatior*, *G. funalis*, *G. orbicularis*, *G. pulvinata* and *G. trichophylla*. They were all described with a perine layer. The authors give a detailed description of the perine, which is presented in form of table 1.3. Perine ultrastructure consists of two different materials, opaque primary elements giving rise to the overall sculpture and of translucent secondary elements partly covering primary elements. All species have a distinct perine layer, which the authors explain with interspecific variability. They also conclude that differences in spore ultrastructure might reflect different ecological requirements, e.g. early germination after dispersal demands a thinner spore wall and *vice versa*.

Species	Perine thickness	Ultrastructural perine elements
<i>G. descipiens</i>	even with 0.8µm	primary: verrucae and bacula, densely covering the spore secondary: interconnecting and covering primary elements
<i>G. elatior</i>	0.5 - 0.6µm	primary: unbranched baculae giving rise to verrucate and clavate sculpture secondary: papillose, sparsely distributed
<i>G. funalis</i>	0.2 - 0.4µm	primary: scattered verrucoid elements secondary: rarely observed
<i>G. orbicularis</i>	0.2 – 0.4µm	primary: fused on their based forming continuous layer secondary: translucent material surrounding primary elements
<i>G. pulvinata</i>	0.2 – 0.4µm	primary: verrucate or clavate elements secondary: abundant and irregularly shaped
<i>G. trichophylla</i>	0.3 – 0.5µm	primary: baculate or verrucate elements secondary: scattered on surface

Table 1.3: Synopsis of perine characters in the bryophyte genus *Grimmia*, based on Estébanez *et al.* (1997).

Luizi-Ponzo and Barth (1998) studied spore morphology in some Bruchiaceae species from Brazil by the means of SEM. This technique limited their observations to spore sculpture, hence they admitted that exine and perine were hard to distinguish and they therefore adopted the term “sclerine”. On the basis of their findings the authors agreed with previous studies that spore wall characters provide useful taxonomic information.

Although this is a brief overview of bryophyte ultrastructure and the occurrence of a perine, it clearly shows that this layer is as common in bryophytes as it is in pteridophytes, which is an important consideration in the evolution of this layer. This means that bryophytes, who have a longer fossil record than pteridophytes, might hold the key for the origin of this layer.

1.5.2 In pteridophytes

Based on the phylogeny generated by Stevenson and Loconte (1996) the genera included therein were consulted in *Spores of the Pteridophyta* (Tryon and Lugardon 1990). I chose the phylogeny by Stevenson and Loconte (1996) instead that of Pryer *et al.* (2004), because although her work comprised 62 taxa and is the most recent phylogeny, that of Stevenson and Loconte took almost double the number of taxa (111) into consideration. The list starting below is the combined information of both references. The numbers in front of

the genera and species were readopted from Tryon and Lugardon. Where genera or species are omitted this means that they were not included into Stevenson and Loconte's phylogeny.

Tryon and Lugardon reviewed 35 families of the Pteridophyta, including 232 genera. Marsileaceae, Salviniaceae and Equisetaceae are said to lack a perispore, instead an episporium seems to be present. The term was coined by Lugardon and was recently discussed (Lugardon 1990). Episporium refers to a layer within the sporoderm of heterosporous pteridophytes, which is formed during the latest stages of exospore development. The episporium's main component is sporopollenin and is largely, if not exclusively, of tapetal origin and, totally different from perispore material in all aspects except its superficial position (Lugardon 1990).

According to Tryon and Lugardon (1990), in megaspores of heterosporous genera such as *Selaginella* and *Isoetes* a true perispore is absent, some microspores, however, develop a true perispore.

In the Lycopodiaceae, a true perispore has been observed in the genera *Phylloglossum*, *Lycopodium* and *Lycopodiella* but not in *Huperzia*. Here the question arises, why in genera of the same family is there not a consistent perispore. The same applies to Hymenophyllaceae with its eight genera. In the genus *Trichomanes* a true perispore has not been observed, whereas the four genera *Hymenophyllum*, *Sphaerocionium*, *Crepidomanes* and *Cardiomanes* show a true perispore, which is usually thin and inconspicuous. In the case of the genera *Hymenoglossum*, *Serpyllopsis* and *Cephalomanes* nothing is said about a perispore, possibly owing to lack of data. All in all, data seem to be missing in quite a few genera of different families. This is the case in:

- a) *Archangiopteris* of the Marattiaceae
- b) *Pterozonium*, *Nephtopteris*, *Cerosora*, *Actiniopteris*, *Coniogramme*, *Anopteris*, *Idiopteris* and *Neurocallis* (Pteridaceae)
- c) *Anetium* (Vittariaceae)
- d) *Oenotrichia*, *Leptolepia* and *Tapeinidium* (Dennstaedtiaceae)
- e) *Drymotaenium*, *Lemmaphyllum*, *Christiopteris*, *Leptochilus*, *Neochheiropteris*, *Dicranoglossum*, *Microgramma*, *Neurodium*, *Niphidium*, *Pleopeltis* and *Marginariopsis* (Polypodiaceae)

- f) *Acrosorus* and *Scleroglossum* (Grammitidaceae)
- g) *Davallodes* (Davalliaceae)
- h) *Acrophorus*, *Peranema*, *Stenolepia*, *Nothoperanema*, *Hypoderris*, *Psomiocarpa*, *Triplophyllum*, *Dryopsis*, *Dryopolystichum* and *Deparia* (Dryopteridaceae)
- i) *Teratophyllum* (Lomariosidaceae)
- j) *Steenisoblechnum* (Blechnaceae)
- k) *Pleurosorus* (Aspleniaceae)

As for the genus *Polypodiopteris* of the Polypodiaceae, SEM pictures show a fractured spore with a relatively thick wall and a surface sculpture of short tubercles (Tryon and Lugardon 1990). The authors assume that this exceptionally large outer wall is a true perispore. However, if it turns out to be something different, this might be one of the few, if not the only genus within the Polypodiaceae without a true perispore.

The following list summarises the occurrence of a true perispore (used in this sense hereafter) in pteridophytes gained by combined information from Stevenson and Loconte (1996) and Tryon and Lugardon (1990):

Isoetaceae Reichenbach

232. *Isoetes* Linnaeus This heterosporous genus has microspores with a compact or sometimes diffuse perispore. Megaspores are described to lack a perispore but often show thick, complex silica coatings on the outer exospore.

Selaginellaceae Milde

231. *Selaginella* Beauvois Heterosporous genus with a perispore or paraexospore found in microspores, megaspores are described to lack a perispore but have a siliceous outer exospore coating, as observed in *Isoetes*.

Lycopodiaceae Mirbel

Genera 227-230

227. *Huperzia* Bernardi No perispore observed

228. *Phylloglossum* Kunze A thin, diffuse perispore which is highly electron permeable with more electron dense spots towards the outer regions.

229. *Lycopodium* Linnaeus A thin perispore of usually one layer.

230. *Lycopodiella* Holub Also a thin perispore of one or two layers, depending on species. In species with two layers, the inner is far more electron dense than the outer.

Psilotaceae Kanitz

Genera 219-220

219. *Tmesipteris* Bernhardt A thin perispore conforming to the exospore, which is highly electron permeable.

220. *Psilotum* Swartz A thin perispore draping the exospore and sometimes filling surface depressions. Perispore material is more electron dense than in *Tmesipteris*.

Equisetaceae A.P. DeCandolle

226. *Equisetum* Linnaeus EPISPORE of one layer forming the outer wall, fused with exospore and cellulosic elaters near the aperture.

Ophioglossaceae Agardh

Genera 1-3

Homogenous perispore pattern in all genera, mostly consisting of thin, fibrillar-granular material.

1. *Botrychium* Swartz The genus comprises 25 species, which are treated in four subgenera (*Sceptridium*, *Botrychium*, *Japanobotrychium*, *Osmundopteris*). 10 species were investigated.

The spore structure is made of a three-layered exospore and a continuous perispore, which is of a very fine fibrillar material.

2. *Helminthostachys* Kaulfuss A monotypic genus of the palaeotropics based on *Helminthostachys zeylanica* (L.) Hook. Four collections have been examined.

Three-layered exospore, the one in the middle shows large cavities, the perispore is a thin fibrillar-granular layer with fine spicules.

3. *Ophioglossum* Linnaeus Genus of about 30 species treated in four subgenera, 10 species have been investigated. The exospore consists of three layers from the inner to the outer: inner - compact, middle - with cavities

and foliation, outer - largest and very compact. A thin perispore of fine fibrillar material is easily detached.

Marattiaceae Berchtold and J.S. Presl

Genera 4-9

The perispore varies in thickness and structure, consisting of different numbers of strata in the six genera investigated, with *Christensenia* showing a unique pattern among pteridophytes.

4. *Angiopteris* Hoffman Genus with over 100 species although 10 or fewer species are normally recognised. 8 species were investigated.

Three-layered exospore and a perispore of several strata or coalescent in a single thick layer.

5. *Protomarattia* Hayata Monotypic genus based on *Protomarattia tonkinensis*, very rare. Spores were examined from a topotype.

Perispore rises above the echinate exospore.

6. *Christensenia* Maxon Also monotypic, based on *Christensenia aesculifolia*. Spores of three collections were examined. Spinous exospore with a fine perispore of discrete parallel laminae. There are three discrete types of deposits which tend to be more complex between the spines. The series of fine, parallel laminae seems to be unique among spores of the Marattiaceae. *Christensenia* is associated with the Pennsylvanian *Cyathotrachus*.

8. *Marattia* Swartz The thin, continuous perispore of two locally divided strata. Monolete spores of *Marattia* are the smallest among monolete ferns.

9. *Danaea* J.E. Smith Complex perispore with three different zones: inner formation of compact spherical elements above the exospore, a central granulate deposit thicker between the spines and an outer palliate deposit on top of the spines.

Osmundaceae Berthold and J.S. Presl

Genus 10

Very thin layer of perispore with fascicled, echinate elements at the apex of exospore tubercles.

10. *Osmunda* Linnaeus Thin, continuous layer of perispore with echinate elements that are formed by fascicles of fibrils. This pattern is common among

all species of *Osmunda* and also applies to the genera of *Todea* Bernhardt (genus 11) and *Leptopteris* Presl. (genus 12).

Hymenophyllopsidaceae Pichi-Sermolli

Genus 81

81. *Hymenophyllopsis* Perispore of one layer with long rodlets, diffuse, fairly electron dense material.

Hymenophyllaceae Link

Genera 22-25, 27

All genera where data are available, the perispore is thin and sometimes discontinuous.

22. *Hymenophyllum* Smith A very thin perispore appearing discontinuous.

23. *Sphaerocionium* Presl A very thin perispore.

24. *Crepidomanes* (Presl) Presl Very similar to the perispore of *Hymenophyllum*.

25. *Trichomanes* Linnaeus No perispore observed

27. *Cardiomanes* Presl Granulate perispore, thin.

Matoniaceae Presl

Genera 16, 17

16. *Matonia* R. Brown A thick, complex perispore with two strongly differentiated strata. Well developed rodlets in the upper part of the perispore have a clear central area both in longitudinal and transverse sections. This pattern is exceptional among spores of the less derived genera.

17. *Phanerosorus* Copeland A thin perispore with some rodlets in irregular masses as in *P. sarmentosus*. However, *P. major* is described without a perispore, which should be further investigated.

For a review on this family see van Kronijenburg-van Cittert (1993).

Cheiropleuriaceae Nakai

Genus 18

Usually a featureless, thin perispore which sometimes is slightly rugulate.

18. *Cheiropleuria* Presl A thin perispore with brittle wall material, quite electron dense in TEM section.

Dipteriadaceae (Diels) Seward and Gale

Genus 19

19. *Dipteris* Reinwardt The thin perispore consists of either one or two layers and is often fragmented.

Gleicheniaceae (R. Br.) Presl

Genera 13-15

The perispore is described as thin and plain or rarely rugulate. In all genera the perispore is fairly electron dense.

13. *Gleichenia* J.E. Schmith In monolete spores the perispore is thin with short irregularly disposed rodlets. Trilete spores in contrast show a thin, brittle perispore.

14. *Dicanopteris* Bernhardt A thin perispore that is rarely covered with rodlets.

15. *Stromatopteris* Mettenius A thin perispore that adheres to the exospore.

Plagiogyriaceae Bower

Genus 74

74. *Plagiogyria* Two-layered perispore, the outer forming short rodlets. Canals in the outer exospore visible (p. 217, figs. 11/12).

Metaxyaceae Pichi-Sermolli

Genus 82

82. *Metaxya* Thick, three layered perispore, the outer forming the granulate surface, the inner being thin, the middle heterogeneous.

Loxomataceae Presl

Genera 72,73

72. *Loxoma* A perispore of two layers, the inner with thin granules, the outer with a more diffuse pattern.

73. *Loxomopsis* Two-layered perispore, surface contours derive from perispore, outer layer usually granulate. Dark electron dense perispore resembles siliceous outer exospore of *Selaginella* megaspore walls (p.213, fig.6).

Lophosoriaceae Pichi-Sermolli

Genus 83

83. *Lophosoria* Granulate perispore deposits are formed above and below an additional outer layer of material, similar to the exospore.

Cyatheaceae Kaulfuss

Genera 84-89

84. *Sphaeropteris* A complex perispore of granulate material in and above pits, forming rodlets. Some species have a complex three-layered perispore (p. 251, figs. 22-26) → hints at intraspecific variability.

85. *Alsophila* A three-layered perispore, quite similar to that of *Sphaeropteris* but with less densely packed wall material.

86. *Nephelea* A three-layered perispore, the outer forming ridges. Layer pattern more like *Alsophila*.

87. *Trichipteris* Perispore of two layers, the outer with granulate deposits hiding pits, or simply rodlets.

88. *Cyathea* A thin perispore of two layers, with rodlets lining and spanning the pits.

89. *Cnemidaria* Perispore of two layers, forming a continuous cover on the surface.

Dicksoniaceae Bower

Genera 75-80

75. *Culcita* Presl Perispore of two layers forming the surface contours, the inner showing artificial lines (p. 220, fig. 10).

76. *Calochlaena* (Maxon) Turner and White Two layers of perispore, the outer above a dark, granulate deposit.

77. *Cibotium* Kaulfuss Two very similar layers, the inner being more diffuse.

78. *Cystodium* Hooker Two layered-perispore, the sinuous ridges are formed by the inner layer, scales in inner part (p. 227, fig. 7) have so far not been investigated in much detail.

79. *Tyrsopteris* Kunze A two-layered perispore forming the papillate surface.

80. *Dicksonia* L'Héritier de Brutelle Two or more layers of irregular perispore, consisting of either inner compact material or more diffuse heterogeneous material, partly coalescent like in *Dicksonia sciurus*.

Salviniaceae Reichenbach

Genera 224,225

224. *Salvinia* Séquier EPISPORE

225. *Azolla* Lamark EPISPORE

Marsileaceae Mirbel

Genera 221-223

221. *Marsilea* Mirbel EPISPORE

222. *Regnellidium* Lindman EPISPORE

223. *Pilularia* Linnaeus EPISPORE

Schizaeaceae Kaulsfuss

Genera 28-31

28. *Lygodium* Swartz A complex, three-layered perispore consisting of three layers. The inner perispore is compact with scales below, the middle layers shows radially aligned elongate elements and the outer is compact again, forming the surface contours. Electron density and structures differ greatly in these layers. The middle layer resembles exospore structures of *Lycopodium* and *Artemisia* described by Rowley as tuft like exine (Rowley 1995; 1996; Rowley and Claugher 1991; Rowley and Skvarla 1993).

29. *Anemia* Swartz A complex perispore whose thickness varies in different species.

30. *Mohria* Swartz A complex perispore with small spherical elements on top and below the surface. The material of the spheres looks extremely electron dense and is worth analysing.

31. *Schizaea* Swartz (including subgenus *Actinostachys*) A thin perispore often conforming to the exospore contours with particulate perisporeal spherules as in *S. intermedia*.

32. *Platyzoma* R. Brown A two layered perispore of coalescent granulate material with varying electron density.

Dennstaediaceae Pichi-Sermolli

Genera 90-106

91. *Dennstaedtia* Moore Perispore forming the surface contours, sometimes with short rodlets, extremely electron dense wall material (p.272, fig.16).

94. *Monachosorum* Kunze Perispore of one layer forming echinate surface. Diffuse material, not as densely packed as in *Dennstaedtia*.

105. *Lindsaea* Dryander Two-layered perispore, the outer usually with rodlets. Material granulate, resembling patchwork like pattern of siliceous *Selaginella* outer exospore material.

Vittariaceae (Presl) Ching

Genera 66-67, 69-71

66. *Rheopteris* Alston A thin, finely granulated perispore, which is partially abraded, seems to form the outer contours.

67. *Antrophytum* Kaulfuss Perispore of two layers, the inner forming papillae. The layers do not seem to be separated so that one could argue for one layer with a granulate stratum (or granulate deposit) towards the exospore.

69. *Vittaria* J.E. Smith A thin, two layered perispore, here the two layers are more distinct than in *Antrophytum*.

70. *Monogramma* Schkur A thin, one-layered perispore.

71. *Hecistopteris* J.E. Smith A thin perispore with fine globules and short rodlets. Material is diffuse but fairly electron dense.

Pteridaceae R. Brown

Genera 33, 46, 47, 59, 62

33. *Ceratopteris* Brongnart A thin perispore with dense rodlets. Very electron dense material of diffuse structure.

46. *Taenitis* Schkur One distinct layer of perispore with rodlets as electron dense as in *Ceratopteris*.

47. *Cheilantes* Swartz Several more or less complex layers, the outer sometimes arrested or with residual tapetal deposit.

59. *Adiantum* Linnaeus Two-layered perispore, the outer forming the rugulate surface. Some species have three complex layers that form the largest part of the sporoderm → hints at intraspecific variability.

62. *Pteris* Linnaeus A perispore of two layers which conforms the contours of the exospore. The lower layer is thin and finely granular, the outer rougher, forming rodlets in some species and sometimes enclosing globules.

Apleniaceae Frank

Genus 212

212. *Asplenium* Linnaeus A cavate perispore with long laminae in the inner part.

Thelypteriaceae Pic.-Ser.

Genus 149

149. *Thelypteris* Schmidel A usually two-layered perispore, the outer cavate or echinate. Both layers firm and of quite electron dense material.

Dryopteridaceae Herter

Genera 159, 184

159. *Dryopteris* Adanson A perispore of one cavate layer usually with short scales below.

184. *Athyrium* Roth A complex multi-layered perispore, the main layer usually cavate. Layers also differ in electron density and texture.

Lomariopsidaceae Alston

Genera 198, 200-202

198. *Lomariopsis* Fée Perispore cavate, the outer part fenestrate or reduced, the inner papillate. A bizarre surface sculpture.

200. *Loxogramma* J. Smith A thin cavate or plain perispore of a smooth texture.
201. *Bolbitis* Schott A reticulate outer perispore and a pillared inner perispore, which can also be found in *Elaphoglossum* and *Lomariopsis*.
202. *Elaphoglossum* J. Smith A single cavate layer often with abundant pillars.

Blechnaceae (Presl) Copeland

Genera 203-204, 206-211

203. *Woodwardia* J.E. Smith Complex cavate perispore with scales above, considered as one layer. Scales show a granulate material which is more electron dense than the cavate stratum below.
204. *Pteridoblechnum* Hennipman A thin perispore with long laminae and fibrous material above.
206. *Doodia* Hennipman Perispore with dense, short pillars.
207. *Blechnum* Linnaeus Laminated perispore, pillared with rodlets and a compact outer surface.
208. *Salpichlaena* J. Smith Also laminated perispore but overlaid by irregular, granulate deposits.
209. *Sadleria* Kaulfuss A complex perispore with inner strands.
210. *Brainea* J. Smith Papillate perispore.
211. *Stenochlaena* J. Smith Laminated thin perispore.

Davalliaceae Frank

Genera 143, 145-148

143. *Leucostegia* Presl A thin perispore forming the rugulae, material of varying electron density.
145. *Araiostegia* Copeland Thin, granulate perispore with a matrix of coalescent material.
146. *Davallia* J.E. Smith Perispore with a thin laminated pattern.
147. *Gymnogrammitis* Griffith Thick perispore of one layer with scales in the innermost part forming the papillae and rods. Rods are quite large in size and resemble cuticle wax ornaments of plant leaves.

148. *Nephrolepis* Schott Perispore of one layer forming the tuberculate or rugate surface. Scales in the inner part adjacent to exospore.

Oleandraceae (J. Smith) Pichi-Sermolli

Genera 196-197

196. *Oleandra* Cavanilles One layer of perispore, cavate with pillars and a very electron dense material.

197. *Athropteris* Hooker One layer of perispore, pillared inner perispore subtends the surface contours.

Polypodiaceae Bercht. and J.S. Presl

Genera 107, 110, 114, 120, 135, 137

107. *Platyserioideae* Desvaux A single layered, thin perispore.

110. *Drynarioideae* (Bory) J. Smith Perispore of one layer forming tubercles or echinae, sometimes thin, following the exospore. Tryon and Lugardon (1990) suggest that the material of the spines is derived from the exospore, however, it could also be of perisporial origin.

114. *Lepisoroideae* (J. Smith) Ching Laminated perispore or thicker and granulate

120. *Microsorioideae* Link Laminated perispore, thin.

135. *Selligueoideae* Bory Perispore of one layer, forming papillae and prominent echinae. Very electron dense material, resembling siliceous coating of *Selaginella* outer exospore.

137. *Loxogrammoideae* (Blume) Presl Usually a thin perispore, laminated pattern, some parts are thickened.

Grammitidaceae (Presl) Ching

Genera 138, 142

138. *Grammitis* Swartz A very thin perispore but a well developed endospore, pseudoendospore present.

142. *Pleurosoriopsis* A thin perispore, pseudoendospore present.

1.6 The Role of the tapetum in perispore development

The sculpture of both living and fossil pollen and spore material is often characterised by a species-specific patterning, which is formed by the perispore in many pteridophytes. Past research has focused on two major questions: the underlying process which gives rise to variation in sculpture patterns and the composition of the material which plants use to form these architectures. However, just a few authors have dedicated their work to a better understanding of spore ontogeny and the role of the tapetum in perispore development. The following section provides a summary.

Generally, three factors are regarded as considerable in spore wall formation: 1) universal restrictions; 2) universal processes such as self-assembly and 3) a genetic component, which seems to govern the process in a very simple way although small genetic changes may have a great impact on pattern differentiation (van Uffelen 1991). In recent years numerous publications have stressed the importance of self-assembly in spore wall formation (Hemsley *et al.* 1994, 1996, 1998, 2000; Hemsley and Griffiths 2000). With respect to the perispore, neither genetic components nor chemical process are understood and therefore fundamental studies are needed.

Ontogenetic studies of embryophyte sporogenesis are becoming more important for the interpretation of sporoderm homologies (Blackmore and Barnes 1987). The tapetum is commonly considered as a source of perispore material and appears to be universally present in land plants (Pacini, Franchi and Hesse 1985). Its main function is the nourishment of the spores and pollen grains during their development. The tapetal cells of the sporangia and anthers have a number of features in common. They are ephemeral and strongly polarised, contain a cytoplasm with many ribosomes and active organelles, are often polyploid and form a plasma membrane and walls (Pacini 1990). Furthermore, these cells are able to secrete wall precursors (figure 1.9), which are polymerised later on and deposited outside the cytoplasm and spore plasma membrane to form the layer, known as the perispore in bryophyte and fern spores. The chemistry of these exine precursors is not well understood, neither is the function of Ubisch bodies.

These orbicules are defined as distinctive granule of sporopollenin produced by the tapetum, particularly in plants with secretorial tapeta (Punt *et al.* 1994) but analogous bodies were also reported in ferns (Pacini 1990), which are referred to as orbicules. This is consistent with the idea that with the addition of tapetal derived sporopollenin from these orbicules new wall layers can be formed and that this was a subsequent step first identified in homosporous land plants (Blackmore and Barnes 1987). Polysaccharides, and proteins are also produced and released by the tapetal cells which has been documented by various authors (Schneider and Pryer 2002; Pettitt 1979b; Lugardon 1990). The polysaccharide callose it believed to play an important role in the control of the formation of sculptural elements in pollen (Barnes and Blackmore 1986) but is thought not to be generally produced in pteridophytes (Lugardon 1978; Pettitt 1979a; van Uffelen 1991). It has only been documented in *Selaginella* and in microspores of *Azolla microphylla* (see Parkinson and Pacini (1995) for references). The most primitive type of tapetum is the strictly secretal (= parietal) one, because of its wide distribution among bryophytes and in the Lycopodiophyta (terminology *sensu* Pacini 1990). According to Pacini, all other types of tapeta can be derived from this primitive one. For angiosperms two kinds of tapeta have so far been described: (1) the parietal or secretory type and (2) the amoeboid or periplasmodial type (Pacini and Franchi 1991). Both types are based on morphological characters, the latter is subdivided into two layers, one of which is found in Psilotophyta, Equisetophyta and Polypodiopsida (terminology *sensu* Pacini 1990), whereas the other is restricted to mono- or dicotyledonous angiosperms. The occurrence of these sublayers is thought to be due to evolutionary convergence (Pacini, Franchi and Hesse 1985). A comprehensive overview on spore wall development in mosses, hepatics and hornworts is given by Brown and Lemmon (1990) on the moss *Timmiella barbuloidea* by Gambardella *et al.* (1993a, 1993b, 1994) and in *Selaginella* by Buchen and Sievers (1981). The following figure summarises the key to tapetum types and the hypothetical phylogeny of the principle tapetum types based on extant taxa.

Tapetal cells with or without walls and more or less retaining their shape	Tapetal cells with persistent walls	Tapetal cells surrounding the locus 1
		Tapetal cells enclosing spores whose walls lignify at the end of their life and become elaters 2
	Tapetal cells lacking walls (except the outer tangential one) after tetrad stage and surrounding the locus (parietal tapetum)	Tapetal cells more or less enclosing spores and retaining a thin wall till degeneration; elaters present or not 4
		Many microspores/pollen grains in a cross section of the anther 5
Tapetal cells not retaining their shape losing their walls	Tapetal cells lose their walls and intrude only after a transient parietal phase	Few microspores/pollen grains (5-12) in a cross section of the anther. Monoaperturate pollen grains, pores oriented towards tapetum 8
		Tapetal cell cytoplasm do not fuse 6
		Tapetal cell cytoplasm fuse to form a real periplasmodium 7 p.p.
	Tapetal cells may lose their walls at different stages but their cytoplasm fuse immediately	Tapetum (amoeboid tapetum in ferns) enclosing iso-, micro- or megaspores 3
		Tapetum (amoeboid tapetum in angiosperms) enclosing microspores/pollen grains 7 p.p.

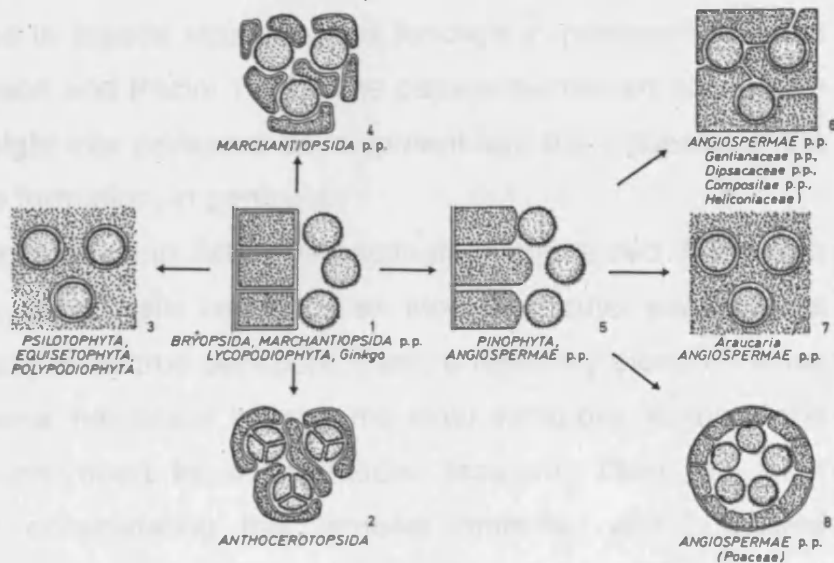


Figure 1.9: Key for tapetum subtypes and their hypothetical phylogeny. From Pacini (1990), p.216+217, table 1 and figure 1.

In the late eighties the tapetal organization in *Psilotum nudum* was closely investigated by Parkinson (1987, 1988). The tapetum in *Psilotum nudum* is described as having two different components. One component is of a cellular nature and is classified as the secretory type. The other is a plasmodial tapetum conforming to the inner tangential wall, which builds the inner surface of the loculus, and is assumed to contain sporopollenin since it is acetolysis resistant (Parkinson 1988). It is clear from studies utilizing TEM and SEM techniques, that the true perispore in *P. nudum* is thin and granulate, conforming to the exospore and partly filling surface depressions (Tryon and Lugardon 1990). The cytological studies made by Parkinson and the assured occurrence of a true perispore strengthen the hypothesis that for perispore development the presence of a tapetum is crucial.

Comprehensive work on *Schizaea pectinata* has been published by Parkinson on sporogenesis (Parkinson 1992), the role of the tapetum in spore wall formation (Parkinson 1995a and b) as well as morphological and ultrastructural variations in the same species originating from different habitats (Parkinson 1994). Later publications compared these data to the findings made in *Psilotum nudum* (Parkinson 1995c) and another article later discussed differences in tapetal structure and function in pteridophytes and angiosperms (Parkinson and Pacini 1995). The papers mentioned above give a comprehensive insight into perispore development and the influence of the tapetum on perispore formation, in particular.

As far as the sporogenesis in *Schizaea pectinata* is concerned (Parkinson 1992, 1995a and b), spore walls consist of an inner and outer exospore as well as of an inner and outer true perispore. First, a relatively electron dense lamella from the plasma membrane initiates the inner exospore. At this stage the tetrad is still surrounded by a plasmodial tapetum. Then the inner exospore forms by consolidating this lamellar material, which showed presence of polysaccharides, established by the Periodic Acid Schiff's test (PAS). Initiation of the outer exospore takes place at specific loci on the inner adjacent plasmodial tapetum. It seems that the plasmodial tapetum is directly involved in the production and deposition of the outer exospore and its differential growth apparently causes the reticulate structure, which characterises the exospore of *Schizaea pectinata*. At the time of the

development of the inner perispore, spherical globules and coiled structures in the inner sporangial loculus are observed. These structures are incorporated into the developing inner perispore, which follows the contours of the exospore. During perispore formation no continuous areas of plasmodial tapetum are present. Composite bodies of sporopollenious material and silicon from the sporangial loculus form the outer perispore. Material detached from these bodies is incorporated into the growing outer perispore and is also deposited on the surface. During processing the spore, Parkinson observed that the outer perispore is often displaced from the spore, a phenomenon that also occurs in *Pteris calomelanos* (figure 4.6A1 and B). Moreover, Parkinson notes that there are very few descriptions of perispore formation based on ultrastructural results in the literature. She also found decisive differences in the spores' morphology and ultrastructure in *Schizaea pectinata* species, which were collected from two habitats of extreme ends of the geographical range in South Africa (Parkinson 1994). These differences included variations in gross morphology, sporangium and spore size, outer exospore sculpture and tapetal organisation. The plant specimen from the Cape is much smaller in appearance with less fronds, whereas the Transvaal specimen is more robust with a large number of fronds and a complex rooting system. The latter specimen also showed longer sporangia. In the Cape material spore diameters range between 84µm and 88.5µm, opposed to the material from Transvaal where spores measure between 105.5µm and 115µm. Outer exospore pattering varies as follows: spores from Transvaal are covered with punctae of about 1µm in diameter, separated by ridges of the same size separating them. The ridges are irregular and the inner surface of the punctae is smooth. In the Cape material these punctae have a bigger and more unequal diameter ranging from 1.5µm to 2µm. The ridges separating them are irregular, too, and the entire uneven surface is covered with small granules. Concerning tapetal organisation, the Cape material showed a cellular, parietal and plasmodial tapetum. In the material from Transvaal only a plasmodial tapetum was observed. Reasons for these variations could either be a change in ploidy between the two species or the influence of the extreme two habitats. A combination of both factors, however, was not discussed but should not be neglected. Bigger spore sizes could be explained with greater

ploidy in the Cape specimen. It is not much known about the trend of pteridophytes for polyploidy but it is assumed that it gives them a certain advantage to maintain their genetic variability, which normally gets lost during intra-gametophyte self-fertilisation (Kramer *et al.* 1995).

After having studied *Psilotum nudum* and *Schizea pectinanta* in great detail, the differences and similarities in the sporogenesis of both species were published in a separate paper (Parkinson 1995c). They are characterised by a so-called "combination tapetum" consisting of two components: a cellular, parietal one and a plasmodial component. One of the main differences between the species is that whereas in *S. pectinata* the tapetum almost entirely disappears towards the end of perispore formation, that of *P. nudum* is still present and surrounds each spore until spore wall formation is completed.

A comparison of tapetal structure and function between pteridophytes and angiosperms lead to doubts that pollen and spore walls share homologous features (Parkinson and Pacini 1995). In the past pollen and spores have been linked due to superficial similarities in structure, function and known evolution. The study found major differences in the formation of the locular fluid, enzyme activity, conveyance of PAS-positive material, formation of exine precursors, sporopollenin production and viscin threads. Furthermore, there are differences in the formation of an acetolysis-resistant membrane, orbicules (Ubisch bodies), sporophytic proteins and the production of pollenkit and tryphine. The authors no longer support direct comparisons between pollen and spores due to fundamental differences in tapetal structure and function.

The tapetum is considered as a key to perispore evolution and development and according to Pettitt (1979b) the perispore is certainly a deposit of the tapetum, however, the exact amount of material involved in both perispore and exospore formation is unknown (see also figure 1.10 for the influence of the tapetum on perispore formation and for the origin of sporopollenin in Chlorophyta, Bryophyta, Pteridophyta and Spermatophyta (Euphyta)).

1.7 Chemical components and ultrastructure of the perispore and other sporoderm layers

1.7.1 Sporopollenin

The chemistry Sporopollenin is one of the most resistant organic materials forming the outer wall of pollen grains and sporoderm layers of spores in plants. The chemical structure of sporopollenin was first studied in the 1960s. The first interpretation of the chemical structure of sporopollenin stated that it is an oxidative polymer of carotenoids and carotenoid esters (Brooks and Shaw 1968). This hypothesis was disproved by Prahl *et al.* (1985, 1986) who discovered that the inhibition of carotenoid biosynthesis did not affect the formation of sporopollenin (for a review, see de Leeuw and Largeau 1993).

In fossil material, two different types of sporopollenin were characterised by pyrolysis and ^{13}C NMR (de Leeuw *et al.* 1991; van Bergen *et al.* 1995). The main building blocks in the first consist of phenolics, which upon thermal stress release alkylphenols and benzaldehydes. A study analysing the sporopollenin from extant *Typha angustifolia* pollen by the means of ^1H NMR techniques also documented the presence of four phenolic compounds in different amounts (Ahlers *et al.* 1999b). It was revealed that the compounds are tri- and tetrasubstituted. The units of the second sporopollenin type are considered to be of aliphatic nature generating extended homologous series of *n*-alkanes, *n*-alk-1-enes and α,ω -alkadiens on pyrolysis. Current systems used for analysing the chemical structure of sporopollenin are pyrolysis GC-MS and solid state NMR. Whereas ^{13}C - and ^1H - NMR revealed the presence of aromatic, aliphatic, and oxygen functionalities (Hemsley *et al.* 1994, 1996; Ahlers *et al.* 1999a, 2000, 2003), pyrolysis GC-MS analysis elucidated a number of structural characteristics of sporopollenin (van Bergen *et al.* 1995, 2004). This GC-MS work proposes that two principal components of sporopollenin are fatty acids ($\text{C}_{24}\text{-C}_{28}$) and oxygenated cinnamic acid derivatives. Latest results, however, show that the sporopollenin of extant *Isoetes* megaspores, isolated with mild chemical treatment and subjected to various mass spectrometry techniques, consists mainly of polymerised *p*-

coumaric acid (de Leeuw *et al.* 2004). No significant aliphatic compound could be found. A general review on organic macromolecules, including sporopollenin, is given by de Leeuw and Largeau (1993) and van Bergen (pers. comm. 2004). Whereas in Chlorophyta sporopollenin is solely produced by the cytoplasm, the role of the cytoplasm of bryophytes and pteridophytes in sporopollenin production is uncertain.

Experimental approaches Since the 1960s researchers have been trying to dissolve and analyse sporopollenin. Experimental approaches have ranged from chemical extractions (Southworth 1974, 1988; Loewus *et al.* 1985; Kress 1986; Tarlyn *et al.* 1993; Rowley *et al.* 2001), TLC and HPLC (Schulze-Osthoff and Wiermann 1987; Wehling *et al.* 1989) to spectroscopy techniques such as GC-MS (Kawase and Takahashi 1996), ^{13}C - and ^1H - NMR (Hemsley *et al.* 1992, 1993, 1994, 1996; Ahlers *et al.* 1999a and b, 2000, 2003) and FT-IR (Domínguez *et al.* 1999; Yule *et al.* 2000). Autoclaving and ultrasonic treatment have also been applied (Southworth 1974, 1988; Herminghaus *et al.* 1988; Thom 1998). Most authors mentioned above combined several of these techniques in their studies of sporopollenin.

A comprehensive study on the solubility of exines revealed that the sporopollenin of pollen exines of *Ambrosia trifida* is soluble in fused potassium hydroxide, strong oxidising solutions and in certain organic bases (Southworth 1974). Interestingly, other organic or inorganic acids, lipid solvents and detergents showed no effect at all and the inner exine of pollen as well as the exospore of pteridophytes seem insoluble, which gives evidence for the existence of different types of sporopollenin. Furthermore, it raises questions about the homology of angiosperm and gymnosperm exines and the exospore of pteridophytes. As far as the outer exine of gymnosperm and angiosperm pollen is concerned, 2-aminoethanol proves to be an efficient solvent. Hence it was proposed as a test to distinguish different types of sporopollenin (Southworth 1974). Herminghaus and co-workers (1988) published a more gentle approach towards the isolation and purification of sporopollenin, describing the use of hydrolytic enzymes such as pronase, lipase, cellulase, amylase and cellulysin and an exhaustive extraction of non-covalently bound components. The authors conclude that phenolic components are part of the

sporopollenin macromolecule and their isolation and purification methods seem successful, however, they also incorrectly assumed that sporopollenin is derived from carotenoids and carotenid esthers.

A different type of sporopollenin was found by Rowley who describes "*receptor-independent sporopollenin*" (Rowley and Claugher 1991; Rowley and Skvarla 1993; Rowley 1996). The exine of some species of the genus *Quercus* is characterised by the presence of very small rod-shaped structure, which in other species is masked by sporopollenin. Oxidation with potassium permanganate removes the sporopollenin between these structures. Rowley assumed that specific receptors for sporopollenin exist and calls the type of sporopollenin between the rod-shaped structure "*receptor-independent sporopollenin*" (RIS). In his 1991 article he suggested giving RIS a simple and positive name such as *masking-sporopollenin* as it is less resistant to oxidation than the sporopollenin in the rod structures of receptor dependant sporopollenin exines.

As described above, to date, several types of sporopollenin have been documented in pollen, spores and fossil material. It is very likely that more types of sporopollenin exist, which have not yet been discovered or described. If as expected sporopollenin is proven to be a randomly cross-linked biomacromolecule that has no repetitive large-scale structure, it will be very difficult to determine its chemical structure.

The evolution The evolutionary history of sporopollenin and that of spore development in land plants are closely interconnected. Figure 1.10 summarises the origin of sporopollenin in Chlorophyta, Bryo- and Pteridophyta and Spermatophyta (Euphyta).

	CHLOROPHYTA	BRYO- & PTERIDOPHYTA	SPERMATOPHYTA
SPOROPHYTIC DOMAIN	Tapetum not present	Tapetum Cytoplasm	Tapetum Cytoplasm
GAMETOPHYTIC DOMAIN	Sporopollenin precursors Cytoplasm	Exine precursors for exine and perine Exine precursors Spore Cytoplasm	Exine precursors Exine precursors Gametophyte Cytoplasm
COMMENTS	Sporopollenin certainly produced by the algal cytoplasm itself	No information on the gametophytic or sporophytic production of sporopollenin is available. Perine is certainly produced by tapetum (PETTITT 1979 a)	At least for some species gametophytic production of sporopollenin is admitted (DICKINSON & HESLOP-HARRISON, 1971, DICKINSON, 1976, PACINI & CRESTI, 1976)

Figure 1.10: The origin of sporopollenin in Euphyta (from Pacini *et al.* (1985), p.163, figure 1).

A study on the thermal evolution of sporopollenin revealed that aliphatic groups play an important role in the colour change of spores (Yule *et al.* 2000). Whereas in the immature phase of spores the colour changes are subtle and slow through a series of different darkening yellows, mature spores change their colour rapidly through a series of orange and brown colours. The first observation correlates with a reduction in the relative proportion of $>C=O$ groups and an increase in the relative proportion of aliphatic CH_2 , CH_3 groups. In mature spores an increase in the $C=C$ content associated with the formation of aromatic rings was reported, suggesting that the aliphatic and aromatic content of spores (and pollen) appear to control colour.

1.7.2 β -lectins, polysaccharides and lipids

Tryon and Lugardon (1990) note that the chemical and physical properties of the perispore in homosporous ferns differ from those of the exospore and that perispore material is absent in the sporoderm of pollen. However, they do not further discuss the chemical nature of the perispore material.

A high activity of spore wall enzymes was found in Marsileaceae mega- and microspores, which are associated with various molecules (Pettitt 1979a). Polysaccharides, β -lectin, proteins and lipids as well as enzymes like esterase, ribonuclease and peroxidase were localised by conventional staining methods. The distribution of chemical compounds in the wall layers intine, perine and the gelatinous layers (terminology *sensu* Pettitt 1979a) of micro- and megaspores were almost identical except for β -lectins, which are completely absent from the megaspores of all six species investigated. The exine is excluded from any enzymatic activity and there is no association with β -lectins, lipids or polysaccharides. One of the major issues of this article is the discussion of the utility of these enzymes and associated molecules in sporogenesis. Pettitt hypothesises connections with wall differentiation, gametophyte nutrition and protection.

Wall differentiation Apparently no new mechanisms are needed to initiate movement and deposition of wall material after the formation of the matrix, except for patterns of differentiation. It was shown that an irregular shaped matrix zone gives rise to various different structures and sculptures (Pettitt 1979b). In the literature this model is described as limited at a molecular level, as there are far more structural and sculptural pattern found in spore walls than could ever be initialised by the limited number of matrix zone variations. However, if one takes into account a process of self-assembly, a matrix zone though limited in chemical components could still give rise to numerous ultrastructural and morphological spore wall patterns (Hemsley *et al.* 1996, 1998, 2000; Hemsley and Griffiths 2000).

Gametophyte nutrition Various studies on gametophyte nutrition have shown that the proteins stored in the spore are hydrolysed by specific enzymes during germination, these hydrolases seem to be synthesised for this special purpose rather than being mobilised by some other endogenous sources (Pettitt 1979a). Exine channels have been described in the spores of *Lycopodium gnidioides* (Pettitt 1976), in *Psilotum* (Lugardon 1979) and in *Marsilea* (Pettitt 1979a). Their function is to provide transport routes for hydrolases and metabolites. These channels only exist for a limited period of

time in the developing exine, acting as a system of interconnected channels filled with fibrillar glycoprotein. It is difficult to prove that the material is transported through a macromolecule such as sporopollenin but staining with iron in *Lycopodium* between and within the channels seems to suggest that diffusion does occur. As an argument against these findings Pettitt himself considered the possibility of an artefact, probably resulting from sectioning. He also speculates on the electron dense surface coat, of which he thinks that it must have been transported either through or between the exine channels. He does not consider the influence of a tapetal membrane.

Protection After being released from the sporangium, spores are exposed to fungal, bacterial or viral infections in all habitats, which makes protection vital. A specially designed spore wall might function as an ideal barrier for any pathogenic attacks from outside. The chemical nature of β -lectins strongly supports the view that these molecules play an important role in the defence mechanisms of plants against the attack of micro-organisms, pests and insects (Lis and Sharon 1973; Etzler 1985). A lectin can be defined as a "sugar-binding protein or glycoprotein of non-immune origin, which agglutinates cells and/or precipitates glycoconjugates" (Goldstein *et al.* 1980). Definitions of lectins were discussed controversially as none of the definitions provided seemed sufficiently comprehensive. Nevertheless, the definition given above was accepted by the Nomenclature Committee of IUB and IUB-IUPAC Joint Commission on Biochemical Nomenclature in 1981 (Etzler 1985). At present little is known about the biological significance of lectins in the plant kingdom. Various biological functions appear to be connected with lectins and a general summary is given in (Etzler 1985), which will briefly be outlined. Since a vast number of lectins are found in legume seeds, a link to seed maturation and germination or in the maintenance of seed dormancy is most likely. As mentioned above, one of the most widespread views is that lectins function as phytochemical protection against various pathogenic attacks. Etzler provides three main evidences for that: (1) the presence of lectins at potential sites for a photogenic attack (2) the ability of binding to fungi and inhibition of their growth and germination (3) a possible correlation between lectin recognition of a micro-organism and its extent of pathogenicity. Finally,

lectins are associated with cell wall extension, cell-cell recognition, growth regulation and carbohydrate transport (Etzler 1985).

Recent studies One of the few recently published articles approaching the question of from what the perispore is made was published by Schneider and Pryer (2002). Marsileaceous megaspores, as in Pettitt's 1979 publication, were treated with histological staining methods to gather more information on possible chemical components. Sporopollenin could be identified in both the exine and the solid perine layer (terminology here following Schneider and Pryer 2002) but is absent in the gelatinous perine layer. In Marsileaceous megaspores the outer sporoderm layer is usually considered as *epispore* (Tryon and Lugardon 1990) and not as a true *perine/perispore* layer.

The results were obtained by using acetolysis and autofluorescence (450-600nm). Both layers, the exine and the solid perine layer, resist acid and acetolysis and the yellow autofluorescence emission indicates the presence of sporopollenin. Furthermore, the yellowish green grading outward to blue autofluorescence of the solid perine layer also indicates that a major component of this layer is not only sporopollenin but also polysaccharides. On the other hand the gelatinous perine layer dissolved by acetolysis and the blue emission of autofluorescence again indicates the presence of polysaccharides. These findings were supported by the use of further histological stains like Alcian blue, Calcufluor white, Ruthenium red, Safranin and the Periodic Acid-Schiff's test (PAS) which clearly showed a positive reaction for polysaccharides in the solid perine layer as well as in the gelatinous perine layer. Weak positive reactions of Ruthenium red and PAS hinted at small quantities of polysaccharides also found in the exine. Callose could not be detected in any of the layers, using Aniline blue, whereas cellulose was distinctly tested positive in the solid perine layer and a weak positive reaction of the exine and the gelatinous perine layer suggests smaller quantities of cellulose in these layers. Proteins, tested with Aniline black, could only be found in the solid perine layer. Lipids, on the other hand were present in all layers but in larger amounts in the solid exine according to tests with Sudan IV.

1.7.3 Silica

In order to avoid confusion over terminology, I will refer to silicon as the element, as for example detected by EDX-analysis, and to silica as the compound present in biological systems and in plants in particular.

Silicon has a relative abundance of about 27.27% in the lithosphere as opposed to only 0.03% in the biosphere, unlike carbon, nitrogen and sulphur which show rapid cycles due to a high biospheric abundance (Exley 1998). It is monosilicic acid, $\text{Si}(\text{OH})_4$, which acts as a precursor for the uptake and deposition of silicon in the biosphere (Epstein 1999). Silicon uptake into plants and the location of deposition are species-specific (Williams 1986). Silicon is present in many vascular plants in the form of solid hydrated silica ($\text{SiO}_2 \cdot n\text{H}_2\text{O}$), also known as opaline silica, silica gel or amorphous silica. Although it occurs in equal amounts like vital nutrients such as calcium, magnesium and phosphorus, silicon is only known to be essential for the growth of *Equisetum* (Chen and Lewin 1969; Epstein 1999), a genus with about 15 species, related to the Carboniferous arborescent group of *Calamites* (Bell and Hemsley 2002). The Poales and some Cyperales, as well as the more primitive plant lineages of the Bryophyta and many Pteridophyta are all known to accumulate silicon in their tissues, with values up to 6.3% of dry weight, as found in rice (Epstein 1999). Silica has been characterised by the means of infra red (IR) and nuclear magnetic resonance (NMR) spectroscopy in the grass *Phalaris canariensis* (Mann *et al.* 1983).

1.7.4 Colloidal structures

A century and a half ago chemists found an intermediate class of materials lying between bulk and molecular dispersed systems, which on the one hand are finely dispersed in one another. On the other hand, their degree of subdivision does not approach that in simple molecular mixtures. These systems are called colloids, which specialities are of great importance. It was Wolfgang Ostwald (1883-1943), Professor for Chemistry at the University of Leipzig (Germany) who first described them appropriately consisting of a dispersed phase (or discontinuous phase) distributed in a finely divided state

in a dispersion medium (or continuous phase) (Everett 1988). There is a large and important class of colloids in which growth is spontaneous but limited by geometric and energy factors to a finite size. Everett puts these colloids in the class of association colloids or, in more general terms, self-assembly systems. These systems can obviously be found in single celled organisms. Looking closer at them many different outstanding architectures can be observed, which arose scientists' interest in the nature of these mechanisms. Soon self-assembly systems were reported for micelles and many more complex forms like vesicles with biological structures such as cell membranes and furthermore for microtubules. Here the microtubules' various conformations are caused by concentration-specific self-assembly patterns (Nédélec *et al.* 1997).

The sporopollenin sculpture of both living and fossil pollen and spore material is often characterised by a species-specific patterning. In the past researchers have been working on two major questions: the underlying process which gives rise to these various sculpture patterns and the composition of the material which plants use to form these architectures. Various experiments regarding this process comprise colloidal simulations of lycophyte wall constructions and exine building in particular (Hemsley and Griffith 2000). Thus, self-assembly is assumed as an important pattern formation process in spore walls. The model system for exine development, used in self-assembly experiments, is a colloidal flocculation of polystyrene resulting in a polystyrene latex dispersion which shares similarities with sporopollenin such as the density or the refractive index. The average colloidal particle size in diameter achieved in experiments was between 0.2-0.5 μm , called polyballs (Hemsley *et al.* 1998). Lately, spherical droplets of over 10 μm with distinct surface patterning were made (Hemsley and Griffiths 2000) and with the introduction of specific surfactants into the reaction, the range of sculpturing patterns was broadened (Hemsley *et al.* 2003). The authors believe that surfactants are naturally occurring in form of fatty acids during spore wall formation.

A wide range of literature covers the behaviour of colloidal polystyrene particles (Everett 1988; Hemsley *et al.* 1992, 1994, 1996; Adams *et al.*, 1998). Previous experiments successfully demonstrated the simulation of all layers

and organizations of the plants studied, which were megaspores of Lycopods (Hemsley *et al.* 1998) and megaspores of *Selaginella* (Hemsley *et al.* 1996). *Selaginella myosurus* Sw. Alston in particular shows a special internal wall structure including a colloidal crystal region consisting of spherical sporopollenin particles, which have an average particle size of about 0.3 μ m. Moreover, the megaspore sculpture is covered with cubic crystals (5-10 μ m) of unknown chemical and crystallographic nature. These cubic crystals have been documented by the means of SEM and TEM by Tryon and Lugardon (1990) and by SEM by Minaki (1988).

2 Material and Methods

2.1 Sources of material

2.1.1 Extant pteridophytes, bryophytes and a gymnosperm

The living material used in this study originates from the Cardiff University Botanical and Research Gardens, Talybont, North Residences, Devon Place, Maindy, Cardiff CF14 3UX. Telephone: +44(0)29208033. The research gardens are maintained and run by Mr Lyndon Tuck (horticulturist).

The only extant plant NOT originating from the Cardiff University Botanical and Research Gardens is *Selaginella myosurus* Sw. Alston, which is a dried specimen originating from Ghana, given to Prof. Dianne Edwards in 1990 and was stored in a glass jar.

2.1.2 List of living species investigated

The following table 2.1 provides a summary of all extant species investigated as well as references to the result chapters. The list was structured according to the systematic classification of bryophytes by Goffinet *et al.* (2001), and the systematic classification of pteridophytes established by Stevenson and Loconte (1996). Although the latter might not be the most recent publication on fern systematics, it is still the most comprehensive available to-date.

Pteridophyte taxonomy is under constant revision (e.g. *Pteris longifolia* is now *Pteris vittata* and *Oreopteris limbosperma* is *Thelypteris limbosperma*). In order to avoid confusion, this list follows Tryon and Lugardon (1990).

Table of extant species investigated

Bryophytes

BRYOPSIDA

Family	Taxon	Results see
POTTIALES Meesiaceae	<i>Leptobryum pyriforme</i> (Hedw.) Wils.	Section 3.5
FUNARIALES Funariaceae	<i>Funaria hygrometrica</i> Hedw.	Section 3.5
BRYALES Bryaceae	<i>Bryum capillare</i> Hedw.	Section 3.5
HYPNALES Brachytheciaceae	<i>Brachythecium velutinum</i> (Hedw.) B.S.G.	Section 3.5

Pteridophytes

LYCOPODIALES		
Family	Taxon	Results see
Selaginellaceae	<i>Selaginella myosurus</i> Sw. Alston	Section 3.2
	<i>Selaginella pallescens</i> (Presl) Spring	Chapter 4
Lycopodiaceae	<i>Lycopodium clavatum</i> L.	Chapter 4
PSILOTALES		
Family	Taxon	Results see
Psilotaceae	<i>Psilotum nudum</i> (L.) Beauv.	Section 3.3
OSMUNDALES		
Family	Taxon	Results see
Osmundaceae	<i>Osmunda regalis</i> L.	Sections 3.3, 3.4, 5
PILULARIALES		
Family	Taxon	Results see
Schizaeaceae	<i>Anemia tomentosa</i> (Sav.) Sw.	Sections 3.3, 3.4
PTERIDALES		
Family	Taxon	Results see
Pteridaceae	<i>Pellaea calomelanos</i> (Swartz) Link	Sections 3.3, 4
	<i>Pellaea rotundifolia</i> (Forst.f.) Hook	Sections 3.3, 3.4
	<i>Pteris cretica</i> L.	Section 3.3
	<i>Pteris longifolia</i> L.	Section 3.3
BLECHNALES		
Family	Taxon	Results see
Thelypteridaceae	<i>Oreopteris limbosperma</i> (All.) J. Holub.	Section 3.3
	<i>Macrothelypteris torresiana</i> (Gaud.) Ching	Section 3.3
	<i>Phegopteris decursive-pinnata</i> (v.Hall) Fee	Sections 3.3, 3.4
	<i>Thelypteris japonicum</i> (Bak.) Ching	Section 3.3
	<i>Cyrtomium falcatum</i> (L.f.) C.Presl	Section 3.3

	<i>Cyrtomium fortunei</i> J. Sm.	Section 3.3
	<i>Diplazium proliferum</i> (Lam.) Thouars	Section 3.3
	<i>Dryopteris erythrosora</i> (Eat.) O. Ktze.	Section 3.3
	<i>Dryopteris stewartii</i> Fraser-Jenk.	Section 3.3
	<i>Hypodematium fauriei</i> (Kodama) Tagawa	Section 3.3
Dryopteridaceae	<i>Lastreopsis microsora</i> (Endl.) Tindale	Section 3.3
	<i>Rumohra adiantiformis</i> (G. Forst.)	Section 3.3
Blechnaceae	<i>Blechnum occidentale</i> L.	Section 3.3
	<i>Blechnum gibbum</i>	Chapter 4
	<i>Doodia aspera</i> R. Br.	Section 3.3
POLYPODIALES		
Family	Taxon	Results see
Davalliaceae	<i>Davallia mariesii</i> Moore ex Baker	Section 3.3
	<i>Nephrolepis hirsutula</i> (Forst.) Pr.	Section 3.3
Polypodiaceae	<i>Phlebodium aureum</i> (L.) J. Smith	Sections 3.3, 3.4
Gymnosperms		
Pinaceae	<i>Pinus sylvestris</i> L.	Chapter 4

Table 2.1: List of species investigated, arranged according to their systematic positions.

2.1.3 Fossil spore material

Fossil sporangia investigated originate from a stream section north of Brown Clee Hill, Shropshire, Early Devonian (Lochkovian) in age. Sedimentary strata (sandstones, marls and conglomerates) from part of the Lower Ditton group and comprise two horizons rich in organic material, vertically separated by about 60m of rock. For details see Habgood (2000). The two sporangia were allocated with specimen numbers HD 437 and HD 407/1.

2.2 Morphological descriptions of extant bryophyte spores, pteridophyte (mega-)spores and gymnosperm pollen

The spore morphology of the untreated species with respect to the size, shape, aperture and surface of the spores is summarised. The format for this description was established by Tryon and Lugardon (1990). Terminology

follows Kremp (1965) and Tryon and Lugardon (1990). SEM pictures of the (mega-)spores and pollen can be found in various results chapters, as cross referenced herein. The relevant page number is located next to the species name. The species are listed alphabetically within their phyla, not taking into account their systematic classification.

Bryophyta

Brachythecium velutinum (Hedw.) B.S.G. (p.169)

Size 11-14 μ m

Shape spheroid

Aperture not observed

Surface densely distributed tubercles, the latter formed by clustered granules

Bryum capillare Hedw. (p.167)

Size 15-18 μ m

Shape spheroid

Aperture not observed

Surface densely distributed low tubercles distally as well as proximally.

Funaria hygrometrica Hedw. (p.165)

Size 8-10 μ m

Shape spheroid

Aperture not observed

Surface densely packed low tubercles, tubercles closer packed than in *B. capillare*

Leptobryum pyriforme (Hedw.) Wils. (p.166)

Size 8-10 μ m

Shape spheroid

Aperture not observed

Surface densely packed low tubercles, tubercles are even closer packed than in *F. hygrometrica*

Pteridophyta

Anemia tomentosa (Sav.) Sw. (p. 122)

Size 110µm

Shape globose with prominent, prolonged angles

Aperture trilete, the laesurae extending $\frac{2}{3}$ to $\frac{3}{4}$ of the spore radius in polar view

Surface coarse ridges, prominent angles with keel-like structures, ridges echinate

Blechnum occidentale L. (p. 99)

Size 35-40µm

Shape ellipsoidal

Aperture monolete, with 25-30µm, over $\frac{3}{4}$ the length of the spore

Surface laevigate true perispore covering a granulate exospore

Cyrtomium falcatum (L. f.) Pr. (p. 105)

Size 58µm

Shape ellipsoidal

Aperture monolete, laesura not observed but usually $\frac{3}{4}$ the spore length

Surface uniformly tuberculate

Cyrtomium fortunei J. Sm. (p. 106)

Size 50µm

Shape ellipsoidal

Aperture monolete, $\frac{3}{4}$ the length of the spore

Surface irregular ridges, sometimes long or compressed or wing-like

Davallia mariesii Moore ex Baker (p. 102)

Size 66µm

Shape ellipsoidal

Aperture monolete, $\frac{3}{4}$ to nearly equal the spore length

Surface prominent verrucae

Diplazium poliferum (Lam.) Thouars (p. 107)

Size 58µm

Shape ellipsoidal

Aperture monolete, laesura obscure but usually $\frac{2}{3}$ to $\frac{3}{4}$ of the spore length

Surface coarse inflated folds, laevigate on folds

Doodia aspera R. Br. (p. 100)

Size 56µm

Shape ellipsoidal

Aperture monolete, $\frac{2}{3}$ to nearly equal the spore length

Surface verrucate

Dryopteris erythrosora (Eat.) O. Ktze. (p. 108)

Size 64µm

Shape ellipsoidal

Aperture monolete, aperture hidden, usually $\frac{1}{2}$ to $\frac{3}{4}$ the spore length

(Tryon and Lugardon 1990)

Surface tuberculate, laevigate between tubercles

Dryopteris stewardii Fraser-Jenk. (p. 109)

Size 72µm

Shape ellipsoidal

Aperture monolete, $\frac{3}{4}$ to full length of spore

Surface irregularly scabrate, flake-like in appearance

Hypodematium fauriei (Kodama) Tagawa (p. 110)

Size 89µm

Shape ellipsoidal

Aperture monolete, $\frac{3}{4}$ to full length of the spore

Surface tuberculate, some tubercles fused to ridges

Lastreopsis microsora (Endl.) Tindale (p. 111)

Size 32µm

Shape spheroid

Aperture monolete, $\frac{2}{3}$ to $\frac{3}{4}$ the spore length

Surface coarse, inflated reticula, reticula and muri are laeviagte

Lycopodium clavatum L. (p. 184)

Size 35-40µm

Shape globose

Aperture trilete, the laesurae extending over $\frac{3}{4}$ to nearly equal the spore radius in polar view (Fig 4.7C).

Surface the proximal and distal faces are reticulate

Macrothelypteris torresiana (Gaud.) Ching (p. 124)

Size 35µm

Shape ellipsoidal

Aperture monolete, $\frac{2}{3}$ to $\frac{3}{4}$ the spore length

Surface irregularly folded, perforated sculpture

Nephrolepis hirsutula (Forst.) Presl (p. 103)

Size 49µm

Shape ellipsoidal

Aperture monolete, $\frac{1}{2}$ the spore length

Surface irregularly tuberculate, some tubercles fused to rugate sculpture

Oreopteris limbosperma (All.) J. Holub (p. 125)

Size 53µm

Shape ellipsoidal

Aperture full length of spore

Surface cristate, with echinate ridges

Osmunda regalis L. (p. 113)

Size 69µm

Shape spheroidal

Aperture trilete, often obscure in immature spores, the laesurae $\frac{1}{2}$ to $\frac{3}{4}$ the spore radius in polar view

Surface coarsely tuberculate

Pellaea calomelanos (Swartz) Link (p. 117)

Size 35-40µm

Shape globose

Aperture trilete, the laesurae are 18µm long, extending over $\frac{3}{4}$ of the spore radius in polar view (Fig 6A)

Surface cristate true perispore (Fig 6C) forming small reticula of 2-4µm in diameter, densely granulate exospore (Fig 6D)

Pellaea rotundifolia (Forst. f.) Hook (p. 118)

Size 35-40µm

Shape globose

Aperture trilete, laesurae obscure

Surface echinate true perispore

Phegopteris decursive-pinnata (v.Hall) Fee (p. 126)

Size 59µm

Shape ellipsoidal

Aperture monolete, $\frac{1}{2}$ to the length of spore

Surface laevigate with some scattered tubercles

Phlebodium aureum (L.) J. Smith (p. 114)

Size 45µm

Shape ellipsoidal

Aperture monolete, the laesura extending over $\frac{3}{4}$ to nearly equal the length of the spore

Surface coarsely tuberculate

Psilotum nudum (L.) Beauv. (p. 115)

Size 65µm

Shape ellipsoidal

Aperture monolete, $\frac{3}{4}$ to full spore length

Surface coarsely rugate

Pteris cretica L. (p. 119)

Size 87.5µm

Shape globose with equatorial flange

Aperture trilete, the laesurae extending over $\frac{3}{4}$ to nearly equal the length of the spore radius in polar view

Surface proximal low flange with partly fused tubercles, distal prominently rugate

Pteris longifolia L. (p. 120)

Size 69µm

Shape globose with equatorial flange

Aperture trilete, the laesurae extending over $\frac{1}{2}$ the length of the spore radius in polar view

Surface tubercles fused adjacent to the aperture, distal surface reticulate with central tubercle

Rumohra adiantiformis (G. Forst) (p. 112)

Size 53µm

Shape ellipsoidal

Aperture monolete, $\frac{2}{3}$ to nearly equal the spore length

Surface irregular low verrucae

Selaginella myosurus Sw. Alston megaspore (p. 79)

Size 500-700µm

Shape globose

Aperture trilete, the laesurae equal the spore radius in polar view

Surface reticulate sculpture with large ridges and muri, cubic crystals visible in muri as well as some scattered crystals on the ridges.

Selaginella pallescens Presl Spring megaspore (p. 185)

Size 300-350µm

Shape globose

Aperture trilete, the laesurae are 150µm long, which equals the spore radius in polar view

Surface proximal: densely verrucate, distal: reticulate. The micro-sculpture is echinulate.

Thelypteris japonica (Bak.) Ching (p. 127)

Size 38µm

Shape ellipsoidal

Aperture monolete, full length of spore

Surface irregularly folded

Gymnosperms

Pinus sylvestris L. (p. 186)

Size 40-45µm

Description saccate with ellipsoidal body outline in polar view, outline even.

Sacs attached to the ventral side of the body, in a small, sharp angle.

Surface finely tuberculate, covering the entire pollen grain

2.3 Microscopy techniques

The techniques used in this study are light microscopy (LM), scanning electron microscopy (SEM) and transmission electron microscopy (TEM). A brief description is also given for energy dispersive x-ray analysis, which was used in combination with SEM and TEM.

2.3.1 Light microscopy (LM)

Microscopy slides were prepared with fresh (mega-)spores embedded into Norland Optical Adhesive 61 photopolymer (Techoptics, Tonbridge Kent TN9 1RF England), covered with a cover slip, and cured under UV light (350-380nm) within 30 minutes. Norland Optical Adhesive 61 is a clear, colourless, liquid photopolymer with a very good adhesion and solvent resistance, ideal for light microscopy. Samples were documented by digital photography with a Leica DC200 camera and saved as a TIFF file (Tagged Image File Format) for plate preparation.

Fluorescence microscopy was used for sporangia and spores of *Osmunda regalis* L., carried out on a Leica DMLB 100S reflected fluorescent light microscope.

2.3.1.1 Staining for callose with aniline blue

Fresh *Osmunda regalis* L. immature sporangia and spores were stained for callose with aniline blue 1% (aqueous), purchased from Fisher Scientific, England.

Two different approaches were pursued:

1. Fresh sporangia and spores were directly incubated in 0.1% aniline blue, and the stain rinsed off with distilled water after 30min. Sporangia and spores were mounted on a slide and viewed under a light and a fluorescence microscope.

2. Sporangia and spores were fixed using 1:3 glacial acetic acid : ethanol for 24 hours and stored in 70% ethanol (Baker *et al.* 1994; Dong *et al.* 2005).

The material was cleared in 5N NaOH for 1.5 hours, stained overnight in 0.1% aniline blue in a ready made buffer solution (pH 9) (Micro Essentials, USA) (Martin 1959). Sporangia and spores were mounted on a slide and viewed under a light and a fluorescence microscope.

2.3.2 Scanning electron microscopy (SEM)

Extant material

Gymnosperm pollen was collected from pine tree strobili and transferred onto aluminium stubs. Pteridophyte spores were scraped off with a razor blade from mature sporangia straight onto aluminium stubs. In order to avoid cross contamination, the razor blade was cleaned between each species, hands were washed and ready prepared stubs were put into a stub box. Rachis and pinnae of five pteridophytes were sectioned with a razor blade and mounted onto stubs. Bryophyte spores were extracted from capsules and directly transferred onto aluminium stubs. Carbon adhesive disks were used (Agar Scientific Ltd., Stansted CM24 8DA, England) and the specimens coated with gold/palladium for 1.5 minutes at a voltage of 15mA and later viewed using a Phillips XL30 FEG ESEM (Environmental Scanning Electron Microscope) with an average working distance of 10mm and a voltage of 15Kv – 20Kv. The detector used was a secondary electron (SE) detector and in some cases (*Selaginella myosurus* Sw. Alston) a backscattered electron detector (BSE). Images were obtained digitally with a LEO digital image capture package and saved as TIFF files.

The Phillips XL30 FEG ESEM in environmental “wet” mode was used once (*Osmunda regalis* L.). Fresh material was observed at low vacuum pressure (640 Pascal (6.4mbar) at 5°C and 100% humidity, water vapour as auxiliary gas) to preserve and document any liquid layers covering immature spores. The detector used was a special gaseous secondary electron (GSED) detector, incorporating a pressure limiting aperture. A cooling Peltier stage combined with high water vapour achieved up to 100% humidity, preventing the drying out of hydrated samples.

Fossil material

Specimen HD437 was removed as part of an undergraduate project following bulk maceration of the siltstone using concentrated hydrochloric acid (HCl) and hydrofluoric acid (HF). No heavy metal separation was used. The >250µm fractions were hand sorted and the sporangium mounted onto stubs as described above. A sporangium was removed from the stub, put in fuming nitric acid for 10 minutes, rinsed and then broken open on a stub for further SEM viewing.

Specimen HD 407/1 was obtained by putting a very small piece of rock into water and left to disintegrate. The latter is possible due to the rocks high clay content. The rock fractions were washed through a 250µm mesh. To remove any adhering rock grains, the residue in the mesh was then put into HCl for 24 hours, incubated into water for 24 hours and transferred into HF for 48 hours under gentle stirring. The HF was replaced with fresh HF for another 48 hours, then filled up with water, poured off and rinsed six times with more water. The residue was poured through a 250µm mesh, further rinsed with water, and placed into a petri dish to air dry. Organic matter was hand sorted under a dissecting microscope and specimens mounted onto stubs for SEM viewing as described above.

2.3.3 Transmission electron microscopy (TEM)

Preparation of (mega-)spores

All living material (*Selaginella myosurus* megaspores, *Osmunda regalis* spores) was rinsed with distilled water and directly transferred into 100% acetone and later embedded into Spurr "hard mix" (Glasspool 2003). The spores were incubated for 24 hours in a mixture of acetone/Spurr 50:50, another 24 hours in 100% Spurr "hard mix" and finally placed in block moulds and polymerised at 70°C for 12h. The material remained unstained. Sections (between 50 and 100nm) were taken on a standard ultramicrotome, using a

diamond knife, collected on coated copper grids (200 mesh) and viewed using a JEOL 1210 TEM at 80Kv.

Preparation of fossil material

A sporangium from specimen HD407/1 was removed from the stub, put into fuming nitric acid (HNO₃) for 14 minutes, rinsed in water and remounted on a stub for further SEM viewing. This was followed by the removal of the sporangium for TEM embedding. A piece of the sporangium was broken off and embedded into an agar block, made from 1% molten agar solution and stained with safranin. Pre-embedding in slightly coloured agar is common in order to improve handling (pers. comm. Lindsey Axe 2005). The specimen was dehydrated over an acetone water series (50:50; 75:25; 90:10; 100) of 30 minutes each and then transferred into Spurr "hard mix" as described above.

2.3.4 Energy dispersive x-ray analysis (EDX)

In order to analyse the elemental composition of spore walls and pteridophyte rachises and pinnae, qualitative EDX was applied to SEM scanned material and, in very few cases, to TEM samples. Qualitative SEM EDX analysis was carried out with a Cambridge Instruments S360 SEM, fitted with an Oxford Instruments analytical LINK system and software package. Stubs with specimen for EDX analysis were carbon coated (e.g. Watt 1997). Accelerating voltage was 20kV. For TEM EDX a JEOL JEM1210 was used, fitted with an Oxford Instruments LINK system and LINK ISIS software package. Accelerating voltage was 80kV.

All spores and fronds analysed by the means of SEM in combination with EDX were carbon coated in order to obtain reliable data on the composition of elements in the spore walls. High resolution pictures of the spores and their sculpture were taken from carbon/palladium coated specimens. Due to the electron beam penetrating through the perispore, it is assumed that, depending on the perispore thickness, chemical information was also picked up from the underlying exospore. Hence I use the general term "spore walls"

throughout *chapter 3* but further discuss the effects of varying perispore thickness on EDX analyses in *section 3.3*.

2.4 Silica in pteridophyte spores, rachises and pinnae / pinnules

24 species of 9 families of pteridophytes were documented with a LM and a SEM in combination with EDX. Of the 24 species mentioned above, in 5 species their rachis and pinnae / pinnules were tested for silica by SEM in combination with EDX. The fronds studied were fertile. For sample preparation and a description of the microscope techniques applied to this study, the reader is referred to *section 2.3* herein.

Family	Species name	LM	SEM (EDX)	Leaf analysis
Blechnaceae	<i>Doodia aspera</i>	✓	✓	
	<i>Blechnum occidentale</i>	✓	✓	
Davalliaceae	<i>Nephrolepis hirsutula</i>	✓	✓	
	<i>Davallia mariesii</i>	✓	✓	
Dryopteridaceae	<i>Cyrtomium falcatum</i>	✓	✓	
	<i>Cyrtomium fortunei</i>	✓	✓	
	<i>Diplazium poliferum</i>	✓	✓	
	<i>Dryopteris eritrosrosa</i>	✓	✓	
	<i>Dryopteris stewardii</i>	✓	✓	
	<i>Hypodematium fauriei</i>	✓	✓	
	<i>Lastreopsis microsora</i>	✓	✓	
	<i>Rumohra adiantiformis</i>	✓	✓	
Osmundaceae	<i>Osmunda regalis*</i>	✓	✓	✓
Polypodiaceae	<i>Phlebodium aureum</i>	✓	✓	✓
Psilotaceae	<i>Psilotum nudum</i>	✓	✓	
Pteridaceae	<i>Pellaea calomelanos</i>	✓	✓	
	<i>Pellaea rotundifolia</i>	✓	✓	✓
	<i>Pteris cretica</i>	✓	✓	
	<i>Pteris longifolia</i>	✓	✓	
Schizaeaceae	<i>Anemia tomentosa</i>	✓	✓	✓
Selaginellaceae	<i>Selaginella pallescens</i>		✓	
	<i>Selaginella myosurus*</i>		✓	
Thelypteridaceae	<i>Oreopteris limbosperma</i>	✓	✓	
	<i>Phegopteris decursive-pinnata</i>	✓	✓	✓
	<i>Thelypteris japonica</i>	✓	✓	
	<i>Macrothelypteris torresiana</i>	✓	✓	

Table 2.2: List of species studied for the presence of silica in spores, rachises and pinnae / pinnules. For the species marked with an asterisk, the spore wall was also investigated by the means of TEM.

2.5 Chemical treatments

2.5.1 Treatment with 1% KMnO₄ solution

Spores of *Pellaea calomelanos*, *P. rotundifolia*, *Lycopodium clavatum* and *Blechnum gibbum* were transferred from distilled water into 1% potassium permanganate solution (KMnO₄) for 48 hours (potassium permanganate purchased at Fisher Scientific, UK), rinsed with distilled water and mounted onto SEM stubs for the documentation of any changes in perispore sculpture.

2.5.2 Treatment with MMNO

Selaginella pallescens megaspores, *Lycopodium clavatum* spores and pollen of *Pinus sylvestris* were incubated in hot (90°C) 4-Methylmorpholine *N*-oxide monohydrate MMNO (purchased at Fisher Scientific, UK) for 30 minutes. The effect of MMNO on the sculpture was documented by SEM. In order to document any products deriving from this treatment ¹H NMR spectra were obtained for all three species investigated. The product was extracted with diethyl ether (Et₂O).

2.5.3 Soxhlet extractions with DCM

Chemical extraction experiments have shown that two solvents have significant effects on spore and pollen walls. 2-Aminoethanol (Southworth 1974; Kress 1986) and MMNO (Loewus *et al.* 1985; Rowley *et al.* 2001) have been shown to successfully dissolve outer spore and pollen layers. Wiermann (2001) reviewed various methodologies, including chemical extractions and mass spectrometry techniques in sporopollenin research.

Mega- and microspores of *Selaginella pallescens*, their leaves as well as *Lycopodium clavatum* isospores were extracted with 100ml dichloromethane (DCM). In order to avoid contamination, thimble, anti-bumping granules and glass wool were pre-extracted for 4 hours. Each spore extraction sequence in DCM was 12 hours. The solvent were evaporated off with a vacuum/pressure evaporator, and extracts were prepared for ¹H and ¹³C NMR and submitted for

analysis. All NMR data were recorded at room temperature in deuterated chloroform (CDCl₃, *d*-Chloroform) with tetramethylsilane (TMS) as internal standard (0ppm). For the ¹³C NMR spectrum of *S. pallescens* leaves the scan rate was increased from 256 to 5000 scans per spectrum to improve its resolution. All other ¹³C NMR spectra were scanned at the conventional rate of 256 scans. A summary is given below in table 2.3.

Sample	Weight	Solvent	Analysis
<i>Selaginella pallescens</i> megaspores	0.006g	DCM	¹ H NMR
<i>S. pallescens</i> microspores	0.024g	DCM	¹ H NMR
<i>S. pallescens</i> leaves	0.5g	DCM	¹ H NMR, ¹³ C NMR
<i>Lycopodium clavatum</i> isospores	1g	DCM	¹ H NMR, ¹³ C NMR

Table 2.3: Summary of spore wall extractions of various species, listing starting material quantities, the solvent used and analytical techniques applied.

2.6 Analytical Chemistry

In order to find out more about the chemical composition of spore wall layers and of sporopollenin in particular, it was necessary to venture into the field of analytical chemistry. Three techniques were applied to palynology in this study, which are NMR, GC-MS and MALDI-ToF MS. Previously, NMR has been successfully applied to palynology by Hemsley *et al.* (1992, 1993, 1994, 1996) and Ahlers *et al.* (1999a and b, 2000, 2003). GC-MS was utilised by Kawase and Takahashi (1996) for the study of pollen extracts and by van Bergen *et al.* (1995, 2004) for fossil material. MALDI-ToF MS has not yet been used in palynology but is a valuable tool for the detection and characterization of bio-macromolecules present in mixtures such as peptides, proteins or synthetic polymers (Kaufmann 1995; Gross and Strupat 1998).

Whereas nuclear magnetic resonance (NMR) spectrometry is based on the nuclei spin of atoms, the two other techniques, GC-MS (gas chromatography mass spectrometry) and MALDI-ToF MS (matrix assisted laser desorption/ionization – time-of-flight mass spectrometry) are analytical

techniques, which separate a mixture by ionization and dissociation into fragments according to their specific mass. All techniques help to elucidate the chemical nature of a sample.

For the reader who might not be familiar with the techniques mentioned above, a brief overview is given but he or she is also referred to publications like Skoog *et al.* (2004), Higson (2003) or to Kealey and Haines (2002) on analytical chemistry and their applications.

2.6.1 NMR and GC-MS

NMR This analytical technique is based on the nuclei spin of atoms and their electrical charge. As soon as a strong external magnetic field is applied, an energy transfer takes place in the atoms between their base energy and a higher energy level. This energy transfer is translated into the wavelength that corresponds to radio frequencies and when the spin returns to its base level, energy is emitted at the same frequency. The signal that matches this transfer is measured and processed and an NMR spectrum is generated giving more information on identity and molecular structure of the sample analyzed.

GC-MS Mass spectrometers nowadays are operated under high vacuum and consist of a sample inlet, ion source, mass analyzer, a detector and a data processing system (figure 2.1). Inside the gas chromatograph oven temperatures up to 400°C immediately vaporise the sample into a gas phase, providing it is stable. It is then transported onto the column by the carrier gas (usually helium), separated in the column and then transported into the capillary column interface, the link between the gas chromatograph and the mass spectrometer. In the ionization chamber the sample is ionised and then brought into the mass analyzer, where positively and negatively charged ions are separated according to their mass. They then enter a detector where they are amplified to enhance the signal. The multiplier then sends the data to a computer, where the data are recorded and transformed into a spectrum. The computer also runs the mass spectrometer.

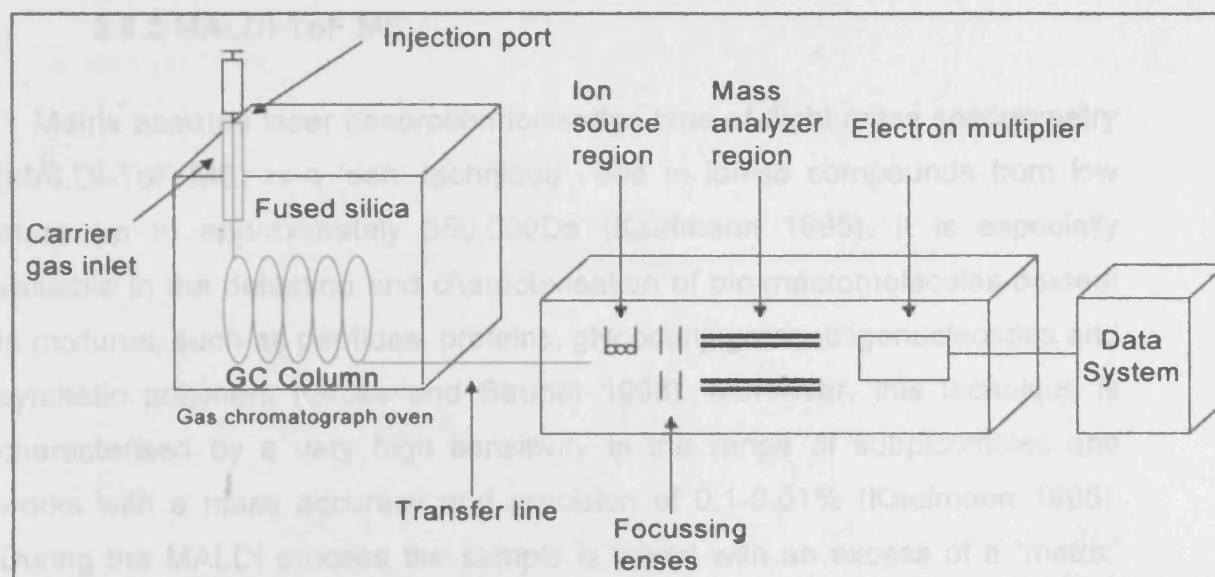


Figure 2.1: Scheme of a GC-MS redrawn from Skoog *et al.* (2004), p. 957, figure 31-12.

Protocols 1g of pollen of *Pinus sylvestris* L. was washed in acetone, incubated in hot (80°C) MMNO for 30 minutes, and cooled to room temperature. Distilled water was added, and the solution was extracted with Et₂O (10ml) and 0.1µl of the product injected into an GC-MS Saturn II, Varian 3400 gas chromatograph. The analysis followed the specifications of Kawase and Takahashi (1996) and was performed on a DB5-MS capillary column (30 m × 0.25 mm, 0.5 µm), 5%-phenyl-methylpolysiloxane, non-polar, (JW Scientific, Folsom, CA). From the same experiment a ¹H NMR spectrum was obtained, performed on a Bruker DPX 400 MHz NMR Spectrometer. All ¹H NMR presented in this chapter were recorded at room temperature CDCl₃ (*d*-Chloroform) with tetramethylsilane as internal standard (0ppm). Parallel to this experiment with pollen grains, a blank using exactly the same chemicals and glassware was carried out without pollen present. The solution obtained from this control experiment was subjected to ¹H NMR.

In a further experiment a new set of spore powder was prepared (see purification process as described above) with 0.025 g *Selaginella pallescens* megaspores, the powder was then acetylated in a solution of 3:1 acetic anhydride:acetyl chloride for 8 hours at 70-80°C. The product was neutralised with sodium bicarbonate (NaHCO₃), extracted with Et₂O, concentrated, and both a GC-MS and an ¹H NMR spectrum were obtained.

2.6.2 MALDI-ToF MS

Matrix assisted laser desorption ionisation time-of-flight mass spectrometry (MALDI-ToF MS) is a 'soft' technique used to ionise compounds from low mass up to approximately 350,000Da (Kaufmann 1995). It is especially valuable in the detection and characterisation of bio-macromolecules present in mixtures, such as peptides, proteins, glycoconjugates, oligonucleotides and synthetic polymers (Gross and Strupat 1998). Moreover, this technique is characterised by a very high sensitivity in the range of subpicomoles and works with a mass accuracy and precision of 0.1-0.01% (Kaufmann 1995). During the MALDI process the sample is mixed with an excess of a "matrix" compound on a plate. A laser is then fired at the mixture and the energy from the laser is passed from the matrix to the analyte (figure 2.2). This process causes ions of the analyte to be produced in the gas phase which are accelerated through a Time of Flight (ToF) tube in which they travel at a speed related to their mass and are detected by a mass analyser to generate the mass spectrum. MALDI-ToF was used in the present study primarily as it allows the detection of compounds of high and low mass with improved sensitivity over previous methods of mass spectrometric analysis. Part of this work has investigated the use of MALDI-ToF MS as a method for the elucidation of the structure of sporopollenin and discusses its possible applications in palynology.

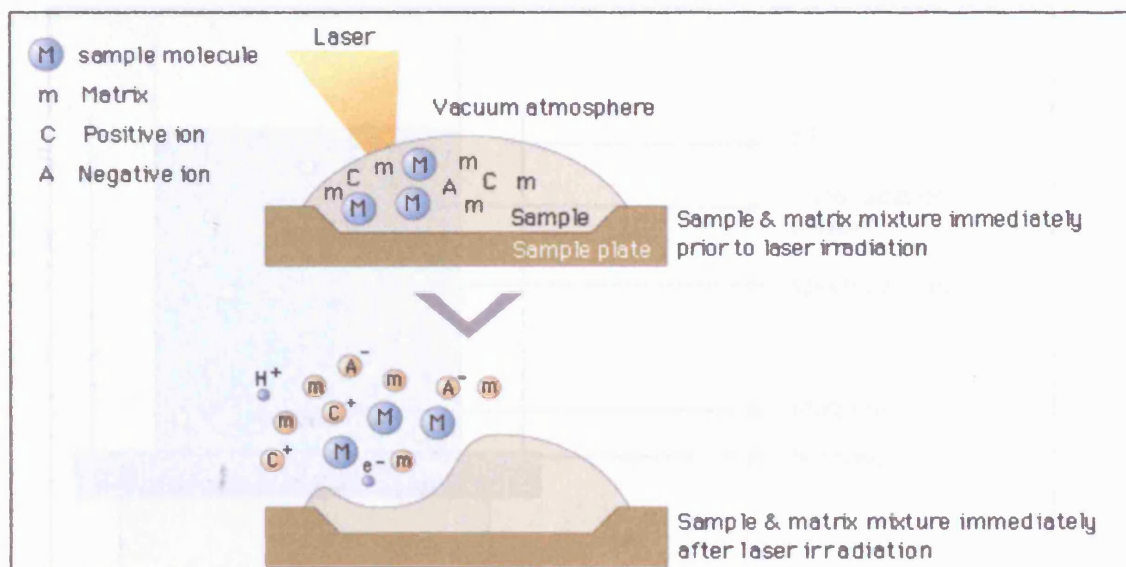


Figure 2.2: The principle of MALDI-TOF MS. The copyright for this figure is with Shimadzu Corporation, Japan, 2003 (company webpage).

Protocols

Purification of sporopollenin 0.025g *Selaginella pallescens* megaspores and 0.1g *Lycopodium clavatum* isospores were collected at the Talybont Research Gardens, Cardiff. The spore samples were washed five times with distilled water and acetone, followed by a 6 hour treatment of a) 80-90°C 5M NaOH b) 80-90°C 3M HCl c) 80-90°C 2-aminoethanol treatment under constant gentle stirring (all chemicals purchased from Fisher Scientific, UK) (figure 2.3). The spore powder obtained from this treatment was subjected to MALDI-ToF MS.

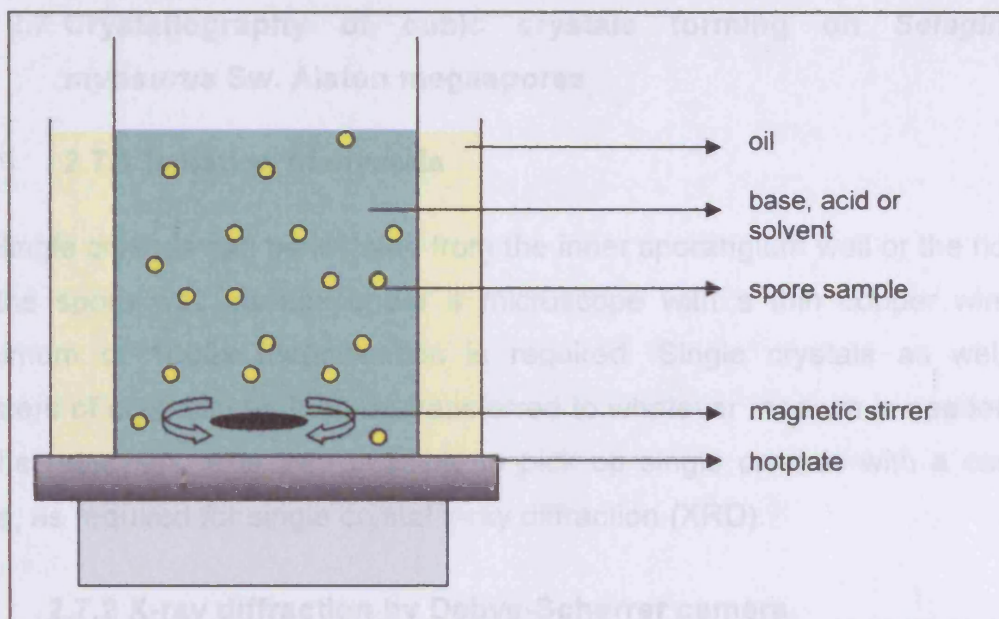


Figure 2.3: Apparatus used for purifying sporopollenin in preparation for MALDI-ToF MS, as described in the text above.

MALDI-ToF MS all chemicals used were purchased from Sigma Aldrich (Dorset, UK). Purified water was produced in-house using an Elix water purification system (Millipore, UK). A proportion of the sporopollenin samples was dissolved in $5\mu\text{l}$ of a 10mg/ml solution of 3-indoleacrylic acid in 50/50 acetonitrile/ water. This was vortex mixed and a $1\mu\text{l}$ aliquot was taken and allowed to dry on the MALDI plate. The plate was introduced into a Voyager DE-STR MALDI mass spectrometer and spectra were obtained in both positive and negative ionisation mode using linear mode analysis, an acceleration voltage of 25000V , an extraction delay time of 750ns , 50 laser shots per spectrum and a mass range of $50 - 100,000\text{Da}$.

Figure 2.4: Schematic sketch of a Debye-Scherrer powder camera. The wall of the cylindrical camera is lined with a film. The sample is placed into the centre of the camera and rotated in an x-ray beam for several hours. The x-rays enter the camera through a collimator, the beam then confines undiffracted beams.

2.7 Crystallography of cubic crystals forming on *Selaginella myosurus* Sw. Alston megaspores

2.7.1 Isolation of crystals

Single crystals can be isolated from the inner sporangium wall or the ridges of the spore wall surface under a microscope with a thin copper wire. A minimum of 1000x magnification is required. Single crystals as well as clusters of crystals can then be transferred to whatever medium is needed for further analyses. It is also possible to pick up single crystals with a carbon fibre, as required for single crystal x-ray diffraction (XRD).

2.7.2 X-ray diffraction by Debye-Scherrer camera

A complete *Selaginella myosurus* Sw. Alston megaspore was mounted and exposed to $\text{CoK}\alpha$ radiation for 17 hours, with rotation in a Debye-Scherrer Camera (figure 2.4). A Philips Automated Powder Diffractometer, model PW1840, was used. The diffractometer was set to 38KV and 28mA. Outlet collimator coordinate was: 90.2mm, inlet collimator coordinate: 270.5mm, difference (d): 180.3mm.

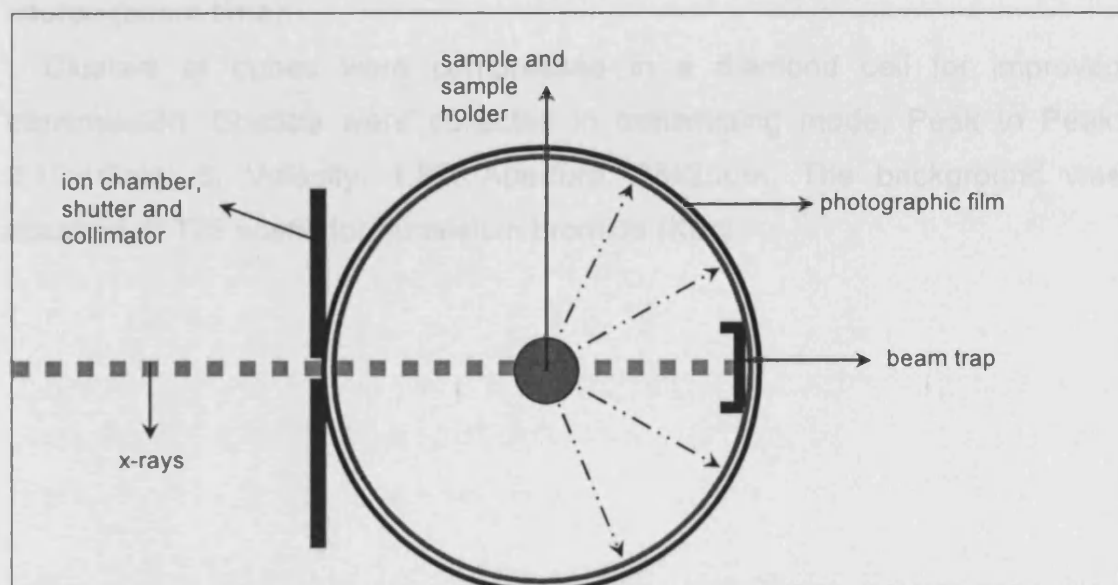


Figure 2.4: Schematic sketch of a Debye Scherrer powder camera. The wall of the cylindrical camera is lined with a film. The sample is placed into the centre of the camera and rotated in an x-ray beam for several hours. The x-rays enter the camera through a collimator; the beam trap confines undiffracted beams.

2.7.3 Synchrotron beam high flux XRD

Synchrotron high flux XRD was carried out on Station 9.8, CCLRC Daresbury Laboratories, Daresbury, UK (Cernik *et al.* 2000) using a standard Bruker-Nonius APEXII diffractometer with side mounted D8 goniometer. The diffractometer hardware was controlled using BIS version 1.2.0.10 and data collection controlled by APEXII version 1.0.27beta. A suitable single crystal was coated in inert perfluoropolyether oil (Fomblin YR-1800) and mounted on a single carbon fibre filament of ca. 8 micron diameter. The single crystal was held in a nitrogen stream at 150K using a 700+ Oxford Cryosystems Cryostream.

2.7.4 IR (Infrared) microspectrometry

IR was carried out using a desktop microspectrometer at CCLRC Daresbury Laboratories, Daresbury, Warrington, Cheshire, WA4 4AD, UK, Synchrotron Station 11.1 (Telephone: +44(0)1925 603000). This work was carried out in order to gain preliminary results, which would support a grant application for IR microspectrometry combined with synchrotron radiation source (beam time).

Clusters of cubes were compressed in a diamond cell for improved transmission. Spectra were collected in transmitting mode; Peak to Peak: 8.10; Gain: 8; Velocity: 1.89; Aperture: 25x25 μ m. The background was scanned at 128 scans for potassium bromide (KBr).

2.7.5 IR microspectrometry with synchrotron radiation source (SRS)

IR with SRS was carried out using an IR microspectrometer at CCLRC Daresbury Laboratories, Synchrotron Station 11.1. Three days of synchrotron radiation source (beam time) were granted (Grant Number 44304). Infrared spectra were recorded using a Nicolet Nexus FT IR spectrometer coupled to a Nicolet Continuum IR microscope fitted with 32x objective, mapping stage, and 50 micron high D* detector. The detector requires cooling with liquid nitrogen to -70°C or below. The system uses a KBr beam-splitter with a spectral range of 750 cm^{-1} to 4000 cm^{-1} . Infrared spectra were manipulated with OmnicTM software. The spectra are presented in absorbance units as a function of the wavenumber (cm^{-1}) in the 750 cm^{-1} to 4000 cm^{-1} range. Molecular vibrations fall into the two main categories “stretching” (often seen as sharp peaks) and “bending” (seen as broader absorption bands).

Single crystals were placed with a thin copper wire onto a diamond cell for improved transmission. Not all spectra obtained were interpretable because they were either too noisy or background calculation errors were present. Single cubic crystals were later crushed between two diamond cells for further analysis.

1. Single crystals: infrared spectrum was collected in transmitting mode; Peak to Peak: 4; Gain: 1 X; Velocity: 1.89; Aperture $10\times 10\mu\text{m}$; 128 scans at a resolution of 8. The background was scanned at 128 scans. Synchrotron beam: Current 207.5mA, Lifetime 22.1 hours.

2. Single crystals: infrared spectrum was collected in transmitting mode; Peak to Peak: 7; Gain: 4; Velocity: 1.89; Aperture $8\times 8\mu\text{m}$; 1024 scans at a resolution of 2. Synchrotron beam: Current 239.6mA, Lifetime 23.6 hours.

3. Crushed crystals: infrared spectrum was collected in transmitting mode; Peak to Peak: 17; Gain: 4; Velocity: 1.89; Aperture $10\times 10\mu\text{m}$; 256 scans at a

resolution of 8, step size of 10 μ m. Background after 15 minutes. Synchrotron beam: Current 192.2mA, Lifetime 25.3 hours.

2.8 Self-assembly experiments

Recently, self-assembly experiments gave rise to ultra-porous hollow particles as seen in *chapter 5* (Griffiths *et al.* 2004). The spore mimic in *chapter 5* was produced from 60ml polystyrene, 670ml distilled water, 20ml cyclohexane, 2g carboxymethylcellulose, 1.25ml sodium chloride (10% solution) and 7ml ammonium persulphate (10% solution) - based on previous work carried out by Hemsley *et al.* (2000) and Hemsley and Griffiths (2000). Distilled water, cyclohexane, carboxymethylcellulose and sodium chloride were heated up to 75°C, after half an hour styrene was added. Another half an hour later the initiator ammonium sulphate was added. The experiment was running for 12 hours in a nitrogen environment and was successfully repeated, confirming its replicability.

3 Mineral content in bryophyte and pteridophyte spore walls

3.1 Silica in *Selaginella* megaspore walls

Previous work in collaboration with the Nees-Institut für Biodiversität der Pflanzen (University of Bonn) and the School of Earth, Ocean and Planetary Sciences (Cardiff University) investigated the correlation between morphology and ultrastructure in *Selaginella* megaspore walls (Moore *et al.* in press a), appendix number 1. One of the main findings of this investigation was a variability of micro-morphology of *Selaginella* outer exospore coatings, as well as an abundance of silica in almost all spore wall layers investigated. The latter led to the question of whether silica is a common feature in pteridophyte spore walls in general or is restricted to lycopsids. Answers to these questions are presented in the following chapters. In order to avoid repetition, only the key discussion points of any published article are incorporated into the chapters. All results and discussion are given in appendix 1.

3.2 An unknown siliceous bio-mineral forming on *Selaginella myosurus* Sw. Alston megaspores

The aim of this study was to analyse and characterise chemically as well as crystallographically cubic crystals that naturally form on the surface of the megaspore of *Selaginella myosurus* Sw. Alston. The following table 3.1 provides a summary of various methodologies carried out and a brief synopsis of the results obtained.

Methodology	Carried out at	Results
SEM combined with EDX	Cardiff Earth Sciences	comprehensive documentation of spore wall and cubic crystal morphology EDX showed composition dominated by Si, O, C (possibly with H, which cannot be analysed by this method)
TEM combined with EDX	Cardiff Bioscience	documentation of spore wall and cubic crystal ultrastructure. EDX showed presence of Si, O, C
Debye Scherrer x-ray diffraction	Cardiff Earth Sciences	ring pattern with sharp rings from crystalline material superimposed on a broad diffuse background from the non-crystalline spore matrix
High Flux XRD	Daresbury Laboratories Station 9.8	diffraction pattern from whole megaspore showing more details of rings against background, and from single cubes showing few, very weak scattered peaks
FT-IR (without and with Synchrotron Radiation Source, SRS)	Daresbury Laboratories Station 11.1	confirmation of Si-O bond in cubes and matrix, and showing loss of components of cubes when crushed

Table 3.1: A synopsis of methods carried out to investigate the unknown bio-mineral, and a brief summary of the results.

3.2.1 Results

3.2.1.1 SEM documentation combined with energy dispersive x-ray analysis (EDX)

The megaspores are coarsely reticulated with prominent ridges (40-95µm in height) and large muri of different shapes (round to elongated, ellipsoidal) (figure 3.1A to F). A large number of cubic crystals appear in the muri between the ridges (figure 3.1A to F). Their size is very variable ranging from 2-7µm (figure 3.1F and G). Some scattered crystals, usually 10µm or larger, can be found on the ridges (figure 3.1C, D and H). A few crystals show interpenetration growth (figure 3.1G and H). A higher magnification of the crystals reveals their Hopper-like habit and in this particular image a dotted surface pattern can be observed on the crystals (figure 3.1G). Halite (rock salt), for example, a crystal wholly formed by ionic bonding, often shows Hopper faces, due to the more rapid deposition of material at the edges than at the centres of the faces (Battey and Pring 1997). Some microspores are attached to the megaspore surface, which can be seen in figure 3.1C and E.

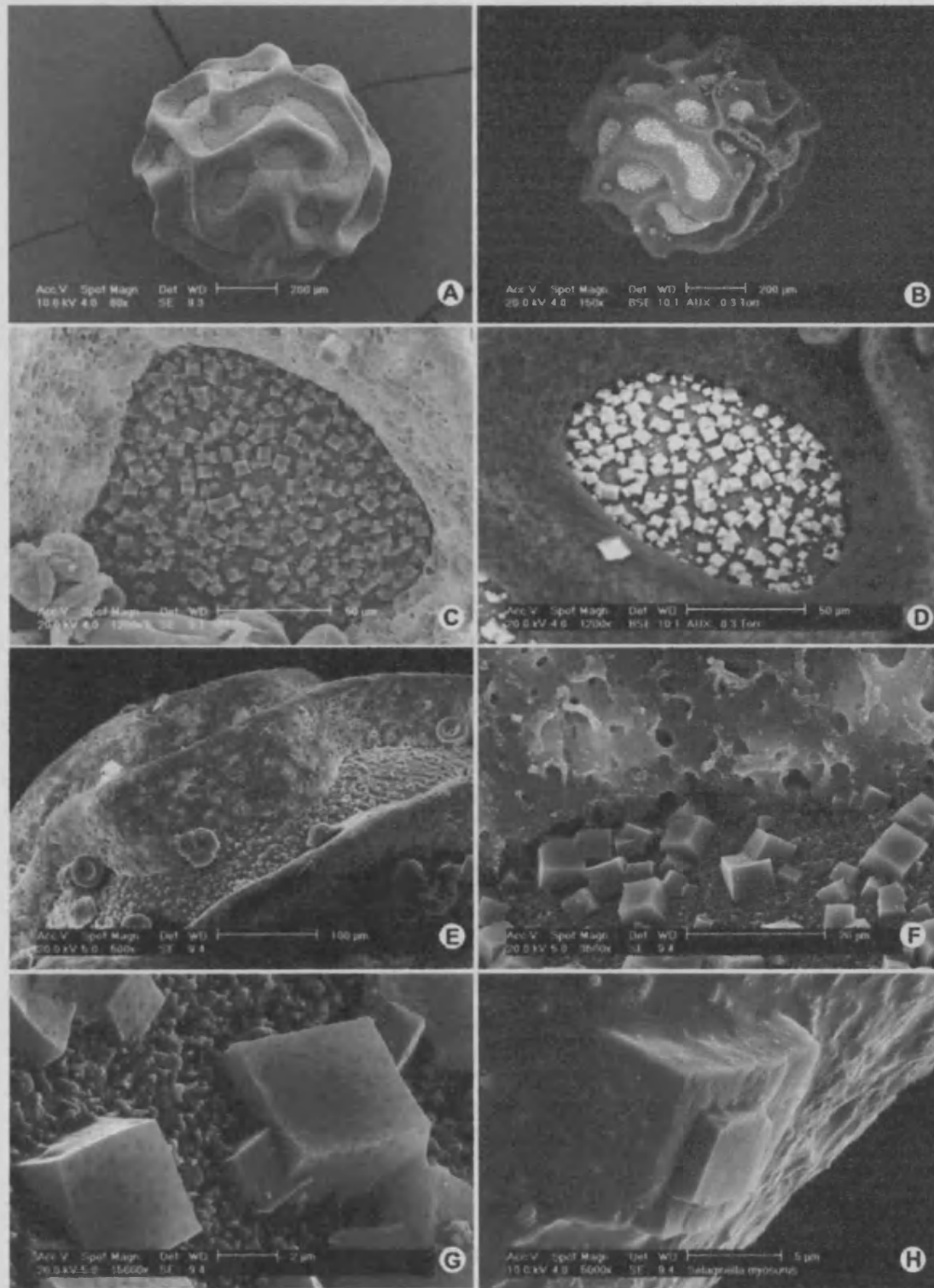


Figure 3.1: **A** *Selaginella myosurus* megaspore as seen by the means of SEM in secondary emission and **B** backscattered electron mode. Cubic crystals accumulate in the muri between ridges, some can also be found on the tips of the ridges as seen in **C** and **D** (**C** secondary emission and **D** backscattered electron mode). **E** Detail of crystals beneath a ridge, note microspores attached, some still in tetrads. **F** to **H** show crystals in higher magnification. The crystal in **H** was found on a ridge. **G** and **H**: note Hopper-like crystal habit and some interpenetration or interference growth.

Closer studies of the inner wall of the sporangium uncovered the occurrence of further cubic crystals. Again, the crystals vary in size ranging from only 1-2 μm to up to 10 μm . They are scattered over the smooth inner surface and were observed next to globules and other aggregates (figure 3.2A) or in isolated clusters (figure 3.2B and C). High magnification of one of the larger crystals revealed surface ornamentation (figure 3.2D).

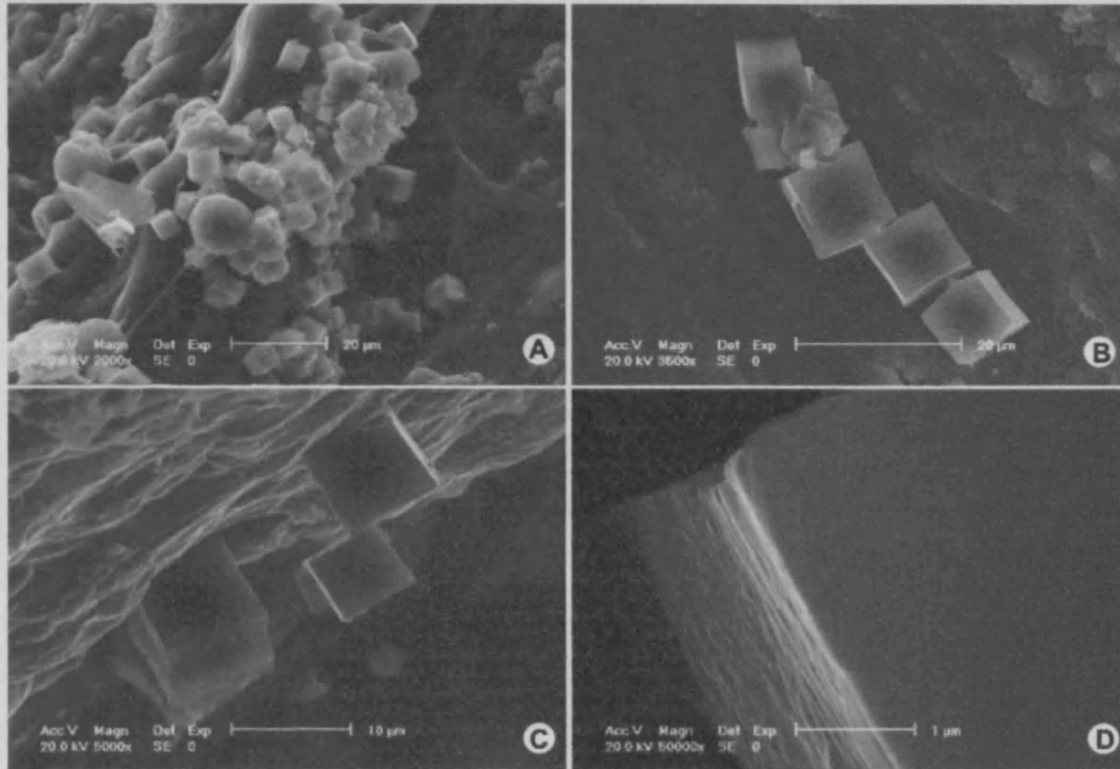


Figure 3.2: A to C crystal growth on the inner wall of the sporangium of *Selaginella myosurus*. The crystals vary in size and accumulate next to spore wall aggregates and globules as seen in A. B and C the largest crystals found on the inner sporangium wall measure up to 10 μm and are bigger than the ones found between the muri on the spores. D is taken at high magnification and clearly shows a surface ornamentation.

Thin-sectioning the entire spore revealed that the crystals do not only occur in the muri but also run underneath the ridges (figure 3.3A and B). The larger white crystals surrounding the spherical gap where the lumen was once situated are contamination particles derived from the polishing process. This was established by analysing both the particles on the section as well as the polishing powder (not shown). An EDX mapping pattern of the thin section of a single crystal (figure 3.3C) showed the presence of three

as well as many elements K and Ca. O to H show the different species. Green: silicon D, Yellow: oxygen E, Red: calcium P, Purple: potassium S, Blue: chlorine H

main elements: silicon, oxygen and carbon (figure 3.3D, E and F) as well as two minor elements potassium and chlorine (figure 3.3G and H).

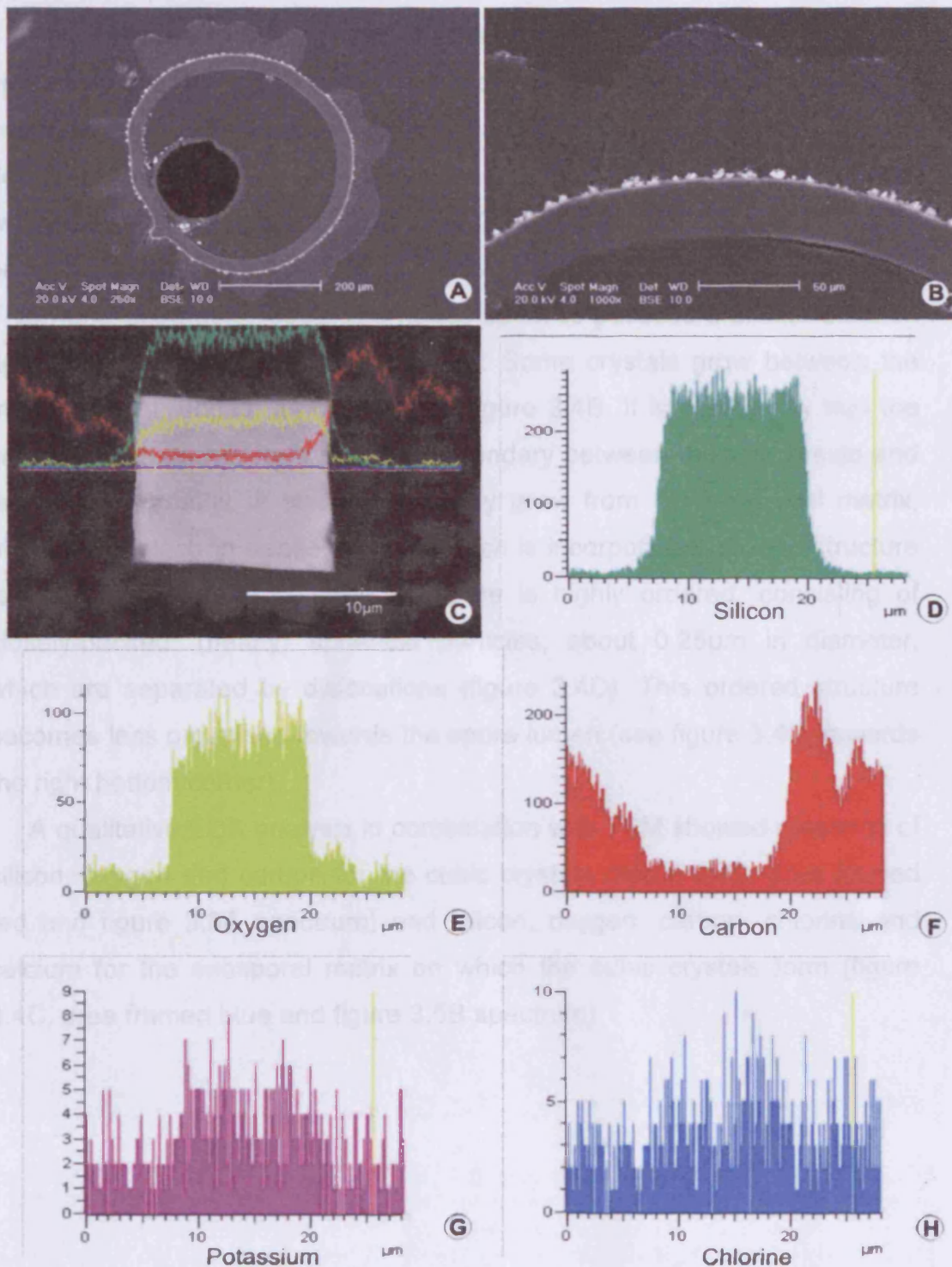


Figure 3.3: A thin section of the complete megaspore of *Selaginella myosurus* and B a detailed view of the section at higher magnification. Note that crystals (in white) run underneath the ridges. C the EDX mapping pattern of a single crystal is showing Si, C, O as well as matrix elements K and Cl. D to H show the different spectra. Green: silicon D; Yellow: oxygen E; Red: carbon F; Purple: potassium G; Blue: chlorine H.

3.2.1.2 TEM documentation combined with energy dispersive x-ray analysis (EDX)

TEM documentation of the crystals as well as the spectrum of the EDX analysis is shown in figure 3.4. The pictures document the occurrence of crystals beneath the ridges (figure 3.4A and B) as well as the electron dense exosporal matrix underneath the crystals (figure 3.4C and D), from which EDX analyses were taken (figure 3.4A and B). The ridges can clearly be seen in figure 3.4A and B, appearing labyrinthine (terminology *sensu* Tryon and Lugardon 1990). The ridges seem to possess a similar electron density to that of the underlying matrix. Some crystals grow between the matrix and the ridges, as observed in figure 3.4B. It is noteworthy that the cubic crystals do not form a distinct boundary between their underside and the adjacent matrix. It seems as if they grow from the exosporal matrix, utilizing the electron dense material which is incorporated into the structure (see figure 3.4B and C). The exospore is highly ordered, consisting of closely-packed, (nearly) spherical particles, about 0.25 μ m in diameter, which are separated by dislocations (figure 3.4D). This ordered structure becomes less organised towards the spore lumen (see figure 3.4D, towards the right bottom corner).

A qualitative EDX analysis in combination with TEM showed presence of silicon, oxygen and carbon for the cubic crystals (figure 3.4C, area framed red and figure 3.5A spectrum) and silicon, oxygen, carbon, chlorine and calcium for the exosporal matrix on which the cubic crystals form (figure 3.4C, area framed blue and figure 3.5B spectrum).

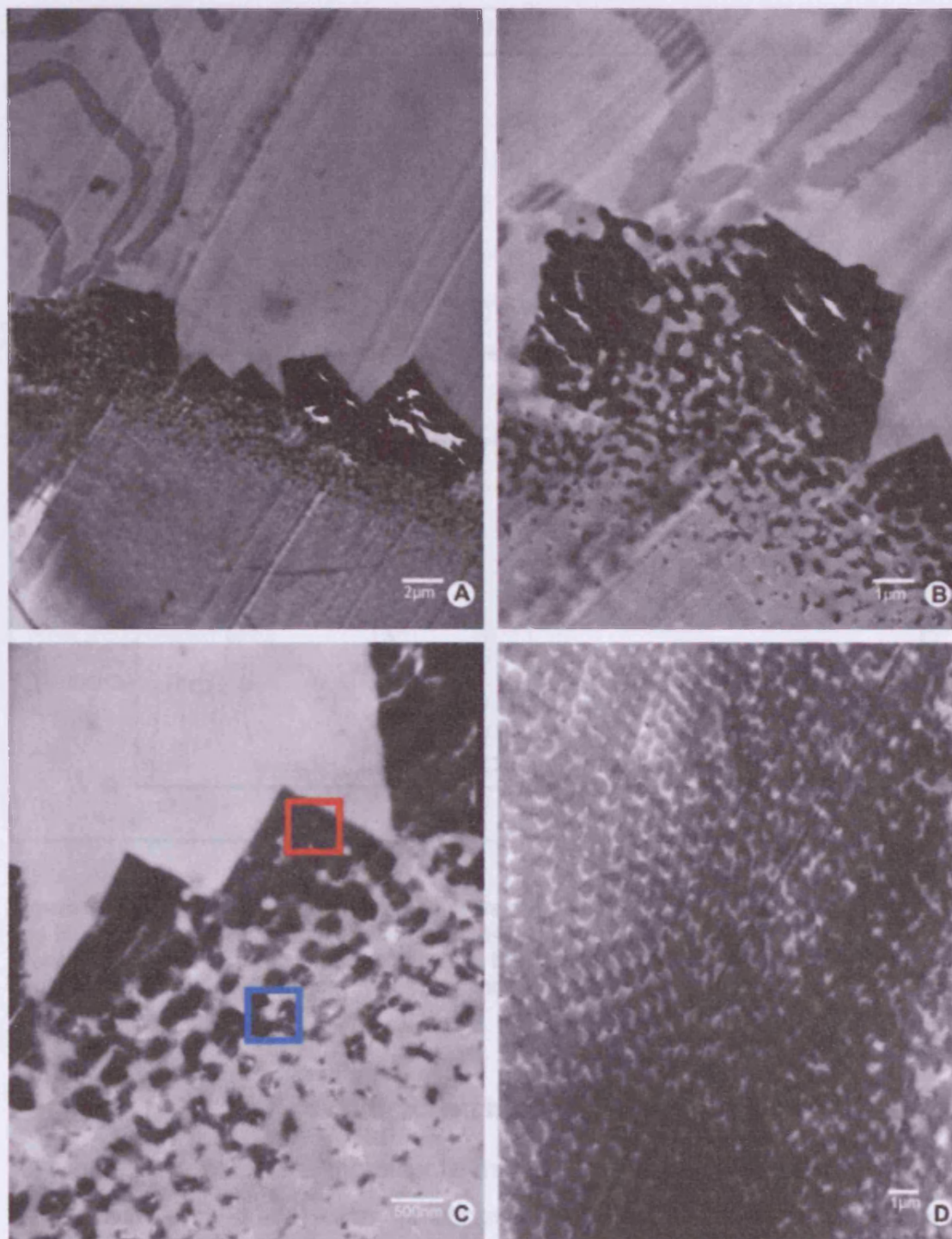


Figure 3.4: A to D TEM sections through crystals and spore matrix (exospore) of *Selaginella myosurus*. A gives an overview showing six crystals, of which the first is beneath the ridge, the second just on the edge between ridge and muri and the other four crystals are on the spore matrix. A detailed view is given in B, where distortions in the crystals can be seen. Note electron dense material incorporated into the exospore. C EDX- analyses were taken from the areas marked red (crystal) and blue (exospore matrix). Exospore of *S. myosurus* consisting of uniform particles with colloidal-crystal like organization.

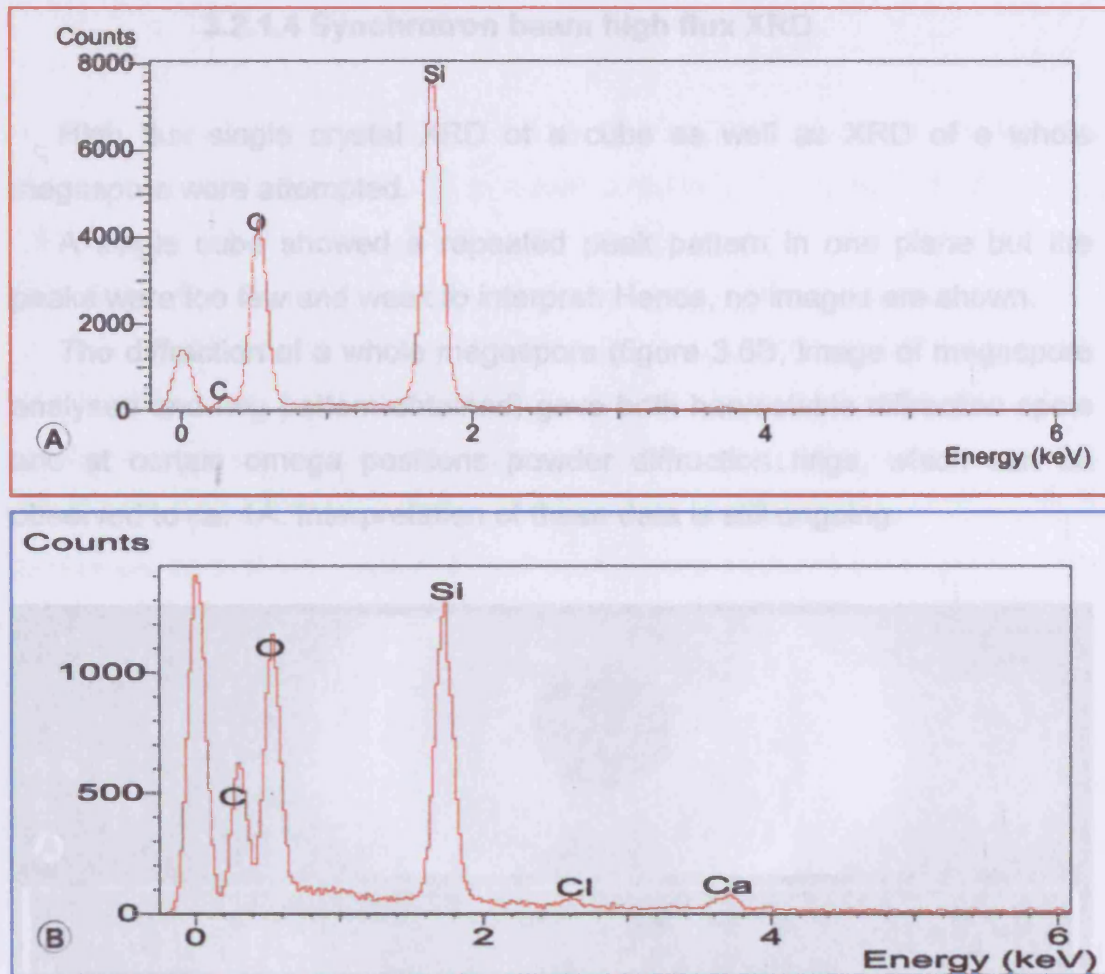


Figure 3.5: EDX analysis of the two areas of *Selaginella myosurus* highlighted red (crystal) and blue (sporopolleninous matrix) in figure 3.4C. **A** the analysis of the crystal revealed the presence of silicon, carbon and oxygen. **B** the same elements were detected in the exosporal matrix, where additionally calcium and chlorine were found.

3.2.1.3 X-ray diffraction by Debye-Scherrer camera

Mounting a complete megaspore into the camera showed a diffraction pattern with a low-d flank of an indistinguishable band which was overlain by an evenly spaced triplet of diffraction lines (figure 3.6A). The black ring in the centre of the ring pattern is the area where the beam entered the camera. The squares of their calculated d -spacings (3.83Å, 3.71Å, 3.58Å) are in ratio 12.1:13.0:13.9. Parsimonious indexing as cubic {222}, {320}, {321} gives lattice repeat $a=13.34\pm 0.06\text{Å}$ ($1.334\pm 0.006\text{nm}$).

Figure 3.6: A Scan of diffraction lines obtained by exposing a complete *Selaginella myosurus* megaspore to a Debye-Scherrer camera and XRD of a whole megaspore (small image top left) and ring pattern obtained.

3.2.1.4 Synchrotron beam high flux XRD

High flux single crystal XRD of a cube as well as XRD of a whole megaspore were attempted.

A single cube showed a repeated peak pattern in one plane but the peaks were too few and weak to interpret. Hence, no images are shown.

The diffraction of a whole megaspore (figure 3.6B, image of megaspore analysed and ring pattern obtained) gave both harvestable diffraction spots and at certain omega positions powder diffraction rings, which can be observed to ca. 1\AA . Interpretation of these data is still ongoing.

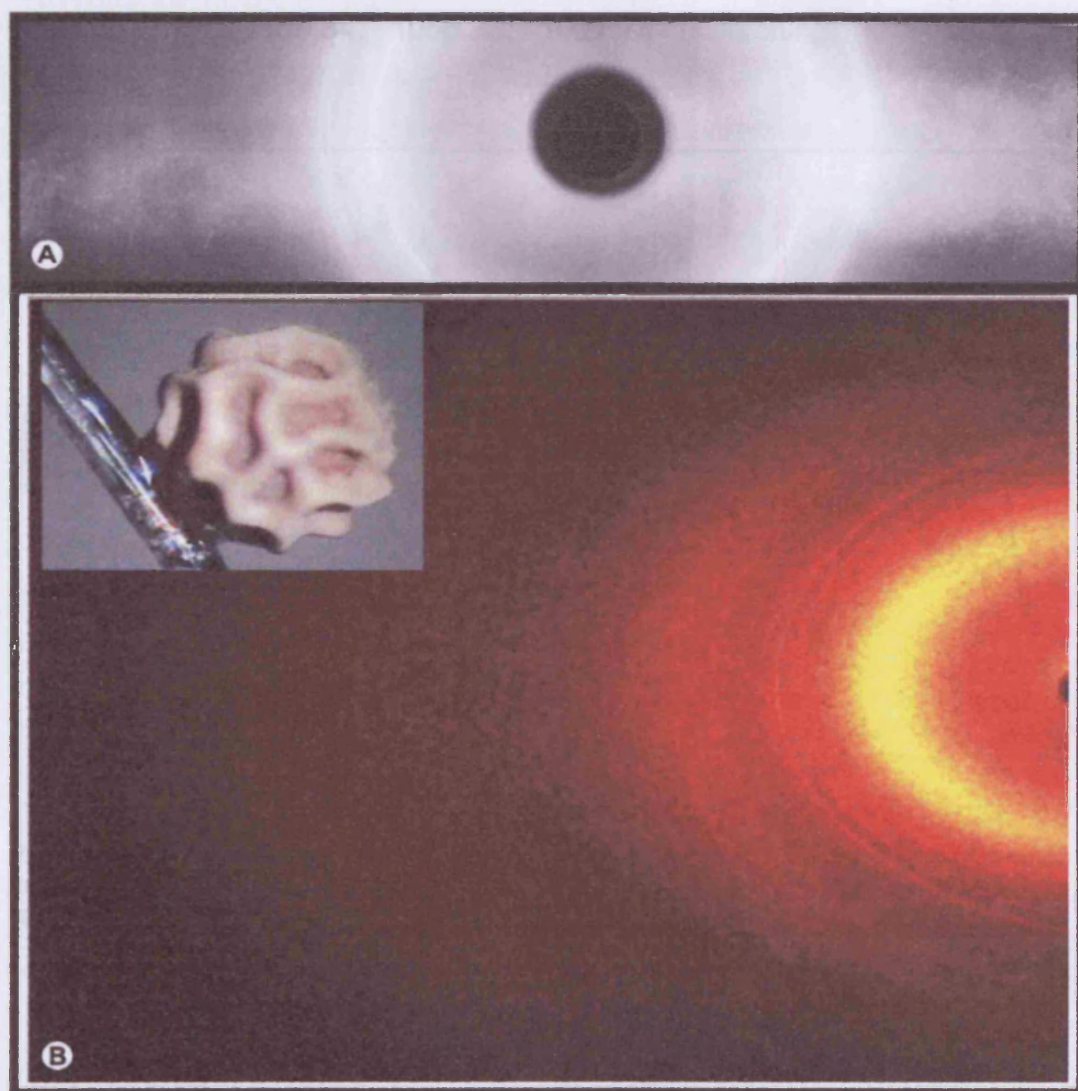


Figure 3.6: A Scan of diffraction film obtained by exposing a complete *Selaginella myosurus* megaspore to a Debye Scherrer camera and XRD of a whole megaspore (small image top left) and ring pattern obtained.

3.2.1.5 IR microspectrometry

The sporopolleninous spore matrix (in red) is characterised by the following group frequencies (all in wavenumbers cm^{-1}) (figure 3.7): 3267.92, 2919.46, 2844.79, 1646.49, 1543.37 (stretching); 2500-1800, 1500-1000 (bending). The crystal cubes (in blue) show group frequencies at: 3267.92, 2919.46, 1159.34, 1056.23, 1027.78 (stretching); 2050-1950, 2150-2050, 2350-2150, 2500-2350, 1950-1800 (bending). It is likely that the cubes analysed were still attached to matrix elements, which would show up in the spectrum. By subtraction of the matrix group frequencies from the crystal cubes we should be looking at the pure crystal group frequencies, which are: 3381.71, 1159.34, 1056.23, 1027.78 (stretching) and 1500-1100 (bending).

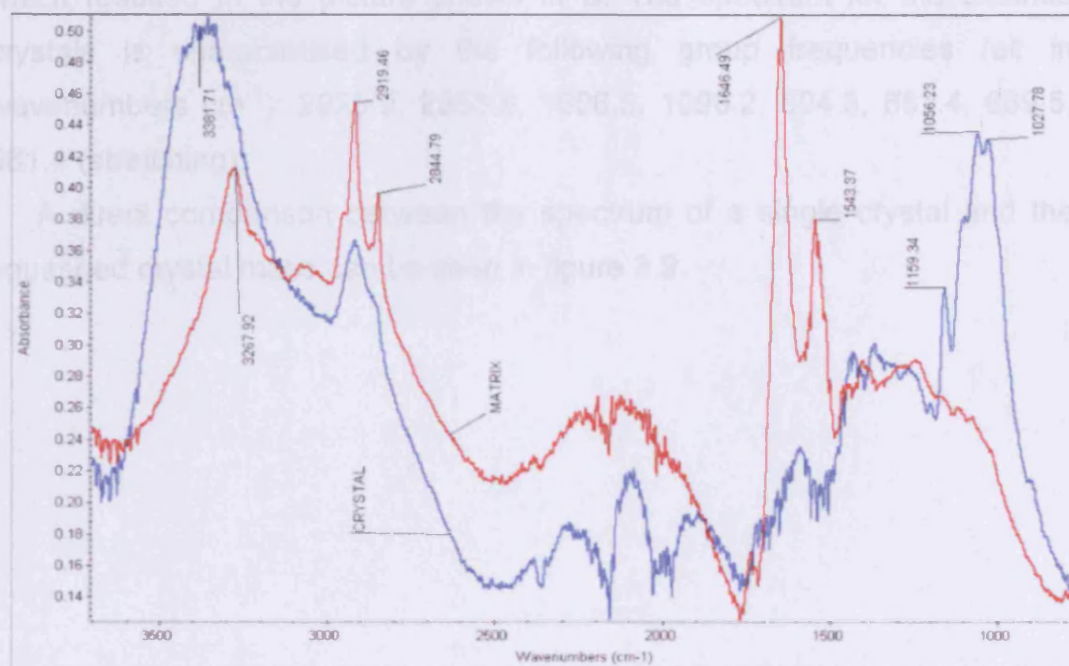


Figure 3.7: FT-IR spectrum of *Selaginella myosurus* spore matrix (red) and of crystal cubes probably still attached to sporopolleninous matrix residue (blue). Note the Si-O region peaking at 1056.23 and 1027.78 cm^{-1} .

3.2.1.6 IR microspectrometry with synchrotron radiation source (SRS)

Figure 3.8A shows three spectra taken from three single crystals (picture seen in A). Although the spectra differ in their absorbance, stretching occurs at the same wavenumbers. The crystals are characterised by the following group frequencies (all in wavenumbers cm^{-1}): 3285.9, 2925.0, 2852.7, 1743.5, 16327.7, 1462.2, and 1019.5 (stretching) and 1200-100 (bending). There are also several peaks between 703.7 and 749.8 as well as at 649.9 (stretching).

Figure 3.8B shows the spectrum of a single crystal (blue) identical to the spectra shown in figure A as well as the spectrum of the squashed crystals (red). The three crystals shown in A were crushed between a diamond cell which resulted in the picture shown in B. The spectrum for the crushed crystals is characterised by the following group frequencies (all in wavenumbers cm^{-1}): 2925.9, 2853.8, 1606.5, 1090.2, 804.3, 681.4, 669.5, 661.4 (stretching).

A direct comparison between the spectrum of a single crystal and the squashed crystal mass can be seen in figure 3.9.

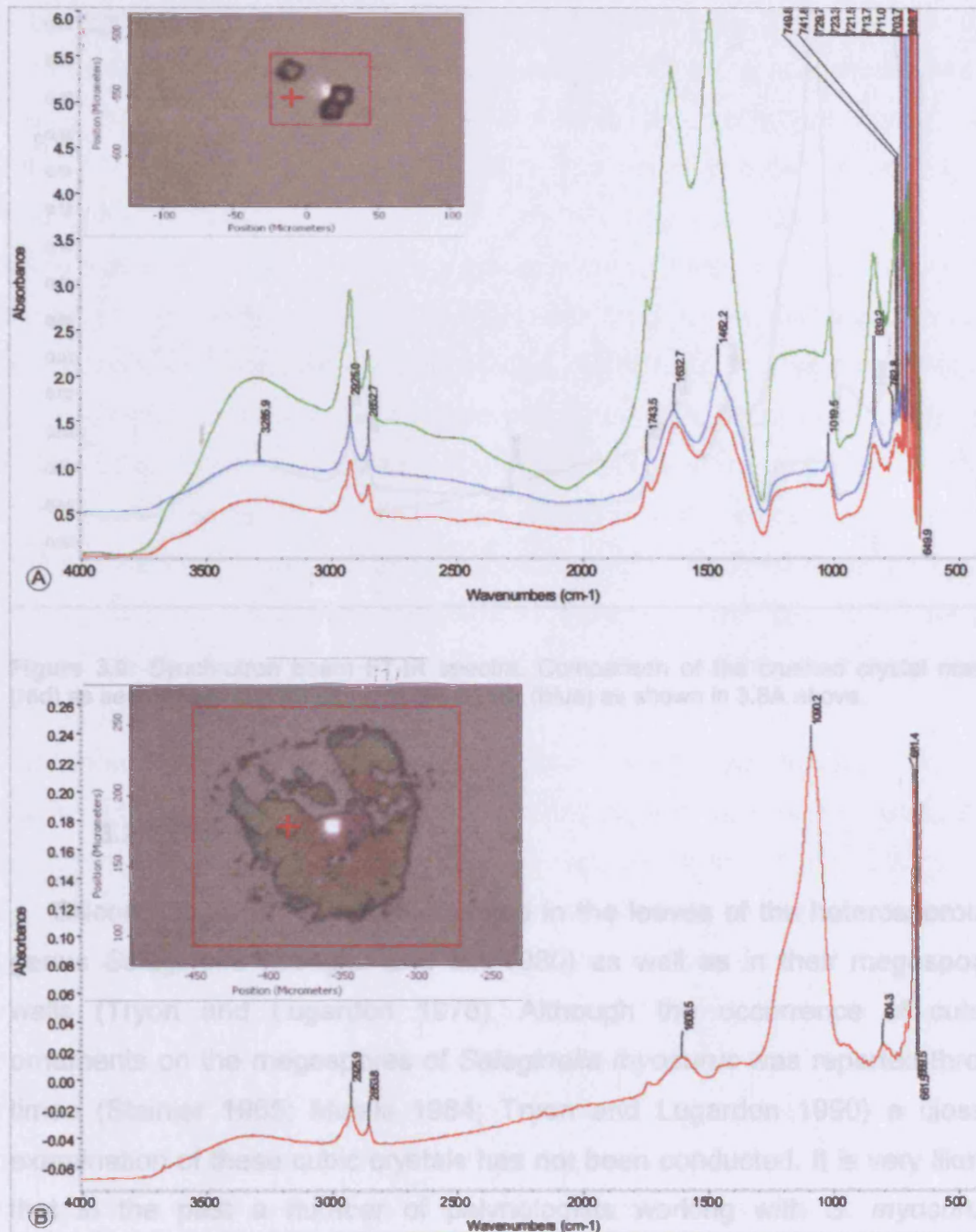


Figure 3.8: Synchrotron beam FT-IR spectra. **A** shows the spectra of three individual crystals from *Selaginella myosurus exospore* (note the picture representing the three crystals). In **B** the red spectrum represents an analysis from a squashed crystal (note the picture showing the crushed crystal mass).

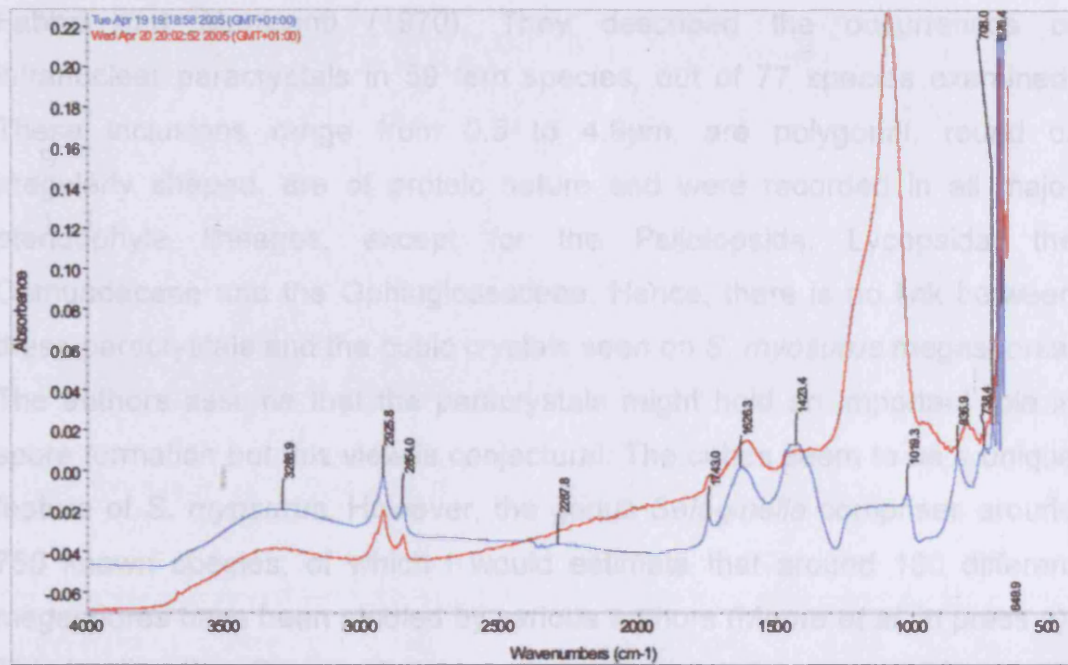


Figure 3.9: Synchrotron beam FT-IR spectra. Comparison of the crushed crystal mass (red) as seen above in 3.8B and a single crystal (blue) as shown in 3.8A above.

3.2.2 Discussion

Silicon has so far been documented in the leaves of the heterosporous genus *Selaginella* (Dengler and Lin 1980) as well as in their megaspore walls (Tryon and Lugardon 1978). Although the occurrence of cubic ornaments on the megaspores of *Selaginella myosurus* was reported three times (Stainier 1965; Minaki 1984; Tryon and Lugardon 1990) a closer examination of these cubic crystals has not been conducted. It is very likely that in the past a number of palynologists working with *S. myosurus* megaspores noted these ornamental cubes but dismissed them as artefacts or contamination. Tryon and Lugardon (1990) described them as “silica crystals” (p. 167f) but provided no proof for the assumption that the crystals are silica. Presumably their hypothesis is based on the fact that the heterosporous genera *Selaginella* and *Isoetes* are characterised by siliceous spore walls, which is well documented in the literature (Tryon and Lugardon 1978; Taylor 1989, 1993; Morbelli 1995). To my knowledge there is no evidence in the literature describing a similar phenomenon occurring in plants. The only account for crystals in pteridophytes was published by

Fabbri and Menicanti (1970). They described the occurrences of intranuclear paracrystals in 59 fern species, out of 77 species examined. These inclusions range from 0.5 to 4.9 μ m, are polygonal, round or irregularly shaped, are of proteic nature and were recorded in all major pteridophyte lineages, except for the Psilotopsida, Lycopsidea, the Osmundaceae and the Ophioglossaceae. Hence, there is no link between these paracrystals and the cubic crystals seen on *S. myosurus* megaspores. The authors assume that the paracrystals might hold an important role in spore formation but this view is conjectural. The cubes seem to be a unique feature of *S. myosurus*. However, the genus *Selaginella* comprises around 750 known species, of which I would estimate that around 100 different megaspores have been studied by various authors (Moore *et al.* in press a). This implies that *Selaginella* megaspores have not been comprehensively studied in order to be certain that cubic crystals do not form on other species as well.

Thin-sectioning of a complete megaspore viewing under the SEM (figure 3.3) confirmed the hypothesis that the cubic crystals are neither artefacts nor contamination. Since they run underneath the ridges (figure 3.3A and B), this indicates that the formation process of these crystals must have taken place during spore wall development. Additionally, a herbarium specimen (Kew Herbarium, A. Fay 1075, figure 3.10) was studied in order to compare megaspore morphology between the species used here, the one investigated by Tryon and Lugardon (1978, 1990) as well as the one documented by Minaki (1984). The following table 3.2 shows that although the species studied originate from different countries, they all have in common the presence of cubic crystals on their megaspore sculpture. This underpins the view that the cubic crystals are genuine features of *S. myosurus* and not contamination.

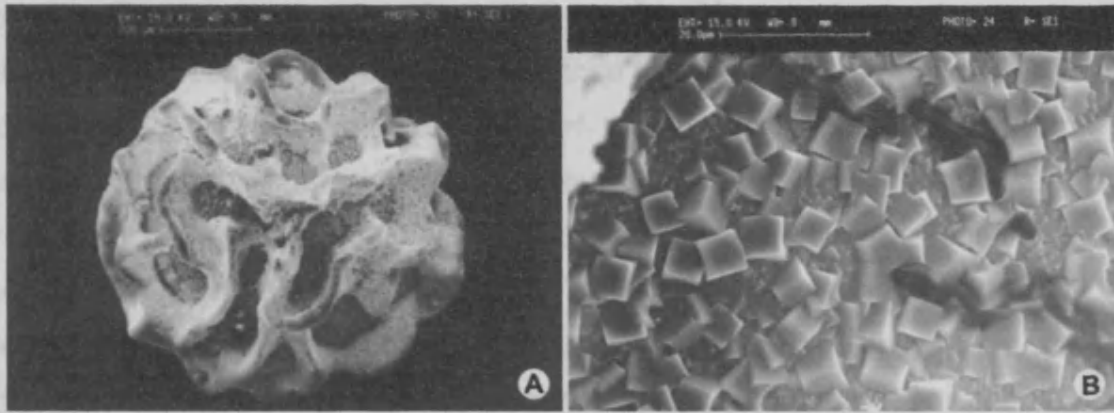


Figure 3.10: A and B SEM documentation of *Selaginella myosurus* megaspore (Kew Herbarium specimen A. Fay 1075). B note the abundance of cubic crystals.

Occurrence of cubic crystals on <i>S. myosurus</i>	Moore 2005, herein	Tryon and Lugardon 1990	Minaki 1984	Kew specimen
Herbarium voucher	leg. anonymos s.n.	Excell 746; Cook 161a (A)	P. Cudjoe 1953.7.35 (KYO)	A. Fay 1075 (K)
Country of origin	Ghana	Cameroon; Liberia	Ghana	Sierra Leone
Cubes present on megaspore sculpture	YES	YES	YES	YES

Table 3.2: Summary of *Selaginella myosurus* megaspores studied by various authors. The table summarises herbarium vouchers, country of origin of the species studied, as well the presence of cubic crystals on the spore sculpture.

All EDX analyses combined with either SEM or TEM, clearly demonstrate the presence of the three main elements silicon, oxygen and carbon in the crystals as well two minor elements potassium and chlorine (figure 3.3G and H). Due to the extremely low counts for chlorine (figure 3.3H) in comparison to silicon, oxygen and carbon, the presence of chlorine is probably due to scattered background noise. Although potassium shows similar low counts, the distribution of potassium correlates with the surface of the crystal. I interpret this as potassium traces in or on the crystals, probably deriving from the underlying spore wall. With the electrons probably also picking up weak signals from the spore wall underneath the crystal's surface and potassium occurring in spore walls (*section 3.3*), weak potassium signal are not surprising.

Silicon is equally distributed across the crystal's surface with high counts (figure 3.3D). This is also true for oxygen but the amount of detected carbon

decreases across the crystal's surface without falling to zero. This means that there is less carbon in the crystal than in the surrounding matrix. Two peaks seen on the right hand side of the oxygen and carbon spectra indicate that the topography of the surrounding spore is very similar, represented by higher peaks where the area is more electron dense (and *vice versa*). The peaks are the result of interactions between the spore wall topography and the electron beam. Hydrogen cannot be analysed by the means of EDX. The high ratio of oxygen to silicon and carbon, and the lack of other atomic species (figure 3.3), indicates that hydrogen is probably the main provider of valency balance. From the results it is suggested that the ratio of the three main elements is approximating $\text{Si}_2\text{C}_5\text{O}_9$ or SiC_3O_5 but very high totals indicate incorrect correction calculations, not fully diagnosed. It is also thought that the cubic habit and deviation from pure SiO_2 composition suggest a loose silica framework structure stabilised by additional elements. Substantial carbon but lack of cationic species indicates a clathrate rather than a zeolite. Zeolites are a family of framework aluminio-silicates containing water molecules along with Na^+ and Ca^{2+} in the spaces of the framework (Battey and Pring 1997). Clathrates are inclusion complexes in which molecules of one substance are completely enclosed within the crystal structure of another (Chatti *et al.* 2005). The dotted sculpture observed on some crystals (figure 3.1G) might be a surface artefact deriving from storage or preparation. It is uncertain as to whether this pattern has any regularity and whether it reflects the organisation of different components in the cubes.

TEM documentation shows that the exospore of *S. myosurus* consists of almost spherical particles, highly ordered, forming compound units separated by dislocations, as shown in figure 3.4D. A very similar pattern can be seen in fossil megaspores of *Erlansonisporites* (Hemsley *et al.* 1994). This ordered pattern is well documented for various extant *Selaginella* species as well as for fossil *Erlansonisporites*, a species with selaginellean affinity (Taylor 1991; Hemsley *et al.* 1992; Collinson *et al.* 1993; Hemsley *et al.* 1994, 1998; Hemsley 1997; Hemsley and Griffiths 2000). Megaspores of extant and fossil species exhibit spore walls with a

varying degree of order and are in many cases also iridescent (Hemsley *et al.* 1992, 1994; Collinson *et al.* 1993). The authors suggest that a monodisperse colloidal crystal is responsible for the iridescent appearance as well as for the highly ordered exine. The only diffraction of this colloidal crystal is of optical nature and has no influence on diffraction patterns obtained by XRD in this study. Iridescence is also common and well documented for plant leaves in general (Lee 1997), for *Selaginella* leaves (Lee and Lowry 1975; Hébant and Lee 1984) and for fern fronds (Graham *et al.* 1993; Gould and Lee 1996), caused by a thin-film interference filter on the upper cell wall of the epidermis.

With IR spectrometry, Si-O-Si compounds appear in a group frequency of 1095-1075 cm^{-1} and 1055-1020 cm^{-1} (Coates 2000). The finding of silicon in this analysis with group frequencies at 1056.23 cm^{-1} and 1027.78 cm^{-1} supports the assumption that silicon is the dominant element in these crystals. A single crystal analysis with IR, however, can only be achieved in combination with a synchrotron radiation source, where an aperture size of 5x5 μm can be applied. The three spectra obtained from single crystals using the SRS (figure 3.8) in combination with IR spectrometry are almost identical with the spectrum obtained from a single crystal using the desktop IR spectrometer (figure 3.7). The main difference is that the peaks representing the diamond cell (figure 3.7 at 3381.71 cm^{-1} and between 2500-1800 cm^{-1}) are not visible in the other spectrum (figure 3.8) due to the use of the SRS. IR combined with a SRS also resulted in an overall less noisy spectrum, compared to IR without SRS (figures 3.7 and 3.8). On the basis of the spectra acquired for the three single crystals combined with SRS it is assumed that the following organic compounds are present (Coates 2000): any broad bending around 3381.71 cm^{-1} is assigned to the diamond cell. The peak at 2925.0 cm^{-1} probably represents an asymmetric methyl C-H stretch, that at 2852.7 cm^{-1} a methyl, methyl ether O-CH₃ or a C-H stretch. 1743.5 cm^{-1} can be assigned to an ester or aldehyde. 16327.7 cm^{-1} and 1462.2 cm^{-1} could represent an aromatic ring. Interpreted separately, they can be assigned to an amide (16327.7 cm^{-1}) and a carboxylate 1462.2 cm^{-1} , which is more likely as the latter peak is lost after squashing the sample

(see below). 1019.5cm^{-1} might represent an organic siloxane Si-O-Si and the bending around $1200\text{-}1000\text{cm}^{-1}$ a phenol. There are skeletal vibrations in the region of $700\text{-}600\text{cm}^{-1}$ representing C-C bonds. A database search combined with the OMNICTM software package used for spectra manipulation confirmed the presence of amides and an organic silicon compound.

Probably the most interesting findings are the loss of peaks at 1423.4cm^{-1} and 1019.5cm^{-1} , the broad bending between $1200\text{-}1000\text{cm}^{-1}$ and a decrease of skeletal vibrations around $700\text{-}600\text{cm}^{-1}$ alongside with the occurrence of a single, strong peak at 1100cm^{-1} (figure 3.8). The loss of some peaks was observed after squashing the single crystals between the diamond cells into one mass. It indicates that crushing the crystals leads to a loss of phenolics and carboxylates and a decrease in C-C bonds but on the other hand increases the absorbance in the organic siloxane region (figure 3.8), supporting the view that the cubes might have an organic siloxane framework stabilised around organic compounds.

X-ray diffraction obtained by Debye Scherrer camera showed a ring pattern with sharp rings from crystalline material superimposed on a broad diffuse background from the non-crystalline spore wall matrix. The calculated d -spacings of 3.83\AA , 3.71\AA , 3.58\AA and a lattice repeat $a=13.34\pm 0.06\text{\AA}$ do not match any classified mineral (databases consulted: Bayliss *et al.* 1986a and b). The closest match is the mineral melanophlogite with its pseudocubic structure based on a cubic (isometric) lattice repeat $a=13.4\text{\AA}$ and because it is unique amongst SiO_2 minerals in its cube crystal habit, sometimes hopped. Melanophlogite, however, is a mineral previously recorded from abiotic environments found in only five sites in the world (Nakagawa *et al.* 2001). It is also the only known natural SiO_2 clathrate (Kolesov and Geiger 2003). The only link between silica in plants (detected in pollen of *Lychnis alba*) and melanophlogite was published by Crang and May (1974). The authors report that the XRD studies of pollen indicate that in dried samples the amorphous silica gel dehydrates, producing a crystalline form with discernible diffraction lines. They assign larger d -spacings to organic compounds and several lines to the strongest

reported lines of melanophlogite, indicating that a positive identification could not be made on the basis of their results. It is assumed that although the organosilicon compounds found in pollen of *Lychnis alba* and in the megaspores of *Selaginella myosurus* share *d*-spacings with melanophlogite, they might be a new form of mineral not yet described.

Single crystal XRD did not give interpretable results due to few, weak and scattered peaks. It is believed that the cubes do not diffract strongly enough to produce a diffraction pattern. The reason for this is unknown. Weak diffraction arises from very little regularity (not crystalline), or if the repeat distance of the crystal is orders of magnitude either greater than the wavelength of the radiation (as seen in proteins, DNA in the case of x-rays and electrons) or smaller (e.g. ordinary inorganic crystals in the case of visible light) (pers. comm. Norman Fry 2005). It is highly unlikely that any silica-containing oxidised crystal would have a repeat distance so large as to reduce the diffraction intensity to that observed herein. Therefore, it is believed that little structurally regular crystal remains, although there must have been some present earlier to constrain the shapes to cubes (pers. comm. Norman Fry 2005). The cubes have reached the analytical limitations of this technique. As for XRD of the whole megaspore, work is ongoing to elucidate the unit cell parameters from the powder pattern.



3.3 Mineral content in pteridophyte spore walls

The following table (3.3) contains all of the species investigated, the results of previous work (Tryon and Lugardon 1990) on the ultrastructure of the true perispore, relevant page number, as well as the results of this study obtained by the means of SEM EDX.

Family	Species investigated	Comments on the true perispore (PS) by Tryon and Lugardon (1990)	Page	Results SEM EDX spore
Blechnaceae	<i>Doodia aspera</i> R. Br.	PS described with dense, short pillars; no TEM available for <i>D. aspera</i>	529	silicon
	<i>Blechnum occidentale</i> L.	PS laminate, pillared with rodlets, a compact outer surface	531, 535	silicon
Davalliaceae	<i>Nephrolepis hirsutula</i> (Forst.) Presl	PS one-layered giving rise to tuberculate or rugate sculpture	383f	no silicon
	<i>Davallia mariesii</i> Moore ex Baker	PS thin, laminate	378f	no silicon
Dryopteridaceae	<i>Cyrtomium falcatum</i> (L. f.) Pr.	PS is a thin coating	439f	no silicon
	<i>Cyrtomium fortunei</i> J. Sm.	PS is a thin coating	439f	no silicon
	<i>Diplazium poliferum</i> (Lam.) Thouars	cavate	476f	silicon
	<i>Dryopteris erythrosora</i> (Eat.) O. Ktze.	cavate	422f	no silicon
	<i>Dryopteris stewardii</i> Fraser-Jenk.	cavate	422f	no silicon
	<i>Hypodematium fauriei</i> (Kodama) Tagawa	cavate	492f	no silicon
	<i>Lastreopsis microsora</i> (Endl.) Tindale	cavate	464f	no silicon
	<i>Rumohra adiantiformis</i> (G. Forst.)	PS thick	417	no silicon
Osmundaceae	<i>Osmunda regalis</i> L.	PS thin	55	no silicon
Polypodiaceae	<i>Phlebodium aureum</i> (L.) J. Smith	no information available	-	no silicon
Psilotaceae	<i>Psilotum nudum</i> (L.) Beauv.	PS thin; well documented; pseudoendospore	561	no silicon
Pteridaceae	<i>Pellaea calomelanos</i> (Swartz) Link	PS present; no TEM available	165	silicon
	<i>Pellaea rotundifolia</i> (Forst. f.) Hook	PS present; no TEM available	165	silicon
	<i>Pteris cretica</i> L.	PS thin	191	silicon
	<i>Pteris longifolia</i> L.	PS thin, two layered	189	silicon
Schizaeaceae	<i>Anemia tomentosa</i> (Sav.) Sw.	PS complex	107f	silicon
Thelypteridaceae	<i>Macrothelypteris torresiana</i> (Gaud.) Ching	cavate	399	silicon
	<i>Oreopteris limbosperma</i> (All.) J. Holub	no information available	-	silicon
	<i>Phegopteris decursive-pinnata</i> (v. Hall) Fee	two types of PS	395	silicon
	<i>Thelypteris japonica</i> (Bak.) Ching	cavate	387f	silicon

Table 3.3: A summary of section 3.3 including species investigated, references to previous work, a brief comment on the ultrastructure of the true perispore and results of spore SEM.

The list of families is arranged alphabetically as are the species within families. *Section 1.3 Systematics* of the *Introduction* provides a general overview on pteridophyte systematics. All perispore descriptions in *section 3.3.1* are used in the sense of a true perispore.

3.3.1 Results

For morphological descriptions of the spores please refer to *Material and Methods, section 2.2*. SEM in combination with Energy Dispersive X-Ray analysis (EDX) showed either presence or absence of silicon (Si) in the spore walls investigated. Generally, analyses also revealed an abundance of other elements such as phosphorus (P), sulphur (S), potassium (K), calcium (Ca), oxygen (O), sodium (Na), chlorine (Cl), carbon (C) or magnesium (Mg).

It is important to mention that the detection of silicon in this study is treated semi-quantitatively only. Although tables with atomic and weight % could be generated from the EDX analysis, these data are treated cautiously as there are several factors which might influence the exact quantitative determination of an element in the spore wall.

The high carbon content in all species investigated is due to the carbon coating applied for SEM. If it is specified in the EDX INKA software that the stub is carbon coated, this will exclude all carbon, which will lead to the loss of elements present in very small quantities. There is no doubt that carbon will be present in spores and since this analysis is treated semi-quantitatively, the exact values can be neglected in this study.

3.3.1.1 Blechnaceae

The spore walls of *Blechnum occidentale* L. and *Doodia aspera* R. Br. were analysed. Silicon was detected in both species investigated. Phosphorus, sulphur, potassium, calcium, carbon and oxygen were found in *Blechnum occidentale*, and oxygen, carbon, sodium, calcium and chlorine in *Doodia aspera*.

Blechnum occidentale

Element	Weight%	Atomic%
C	72.26	78.25
O	25.58	20.80
Si	1.58	0.73
P	0.22	0.09
S	0.07	0.03
K	0.15	0.05
Ca	0.14	0.05

Table 3.4: Occurrence of silicon and other elements (in weight % and atomic %) in the spore wall of *Blechnum occidentale*.

Doodia aspera

Element	Weight%	Atomic%
C	65.03	72.88
O	29.12	24.48
Na	1.04	0.61
Si	2.60	1.25
Cl	0.80	0.31
Ca	1.40	0.47

Table 3.5: Occurrence of silicon and other elements (in weight % and atomic %) in the spore wall of *Doodia aspera*.

Figure 3.11: A *Blechnum occidentale* spore as observed under the SEM and B-C the EDX. G a 0.4-0.5µm thick, lamella perforate covers the fully grown spore. E in many spores observed the perforate lamella and often erodes the lamella completely. F shows the results of the EDX analysis, note silicon peak at 1.5. The SEM picture in F shows the area where the EDX analysis was taken.

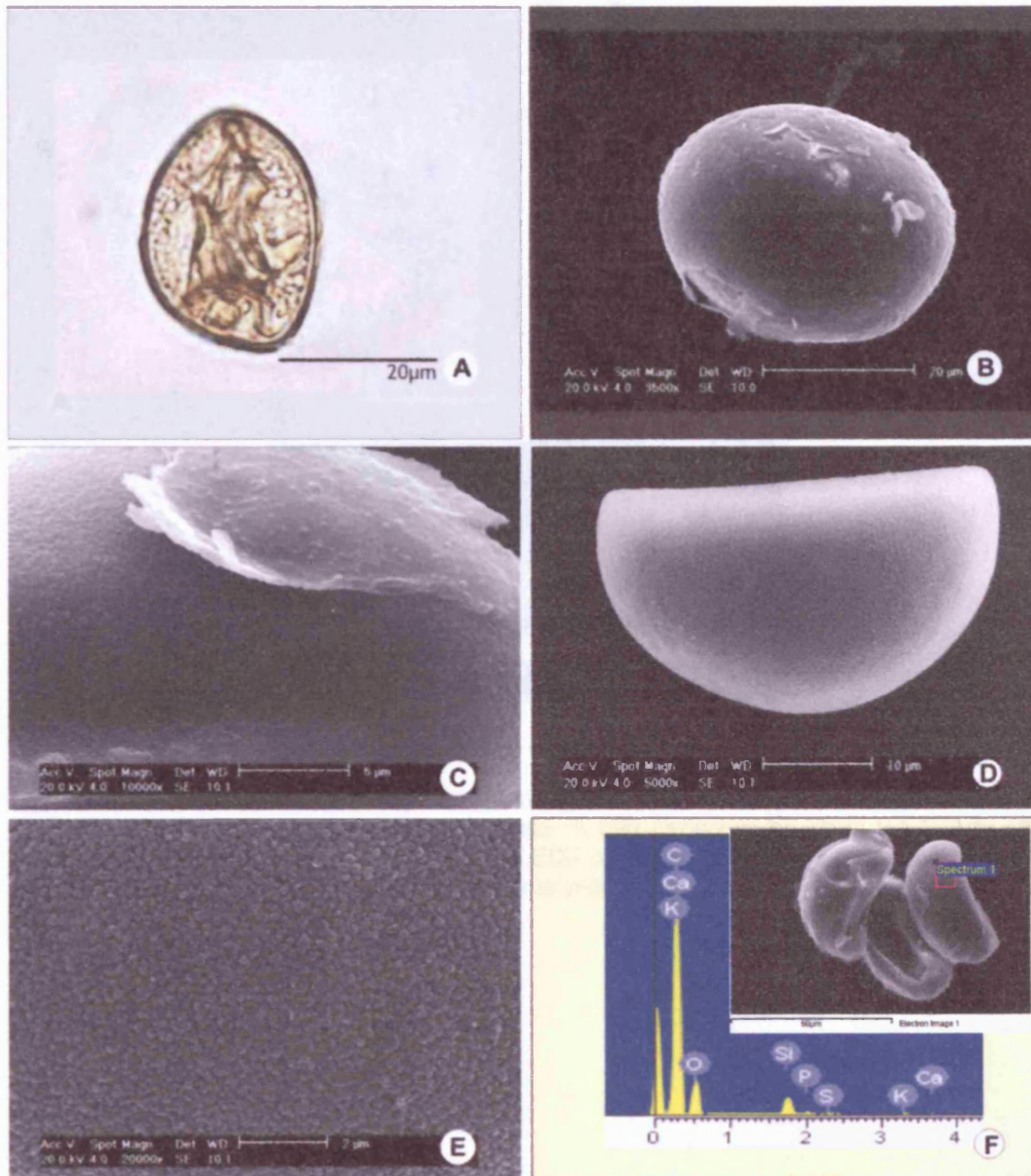


Figure 3.11: *A* *Blechnum occidentale* spores as observed under the LM and **B–E** the SEM. **C** a 0.4-0.6µm thick, laevigate perispore covers the finely granulate exospore. **E** in many spores observed the perispore brittle and often exposes the exospores completely. **F** shows the results of the EDX analysis, note silicon peak at 1.8. The SEM picture in **F** shows the area where the EDX analysis was taken.

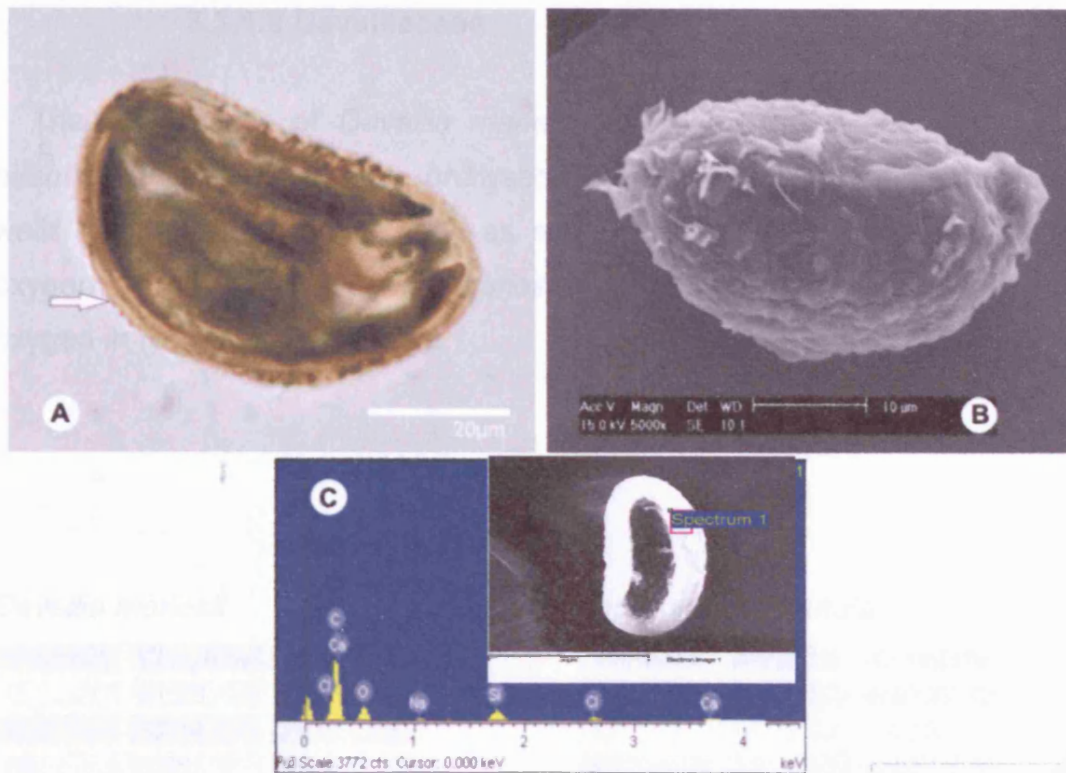


Figure 3.12: **A** *Doodia aspera* spores as observed by LM and **B** the SEM. The spore is characterised by a coarsely verrucate surface. A thin perispore of about 0.1-0.2µm can be seen in **A** (arrow). **C** shows the results of the EDX analysis, note silicon peak at 1.8. The SEM picture in **C** shows the area where the EDX analysis was taken.

3.3.1.2 Davalliaceae

The spore walls of *Davallia mariesii* Moore ex Baker and *Nephrolepis hirsutula* (Forst.) Presl. were analysed. There is no silicon present in either walls, but other elements such as sodium, sulphur, calcium, carbon and oxygen are present in *Davallia mariesii* and carbon, potassium, calcium and oxygen in *Nephrolepis hirsutula*.

Davallia mariesii

Element	Weight%	Atomic%
C	67.28	73.39
O	32.14	26.32
Na	0.36	0.21
S	0.10	0.04
Ca	0.11	0.03

Table 3.6: Absence of silicon but abundance of other elements (in weight % and atomic %) in the spore wall of *Davallia mariesii*.

Nephrolepis hirsutula

Element	Weight%	Atomic%
C	80.39	84.79
O	18.93	14.99
K	0.29	0.09
Ca	0.39	0.12

Table 3.7: Absence of silicon but abundance of other elements (in weight % and atomic %) in the spore wall of *Nephrolepis hirsutula*.

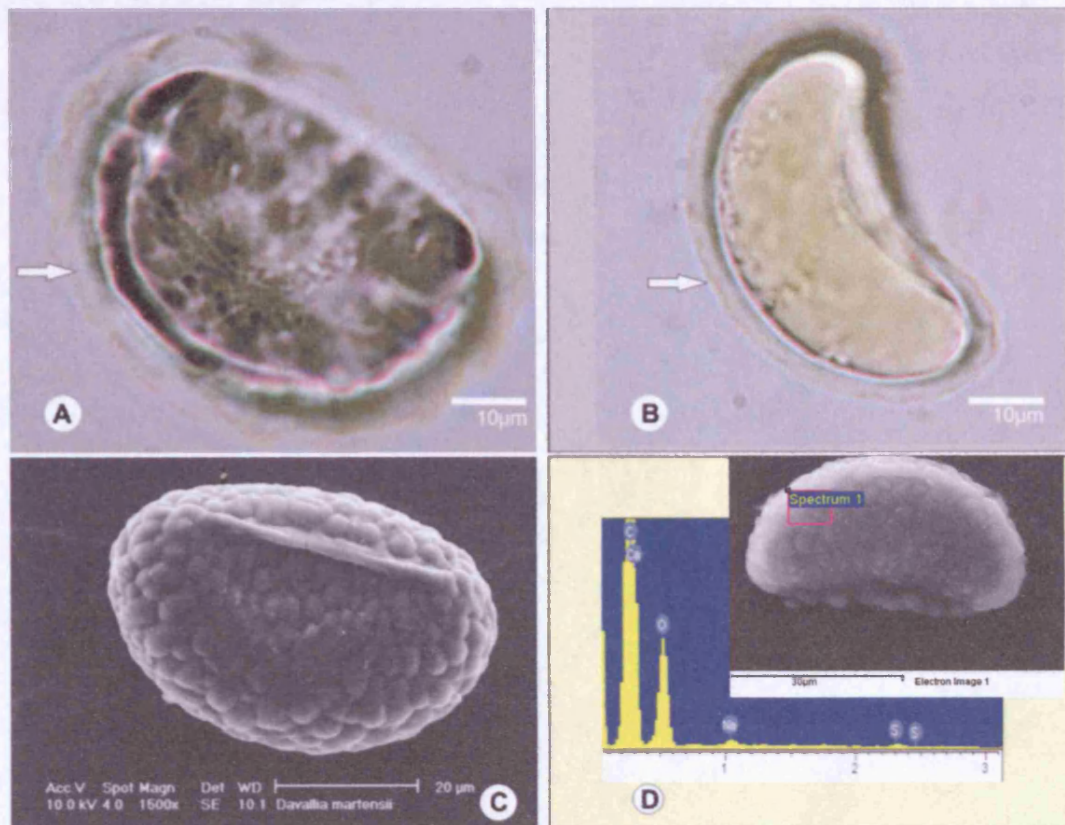


Figure 3.13: A and B *Davallia mariesii* spores documented by LM and C by SEM. The surface consists of prominent verrucae. Note the thick (2-5 µm) exospore in A and an about 0.1µm thick perispore in B (arrow). D shows the results of the EDX analysis. No silicon was detected. The SEM picture in D shows the area where the EDX analysis was taken.

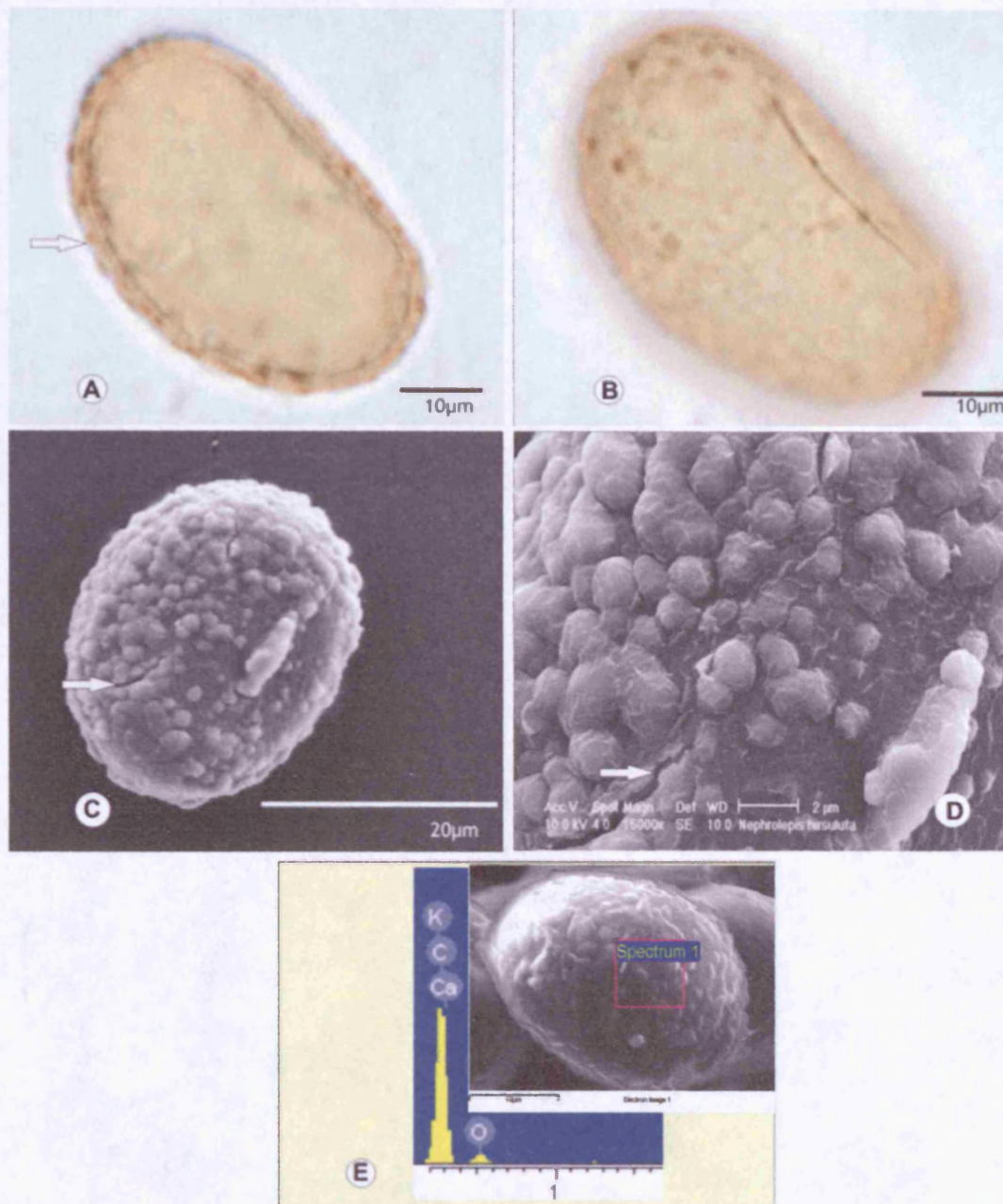


Figure 3.14: A and B *Nephrolepis hirsutula* spores observed by LM and C and D SEM. The sculpture is tuberculate. The perispore is brittle as seen in C and D (arrow) and is about 0.1µm thick, A (arrow). E shows the results of the EDX analysis. No silicon was detected. The SEM picture in E shows the area where the EDX analysis was taken.

3.3.1.3 Dryopteridaceae

The spore walls of *Cyrtomium falcatum* (L.f.) Pr. , *Cyrtomium fortunei* J. Sm., *Diplazium poliferum* (Lam.) Thouars, *Dryopteris erythrosora* (Eat.) O. Ktze., *Dryopteris stewardii* Fraser-Jenk., *Hypodematium fauriei* (Kodama) Tagawa, *Lastreopsis microsora* (Endl.) Tindale and *Rumohra adiantiformis* (G.Forst.) were analysed. Silicon was found only in the spore wall of *Diplazium proliferum*. *Cyrtomium falcatum* spore walls showed the presence of carbon, oxygen and calcium, *Cyrtomium fortunei* of carbon and oxygen only, *Dryopteris erythrosora* of carbon, phosphorus, chlorine, potassium and oxygen, *Dryopteris stewardii* of carbon, sodium, magnesium, phosphorus, sulphur, chlorine, potassium, calcium and oxygen. The spore walls of *Hypodematium fauriei* contain sodium, magnesium, sulphur, chlorine, calcium, carbon and oxygen, those of *Lastreopsis microsora* oxygen, phosphorus, potassium, carbon and calcium and in the spore walls of *Rumohra adiantiformis* carbon, oxygen and calcium were detected.

Cyrtomium falcatum

Element	Weight%	Atomic%
C	74.11	75.43
O	25.33	24.40
Ca	0.56	0.17

Table 3.8: Absence of silicon but abundance of other elements (in weight % and atomic %) in the spore wall of *Cyrtomium falcatum*.

Cyrtomium fortunei

Element	Weight%	Atomic%
C	72.38	77.75
O	27.62	22.25

Table 3.9: Absence of silicon but occurrence of other elements (in weight % and atomic %) in the spore wall of *Cyrtomium fortunei*.

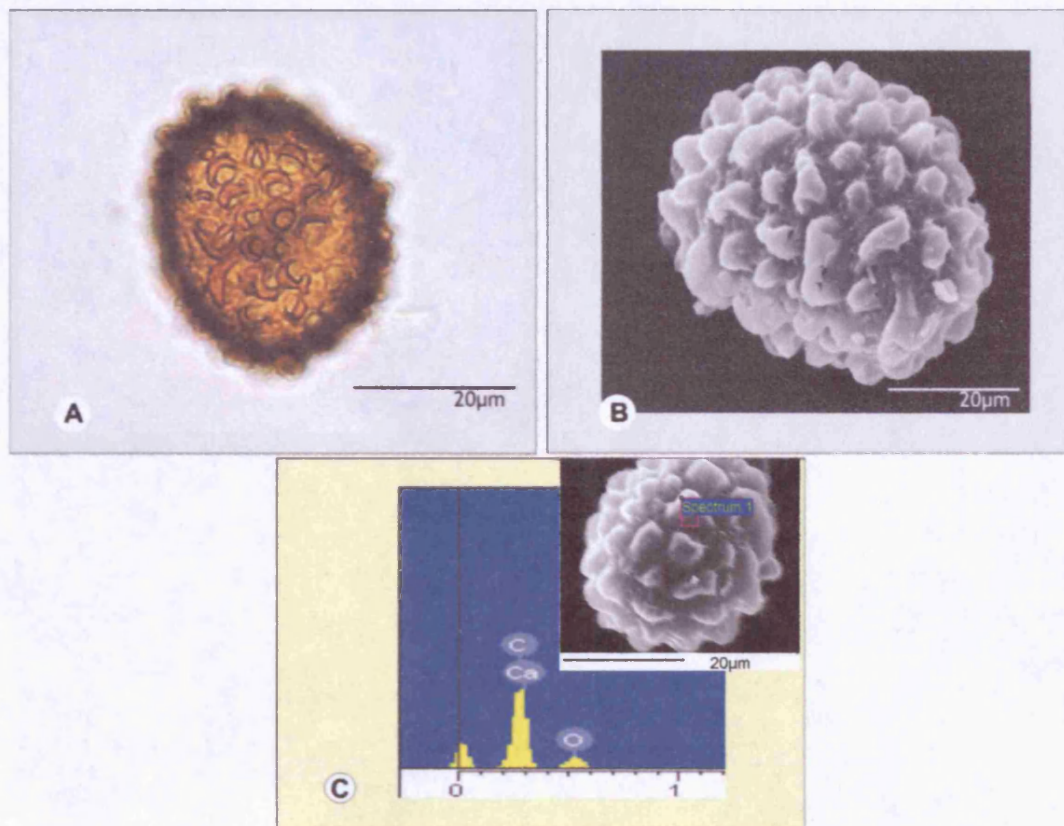


Figure 3.15: A *Cyrtomium falcatum* spores documented by LM and B SEM. The sculpture is uniformly tuberculate. C shows the results of the EDX analysis. No silicon was detected. The SEM picture in C shows the area where the EDX analysis was taken.

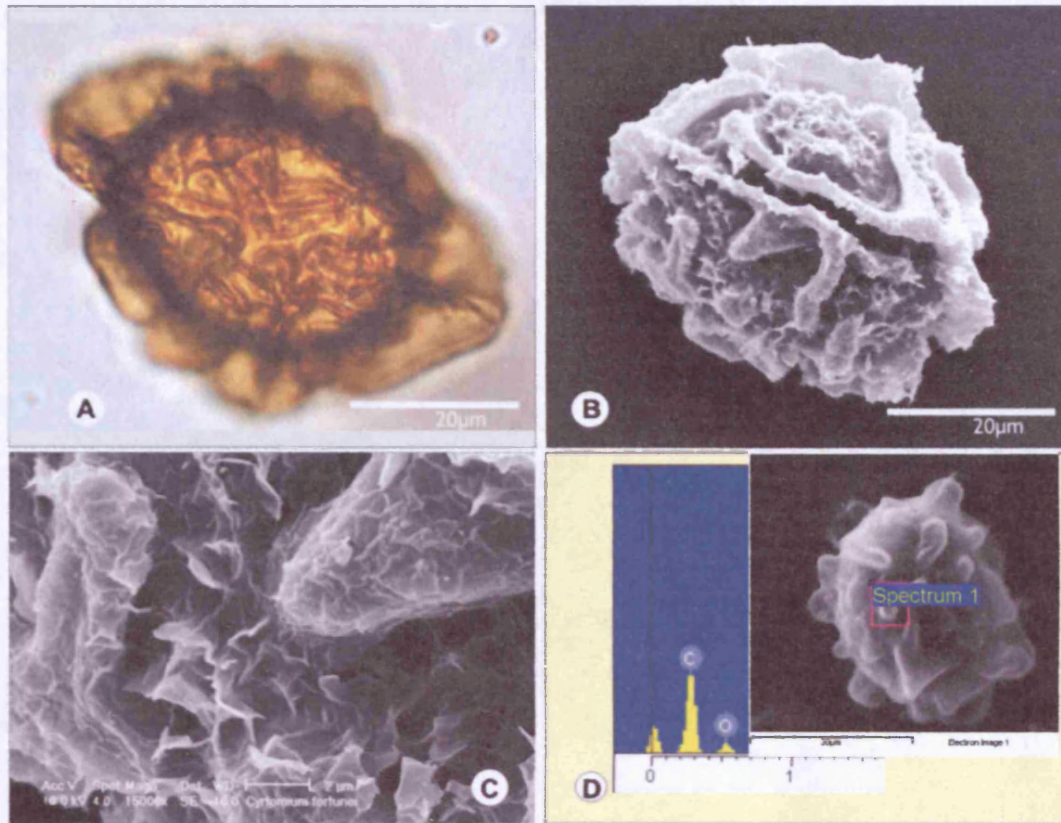


Figure 3.16: *Cyrtomium fortunei* as observed by LM **A** and SEM **B** and **C**. **A** and **B** the sculpture is characterised by coarse ridges, which are often wing-like. **D** shows the results of the EDX analysis. No silicon was detected. The SEM picture in **D** shows the area where the EDX analysis was taken.

Diplazium poliferum

Element	Weight%	Atomic%
C	58.96	67.25
O	35.80	30.65
Mg	0.33	0.19
Si	1.13	0.55
P	0.31	0.14
S	0.21	0.09
K	2.46	0.86
Ca	0.80	0.27

Table 3.10: Occurrence of silicon and other elements (in weight % and atomic %) in the spore wall of *Diplazium proliferum*.

Dryopteris erythrosora

Element	Weight%	Atomic%
C	74.57	79.78
O	24.98	20.06
P	0.11	0.05
Cl	0.14	0.05
K	0.19	0.06

Table 3.11: Absence of silicon but abundance of other elements (in weight % and atomic %) in the spore wall of *Dryopteris erythrosora*.

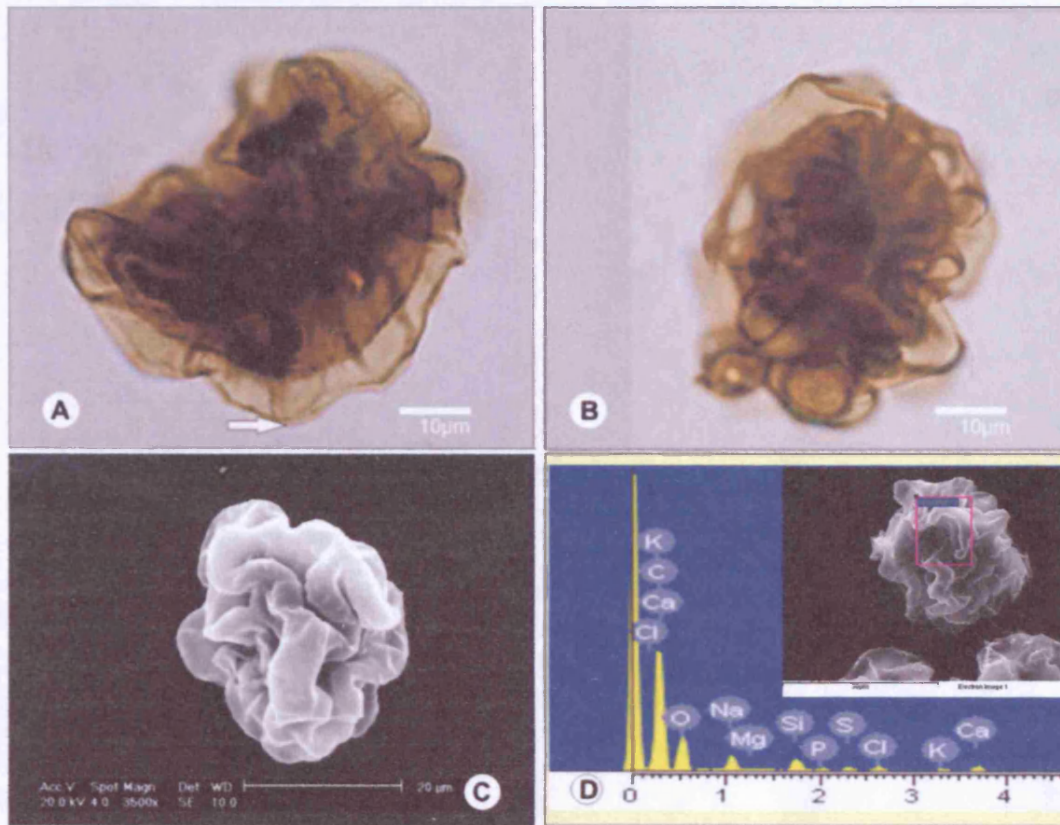


Figure 3.17: *Diplazium proliferum* spores documented by LM **A** and **B** and SEM **C**. Coarse, inflated folds form the spore sculpture. The folds are laevigate. **A** the about 0.05-0.1µm thick outer part of the cavate perispore layer (arrow) can be distinguished in. **D** shows the results of the EDX analysis, note silicon peak at 1.8. The SEM picture in **D** shows the area where the EDX analysis was taken.

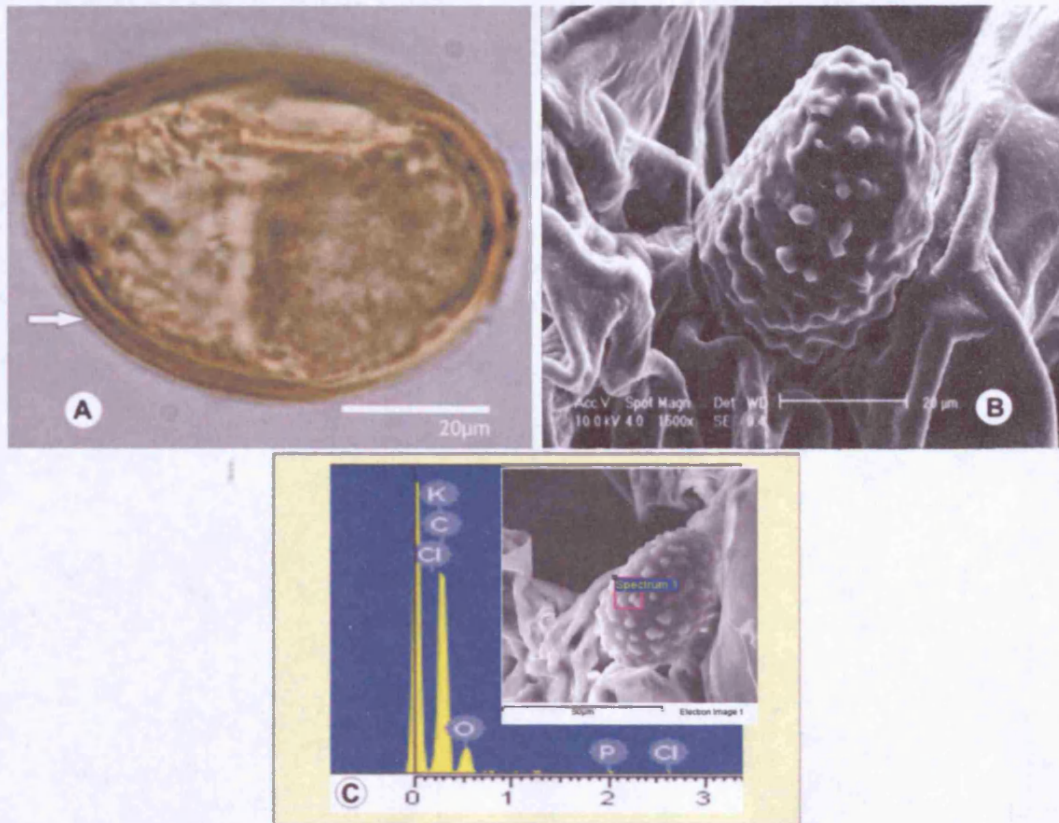


Figure 3.18: *Dryopteris erythrosora* as observed by LM **A** and **B** and by SEM **C** and **D**. The overall sculpture is tuberculate, and laevigate between tubercles. **A** and **B** note the about 0.05-0.1µm thick outer part of the perispore (arrow). **E** shows the results of the EDX analysis. No silicon was detected. The SEM picture in **C** shows the area where the EDX analysis was taken.

Dryopteris stewardii

Element	Weight%	Atomic%
C	70.91	78.88
O	22.11	18.46
Na	0.22	0.13
Mg	0.41	0.22
P	0.78	0.34
S	0.35	0.15
Cl	1.58	0.59
K	2.16	0.74

Table 3.12: Absence of silicon but abundance of other elements (in weight % and atomic %) in the spore wall of *Dryopteris stewardii*.

Hypodematium fauriei

Element	Weight%	Atomic%
C	58.28	66.35
O	37.30	31.88
Na	0.74	0.44
Mg	0.18	0.10
S	0.25	0.11
Cl	0.27	0.10
Ca	2.98	1.02

Table 3.13: Absence of silicon but abundance of other elements (in weight % and atomic %) in the spore wall of *Hypodematium fauriei*.

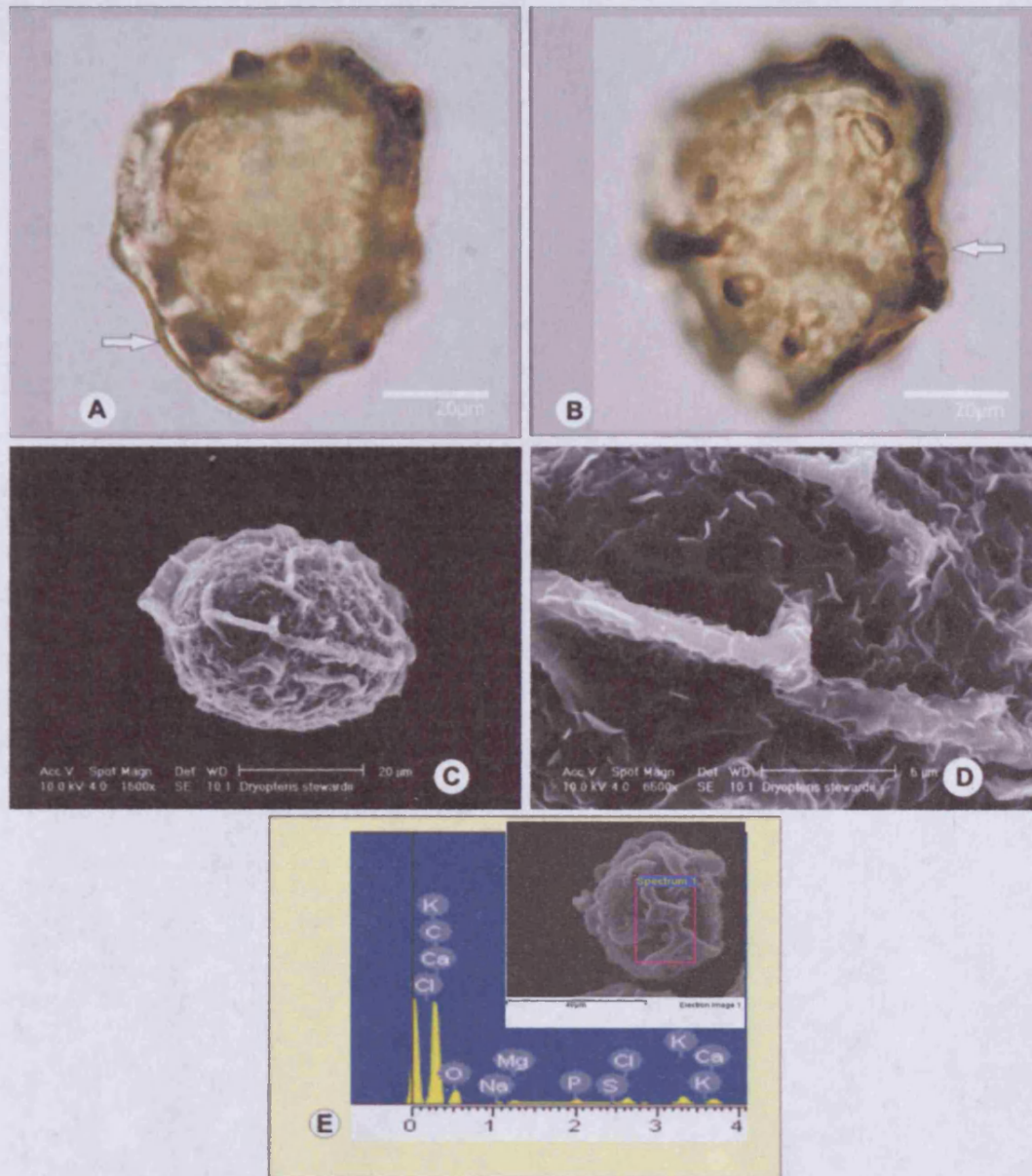


Figure 3.19: *Dryopteris stewardii* documented by LM **A** and by SEM **B**. The sculpture is irregularly scabrate and laminate in appearance. **A** note the about 0.05-0.1 µm thick outer part of the perispore (arrow). **C** shows the results of the EDX analysis. No silicon was detected. The SEM picture in **E** shows the area where the EDX analysis was taken.

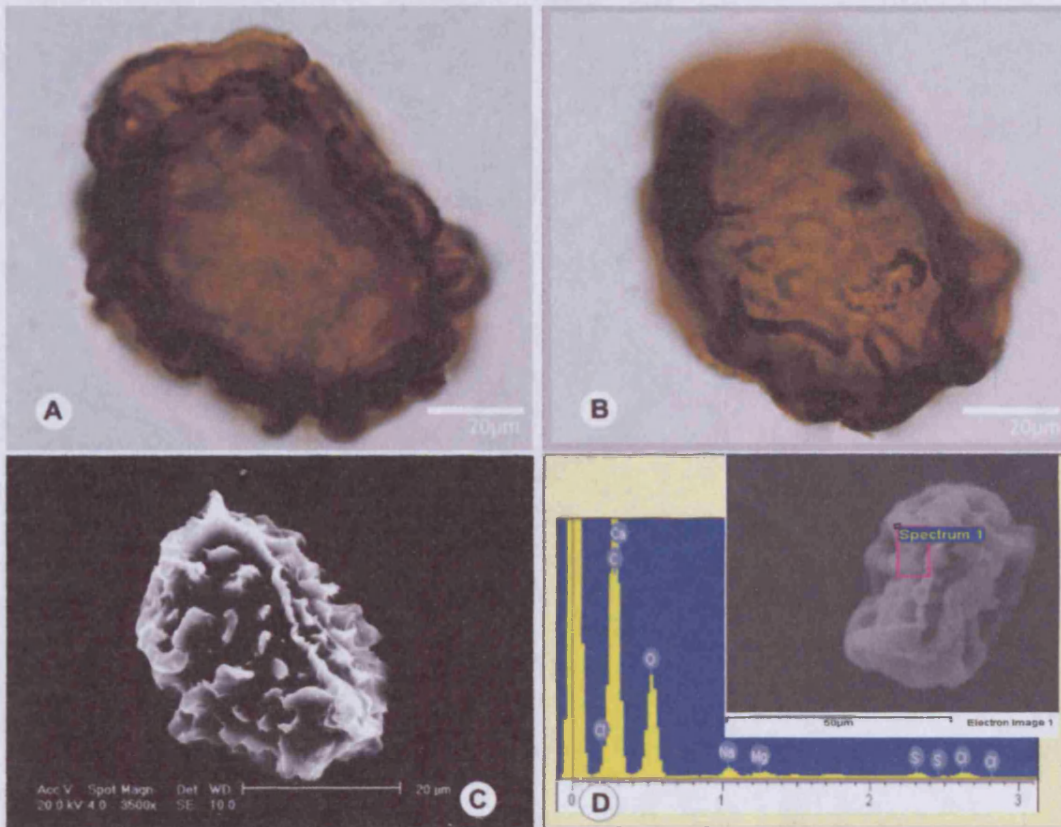


Figure 3.20: *Hypodematium fauriei* documented by LM **A** and **B** and by SEM **C**. **B** and **C** the sculpture is tuberculate, some tubercles are fused and form ridges. **D** shows the results of the EDX analysis. No silicon was detected. The SEM picture in **D** shows the area where the EDX analysis was taken.

Lastreopsis microsora

Element	Weight%	Atomic%
C	68.89	75.19
O	29.64	24.29
P	0.37	0.16
K	0.18	0.06
Ca	0.93	0.30

Table 3.14: Occurrence of silicon and other elements (in weight % and atomic %) in the spore wall of *Lastreopsis microsora*.

Rumohra adiantiformis

Element	Weight%	Atomic%
C	69.94	76.15
O	29.28	23.60
Ca	0.76	0.25

Table 3.15: Absence of silicon but occurrence of other elements (in weight % and atomic %) in the spore wall of *Rumohra adiantiformis*.

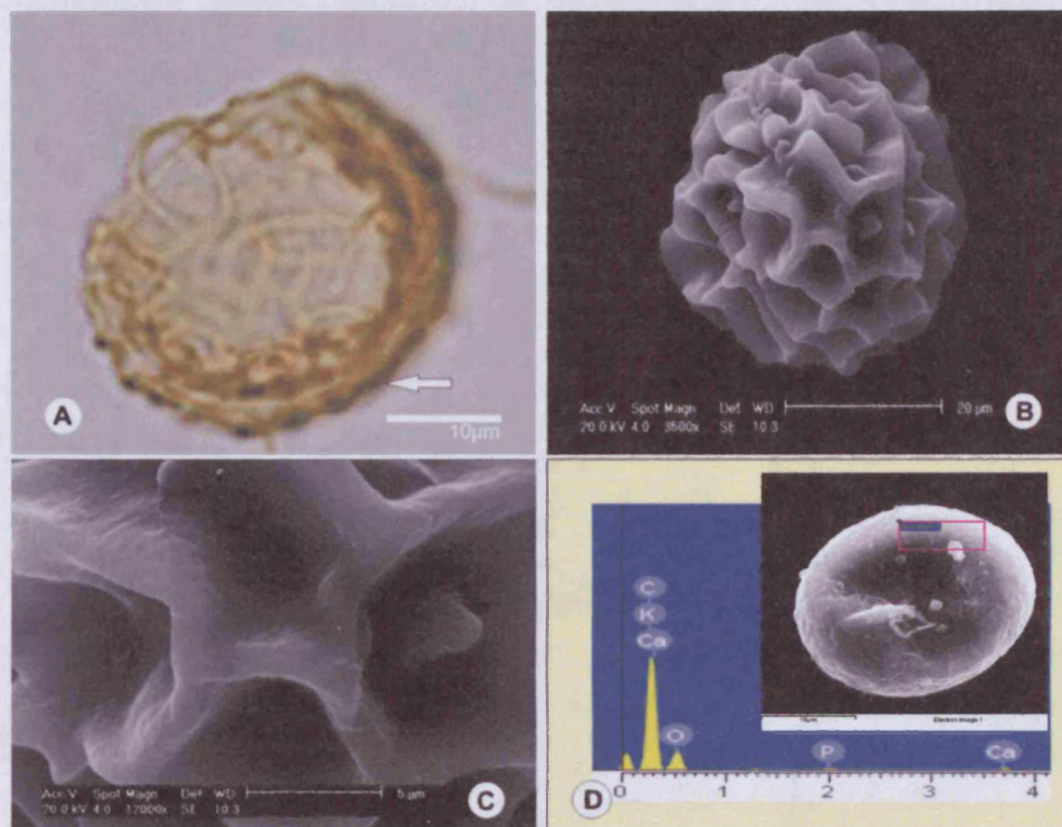


Figure 3.21: *Lastreopsis microsora* as observed by LM **A** and SEM **B** and **C**. The sculpture shows coarse, inflated reticula. **A** note the about 0.05-0.1µm thick perispore (arrow). **D** shows the results of the EDX analysis. No silicon was detected. The SEM picture in **D** shows the area where the EDX analysis was taken.

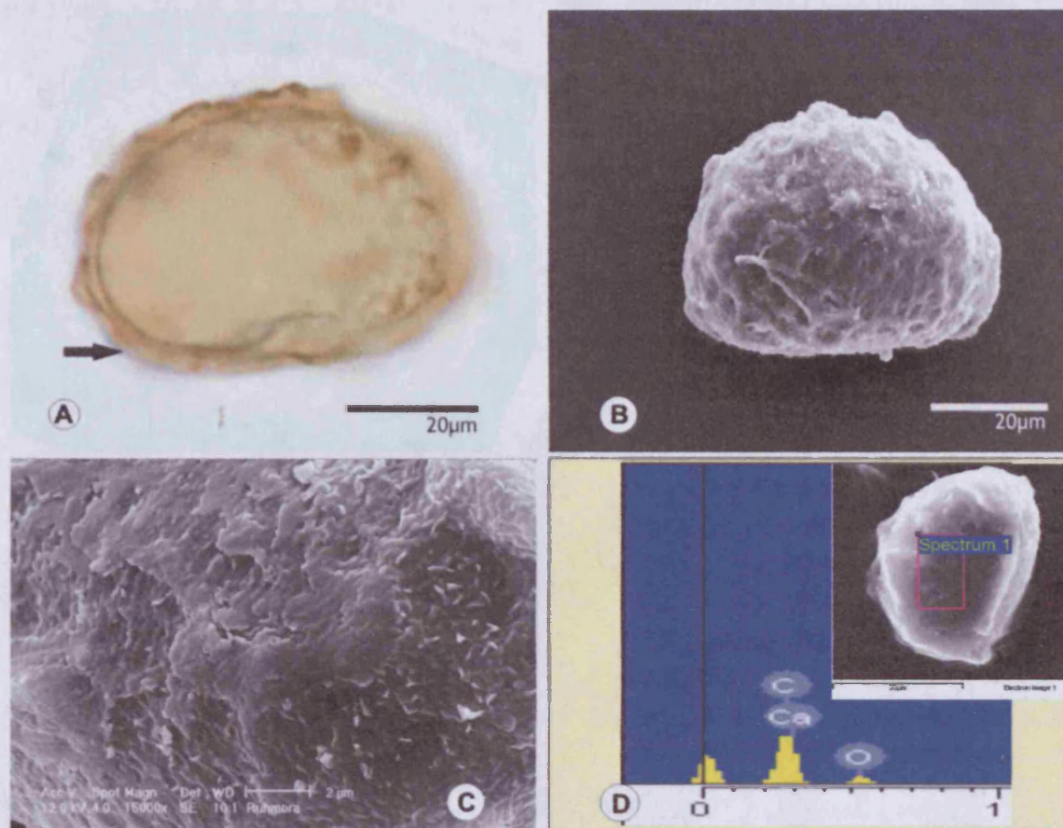


Figure 3.22: *Rumohra adiantiformis* as documented by LM **A** and SEM **B** and **C**. The sculpture shows irregular low verrucae. **A** note the about 0.05–0.1 μ m thick outer part of the perispore (arrow). **D** shows the results of the EDX analysis. No silicon was detected. The SEM picture in **D** shows the area where the EDX analysis was taken.

3.3.1.4 Osmundaceae

Osmunda regalis L. spore walls do not have silicon. Instead carbon, potassium and oxygen were found.

Osmunda regalis

Element	Weight%	Atomic%
C	27.22	33.31
K	0.16	0.06
O	72.63	66.64

Table 3.16: Absence of silicon but occurrence of other elements (in weight % and atomic %) in the spore wall of *Osmunda regalis*.

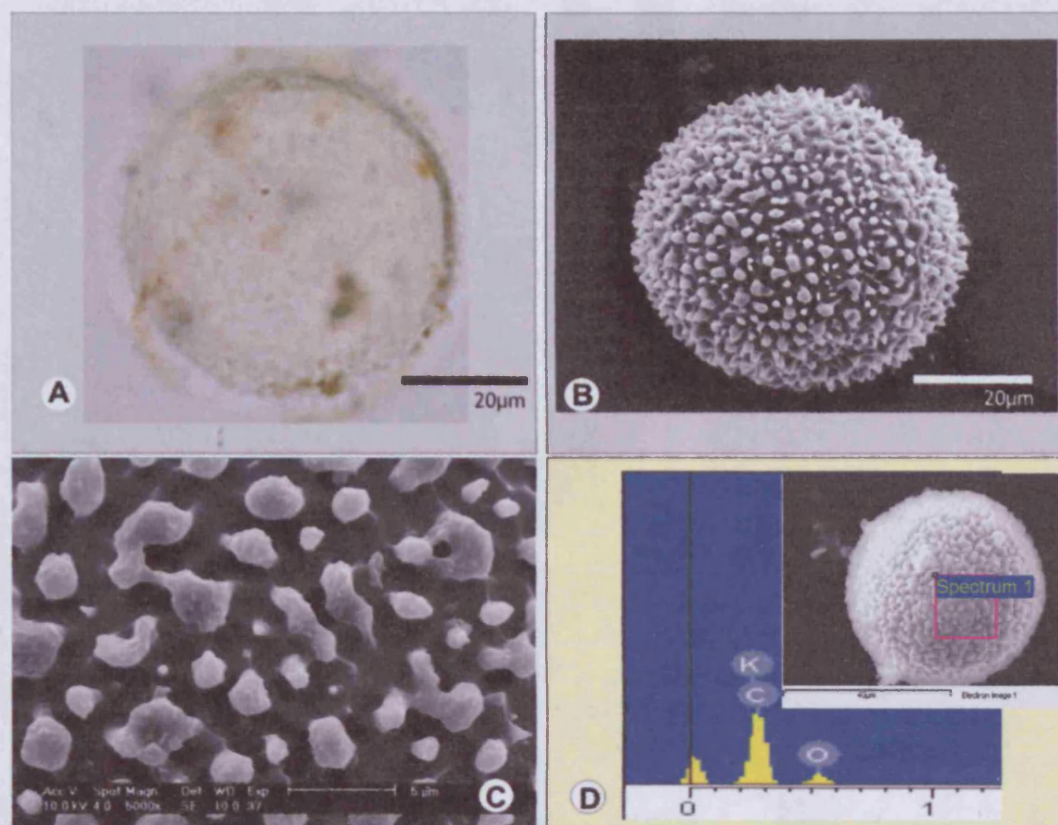


Figure 3.23: *Osmunda regalis* observed by LM **A** and SEM **B** and **C**. **A** and **C** the sculpture is coarsely tuberculate. **D** shows the results of the EDX analysis. No silicon was detected. The SEM picture in **D** shows the area where the EDX analysis was taken.

3.3.1.5 Polypodiaceae

The spore walls of *Phlebodium aureum* (L.) J. Smith show no evidence of silicon. Only oxygen, carbon and potassium were found.

Phlebodium aureum

Element	Weight%	Atomic%
C	72.77	78.13
O	27.06	21.82
K	0.17	0.06

Table 3.17: Absence of silicon but occurrence of other elements (in weight % and atomic %) in the spore wall of *Phlebodium aureum*.

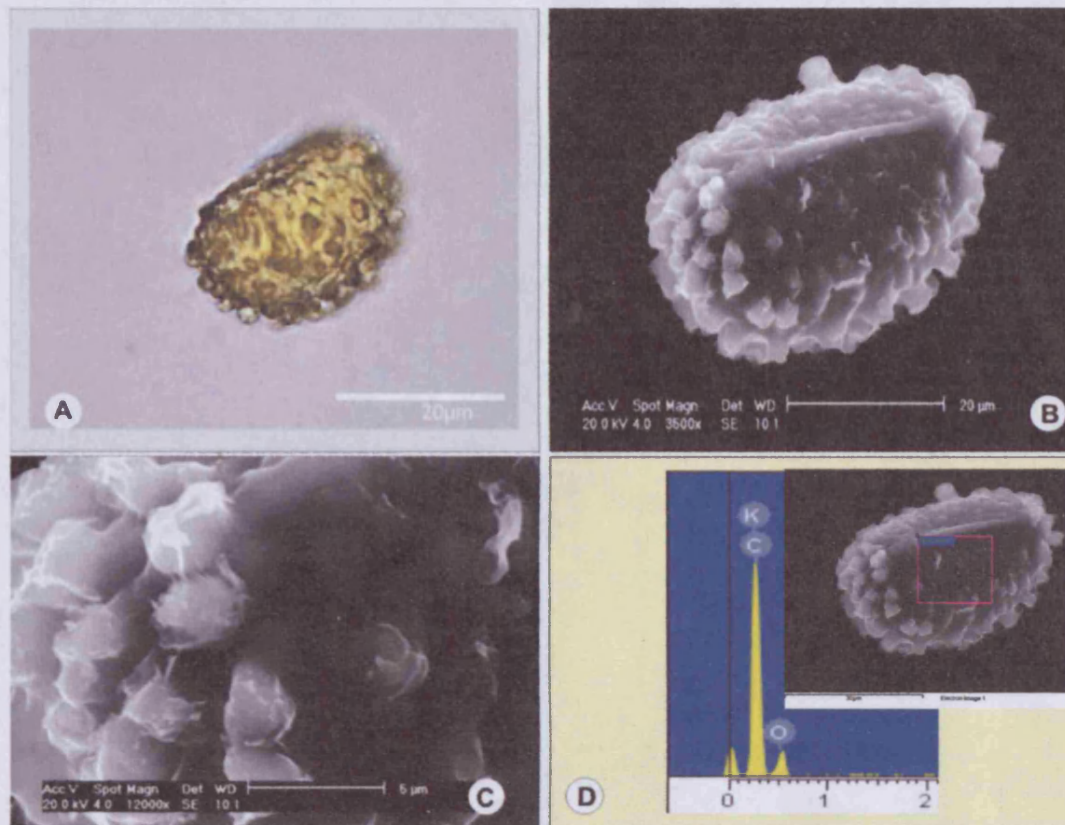


Figure 3.24: *Phlebodium aureum* as observed by LM **A** and SEM **B** and **C**. The sculpture is tuberculate. **D** shows the results of the EDX analysis. No silicon was detected. **B** the area where the EDX analysis was taken is marked by a white frame. **D** the SEM picture shows the area where the EDX analysis was taken.

3.3.1.6 Psilotaceae

The spore wall of *Psilotum nudum* (L.) Beauv. contains carbon and oxygen. No silicon was found.

Psilotum nudum

Element	Weight%	Atomic%
C	66.20	72.31
O	33.80	27.69

Table 3.18: Absence of silicon but occurrence of other elements (in weight % and atomic %) in the spore wall of *Psilotum nudum*.

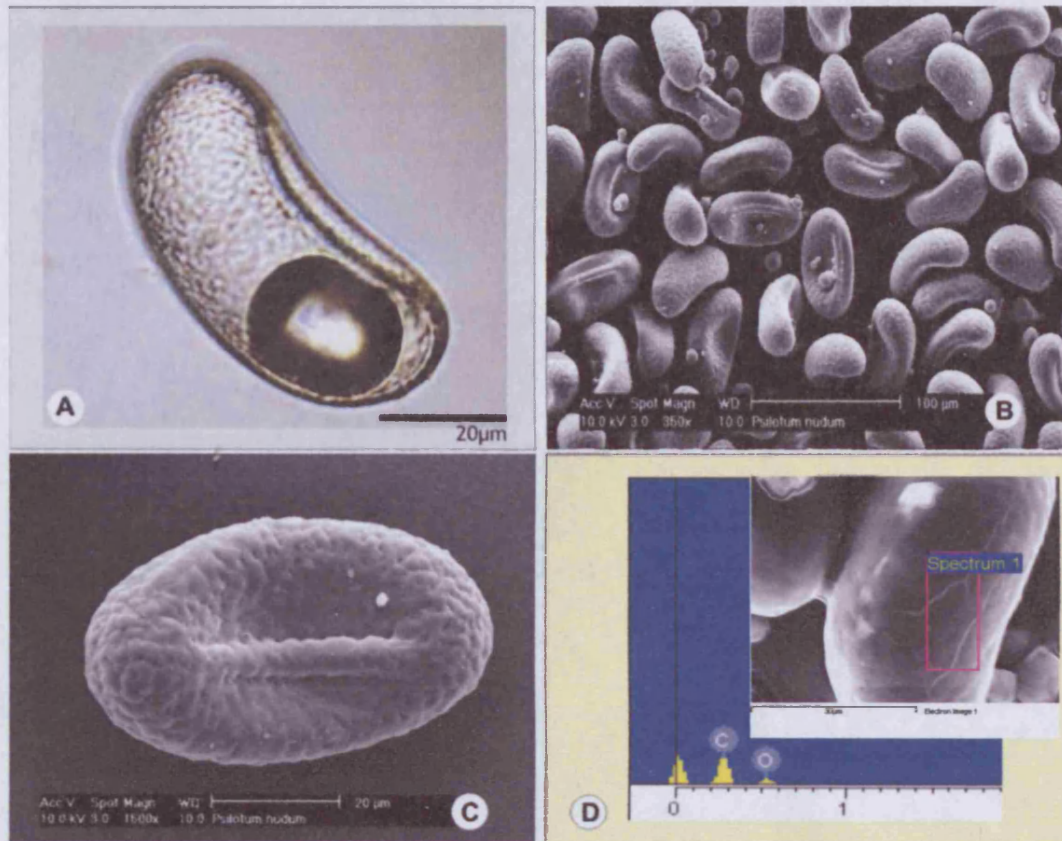


Figure 3.25: *Psilotum nudum* as observed by LM **A** and SEM **B** and **C**. The sculpture is coarsely rugate. **D** shows the results of the EDX analysis. No silicon was detected. The SEM picture in **D** shows the area where the EDX analysis was taken.

3.3.1.7 Pteridaceae

The spore walls of *Pellaea calomelanos* (Swartz) Link, *Pellaea rotundifolia* (Forst.f.) Hook, *Pteris cretica* L. and *Pteris longifolia* L. were analysed. All spore walls contain silicon. Those of *Pellaea calomelanos* also show presence of carbon and oxygen. Whereas immature spores of *Pellaea rotundifolia* contain carbon, oxygen, sodium, magnesium, phosphorus and potassium, in mature spore walls the same elements were detected apart from potassium. Instead sulphur and calcium were detected. In the spore walls of *Pteris cretica* carbon, oxygen, chlorine and calcium were detected and in *Pteris longifolia* carbon, potassium, calcium and oxygen.

Pellaea calomelanos

Element	Weight%	Atomic%
C	63.08	69.88
O	35.29	29.35
Si	1.64	0.77

Table 3.19: Occurrence of silicon and other elements (in weight % and atomic %) in the spore wall of *Pellaea calomelanos*.

Pellaea rotundifolia

Element	Weight%	Atomic%
C	69.76	75.83
O	28.89	23.57
Na	0.37	0.21
Mg	0.14	0.07
Si	0.12	0.06
P	0.22	0.09
K	0.50	0.17

Table 3.20: Occurrence of silicon and other elements (in weight % and atomic %) in the spore wall of *Pellaea rotundifolia* (immature spore).

Pellaea rotundifolia

Element	Weight%	Atomic%
C	61.08	68.75
O	34.85	29.45
Na	0.51	0.30
Mg	0.30	0.16
Si	1.27	0.61
P	0.29	0.12
S	0.29	0.12
Ca	1.41	0.48

Table 3.21: Occurrence of silicon and other elements (in weight % and atomic %) in the spore wall of *Pellaea rotundifolia* (mature spore).

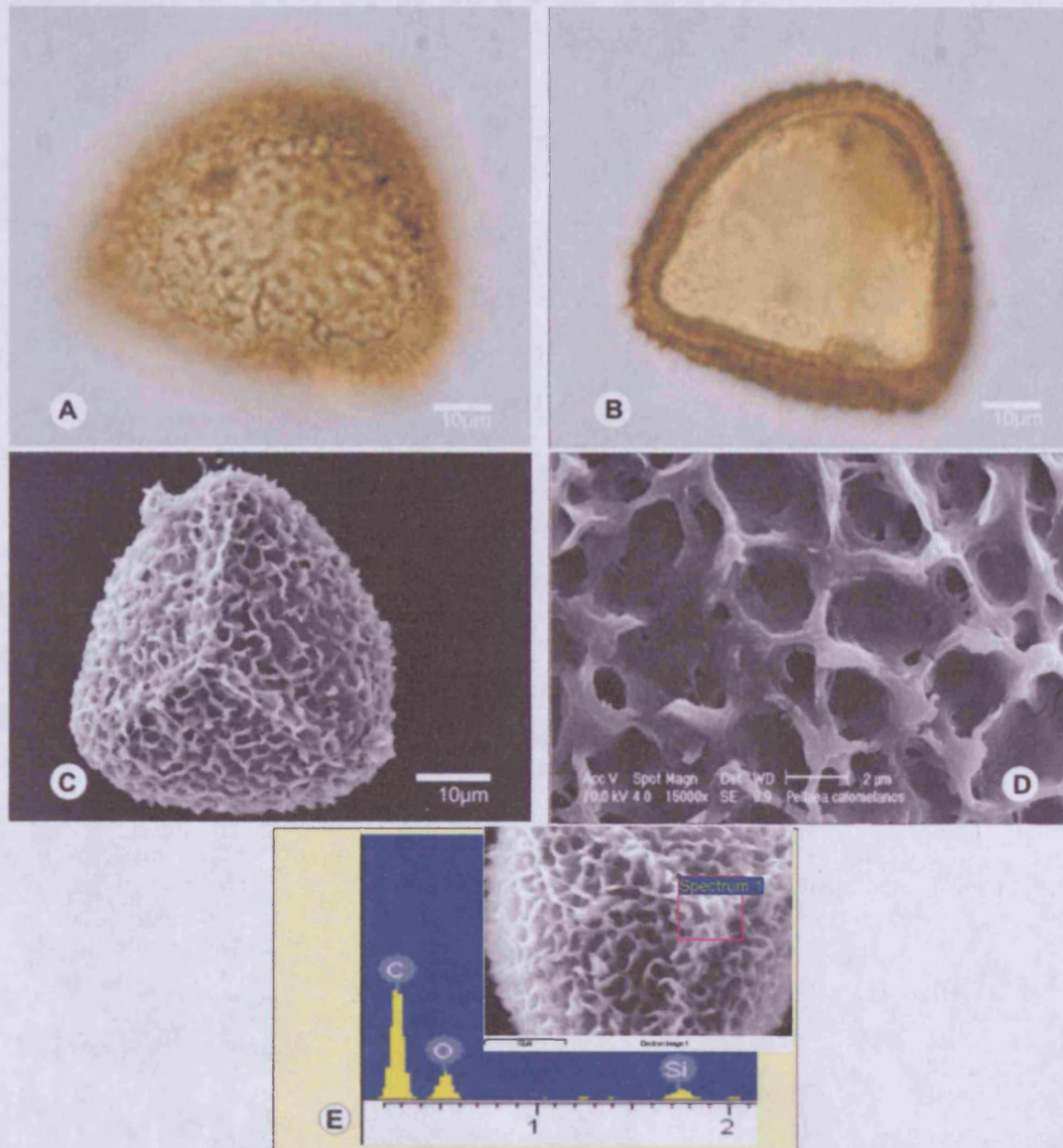


Figure 3.26: *Pellaea calomelanos* documented by LM **A** and by SEM **C-D**. **B** note a cristate perispore, which forms small reticula of 2-4µm in diameter **C**. **D** the exospore is densely granulate. **E** shows the results of the EDX analysis, note silicon peak at 1.8. The SEM picture in **E** shows the area where the EDX analysis was taken.

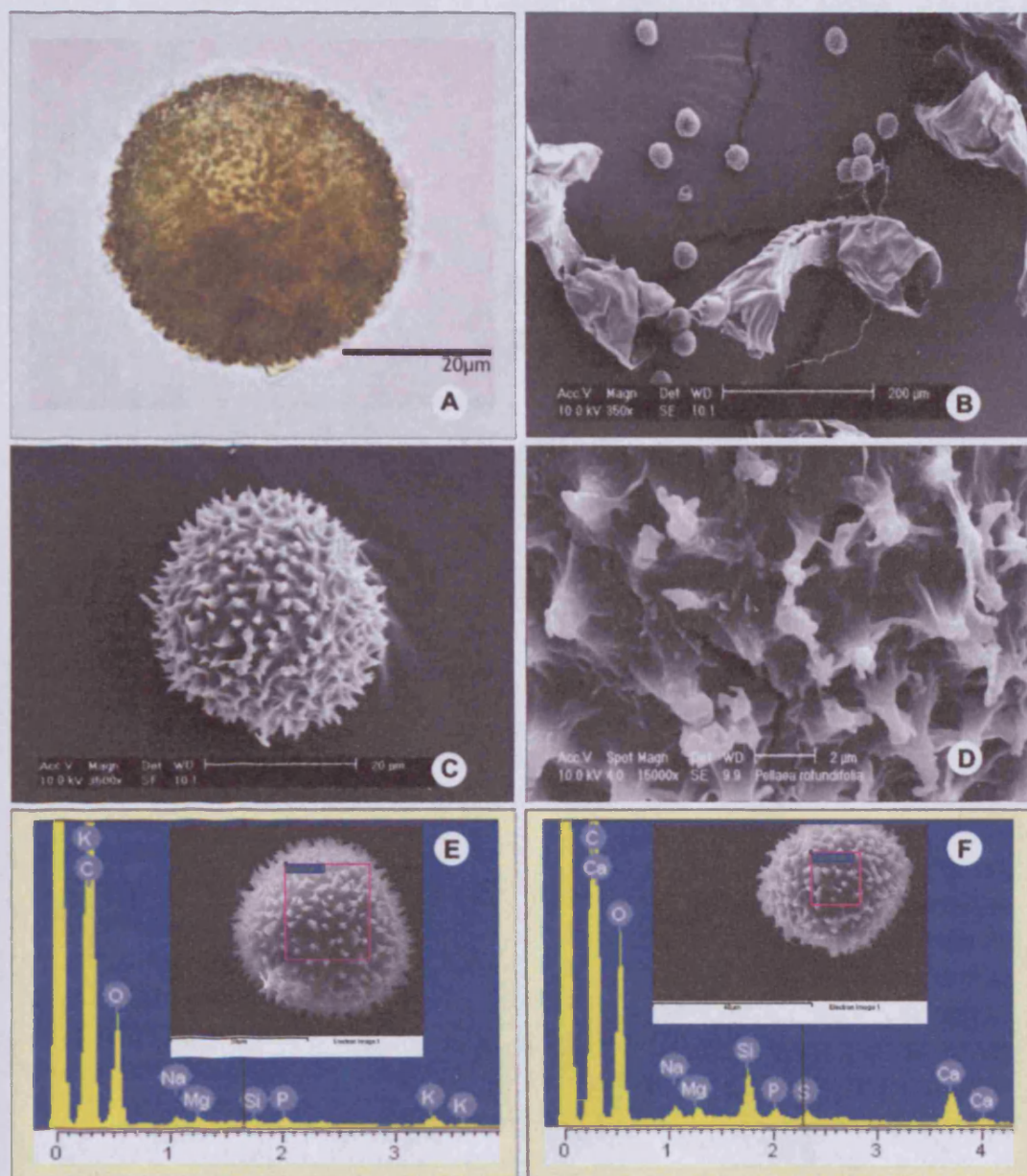


Figure 3.27: *Pellaea rotundifolia* as observed by LM **A** and SEM **B-D**. The sculpture is echinate **C** and **D**. **E** shows the results of the EDX analysis for an immature spore, **F** the results for a mature spore. Note silicon peaks at 1.8. The SEM pictures in **E** and **F** show the area where the EDX analysis was taken.

Pteris cretica

Element	Weight%	Atomic%
C	56.54	64.73
O	38.19	32.79
Si	4.36	2.14
Cl	0.41	0.16
Ca	0.50	0.17

Table 3.22: Occurrence of silicon and other elements (in weight % and atomic %) in the spore wall of *Pteris cretica*.

Pteris longifolia

Element	Weight%	Atomic%
C	68.19	74.67
O	29.78	24.49
Si	0.96	0.45
P	0.33	0.14
Cl	0.17	0.06
K	0.17	0.06
Ca	0.40	0.13

Table 3.23: Occurrence of silicon and other elements (in weight % and atomic %) in the spore wall of *Pteris longifolia*.

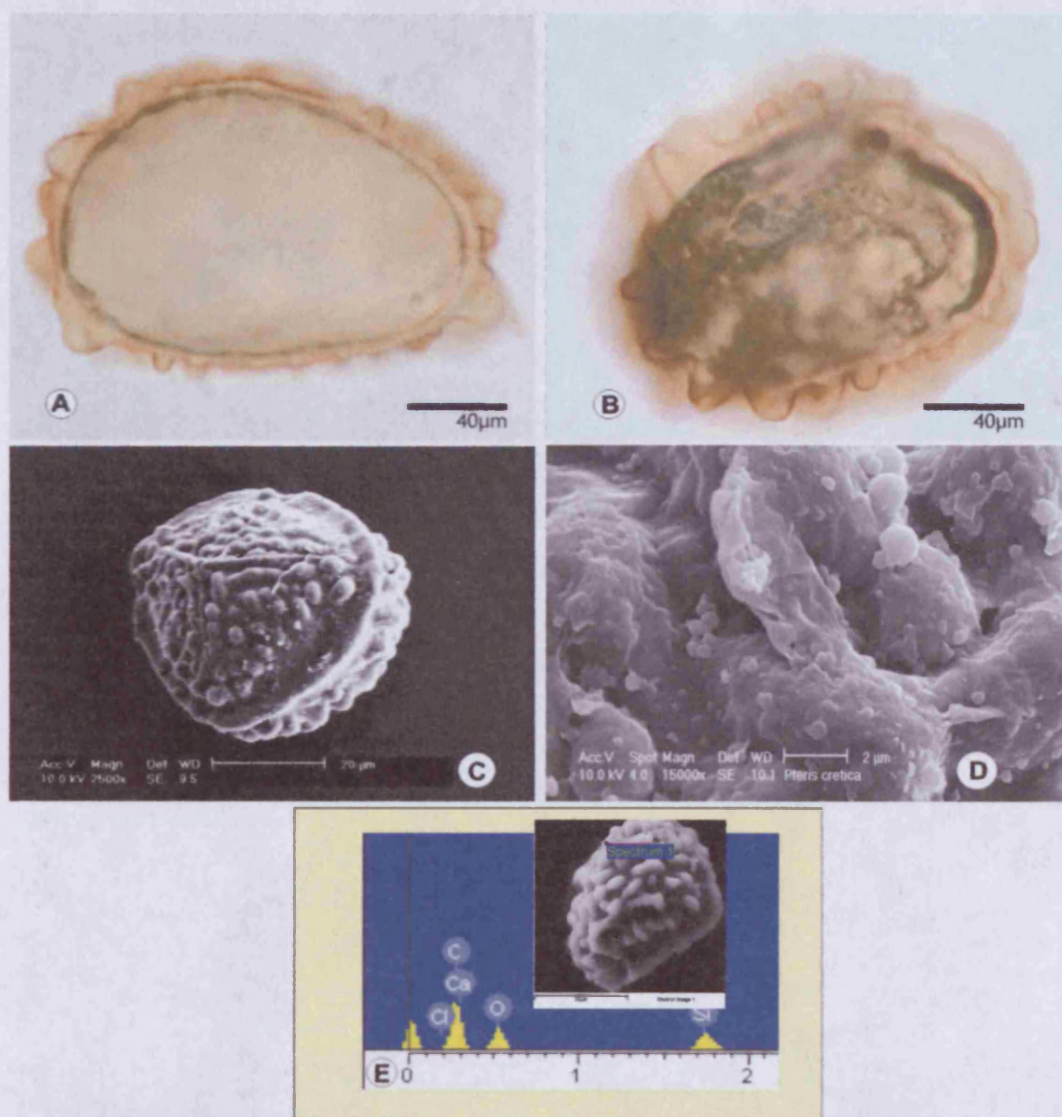


Figure 3.28: *Pteris cretica* documented by LM A and B and by SEM C and D. C and D the sculpture shows proximally a low flange with partly fused tubercles and distally a prominently rugate sculpture. A and B note an about 0.2µm thick perispore (arrow). E shows the results of the EDX analysis, note silicon peak at 1.8. The SEM picture in E shows the area where the EDX analysis was taken.

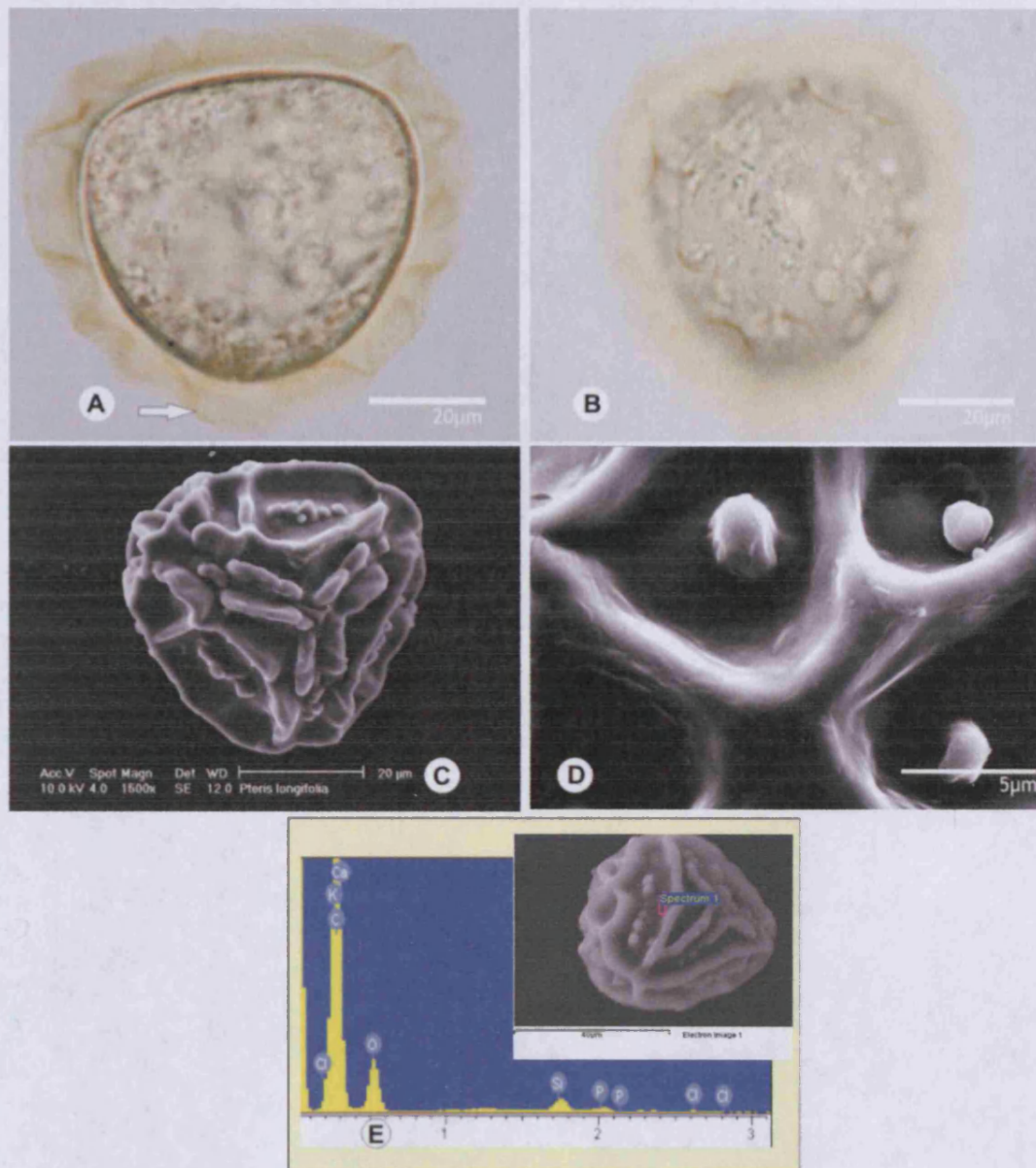


Figure 3.29: *Pteris longifolia* observed by LM **A** and **B** and by SEM **C** and **D**. **C** and **D** the sculpture shows tubercles fused adjacent to the aperture, the distal surface is reticulate with central tubercle. **A** note an about 0.1-0.2µm thick perispore (arrow). **E** shows the results of the EDX analysis, note silicon peak at 1.8. The SEM picture in **E** shows the area where the EDX analysis was taken.

3.3.1.8 Schizaeaceae

Silicon was detected in the spore wall of *Anemia tomentosa* (Sav.) Sw.. Whereas immature spores the walls contain carbon, oxygen, sodium, magnesium, phosphorus, chlorine, potassium and calcium, nearly mature spores additionally show sulphur. In mature spore walls carbon, oxygen, sodium, chlorine and calcium were detected.

Anemia tomentosa

Element	Weight%	Atomic%
C	69.48	75.78
O	28.60	23.42
Na	0.33	0.19
Mg	0.14	0.07
Si	0.13	0.06
P	0.13	0.06
Cl	0.61	0.22
K	0.40	0.13
Ca	0.19	0.06

Table 3.24: Occurrence of silicon and other elements (in weight % and atomic %) in the spore wall of *Anemia tomentosa* (immature).

Anemia tomentosa

Element	Weight%	Atomic%
C	56.11	64.26
O	38.94	33.48
Na	0.65	0.39
Mg	0.22	0.12
Si	1.87	0.91
P	0.15	0.07
S	0.31	0.13
Cl	0.62	0.24
K	0.87	0.31
Ca	0.25	0.09

Table 3.25: Occurrence of silicon and other elements (in weight % and atomic %) in the spore wall of *Anemia tomentosa* (nearly mature).

Anemia tomentosa

Element	Weight%	Atomic%
C	57.79	65.67
O	38.05	32.46
Na	0.34	0.20
Si	2.45	1.19
Cl	0.22	0.08
Ca	1.15	0.39

Table 3.26: Occurrence of silicon and other elements (in weight % and atomic %) in the spore wall of *Anemia tomentosa* (mature).

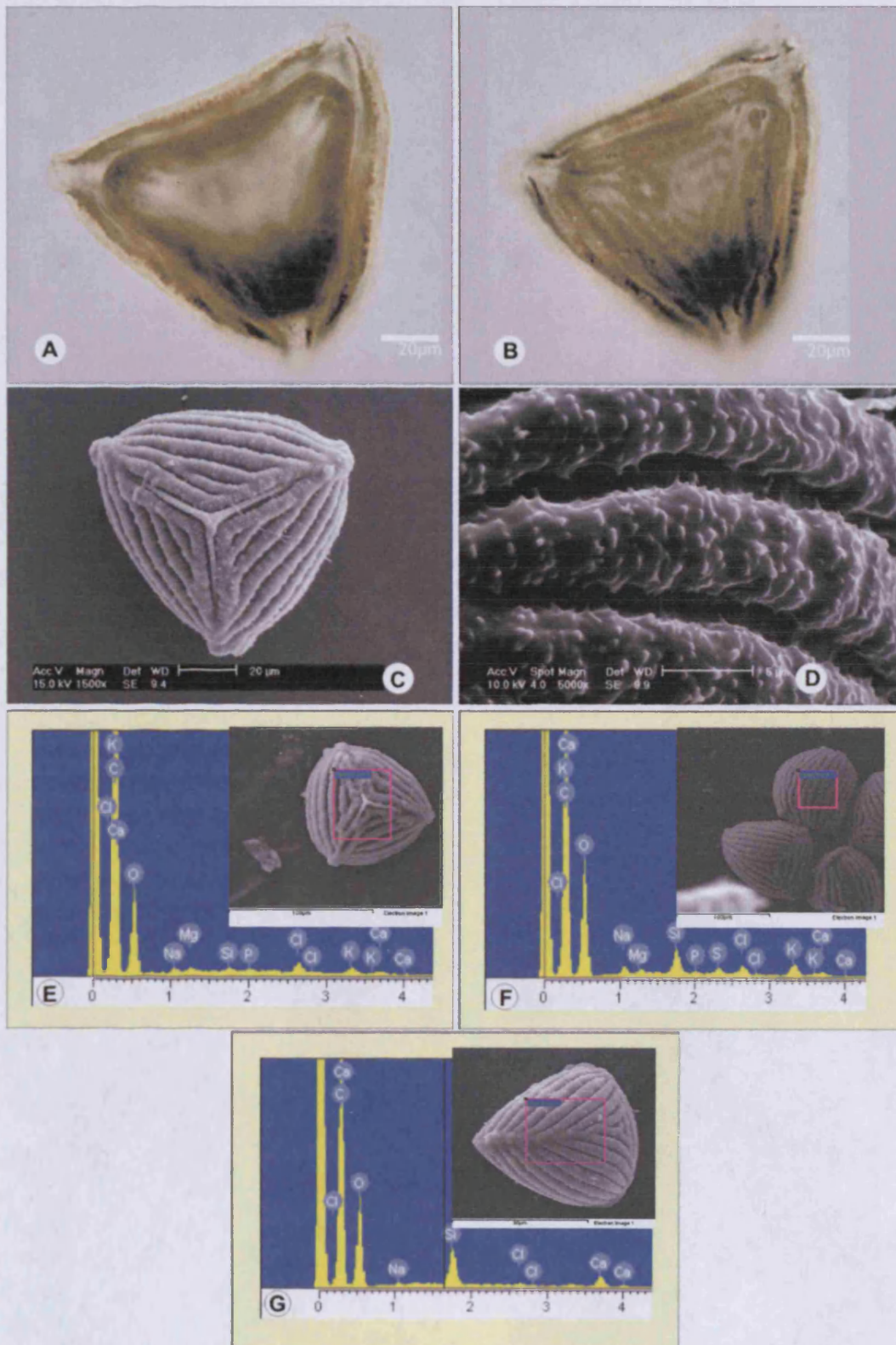


Figure 3.30: *Anemia tomentosa* as observed by LM **A** and **B** and SEM **C** and **D**. **C** and **D** The sculpture is characterised by coarse ridges featuring prominent angles with keel-like structures. **D** the ridges are echinate. **E** shows the results of the EDX analysis for an immature spore, **F** for a nearly mature spore and **G** for a mature spore. Note silicon peaks at 1.8. The SEM pictures in **E-G** show the area where the EDX analysis was taken.

3.3.1.9 Thelypteridaceae

The spore walls of *Macrothelypteris torresiana* (Gaud.) Ching, *Oreopteris limbosperma* (All.) J. Holub, *Phegopteris decursive-pinnata* (v.Hall) Fee and *Thelypteris japonica* (Bak.) Ching and were analysed. All spore walls contain silicon. The spore walls of *Macrothelypteris torresiana* also contain carbon, phosphorus, chlorine, potassium, calcium and oxygen, those of *Oreopteris limbosperma* carbon, magnesium, phosphorus, calcium and oxygen. Whereas immature spores of *Phegopteris decursive-pinnata* contain carbon, oxygen, sodium, phosphorus, sulphur and calcium, mature spores are only lacking phosphorus. Oxygen, carbon and calcium were also detected in *Thelypteris japonica*.

Macrothelypteris torresiana

Element	Weight%	Atomic%
C	66.24	73.05
O	31.59	26.15
Si	0.41	0.19
Cl	0.29	0.11
K	0.57	0.19
Ca	0.91	0.30

Table 3.27: Occurrence of silicon and other elements (in weight % and atomic %) in the spore wall of *Macrothelypteris torresiana*.

Oreopteris limbosperma

Element	Weight%	Atomic%
C	26.75	32.88
Mg	0.11	0.07
Si	0.58	0.31
P	0.10	0.05
Ca	0.16	0.06
O	72.28	66.63

Table 3.28: Occurrence of silicon and other elements (in weight % and atomic %) in the spore wall of *Oreopteris limbosperma*.

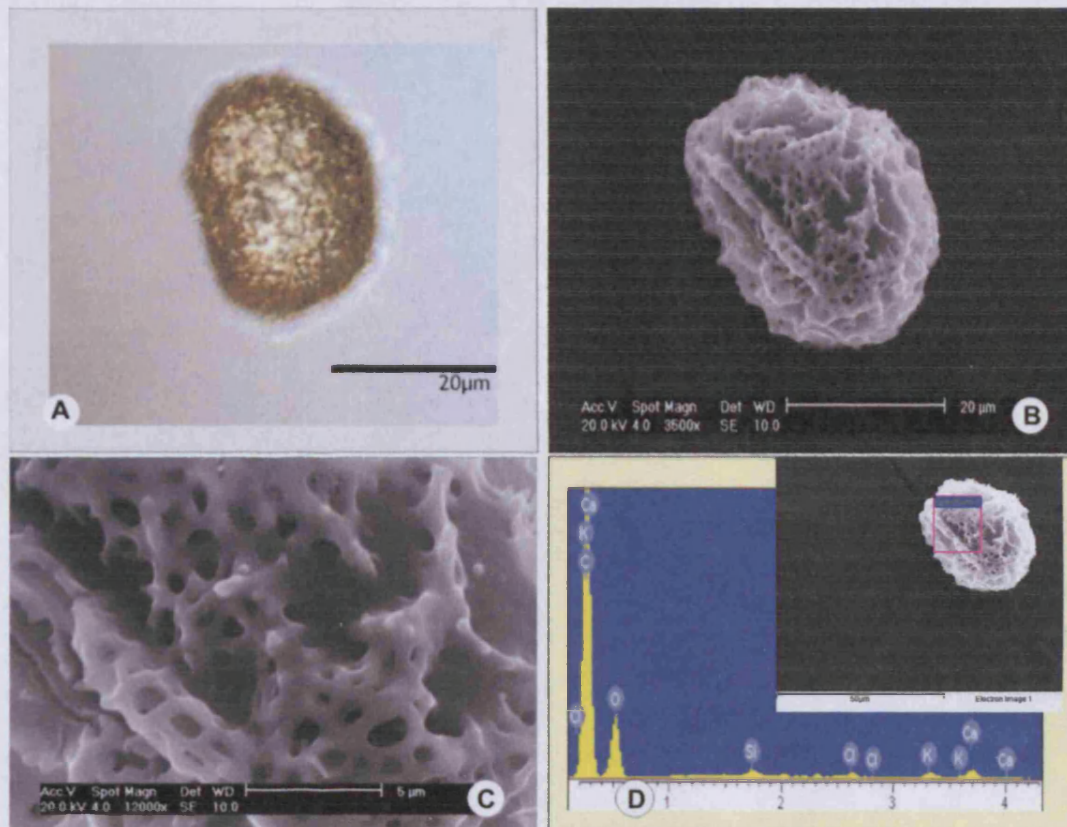


Figure 3.31: *Macrothelypteris torresiana* documented by LM **A** and by SEM **B** and **C**. **B** and **C** the sculpture is irregularly folded and perforated. **D** shows the results of the EDX analysis, note silicon peak at 1.8. The SEM picture in **D** shows the area where the EDX analysis was taken.

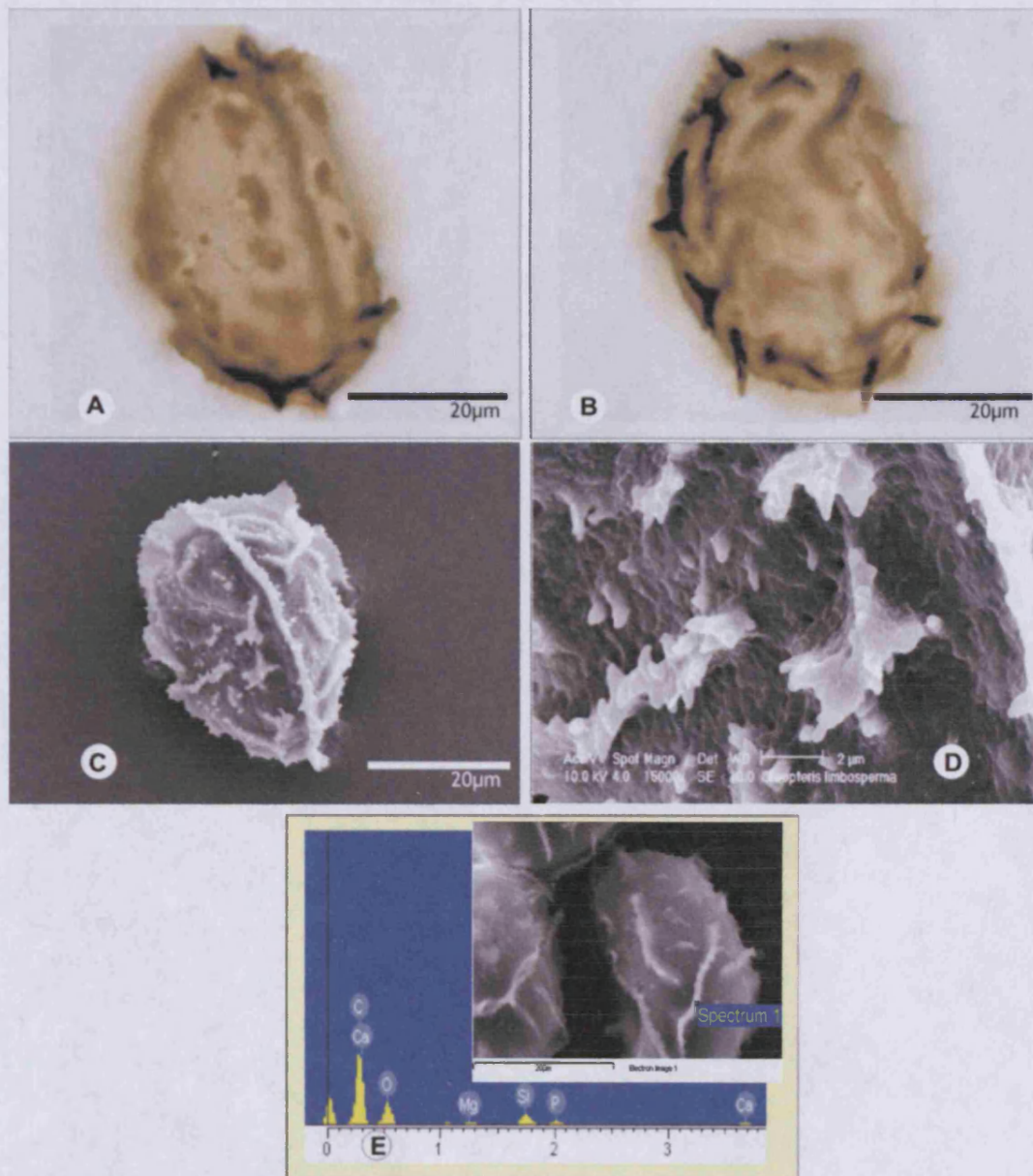


Figure 3.32: *Oreopteris limbosperma* as observed by LM **A** and **B** and SEM **C** and **D**. **C** and **D** the sculpture is cristate with echinate ridges. **E** shows the results of the EDX analysis, note silicon peak at 1.8. The SEM picture in **E** shows the area where the EDX analysis was taken.

Phegopteris decursive-pinnata

Element	Weight%	Atomic%
C	63.73	70.78
O	33.52	27.95
Na	0.64	0.37
Si	1.17	0.56
P	0.14	0.06
S	0.18	0.07
Ca	0.62	0.21

Table 3.29: Occurrence of silicon and other elements (in weight % and atomic %) in the spore wall of *Phegopteris decursive-pinnata* immature spore).

Phegopteris decursive-pinnata

Element	Weight%	Atomic%
C	64.61	72.10
O	30.63	25.66
Na	0.74	0.43
Si	3.08	1.47
S	0.36	0.15
Ca	0.58	0.19

Table 3.30: Occurrence of silicon and other elements (in weight % and atomic %) in the spore wall of *Phegopteris decursive-pinnata* (mature spore).

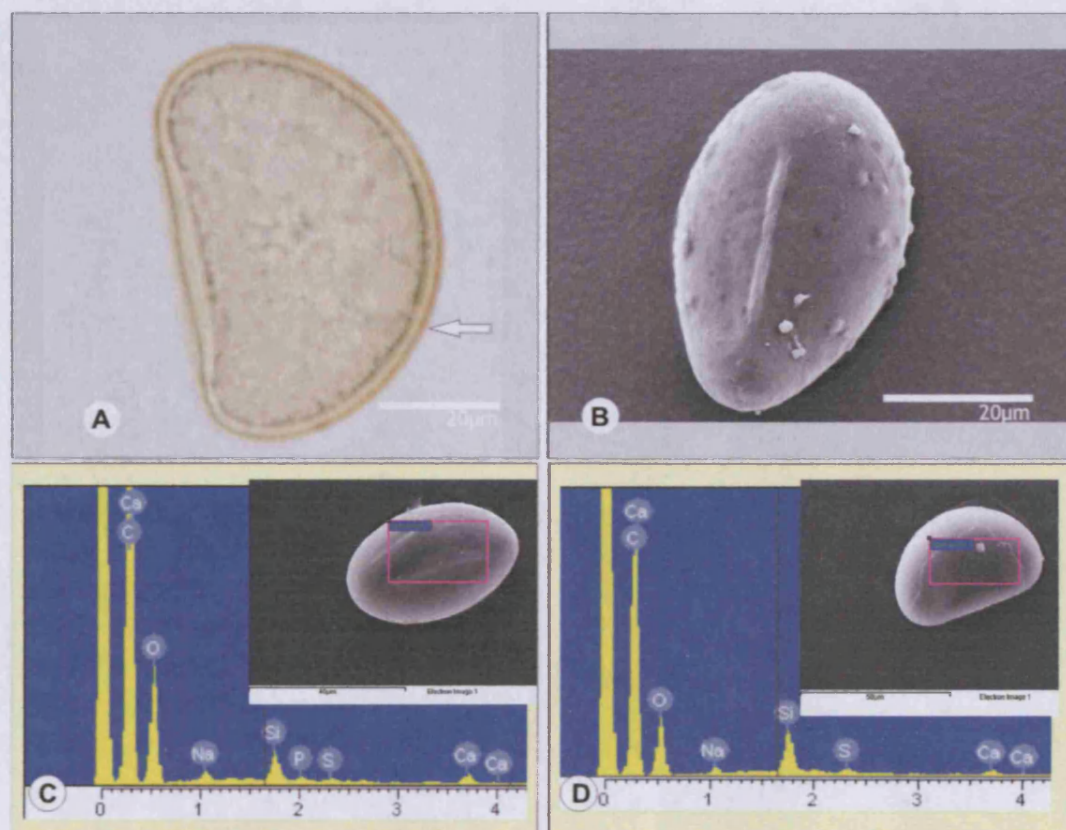


Figure 3.33: *Phegopteris decursive-pinnata* documented by LM **A** and SEM **B**. **B** the sculpture is laevigata with some scattered tubercles. Note the about 0.2µm thick perispore in **A** (arrow). **C** shows the results of the EDX analysis for an immature spore, **D** the results for a mature spore. Note silicon peaks at 1.8. The SEM pictures in **C** and **D** show the area where the EDX analysis was taken.

Thelypteris japonica

Element	Weight%	Atomic%
C	63.85	70.54
O	35.01	29.04
Si	0.36	0.17
Ca	0.78	0.26

Table 3.31: Occurrence of silicon and other elements (in weight % and atomic %) in the spore wall of *Thelypteris japonica*.

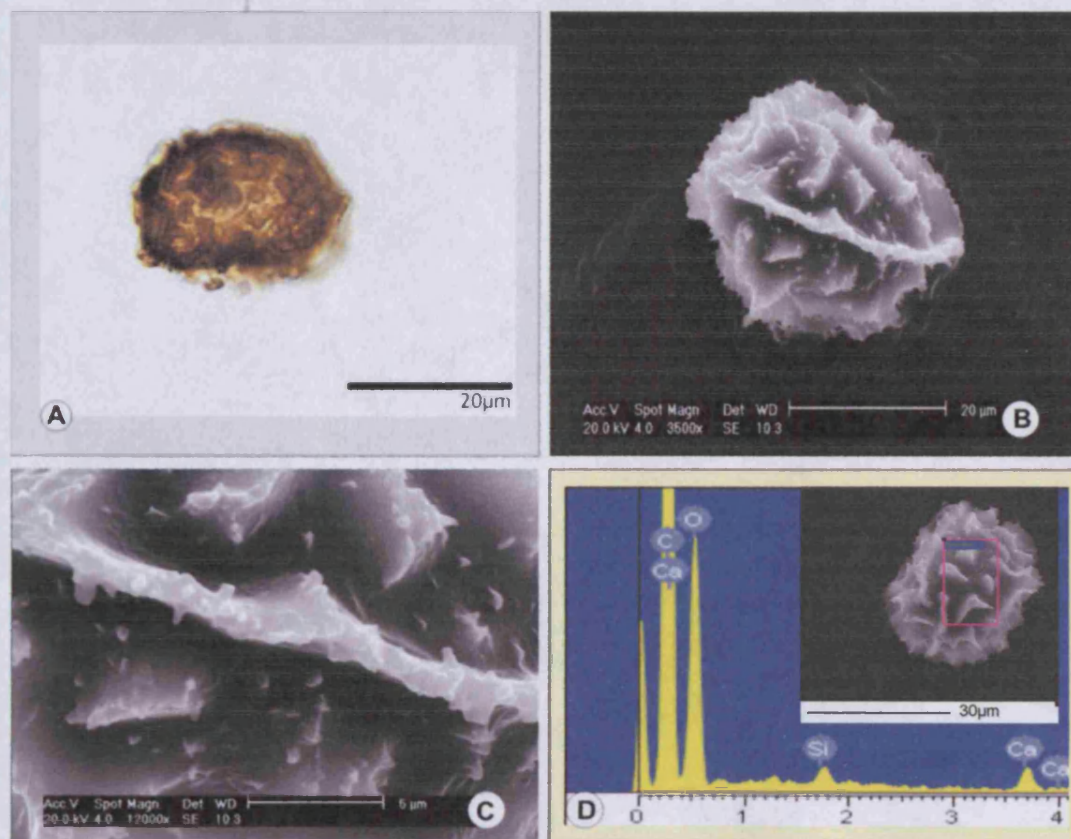


Figure 3.34: *Thelypteris japonica* as observed by LM **A** and by SEM **B** and **C**. **C** the sculpture is irregularly folded. **D** shows the results of the EDX analysis, note silicon peak at 1.8. The SEM picture in **D** shows the area where the EDX analysis was taken.

3.3.2 Discussion

Detection of silicon by EDX analysis EDX-analysis combined with SEM is a standard technique often used in plant science in order to determine chemical components in various parts of a plant. This technique has also been utilised for the detection of silicon in plants (Crang and May 1974; Tryon and Lugardon 1978; Dengler and Lin 1980; Sangster and Hodson 1986; Parry *et al.* 1986; Hodson and Sangster 2002).

Since spore walls are extremely diverse in their morphology, the sculpture can range from entirely laevigate to reticulate, echinate, rugate, tuberculate or flanged. This means that the spore surface itself can be very uneven and therefore poses the first hurdle when carrying out EDX analysis. Rough-surfaced specimen can alter the detection of its own emission, often resulting in misleading and inaccurate data (Watt 1997). Apart from problematic spore morphologies, it would also be necessary to orientate spores into the same angle towards the detector in order to gain comparable data. With spores being globose, spherical or ellipsoidal, in other words often having very different shapes, this is quite a challenge, particularly in respect to sample preparation. Spore diameters normally range between 20-50µm. Another important aspect is the calibration of the EDX system. Ideally, a spore with known silicon content should be used as standard. This, however, is impossible, mainly because the extraction of silicon from a single spore cannot be achieved. This, as well as the interaction of silicon with sporopollenin and other spore wall components, is discussed in more detail below. I will continue to use the term silica, as I will be discussing the compound (silica) and not the element (silicon). Whenever the work of other authors is cited, I will, however, use their terminology.

The main aim of this investigation was to gain preliminary data on the occurrence and distribution of silica in pteridophyte spore walls, which has not been studied before.

Evolutionary levels in spore walls and silica Although the occurrence of silica was reported in *Selaginella* megaspores (Tryon and Lugardon 1978; Moore *et al.* in press a), in *Anemia phyllitidis* (Schizaeaceae)

spores (Schraudorf 1984) and in the spores of *Lygodium* (Schizaeaceae) (Edman 1932), the extent to which it occurs in other pteridophyte spore walls is unclear. Therefore, 24 pteridophyte species from 9 different families (Blechnaceae, Davalliaceae, Dryopteridaceae, Osmundaceae, Polypodiaceae, Psilotaceae, Pteridaceae, Schizaeaceae and Thelypteridaceae) were investigated. The study includes primitive, derived and "specialised" (*sensu stricto* Tryon 1990; Tryon and Lugardon 1990) families. The terminology refers to the evolutionary levels in the spore walls and the distribution of various fern families into these three categories is provided in figure 3.35, below.

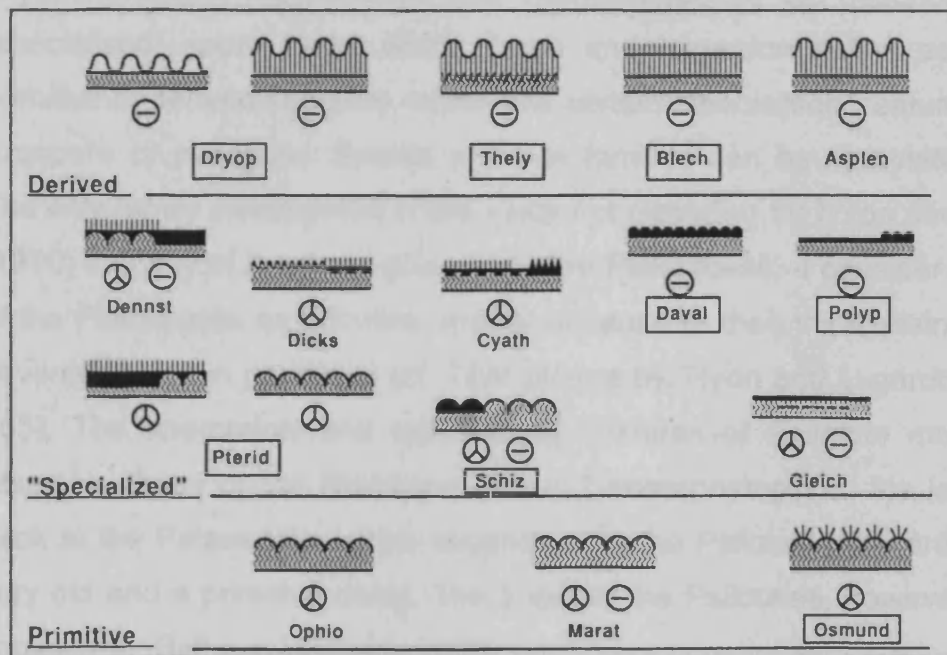


Figure 3.35: Modified after Tryon and Lugardon (1990), p.21 Introduction. The figure shows the three evolutionary levels of wall structure in fern spores: primitive, derived and "specialised". A box frames the families investigated in this study. Aperture: trilete (three radii in a circle) or monolete (bar in circle). Exospore: undulate lines in lower layer. Perispore: solid black. Inner perispore: vertical lines below surface. Rodlets: short lines perpendicular to outer surface. Flanged exospore: broken line. Family abbreviations: **Aspleniaceae**, **Blechnaceae**, **Cyatheaceae**, **Davalliaceae**, **Dennstaedtiaceae**, **Dicksoniaceae**, **Dryopteridaceae**, **Gleicheniaceae**, **Marattiaceae**, **Ophioglossaceae**, **Osmundaceae**, **Polypodiaceae**, **Pteridaceae**, **Schizaeaceae**, **Thelypteridaceae**.

The fern families investigated in the present study are categorised as follows: Osmundaceae are classified as a primitive family, Pteridaceae, Schizaeaceae and Davalliaceae as derived and Dryopteridaceae, Blechnaceae,

Thelepteridaceae as “specialised”. According to Tryon and Lugardon a primitive wall structure is characterised by a thick exospore overlain by a thin perispore, as found in Osmundaceae. With their trilete spores *Osmunda* spores show the feature mentioned above and are very similar in all three genera. It is noteworthy that *Osmunda* spores (often called “green spores”) incorporate chloroplasts, which gives them a green appearance. Pteridaceae, Schizaeaceae and Davalliaceae have derived spore walls, which means that their spore wall is usually formed by an elaborate perispore that overlies a relatively plain, thinner exospore. Their spores are often monolete and perispore development varies in number and thickness of individual layers. Dryopteridaceae, Blechnaceae and Thelepteridaceae are described to have “specialised” spore walls, which Tryon and Lugardon define as an either primitive or derived structure, which has certain “specialised” features in either exospore or perispore. Spores of these families can be monolete or trilete. The only family investigated in this study not classified by Tryon and Lugardon (1990) into any of the three groups are the Psilotaceae. I consider the spores of the Psilotaceae as primitive, mainly because of their thick, plain exospore, covered by a thin perispore (cf. TEM picture by Tryon and Lugardon 1990, p. 563). The anatomical and reproductive features of *Psilotum* more or less resemble those of the Rhyniopsida and Trimerophytopsida, the latter dating back to the Palaeozoic, which suggests that the Psilotales are presumably a very old and a primitive clade. The origin of the Psilotales, however, remains conjectural (Bell and Hemsley 2000).

With *Osmunda regalis* (Osmundaceae) and *Psilotum nudum* (Psilotaceae) showing no silica in their spore walls (see tables 3.16 and 3.18), the results suggest that silica incorporation into spore walls could be restricted to the derived and “specialised” families. Since neither Marattiaceae, Ophioglossaceae nor further species of the Osmundaceae or Psilotaceae were investigated, it remains unclear whether this is a general trend.

Among the derived families, all species investigated of the Blechnaceae (*Doodia aspera* and *Blechnum occidentale*) as well as the Thelepteridaceae (*Oreopteris limbosperma*, *Macrothelypteris torresiana*, *Phegopteris decursive-pinnata* and *Thelypteris japonicum*) are characterised by a siliceous spore wall. This stands in contrast to the Dryopteridaceae, in which out of 8 species

investigated (*Cyrtomium falcatum*, *Cyrtomium fortunei*, *Diplazium proliferum*, *Dryopteris eritrorosa*, *Dryopteris stewartii*, *Hypodematium fauriei*, *Lastreopsis microsora*, *Polystichum polyphyllum* and *Rumohra adiantiformis*) only one species (*Diplazium proliferum*) contains silica. There seems no correlation between the evolutionary level of the spore wall and the occurrence of silica in the spore walls. This view is reinforced by the insights gained from the “specialised” families. Whereas the 4 species examined in the Pteridaceae (*Pellaea calomelanos*, *Pellaea rotundifolia*, *Pteris cretica*, *Pteris longifolia*) and *Anemia tomentosa* (Schizaeaceae) all incorporate silica into their spore walls, for two species of the Davalliaceae (*Davallia mariesii*, *Nephrolepis hirsutula*) and *Phlebodium aureum* (Polypodiaceae) no silica was found. It is acknowledged, that in relation to the vast number of species in families like the Polypodiaceae or Dryopteridaceae, only a very small number of fern spore were investigated in this study. The results add weight to the hypothesis that silica occurrence in pteridophyte spore walls is a random feature, which has so far been overlooked and seems independent from the evolutionary level of spore wall organisation.

Silica and pteridophyte systematics When comparing the occurrence of silica in spore walls with the systematic positions of the individual families studied, it becomes obvious that there is no correlation between silica distribution and phylogenetic relationships (figure 3.36).

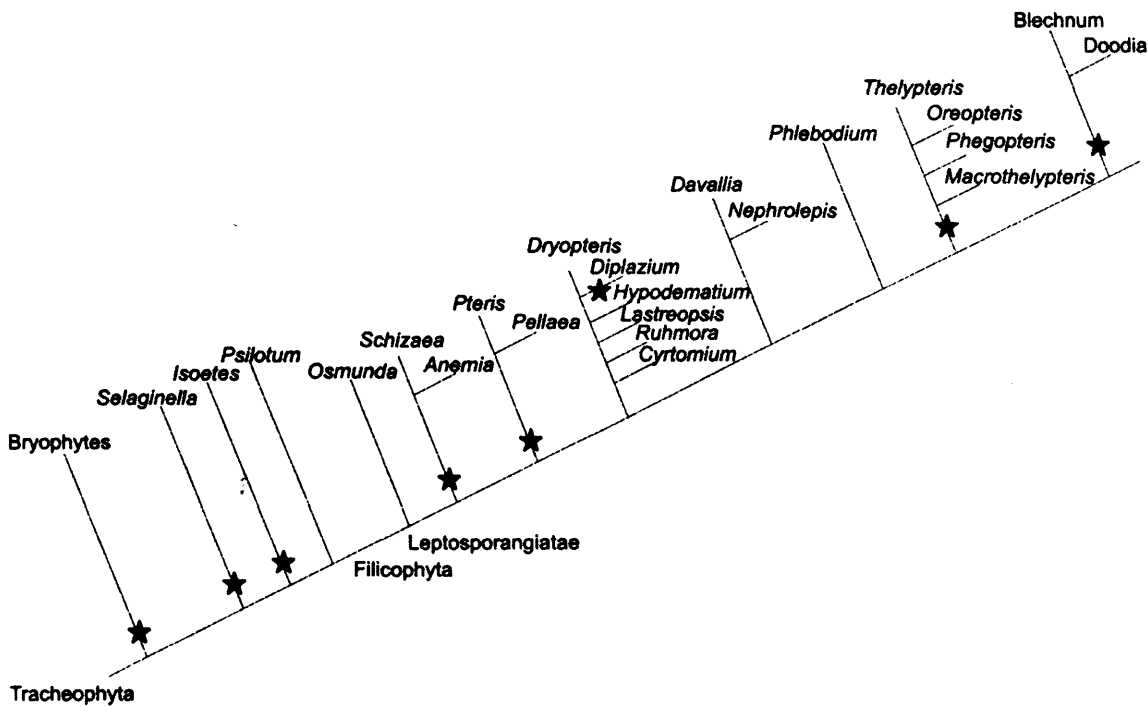


Figure 3.36: Occurrence of silica (asterisk) in bryophyte and pteridophyte spore walls. The figure is based on a phylogramme by Stevenson & Loconte (1996). Silica distribution is random as there is no correlation between pteridophyte systematics and the accumulation of silica. The feature must have evolved in parallel. Habitat and ecology of the different fern genera also provide no explanations for the occurrence of silica in spore walls.

Bryophytes incorporate small quantities of silica into their spore walls (*section 3.5*) and are also known to be silicon-accumulators (Epstein 1999). Silicon-accumulation could have evolved very early in evolution since the fossil record of bryophytes probably dates back to the Ordovician (Wellman *et al.* 2003). Maceration and acetolysis techniques as well as diagenesis, however, would have destroyed all evidence of silica in fossil bryophyte spore walls, since silica is not resistant to HF treatment. The random distribution of silica among pteridophytes, however, suggests that this feature evolved in parallel in different families at different times and is independent from phylogenetic relationships and probably also from their ecology or habitat. A study carried out by Parkinson (1994) looking at *Schizaea pectinata* species from two very different habitats, revealed an intra-specific variability in spore wall morphology. This is a very important and interesting study with much impact on the interpretation of spore walls and the establishment of characters for systematic relationships. This is not as much a problem for extant pteridophyte systematics, as it is for the fossil record. Whereas for the systematics of extant pteridophytes abundant genetic, anatomical and

morphological characters can be taken into consideration, this is often very difficult to achieve with spores from the fossil record. In my opinion, Parkinson's results question attempts to reconstruct systematic relationships of dispersed spore species, for which palynologists sometimes might overestimate the information derived from spore wall characters. The extant species *Pteris longifolia* (Pteridaceae) has both monolete and trilete spores (Tryon and Lugardon 1990, p.189). One has to ask the question whether studies would have placed these spores into the same species, were they to have been fossil, dispersed spores. These spores would have presumably undergone harsh chemical treatment, which might have affected spore morphology, making sporoderm identification more difficult.

Silica in exospore and perispore / spore wall interaction It is suggested from the results that the perispore and presumably also, to some extent, the exospore of pteridophytes can either be siliceous or not. It is, however, extremely difficult to judge if a presence of silica means that both layers are siliceous or only one of them and a definite answer as to which of the two layers contains silica cannot be achieved with this technique. With a varying degree of true perispore thickness (between 0.17 μm in *Psilotum nudum* and 1.4 μm in *Blechnum occidentale*, measured from TEM pictures by Tryon and Lugardon, 1990) and the electron beam normally penetrating into the sample at a depth of up to 4 μm (Watt 1997), EDX-analysis also picks up signals from the underlying exospore. Attempts to isolate the perispore are described in *chapter 4* and have clearly demonstrated that only a harsh treatment with MMNO successfully removed the perispore in *Selaginella pallescens* (Selaginellaceae). Since it is unknown how and to what extent MMNO reacts with the spore wall compounds and because reactions of MMNO with silica complexes cannot be excluded, it is assumed that further studies into this direction may well prove futile. Moreover, the quantities isolated are too small for tests on organo-silicon compounds and these have therefore not been carried out.

The pathway of silica transport into the spores is unknown. Some authors looked at the mineral content of spores (Edman 1932; Kempf 1970; Tryon and Lugardon 1978; Schraudorf 1984; Rowley and Morbelli 1995; Morbelli 1995)

and pollen (Crang and May 1974) but only speculated on silica and spore wall interactions. Most of the studies on silica and spore wall interaction were done using *Selaginella* megaspores. For details on spore wall terminology in *Selaginella*, see figure 1.2 in section 1.4.2 Terminology.

Kempf (1970) studied the spores of *Selaginella galeottii*, *S. selaginoides*, *S. usta* and closer investigated the silification of the spore walls. He noted that the siliceous coating consists of 0.5-1 μ m long and 0,03 μ m wide needles, which can also occur within the perine (terminology *sensu* Kempf). A needle or sheet like structure in the siliceous coating was also reported by Edman (1932). These needles can clearly be seen in TEM section (figure 3.37B below), as observed in an unidentified *Selaginella* species (Moore 2001). A comparison with SEM pictures of the spore sculpture (figure 3.37A and B below) reveals that these siliceous needles reflect spore micro-morphology, especially in species which exhibit an echinate micro-sculpture. The broader sheets, as described by Edman (1932) are also shown on the TEM picture (figure 3.37B).

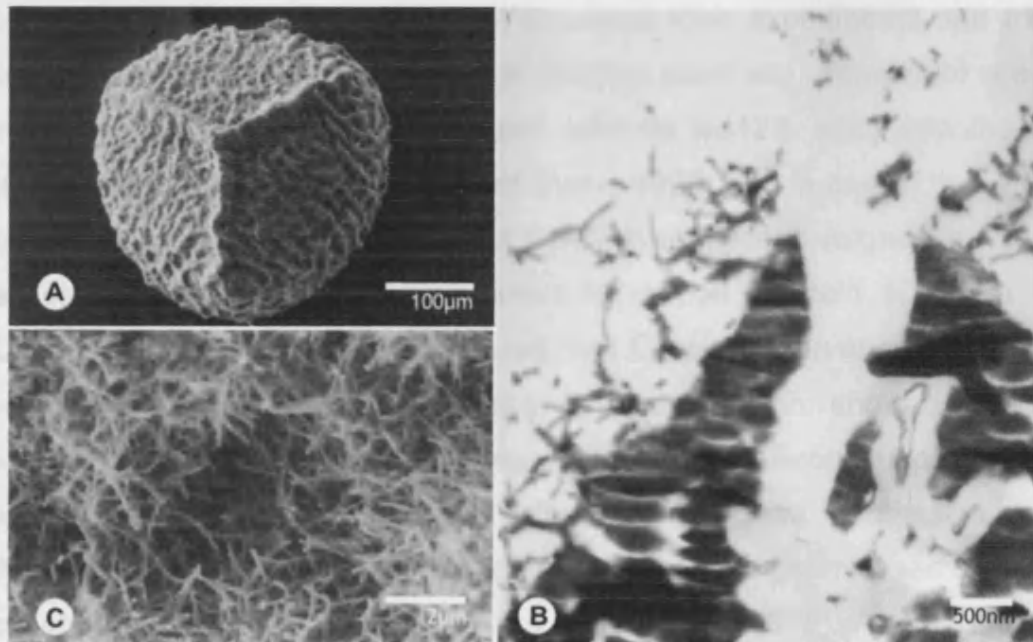


Figure 3.37: An unidentified *Selaginella* species, referred to as *Selaginella* sp.12 in Moore (2001). **A** shows the proximal face of the megaspore and **C** the finely echinate micro-sculpture. Note fine siliceous needles on the TEM picture **B** as well as the broad sheets of silica coating (electron dense material) as described by Edman (1932).

On higher magnification Kempf observed that some needles have a white central line of 5nm width, which he interpreted as cellulose. He suggests that

cellulose and sporopollenin could favour the incorporation of silica into the spore wall but does not discuss this any further. Since not much is known about silica and spore wall interactions this process remains conjectural.

Crang and May (1974) demonstrated the presence of silica in pollen walls of *Lychnis alba* Mill. (Caryophyllaceae) and *Impatiens sultanii* Hook. f. (Balsaminaceae) by X-ray diffraction analysis of both fresh (undried) and air-dried samples and by EDX analysis in combination with SEM. They observed a tendency of silica accumulation in mature pollen rather than in immature pollen of *Lychnis alba*, which was documented by EDX analysis. Although the results suggest a similar trend for *Pellaea rotundifolia* (Pteridaceae) (tables 3.20 and 3.21), *Phegopteris decursive-pinnata* (Thelypteridaceae) (tables 3.29 and 3.30) and *Anemia tomentosa* (Schizaeaceae) (tables 3.24-3.26), the detection of silica in the spore walls is treated qualitatively purely and any interpretations of putative trends in the data are hypothetical and would need further analyses.

Based on findings by Lovering and Engel (1967), revealing that silicon transport in *Equisetum arvense* L. (Equisetaceae) involved a silicon-phenyl complex, Peggs and Bowen (1984) repeated their experiments and tried to isolate silicon from 1ml of *Equisetum arvense* plant sap. *Equisetum* is a well-known silicon-accumulator, which can take up to 12% silica into the shoot (Chen and Lewin 1969; Hodson and Evans 1995) and is one of the very few organisms, apart from diatoms and the Chrysophyceae (algae), to have an absolute and quantitatively major need for silicon (Epstein 1999). In 1969, Chen and Lewin clearly demonstrated that *Equisetum arvense* plants grown without a supply of silicon in the nutrient solution showed deficiency symptoms, unlike the plants grown with sufficient silicon supply (40-80mg silicon/litre). Peggs and Bowen also attempted to synthesise tris-(β -thujaplicine)silicon complexes to then extract the same complexes from *Thuja plicata* plants, as described by Weiss and Herzog (1978). As for *Equisetum arvense*, Peggs and Bowen showed that the most likely component in the sap was monosilicic acid with a very low molecular mass of 96, unlike Lovering and Engel, who claimed to have found a phenyl-silicon compound. All attempts to extract tris (β -thujaplicine)silicon complexes from bark and leaves of *Thuja plicata* were unsuccessful and the authors also failed to obtain

crystals from the extract by adding potassium hexafluorophosphate, as reported by Weiss and Herzog. Peggs and Bowen concluded that Herzog and Weiss must have isolated artefacts, arguing that impurities of dissolved or particulate silica are able to react with β -thujaplicine *in vitro* to form the complex. Although Peggs and Bowen synthesised the tris (β -thujaplicine)silicon complex from SiI_4 or SiCl_4 with β -thujaplicine they did not manage to produce high yields when synthesizing the complex from silica solutions with β -thujaplicine, as the product is highly insoluble. Peggs and Bowen's study obviously underpins the hypothesis that any products obtained from spore extractions are too low in quantity to pursue further analyses and that the risk of contamination and impurities when dealing with such low quantities is particularly high (Moore *et al.* in press b, appendix 2).

Parkinson (1996) found silica in *Schizaea pectinata* (L.) Sw. sporangium walls, the perispore and in composite bodies present in the sporangial locus at the time of perispore formation. She pointed out that the close association of silicon/silica interaction with phenolics, as described for angiosperms by Scurfield *et al.* (1974) (quoted in Parkinson 1996), might imply that both processes are interlinked, which was also earlier suggested by Raven (1983). Parkinson also referred to a publication by Taylor (1988), which proposes that silicon is involved in spore wall assembly processes in *Selaginella*. I agree with Taylor's idea that silica might be involved in spore wall assembly processes and probably also in self-assembly processes as described by Hemsley *et al.* (1994, 1996, 1998, 2000, 2003) and Hemsley and Griffiths (2000) for various pteridophyte spore walls. In *Selaginella* megaspores silica was detected not only in the perispore but also throughout the exospore (Moore *et al.* in press a, appendix 1). This distribution pattern was also documented by Kempf (1970), Tryon and Lugardon (1978) and Morbelli (1995) and is indicative for silica being present after the completion of exospore formation and hence might play a significant role in spore wall formation. It remains unclear how the siliceous coating in *Selaginella* spore walls materialises but the tapetum is commonly considered as a source of peri- and exospore compounds (Pacini *et al.* 1985). In *Selaginella* a cellular tapetum was described by Pacini and Franchi (1991) but there is little evidence in the literature that the tapetum is the source of silica in *Selaginella*

megaspores, although Taylor (1992) strongly favours this hypothesis for *Isoetes*.

Other elements detected Apart from silica, numerous other elements were identified in all spore walls investigated. The following table 3.32 provides a summary of these elements, revealing their distribution and their approximate atomic weight %, where less than 10 weight % are scored with "+", 10-50 weight % as "++" and over 50 weight % as "+++".

Family	Species investigated	Other Elements found (SEM EDX) in Atomic %									
		+ >10%		++ 10-50%			+++ over 50%				
		Na	K	Mg	Ca	C	Si	P	O	S	Cl
	<i>Doodia aspera</i>	+			+	++	++		++		+
Blechnaceae	<i>Blechnum occidentale</i>		+		+	+++	+	+	++		+
Davalliaceae	<i>Nephrolepis hirsutula</i>		+		+	+++			++		
	<i>Davallia mariesii</i>	+			+	+++			++		+
	<i>Cyrtomium falcatum</i>				+	+++			++		
	<i>Cyrtomium fortunei</i>					+++			++		
	<i>Diplazium poliferum</i>		+	+	+	+++	+	+	++		+
	<i>Dryopteris erythrosora</i>		+			+++		+	++		+
Dryopteridaceae	<i>Dryopteris stewardii</i>	+	++	+	++	+++		+	++	+	++
	<i>Hypodematium fauriei</i>	+		+	+	+++			++	+	+
	<i>Lastreopsis microsora</i>		+		+	+++		+	++		
	<i>Rumohra adiantiformis</i>				+	+++			++		
Osmundaceae	<i>Osmunda regalis</i>		+			++			+++		
Polypodiaceae	<i>Phlebodium aureum</i>		+			+++			++		
Psilotaceae	<i>Psilotum nudum</i>					+++			++		
	<i>Pellaea calomelanos</i>					+++	+		++		
Pteridaceae	<i>Pellaea rotundifolia</i>	+		+	+	+++	+	+	++	+	
	<i>Pteris cretica</i> L.				+	+++	+		++		+
	<i>Pteris longifolia</i>		+		+	+++	+	+	++		+
Schizaeaceae	<i>Anemia tomentosa</i>	+			+	+++	+		++		+
	<i>Oreopteris limbosperma</i>			+	+	+	+	+	++		
	<i>Phegopteris decursive-pinnata</i>	+			+	+++	+		++	+	
Thelypteridaceae	<i>Thelypteris japonica</i>				+	+++	+		++		
	<i>Macrothelypteris torresiana</i>		+		+	+++	+		++		+
Accounts of element in various fern species		7	10	5	18	24	13	7	24	7	8

Table 3.32: Distribution of Na, K, Mg, Ca, C, Si, P, O, S and Cl in atomic % in the spore walls investigated.

Various experiments have demonstrated that the following 10 elements are vital for healthy plant growth: carbon, hydrogen, oxygen, nitrogen, sulphur, phosphorus, potassium, calcium, magnesium and iron (Linder 1992; Strasburger 1998). Since EDX analysis cannot detect hydrogen due to its light atomic properties, hydrogen could not be included into this study. It is assumed that hydrogen is part of the spore wall, bound to oxygen in form of water and hydrocarbons. The only elements present in the spores, which are

not essential for plant growth, are silicon and sodium. Both elements, however, have been detected in spore walls in this study. For reference on silicon in spore walls, please refer to the sections above. As for sodium, Schraudolf (1984) examined ultrastructural events during sporogenesis in *Anemia phyllitidis* (L.) Sw. (Schizaeaceae). This process is characterised by participation of a periplasmodial tapetum in the formation of both the exine and perine (terminology *sensu* Schraudolf). He studied the mineral content (ash weight) of dry spores by the means of EDX analysis and found that more than 75% of the material of the ash is SiO₂. He also detected, in small amounts, sodium, calcium and magnesium. Morbelli (1995) focused her work on the ultrastructure of *Selaginella* megaspores and carried out EDX analysis in combination with SEM on *S. convoluta*. Although she acetolyzed the megaspore, enough information was preserved in order to detect in addition to silica, aluminium, sulphur and calcium in the tubular exospore structures of this species.

The results of this study as well as the findings of Schraudolf (1984) and Morbelli (1995) support the view that spores are not only a reproductive unit hosting genetic information but also seem to provide storage for nutrients. It remains unclear if these nutrients play an active role in spore development, in gametophyte growth, or both, or whether these nutrients are merely “dumped” in the spores without any particular function. As for silicon and sodium, it is suspected that these elements are taken up by the roots and transported into the sporangia where they remain during spore wall formation and thus become incorporated into the spore walls. Hence silica forms not only the outermost spore wall layer in form of a siliceous coating but is also found throughout the exospore (for details see Moore *et al.* in press a, appendix 1).

I have summarised the presence of the elements sodium, potassium, magnesium, calcium, phosphorus, sulphur and chlorine in a table below, correlated with pteridophyte classification. Silica was omitted, since its presence in spore walls and its systematic distribution were discussed above. I also did not include carbon and oxygen as both elements are basic elements present in all organic systems. In table 3.33 the fern families are listed according to their systematic positions, starting with primitive families and ending with more derived families. I have separated the primitive families from

the specialised and derived families (*sensu* Tryon and Lugardon 1990) by inserting an empty row and labelling the families accordingly. Again, no correlation between systematics and the occurrence of a particular element or groups of elements was found. In species like *Pellaea calomelanos* and *P. rotundifolia* there is a significant difference of elements found in the spore walls. Whereas the spores of *P. calomelanos* do not contain any other elements apart from silicon, oxygen and carbon, spores of *P. rotundifolia* additionally contain sodium, magnesium, calcium, phosphorus and sulphur. Similarly, in *Pteris cretica* only calcium and chlorine are present, apart from silicon. This stands in contrast with *P. longifolia* where, additionally, potassium and phosphorus are present. Both *Cyrtomium* species investigated show very few elements in their spores, apart from *C. falcatum*, which also incorporates calcium into its spore walls. Whereas in *Dryopteris erythrosora* spores only potassium, phosphorus and chlorine were found, spores of *D. stewardii* also show the presence of sodium, magnesium, calcium and sulphur. One might expect a consistency of elements present in spore walls within families or genera, but to find intra-generic variability in not only one, but four different genera (*Cyrtomium*, *Dryopteris*, *Pteris* and *Pellaea*) implies no specific or easily observed pattern behind this phenomenon. This is also supported by the results obtained from the Dryopteridaceae, of which 8 species were studied. When looking at the occurrence of elements in this family, it becomes obvious that the distribution pattern is indeed random. There is little evidence that in primitive families fewer elements are incorporated into the spore than in specialised or derived fern families. Since only two species from two primitive families were investigated, this trend cannot be confirmed in the present study. It remains a mystery why such a high number of elements can be detected in spore walls and what their function might be. I can only speculate that their presence may relate to nutrient up-take, which will be discussed in more detail in *section 3.4*.

Family	Evolutionary Level (<i>sensu</i> Tryon and Lugardon 1990)	Species	Other Elements found (SEM EDX) in Atomic %							
			+ >10%	++ 10-50						
			Na	K	Mg	Ca	P	S	Cl	
Psilotaceae	PRIMITIVE	<i>Psilotum nudum</i>								
Osmundaceae		<i>Osmunda regalis</i>		+						
Schizaeaceae	SPECIALISED	<i>Anemia tomentosa</i>	+			+			+	
Pteridaceae		<i>Pellaea calomelanos</i>								
		<i>Pellaea rotundifolia</i>	+		+	+	+	+		
		<i>Pteris cretica</i> L.					+		+	
		<i>Pteris longifolia</i>			+		+	+	+	
Dryopteridaceae		<i>Cyrtomium falcatum</i>					+			
		<i>Cyrtomium fortunei</i>								
		<i>Diplazium poliferum</i>			+	+	+	+	+	
		<i>Dryopteris erythrosora</i>			+			+	+	
		<i>Dryopteris stewardii</i>	+		++	+	++	+	+	++
		<i>Hypodematium fauriei</i>	+			+		+	+	
		<i>Lastreopsis microsora</i>			+				+	
		<i>Rumohra adiantiformis</i>					+			
Davalliaceae			<i>Nephrolepis hirsutula</i>		+		+			
			<i>Davallia mariesii</i>	+			+		+	
Polypodiaceae		<i>Phlebodium aureum</i>		+						
Thelypteridaceae	DERIVED	<i>Oreopteris limbosperma</i>			+	+	+			
		<i>Pheg. decursive-pinnata</i>	+			+		+		
<i>Thelypteris japonica</i>						+				
<i>Macrothelypteris torresiana</i>				+		+		+		
Blechnaceae		<i>Doodia aspera</i>	+			+			+	
	<i>Blechnum occidentale</i>			+		+	+	+		

Table 3.33: Distribution of Na, K, Mg, Ca, P, S and Cl their approximate atomic weight %, where less than 10 atomic weight % are marked as "+", 10-50 atomic weight % as "++". This information is plotted against the systematic position of the pteridophyte families in which the elements occur. There is no obvious correlation between the presence of certain elements and the systematic position of the fern species.

3.4 Mineral content in pteridophyte fronds

This study was undertaken to establish whether there is a correlation between the occurrence of silica in spore walls and fronds. In the light of the results gained so far it is assumed that if silica and other elements are sufficiently present in spores, they might also occur in fronds, as previously described (Kaufman *et al.* 1971; Dengler and Lin 1980; Höhne and Richter 1981; Parry *et al.* 1985; von Aderkans *et al.* 1986; Perry and Fraser 1991). The fronds of five fern species were studied and the following table outlines the occurrence of silicon in rachis or pinna/pinnule. The results from the previous section 3.3 have been included into this table in order to provide a comprehensive summary.

Family	Species investigated	Results SEM EDX analysis spore wall	SEM EDX analysis rachis/pinna/pinnule
Polypodiaceae	<i>Phlebodium aureum</i> (L.) J. Smith	no silicon	no silicon
Osmundaceae	<i>Osmunda regalis</i> L.	no silicon	silicon in rachis and pinnule
Pteridaceae	<i>Pellaea rotundifolia</i> (Forst. f.) Hook	silicon	silicon in rachis but none in pinna
Schizaeaceae	<i>Anemia tormentosa</i> (Sav.) Sw.	silicon	silicon in pinnule but none in rachis
Thelypteridaceae	<i>Phegopteris decursive-pinnata</i> (v.Hall) Fee	silicon	silicon pinnule but none in rachis

Table 3.34: A summary of section 3.4 *Mineral content in pteridophyte fronds* including species investigated and results of SEM EDX analyses of the spores and fronds.

3.4.1 Results

SEM in combination with Energy Dispersive X-Ray analysis (EDX) showed either presence or absence of silicon (Si) in rachis and pinnae/pinnules of five fern species investigated. Most analyses also revealed an abundance of other elements such as phosphorus (P), sulphur (S), potassium (K), calcium (Ca), oxygen (O), sodium (Na), chlorine (Cl), carbon (C) or magnesium (Mg), manganese (Mn) and molybdenum (Mo).

3.4.1.1 Polypodiaceae

Four different areas of the cross section through the rachis of *Phlebodium aureum* (L.) J. Smith (figure 3.38A) were analysed: the epidermis (figure 3.38C and D), parenchyma (figure 3.38E and F), vascular bundle (figure 3.38G and H) and the central parenchyma (figure 3.38I and J). Five different elements were detected, oxygen, potassium, phosphorous, calcium and chlorine. There is apparently no silicon in the rachis of *Phlebodium aureum*.

Rachis

Element	Weight%	Atomic%
C	61.71	68.64
O	37.04	30.93
K	1.25	0.43

Table 3.35: Presence of potassium and oxygen in the epidermis of *Phlebodium aureum* (in weight % and atomic %). This table corresponds to the chart in figure 3.38D.

Rachis

Element	Weight%	Atomic%
C	49.88	58.63
O	44.63	39.39
K	5.49	1.98

Table 3.36: Presence of potassium and oxygen in the parenchyma of *Phlebodium aureum* (in weight % and atomic %). This table corresponds to the chart in figure 3.38F.

Rachis

Element	Weight%	Atomic%
C	53.69	61.17
O	44.77	38.29
K	1.54	0.54

Table 3.37: Presence of potassium and oxygen in the vascular bundle of *Phlebodium aureum* (in weight % and atomic %). This table corresponds to the chart in figure 3.38H.

Rachis

Element	Weight%	Atomic%
C	32.47	53.17
O	15.87	19.51
Mg	1.59	1.28
P	2.67	1.69
S	1.47	0.90
Cl	7.67	4.26
K	32.98	16.59
Ca	5.28	2.59

Table 3.38: Elements detected in the central parenchyma of *Phlebodium aureum* (in weight % and atomic %). This table corresponds to the chart in figure 3.38J.

Figure 3.38: (A) A cross-section through a rachis of *Phlebodium aureum* (L.) J. Smith. (B) An enlarged view of the rachis. (C) and (D) are the EDX-analysis charts of the epidermis. (E) and (F) are the EDX-analysis charts of the parenchyma. (G) and (H) are the EDX-analysis charts of the vascular bundle. (I) and (J) are the EDX-analysis charts of the central parenchyma. (C) shows the epidermis, (D) shows the epidermis, (E) shows the parenchyma, (F) shows the parenchyma, (G) shows the vascular bundle and (H) shows the vascular bundle.

3.4.1.2 Osmundaceae

Three areas of a cross section through the rachis of *Osmunda regalis* L. (figure 3.39A) were analysed. The epidermis (figure 3.39B and C), the parenchyma (figure 3.39D and E) and the vascular bundle (figure 3.39F and G). Silicon was detected in all parts of the rachis. Additionally, carbon, oxygen, chlorine, potassium and calcium are present in the epidermis and parenchyma. The vascular bundle also showed the presence of magnesium, sodium and phosphorous.

Rachis

Element	Weight%	Atomic%
C	50.77	58.94
O	45.38	39.54
Si	0.82	0.41
Cl	1.12	0.44
K	1.01	0.36
Ca	0.89	0.31

Table 3.39: Silicon as well as other elements detected in the epidermis and adjacent hypodermis of *Osmunda regalis* (in weight % and atomic %). This table corresponds to the chart in figure 3.39C.

Rachis

Element	Weight%	Atomic%
C	55.11	63.58
O	39.90	34.55
Si	0.22	0.11
Cl	2.02	0.79
K	2.08	0.74
Ca	0.67	0.23

Table 3.41: Silicon as well as other elements detected in the vascular bundle of *Osmunda regalis* (in weight % and atomic %). This table corresponds to the chart in figure 3.39G, area framed in pink.

Rachis

Element	Weight%	Atomic%
C	51.68	60.37
O	42.69	37.43
Si	0.90	0.45
Cl	1.91	0.76
K	1.22	0.44
Ca	1.59	0.56

Table 3.40: Silicon as well as other elements detected in the parenchyma of *Osmunda regalis* (in weight % and atomic %). This table corresponds to the chart in figure 3.39E.

Rachis

Element	Weight%	Atomic%
C	52.28	60.97
O	41.92	36.70
Na	0.40	0.24
Mg	0.24	0.14
Si	0.19	0.09
P	0.26	0.12
Cl	1.63	0.65
K	1.74	0.62
Ca	1.34	0.47

Table 3.42: Silicon as well as other elements detected in the vascular bundle of *Osmunda regalis* (in weight % and atomic %). This table corresponds to the chart in figure 3.39G, area framed in blue.

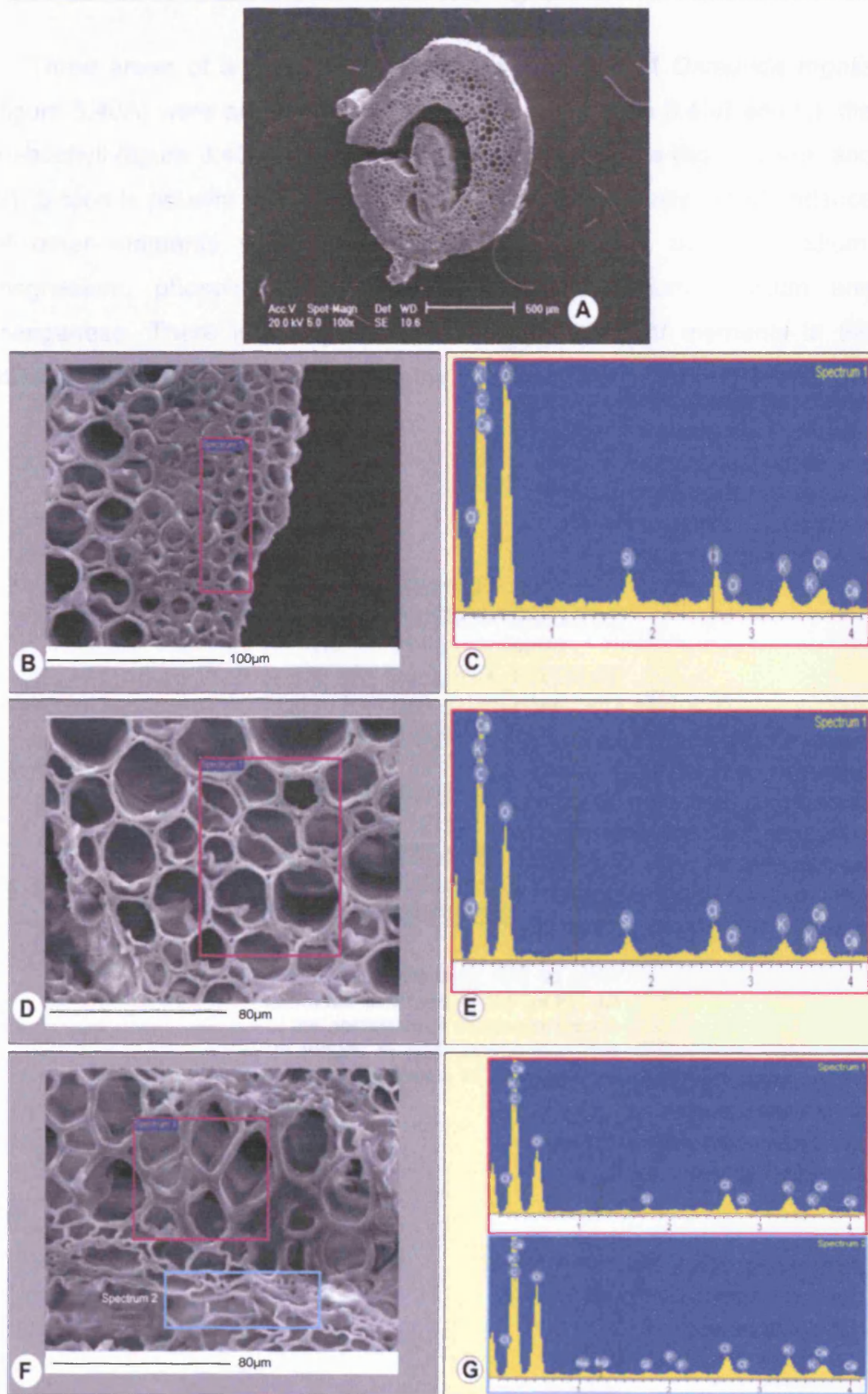


Figure 3.39: A SEM of a cross-section through a rachis of *Osmunda regalis*. The SEM pictures of the area from which the EDX-analyses were taken (B, D, F) as well as the EDX-analysis charts (C, E, G) are arranged as matching pairs (B-C, D-E, F-G). B shows the epidermis/hypodermis area, D the parenchyma and F two areas of the vascular bundle.

Three areas of a cross section through a pinnule of *Osmunda regalis* (figure 3.40A) were analysed. The axial epidermis (figure 3.40B and C), the mesophyll (figure 3.40D and E) and the abaxial epidermis (figure 3.40F and G). Silicon is present in all areas of the pinnule. Additionally, an abundance of other elements were detected such as carbon, oxygen, sodium, magnesium, phosphorous, sulphur, chlorine, potassium, calcium and manganese. There is a slightly higher accumulation of elements in the abaxial part of the epidermis than in the adaxial epidermis.

Pinnule

Element	Weight%	Atomic%
C	61.27	70.09
O	31.33	26.91
Na	0.25	0.15
Mg	0.36	0.20
Si	2.00	0.98
P	0.25	0.11
S	0.21	0.09
Cl	1.12	0.44
K	0.56	0.20
Ca	1.93	0.66
Mn	0.72	0.18

Table 3.43: Silicon as well as other elements detected in the axial part of the epidermis of *Osmunda regalis* (in weight % and atomic %). This table corresponds to the chart in figure 3.40C.

Pinnule

Element	Weight%	Atomic%
C	25.14	46.27
O	12.06	16.66
Si	0.79	0.62
P	1.28	0.92
S	3.63	2.50
Cl	20.57	12.83
K	3.91	2.21
Ca	32.62	17.99

Table 3.44: Silicon as well as other elements detected in the mesophyll of *Osmunda regalis* (in weight % and atomic %). This table corresponds to the chart in figure 3.40E.

Pinnule

Element	Weight%	Atomic%
C	50.65	60.89
O	36.99	33.39
Na	0.44	0.28
Si	6.48	3.33
P	0.40	0.19
Cl	2.04	0.83
K	1.15	0.43
Ca	1.85	0.67

Table 3.45: Silicon as well as other elements detected in the abaxial part of the epidermis of *Osmunda regalis* (in weight % and atomic %). This table corresponds to the chart in figure 3.40G.

Figure 3.40: A SEM of cross-section through a pinnule of *Osmunda regalis*. The SEM pictures of the area right which the EDS-analysis was taken (B, D, F) is written as the EDS-analysis charts (C, E, G) are arranged as matching pairs (B-C, D-E, F-G). B focuses on the cell wall of a mesophyll cell, C on the mesophyll cell, D on the abaxial part of the epidermis.

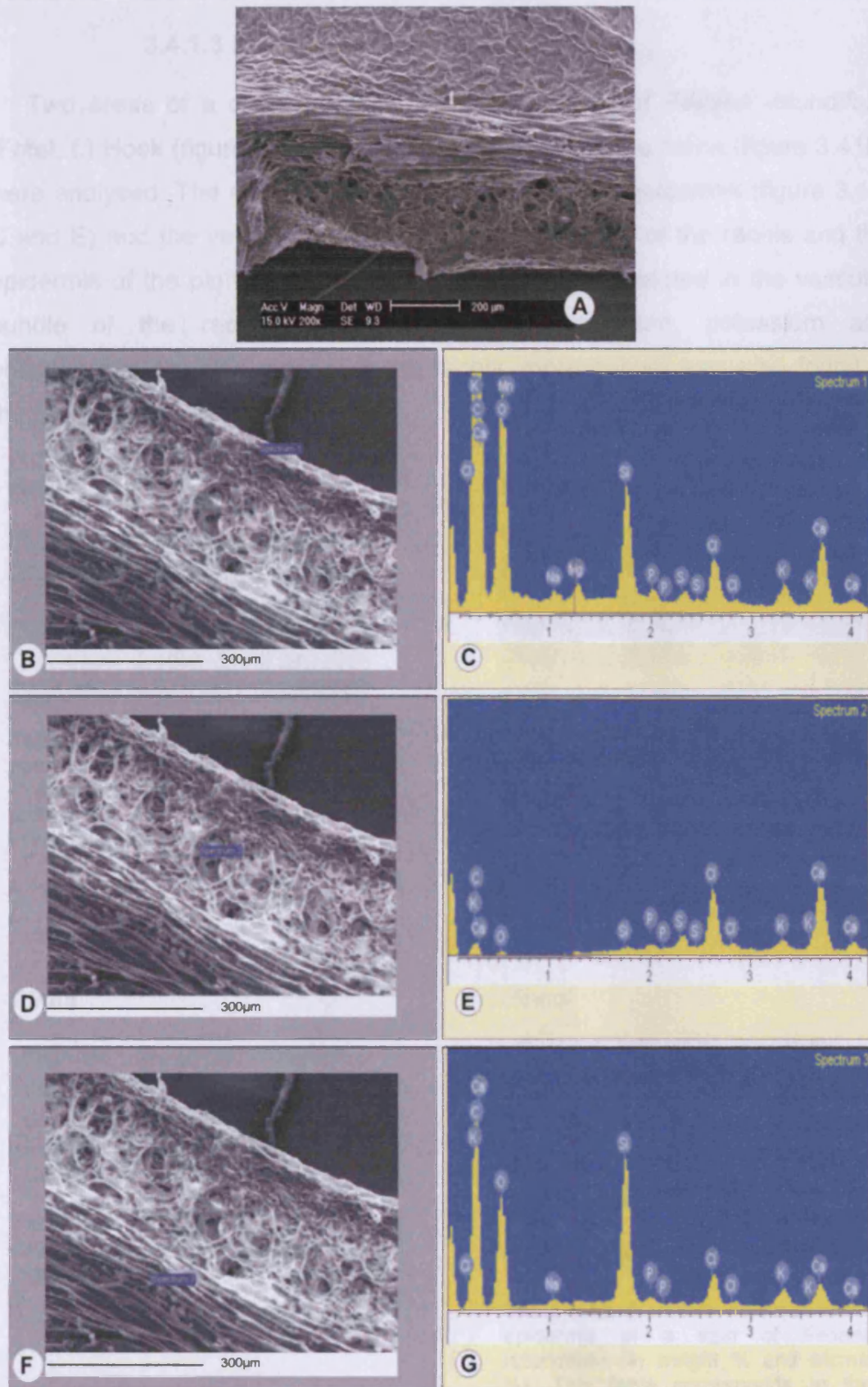


Figure 3.40: A SEM of cross-section through a pinnule of *Osmunda regalis*. The SEM pictures of the area from which the EDX-analyses were taken (B, D, F) as well as the EDX-analysis charts (C, E, G) are arranged as matching pairs (B-C, D-E, F-G). B focusses on the axial part of the epidermis, D on the mesophyll and F on the abaxial part of the epidermis.

3.4.1.3 Pteridaceae

Two areas of a cross section through the rachis of *Pellaea rotundifolia* (Forst. f.) Hook (figure 3.41A) as well as two areas of the pinna (figure 3.41B) were analysed. The areas investigated comprised the epidermis (figure 3.41. C and E) and the vascular bundle (figure 3.41G and I) of the rachis and the epidermis of the pinna and a vein. Silicon was only detected in the vascular bundle of the rachis. Oxygen, carbon, magnesium, potassium and phosphorous are also present in the rachis, molybdenum was also found in the pinna.

Rachis

Element	Weight%	Atomic%
C	60.77	68.15
O	36.72	30.91
Mg	0.25	0.14
P	0.18	0.08
K	2.08	0.72

Table 3.46: Elements detected in the epidermis and adjacent hypodermis of *Pellaea rotundifolia* (in weight % and atomic %). This table corresponds to the chart in figure 3.41E.

Rachis

Element	Weight%	Atomic%
C	57.69	65.25
O	39.89	33.87
Si	0.27	0.13
K	2.15	0.75

Table 3.47: Carbon, silicon, oxygen and potassium detected in the vascular bundle of *Pellaea rotundifolia* (in weight % and atomic %). This table corresponds to the chart in figure 3.41I.

Pinna

Element	Weight%	Atomic%
C	60.76	73.82
O	21.47	19.58
K	14.25	5.32
Ca	3.52	1.28

Table 3.48: Oxygen, potassium and calcium detected in the epidermis of a pinna of *Pellaea rotundifolia* (in weight % and atomic %). This table corresponds to the chart in figure 3.41F.

Pinna

Element	Weight%	Atomic%
C	59.43	67.81
O	35.53	30.43
Mg	0.45	0.25
P	0.47	0.21
K	2.93	1.03
Ca	0.54	0.18
Mo	0.66	0.09

Table 3.49: Elements detected in the epidermis of a vein of *Pellaea rotundifolia* (in weight % and atomic %). This table corresponds to the chart in figure 3.41J.

Figure 3.41: SEM of cross-section through A a rachis and B a pinna of *Pellaea rotundifolia*. B, D, G and H show the SEMs of the areas that were analysed. The EDS-analysis were taken on E, F, I and J the square obtained. Matching were set along the horizontal C-E, G-I and D-F, H-J. G shows the epidermis and hypodermis with the vascular bundle. D is a detail of the epidermis of the pinna and H the epidermis of a vein.

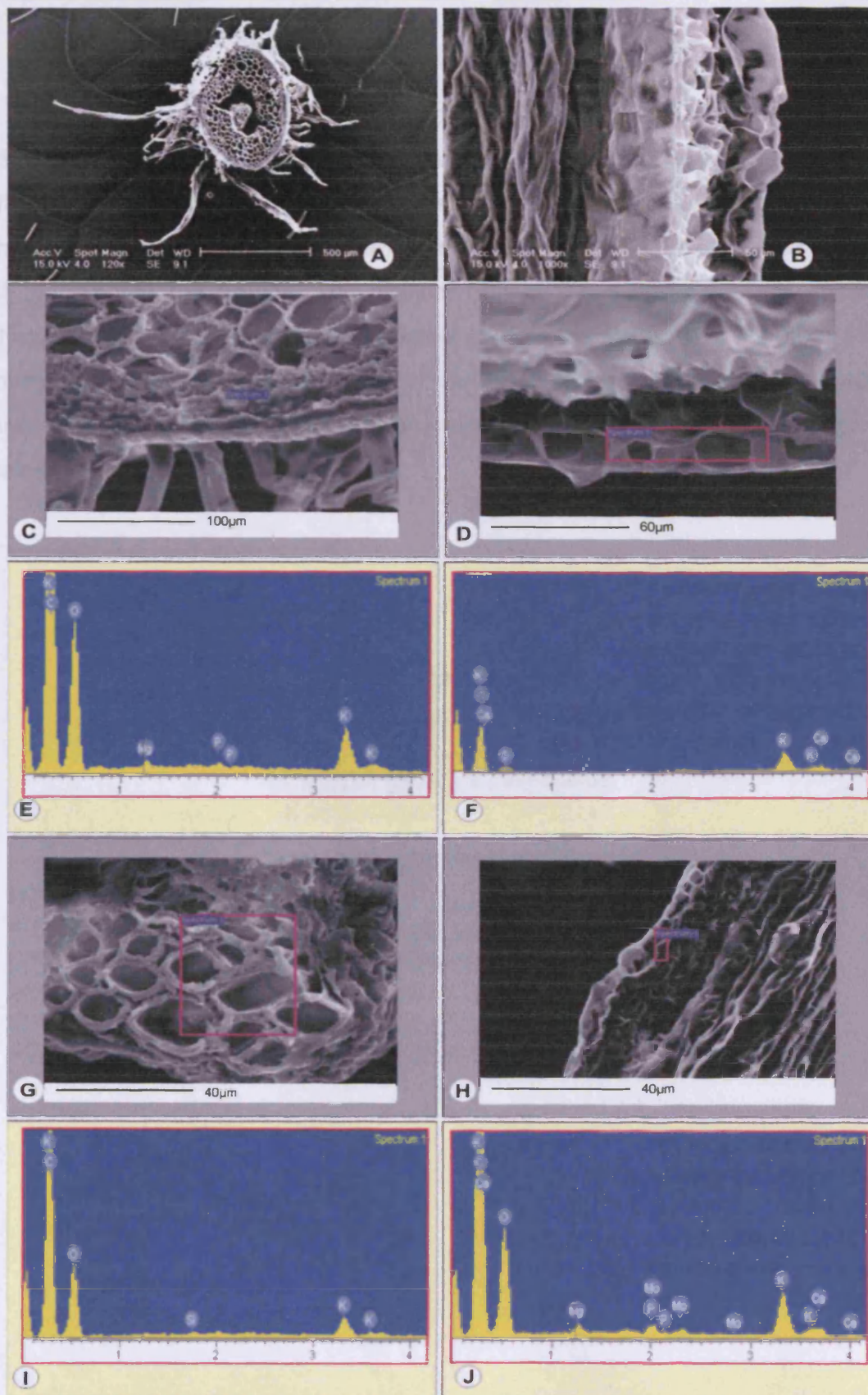


Figure 3.41: SEM of cross-section through **A** a rachis and **B** a pinna of *Pellaea rotundifolia*. **B**, **D**, **G** and **H** show the SEMs of the area from where the EDX-analyses were taken and **E**, **F**, **I** and **J** the spectra obtained. Matching pairs are arranged horizontally (**C-E**, **G-I** and **D-F**, **H-J**). **C** shows the epidermis and hypodermis area, **G** the vascular bundle. **D** is a detail of the epidermis of the pinna and **H** the epidermis of a vein.

3.4.1.4 Schizaeaceae

Two areas of a cross section through the rachis of *Anemia tomentosa* (Sav.) Sw. (overview figure 3.42A) as well as a cross section of a pinnule (figure 3.42F) were analysed. The areas investigated in the rachis comprised the epidermis, the parenchyma and the vascular bundle. In the cross section of the pinnule the adaxial and abaxial part of the epidermis were studied. Silicon was only detected in the abaxial part of the epidermis. All other sites investigated showed the presence of carbon, oxygen, chlorine, phosphorous and potassium (rachis) and carbon, oxygen, chlorine, potassium, sulphur, calcium and phosphorous (pinnule).

Rachis

Element	Weight%	Atomic%
C	54.06	61.84
O	43.34	37.21
Cl	0.99	0.38
K	1.62	0.57

Table 3.50: Elements detected in the epidermis and adjacent hypodermis of *Anemia tomentosa* (in weight % and atomic %). This table corresponds to the chart in figure 3.42C.

Rachis

Element	Weight%	Atomic%
C	52.37	60.98
O	42.38	37.05
P	0.50	0.23
Cl	1.22	0.48
K	2.71	0.97
Ca	0.82	0.29

Table 3.51: Elements detected in the parenchyma of *Anemia tomentosa* (in weight % and atomic %). This table corresponds to the chart in figure 3.42E, framed in pink.

Rachis

Element	Weight%	Atomic%
C	56.80	64.64
O	39.97	34.15
P	0.65	0.29
Cl	0.61	0.24
K	1.97	0.69

Table 3.52: Elements detected in the vascular bundle of *Anemia tomentosa* (in weight % and atomic %). This table corresponds to the chart in figure 3.42E, framed in blue.

Pinnule

Element	Weight%	Atomic%
C	55.87	63.48
O	41.83	35.68
S	0.22	0.09
Cl	0.54	0.21
K	1.00	0.35
Ca	0.54	0.18

Table 3.53: Elements detected in the axial part of the epidermis of *Anemia tomentosa* (in weight % and atomic %). This table corresponds to the chart in figure 3.42G, framed in pink.

Pinnule

Element	Weight%	Atomic%
C	53.83	61.86
O	42.55	36.71
Si	0.83	0.41
S	0.24	0.10
Cl	0.70	0.27
K	1.03	0.36
Ca	0.82	0.28

Table 3.54: Silicon as well as other elements detected in the abaxial part of the epidermis of *Anemia tomentosa* (in weight % and atomic %). This table corresponds to the chart in figure 3.42G, framed in blue.

Figure 3.42: A-SEM of a cross section through the epidermis of *Anemia tomentosa*. The SEM picture of the area from which the EDS analysis was taken (B, D, F) is shown in the left column, while the corresponding EDS analysis charts (C, E, G) are arranged in columns (B-C, D-E, F-G). A shows the area of the epidermis and hypodermis; B the pinnule midrib and the vascular bundle; F and G show the pinnule showing the axial (framed in pink) and abaxial (framed in blue) part of the epidermis with the mesophyll in the centre (not visible).

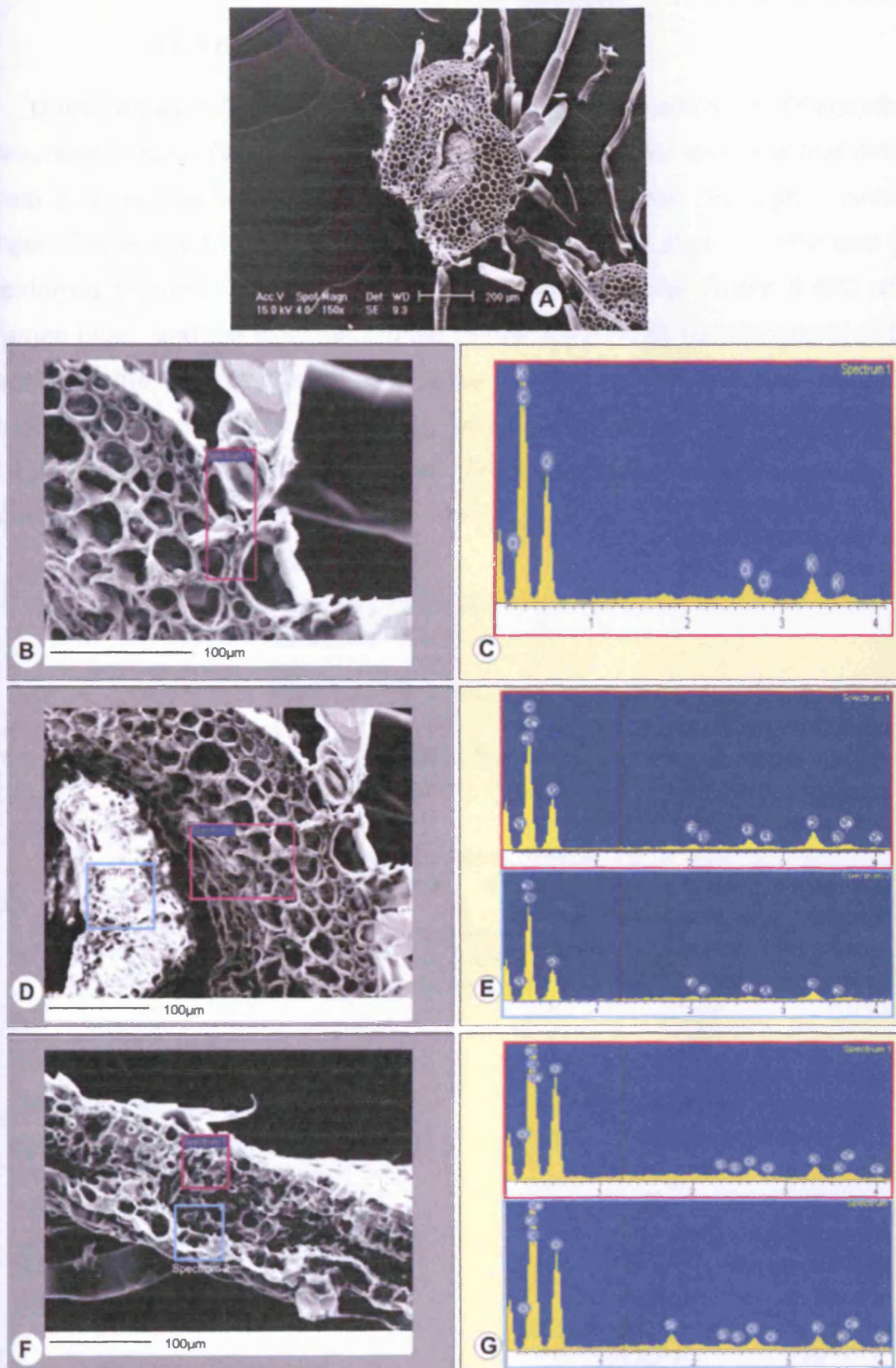


Figure 3.42: A SEM of a cross section through the rachis of *Anemia tomentosa*. The SEM pictures of the area from which the EDX-analyses were taken (B, D, F) as well as the EDX-analysis charts (C, E, G) are arranged as matching pairs (B-C, D-E, F-G). B shows the area of the epidermis and hypodermis, D the parenchyma and the vascular bundle. F is a detail of the pinnule showing the axial (framed in pink) and abaxial (framed in blue) part of the epidermis with the mesophyll in the centre (not studied).

3.4.1.5 Thelypteridaceae

Three areas of a cross section through the rachis of *Phegopteris decursive-pinnata* (Van Hall) Fee (figure 3.43A and C for overview and detail) were analysed as well as three areas of a cross section through a pinnule (figure 3.43B and D for overview and detail). The areas studied comprised the epidermis (figure 3.43C area framed pink), parenchyma (figure 3.43C area framed blue), and the vascular bundle (figure 3.43C area framed green) of the rachis. In the pinnule the abaxial epidermis (figure 3.43C spectrum 1), the axial epidermis overlying the vein (figure 3.43C spectrum 2) and a hair (figure 3.43C spectrum 3) were investigated. Silicon was only detected in the axial part of the epidermis and in the hair. No silicon was found in the rachis.

Rachis

Element	Weight%	Atomic%
C	50.46	60.42
O	39.90	35.87
P	0.98	0.46
Cl	2.74	1.11
K	2.87	1.06
Ca	3.04	1.09

Table 3.55: Elements detected in the epidermis and adjacent hypodermis of *Phegopteris decursive-pinnata* (in weight % and atomic %). This table corresponds to the chart in figure 3.43E.

Rachis

Element	Weight%	Atomic%
C	44.73	55.01
O	43.79	40.43
P	1.25	0.60
Cl	3.46	1.44
K	3.65	1.38
Ca	3.11	1.15

Table 3.56: Elements detected in the parenchyma of *Phegopteris decursive-pinnata* (in weight % and atomic %). This table corresponds to the chart in figure 3.43G.

Rachis

Element	Weight%	Atomic%
C	50.98	60.64
O	39.85	35.58
Na	0.37	0.23
Mg	0.40	0.24
P	1.35	0.62
S	0.33	0.15
Cl	2.69	1.08
K	2.51	0.92
Ca	1.52	0.54

Table 3.57: Elements detected in the vascular bundle of *Phegopteris decursive-pinnata* (in weight % and atomic %). This table corresponds to the chart in figure 3.43I.

Pinna

Element	Weight%	Atomic%
C	75.93	82.38
O	19.86	16.17
S	0.40	0.16
Cl	0.89	0.33
K	1.05	0.35
Ca	1.88	0.61

Table 5.58: Elements detected in the abaxial part of the epidermis of *Phegopteris decursive-pinnata* (in weight % and atomic %). This table corresponds to the chart in figure 3.43F.

Pinna

Element	Weight%	Atomic%
C	66.17	76.70
O	21.38	18.61
Mg	0.30	0.17
Si	0.24	0.12
S	0.43	0.19
Cl	4.31	1.69
K	3.76	1.34
Ca	3.42	1.19
Totals	100	100

Table 3.59: Silicon as well as other elements detected in the axial part of the epidermis of *Phegopteris decursive-pinnata* (in weight % and atomic %). This table corresponds to the chart in figure 3.43H.

Pinna

Element	Weight%	Atomic%
C	63.08	70.98
O	32.28	27.27
Si	0.56	0.27
S	0.17	0.07
Cl	1.69	0.64
K	1.27	0.44
Ca	0.94	0.32

Table 3.60: Silicon as well as other elements detected in the hair on the pinnule of *Phegopteris decursive-pinnata* (in weight % and atomic %). This table corresponds to the chart in figure 3.43J.

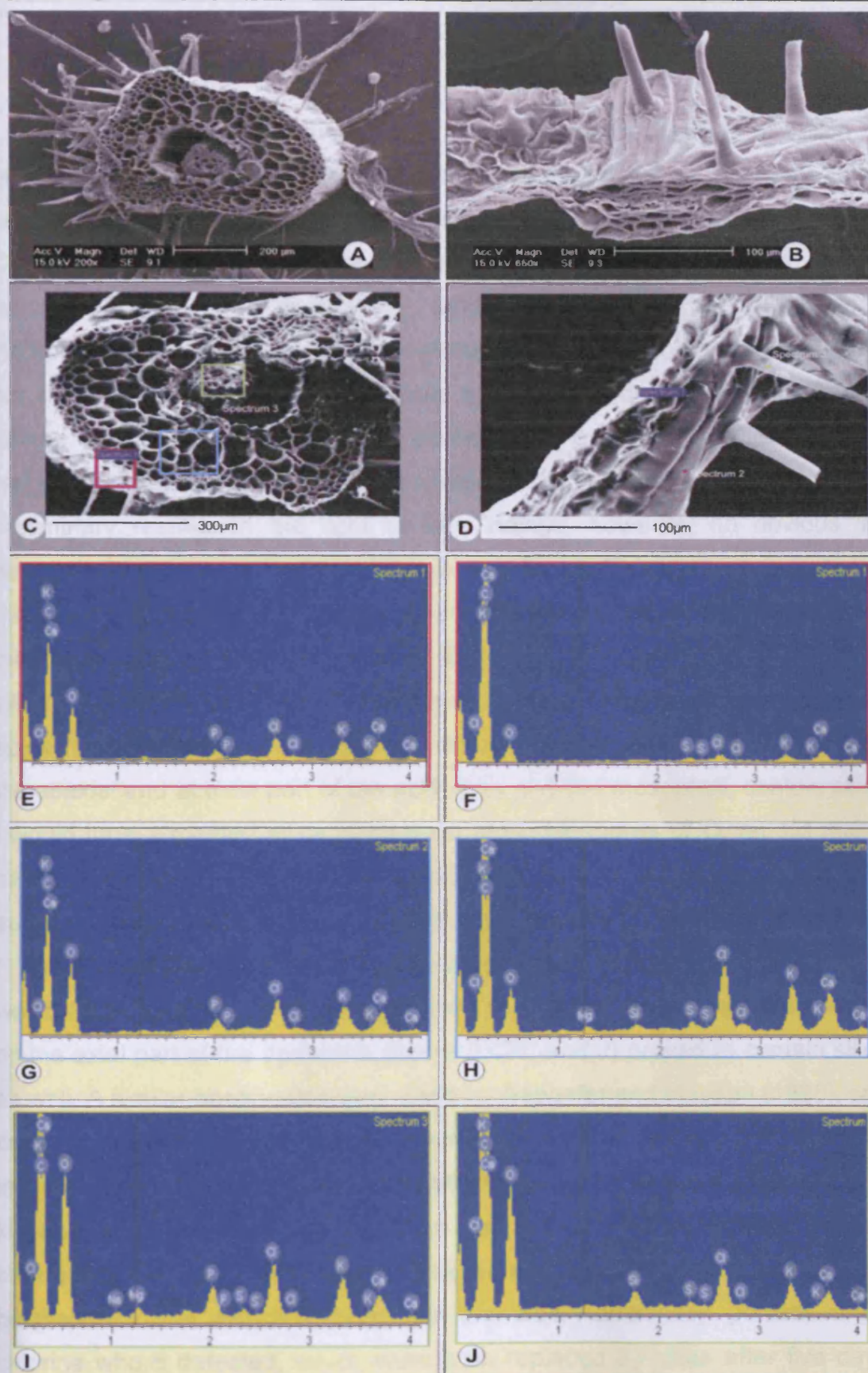


Figure 3.43: A SEM of a cross-section through a rachis of *Phegopteris decursive-pinnata* and B a pinnule. C and D show the SEMs of the areas from where the EDX-analyses were taken and E- J the spectra obtained. Matching pairs are arranged horizontally (C - E, G, I and D - F, H, J). C shows the three areas epidermis (pink), parenchyma (blue) and vascular bundle (green). D shows the abaxial part of the epidermis (spectrum 1), the axial part of the epidermis (spectrum 2) and a hair of a pinnule (spectrum 3).

3.4.2 Discussion

It seems clear from the results that the accumulation of silica in pteridophyte fronds does not follow any regular patterns (e.g. accumulation only occurring in the rachis or certain sites of the pinna/pinnule). Whereas in *Osmunda regalis* both rachis and pinnule show a presence of silica, *Pellaea rotundifolia*, *Anemia tomentosa* and *Phegopteris decursive-pinnata* incorporate silica in either rachis or pinna/pinnule. *Phlebodium aureum* does not show any silica in its fronds. It was hoped that a deeper insight might be gained into a possible correlation between the presence of silica in spore walls and in fern fronds. Hence, five species were studied in order to get some preliminary results. In the light of the findings, however, no obvious link between silica in spore walls and fronds was found. This view is supported by the results from *Osmunda regalis*, where the spores are free of silica but not the fronds. Of all five species studied, *O. regalis* had the highest deposition of silica in fronds. All parts of the frond studied, the rachis including the epidermis, parenchyma and vascular bundle as well as the pinnule including the adaxial and abaxial part of the epidermis and the mesophyll, contain silica. I would have expected silica to be present in the spores of *O. regalis* mainly because the fronds show an abundance of silica. This stands in contrast to *P. aureum* where no silica was found in the spores and fronds. In *A. tomentosa*, *P. rotundifolia* and *P. decursive-pinnata* silica was detected in the spores as well as in at least rachis or pinna/pinnule. In *P. decursive-pinnata* macro-hairs on the axial part of the epidermis (figure 3.43D and J) proved to contain silica, as well. A similar observation was made by Sangster and Hodson (1986), who carried out a study on unicellular macro-hairs of the outer epidermis on the inflorescence of bracts of *Phalaris canariensis* L. (Poaceae), a plant that is known to accumulate silicon. No silicon was detected in the micro-hairs before emergence but silicon deposition increased after three days and was found to be present in the vacuoles, cytoplasm and wall. Additionally, potassium and chlorine were detected, which were both replaced by silica after five days. The EDX-analysis of the macro-hair in *P. decursive-pinnata* revealed, in addition to silicon, the occurrence of sulphur, chlorine, potassium and calcium. The fertile frond of *P. decursive-pinnata* was fully mature at the time

of collection and it therefore seems that the macro-hair accumulates various elements, including silicon.

It is acknowledged that a study of just five pteridophyte species allows only a very limited interpretation of the data. Hence, it remains unclear why the distribution pattern of silica in fern fronds is not confined to any particular area in the rachis or pinna/pinnules. Although there is comprehensive information on silica in higher plants (Mann *et al.* 1983; Sangster and Hodson 1986; Williams 1986; Hodson and Evans 1995; Epstein 1999), the literature focusing on the occurrence of silica in plant leaves is often limited to studies of Urticales, Poales and some Cyperales, which are all known to be silicon accumulators (Epstein 1999), as well as to needles of Pinaceae (Hodson and Sangster 2002). All investigations of silicon in leaves were carried out by the means of EDX-analysis (Dengler and Lin 1980; Parry *et al.* 1985; von Aderkans *et al.* 1986; Hodson and Evans 1995; Hodson and Sangster 2002). The only data available on silica in pteridophyte leaves were published by Dengler and Lin (1980) who looked at *Selaginella emmiana*, by Höhne and Richter (1981) on *Matteuccia struthiopteris*, *Gymnocarpium dryopteris* and *Phegopteris connectilis*, by Parry *et al.* (1985) studying the fronds of *Pteridium aquilinum* and von Aderkans *et al.* (1986) looking at the fronds of *Matteuccia struthiopteris*. Two publications describe silica distribution in leaves of *Equisetum*, a silicon accumulator (Kaufman *et al.* 1971; Perry and Fraser 1991). Both authors noted some correlations between anatomical features (e.g. stomata or micromorphological sculpturing) and silica deposition. The distribution pattern, however, does vary inter-specifically and seems to be selective (Kaufman *et al.* 1971). There are not many indications in the literature which would help to explain the irregular distribution of silica in pteridophyte spores and fronds. von Aderkans *et al.* (1986) pointed out that the pattern of silica accumulation in fronds is random, a hypothesis also favoured herein. Dengler and Lin (1980) provide a detailed summary of where silica is deposited in leaves (e.g. as bodies in the lumen of epidermal cells, between cellulose microfibrils, within the wall of various cell types, or as occlusions of intercellular spaces). Their own study showed high levels of silicon in the marginal sclereids and in half of the abaxial epidermal cells on the ventral leaves of *Selaginella emmiana*. 6% of the stomata also contain

high levels of silicon, which are restricted to a broad band of cells on the abaxial surface, overlying a single vascular bundle. The authors could not find any straightforward explanation for the distribution pattern of silica but suspect that this process might be under metabolic control. They refer to another concept, which describes the deposition of monosilicic acid being carried passively in the transpiration stream to be deposited later on at sites of greatest transpiration (Jones and Handreck 1967, cited in Dengler and Lin 1980). Dengler and Lin, however, did not find any evidence that would support the concept mentioned above, mainly because they documented a widely scattered distribution pattern within the leaves and not one that is confined to sites of greatest transpiration. Parry *et al.* (1985) did not document any isolated deposits of silica associated with cell shapes. After wet ashing of midrib tissues in nitric acid, silica was found along the midrib regions of the laminae in form of silicified fibre-like structures (about 5µm in diameter and up to 300 µm long). Only very few silicified epidermal cells were found and no elements other than silicon were detected. SEM in combination with EDX analysis revealed that silica accumulation seemed to concentrate in the abaxial epidermal cells of the lamina and the epidermal cells of the petiole. These findings are similar to the results presented in this chapter. Whereas in *A. tomentosa* silica was also located in the abaxial epidermal cells but not in the rachis, in *P. decursive-pinnata* silica only occurred in the adaxial epidermal cells. In *O. regalis* both adaxial and abaxial epidermal cells and the rachis accumulate silica. A comparison between the siliceous rachis of *O. regalis* and *P. rotundifolia* revealed that in both cases the vascular bundles show the presence of silica. This suggests that at least in these two species silica is transported through the vascular bundles. It does not, however, explain the presence of silica in the pinnules of *A. tomentosa* and *P. decursive-pinnata* mainly because their rachis did not show any silica deposits. von Aderkans *et al.* (1986) reported similar discrepancies in their study on *Matteuccia struthiopteris* fronds and speculate that the lignification of many cell walls in fertile fronds might actually prevent the deposition of silica. I concur with the general idea developed by von Aderkans *et al.* (1986) that the growth of different leaf types (e.g. vegetative and fertile) might influence silica accumulation. They documented a higher silica contents in vegetative than in fertile fronds, which they explain with the fact that fertile fronds develop later,

are green for only short periods and therefore transpire less. Hence, the time for silica deposition is far more restricted than in vegetative fronds. If one also takes into consideration the lignification of cell walls in fertile fronds, these two aspects most certainly have a negative effect on the accumulation of silica in fertile fronds. This, however, does not answer the question of why spores of *O. regalis* contain silica but the fertile fronds do not and why in some species (*A. tomentosa* and *P. decursive-pinnata*) the spores incorporate silica but the rachis does not when the pinnules of fertile fronds clearly do. In the light of the results from this study as well as from the various authors mentioned above I suspect that silica distribution in fronds as well as in the spores is random and does not seem to follow any particular pattern.

The presence of all the other elements detected in fern fronds is probably related to nutrient uptake by the roots. Marschner (1995), Strasburger (1998) and von Sengbush (2003) give a comprehensive overview on the uptake, transport and function of various nutrients in plants. The information from these publications is cited and summarised in the following section.

As mentioned before (*chapter 3.3*), the elements C, O, H, N, S, P, K, Ca, Mg and Fe are considered essential for plant growth (Marschner 1995; Strasburger 1998; von Sengbusch 2003). Whereas the first three elements are taken up by the plant from the air and water in form of CO₂ and O₂, the remaining seven elements have to be taken from the soil as ions vital for plants. All elements mentioned above are macronutrients. This means that they need to be at the disposal for plants at > 20mg/l (Strasburger 1998). Macronutrients are also referred to as “essential mineral elements” and “mineral nutrients”. Trace elements (< 0.5mg/l) are Mn, B, Zn, Cu, Mo and Cl and are, as the name suggest, only required in very small quantities and are generally referred to as micronutrients (Marschner 1995). Generally, N, S, P, Cl, B and Mo are taken up in form of ions (N also as NH₄⁺ and in some cases as N₂), whereas the remaining elements are taken up in form of cations (K⁺, Mg²⁺, Ca²⁺, Fe²⁺, ³⁺, Mn²⁺, Zn²⁺, Cu²⁺) (Strasburger 1998). Some plants only need a certain combination of additional elements such as Na, Se, Co, Ni or Si. These elements are often called “beneficial mineral elements” because they are not strictly essential for the plant but assist important functions such

as osmotic pressure or the compensation of other toxic elements (Marschner 1995).

Nutrients have very different mobility in the phloem, which affects their availability and distribution. Whereas potassium, sodium, magnesium, phosphorus, sulphur and chlorine are highly mobile, some other elements such as molybdenum are less transportable, or totally immobile such as calcium, for example (Strasburger 1998). In this study, calcium was abundant in pteridophyte as well as bryophyte spore walls (*chapter 3.5*) as well as in all fronds investigated. Calcium is taken up in the roots by mass flow through the apoplast and accumulates passively and irreversibly in sites of highest transpiration (e.g. the leaves). Plant cells also bind excessive calcium in form of phytate, oxalate, and carbonate or sometimes even as phosphate or sulphate (Strasburger 1998). In plant cells calcium also plays an active role in the synthesis of callose, an amorphous polymer also found in pollen and spore development (Strasburger 1998; Paxon-Sowders *et al.* 2001). It is assumed that in plant cells an increase in calcium ions is responsible for switching from cellulose to callose production, if necessary. This would explain the occurrence of calcium in many pteridophyte and bryophyte spore walls but also in pteridophyte fronds.

Seven pteridophyte species had sodium in their spore walls and of the four fronds studied, only two showed presence of sodium. Sodium is a so-called beneficial mineral element (Marschner 1995). It is noteworthy that the spores of *O. regalis* did not contain sodium whereas the fronds do, contrary to *P. decursive-pinnata*, where both spores and fronds contain sodium. Again, no constancy in the distribution pattern can be observed. The English edition of Strasburger (1976) states: "apparently their (sodium, aluminium, chlorine, silicon) presence in these plants represents nothing more than an inert component of the plant body" (p. 231). On the basis of the results presented here, this view might well be correct. It is not surprising to find potassium, magnesium, phosphorous and sulphur in the fronds since they are macronutrients and play important roles in the plant metabolism. This also applies to the micronutrients molybdenum, manganese and chlorine. The functions of macro- and micronutrients in plants are summarised in table 3.61 below.

Nutrient Classification	Element	Abbr.	Presence in fronds	Significance in plants
Macronutrient	Potassium	K	√	activates many enzymes, regulates guard cell movements and protein biosynthesis; vital for all plants
	Calcium	Ca	√	regulatory functions; stabilises cell wall structures and membranes, controls movements
	Phosphorus	P	√	energetic bonds (ATP), component of nucleic acids
	Magnesium	Mg	√	chlorophyll component, counter ion of ATP, important for protein biosynthesis
	Sulphur	S	√	amino acid and protein component, coenzyme A
	Nitrogen	N	X	amino acids, proteins, nucleotides, chlorophyll, etc.
Micronutrients	Copper	Cu	X	co-factor of some enzymes
	Chloride	C	√	takes part in osmotic processes
	Manganese	Mn	√	like copper, component of protein biosynthesis
	Molybdenum	Mo	√	controls nitrate metabolism, metal component of enzymes
	Zinc	Zn	X	like copper (for example carboxypeptidase, DNA-dependent RNA polymerase)
	Boron	B	X	influences use of Ca ²⁺
	Iron	Fe	X	necessary for chlorophyll synthesis

Table 3.61: Plant nutrients and their functions. The table was modified from von Sengbusch (2003) with further information added from the present study as well as from Marschner (1995) and Strasburger (1998).

It seems more appropriate to discuss the presence of macro- and micronutrients in pteridophyte fronds than in spore walls. This is mainly because of a lack of studies carried out on spore wall constituents in the general literature (see also *1.7 Chemical components and ultrastructure of the perispore*). It is known that for pollen formation elements such as boron, copper, manganese and molybdenum are important and often regulate complex processes such as pollen tube growth (Marschner 1995). Although manganese and molybdenum were successfully detected in pteridophyte fronds, none of the elements important in pollen formation were found in pteridophyte spores. Although some authors (Pettitt 1974, 1976, 1979a, 1979b; Schneider and Pryer 2002) described chemical components in pteridophyte spores, up to now no study has looked at spore wall elements

such as nutrients. A possible explanation for the occurrence of silica and the other elements detected is that they are simply “dumped” in the spore walls after spore formation. Although some of these elements might be needed for spore development such as potassium, calcium, magnesium or phosphorous (see table 3.61), others that cannot be utilised or that are too abundant, become incorporated into the walls. I can only speculate on other possible functions for silica and nutrient elements in spore walls, for which I refer the reader to the general discussion (*chapter 7*).

3.5 Mineral content in bryophyte spore walls

The following table summarises the occurrence of silica in the spore clusters of four bryophyte species.

Family	Species investigated	Result EDX analysis of spore clusters
Funariaceae	<i>Funaria hygrometrica</i> Hedw.	silica
Meesiaceae	<i>Leptobryum pyriforme</i> (Hedw.) Wils.	no silica
Bryaceae	<i>Bryum capillare</i> Hedw.	silica
Brachytheciaceae	<i>Brachythecium velutinum</i> (Hedw.) B.S.G.	silica

Table 3.62: A summary of section 3.5 Mineral content in bryophyte spore walls including species investigated and results of SEM EDX analyses of the spore clusters.

3.5.1 Results

Since bryophyte spores (up to 10µm in diameter) are much smaller than pteridophyte spores (between 35 and 100µm in diameter), spore clusters instead of single spores were analysed by the means of SEM in combination with EDX-analysis. This revealed the presence of silica (Si) in three different spore clusters out of four species investigated. Most analyses also showed an abundance of other elements such as phosphorus (P), sulphur (S), potassium (K), calcium (Ca), oxygen (O), carbon (C), sodium (Na), chlorine (Cl), magnesium (Mg) or molybdenum (Mo). The high carbon content in all species investigated is due to the carbon coating applied for SEM, which had already been discussed in section 3.3.

3.5.1.1 Funariaceae

The analysis of spore clusters of *Funaria hygrometrica* Hedw. revealed the presence of silica as well as other elements such as carbon, oxygen, sodium, magnesium, phosphorus, sulphur, potassium and calcium.

Element	Weight%	Atomic%
C	74.97	80.81
O	22.45	18.16
Na	0.26	0.15
Mg	0.15	0.08
Si	0.11	0.05
P	0.61	0.25
S	0.21	0.08
K	0.90	0.30
Ca	0.34	0.11

Table 3.63: Silica was detected in the spore cluster of *Funaria hygrometrica* alongside with various other elements (in weight% and atomic%).

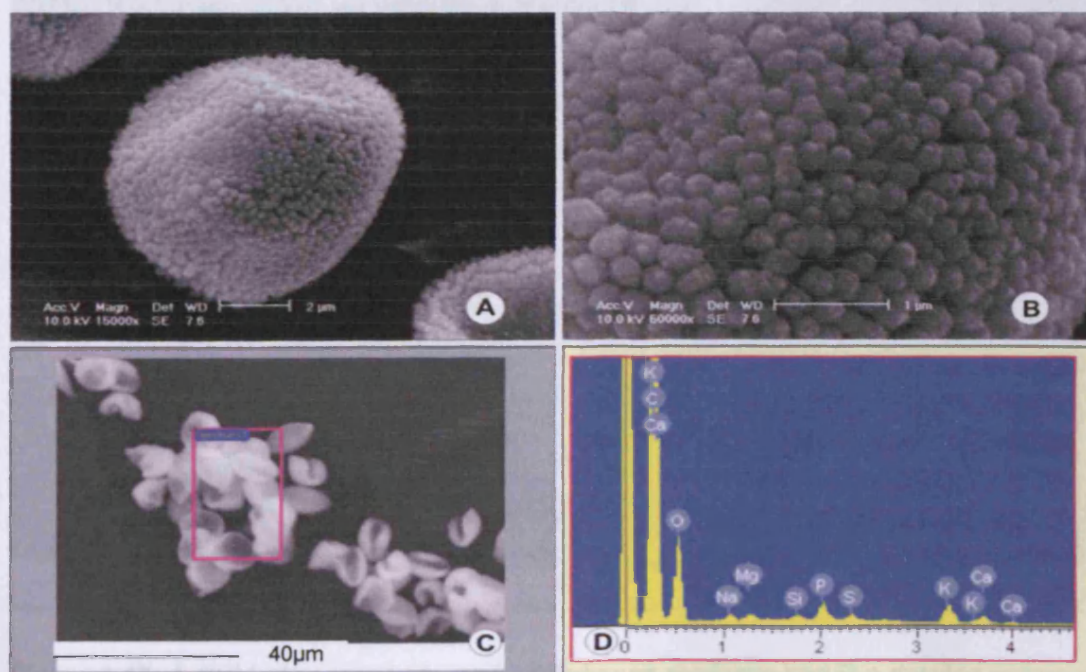


Figure 3.44: **A** SEM of individual spores of *Funaria hygrometrica* and **B** a detailed picture of the densely verrucate sculpture. **C** shows the area from where the EDX analysis was taken (spore clusters) and **D** the spectrum obtained. Note the silicon peak at 1.8.

3.5.1.2 Meesiaceae

Spore clusters of *Leptobryum pyriforme* (Hedw.) Wils. show no sign of silicon but an abundance of elements such as carbon, oxygen, sodium, phosphorous, sulphur and calcium.

Element	Weight%	Atomic%
C	75.64	81.18
O	22.16	17.85
Na	0.77	0.43
P	0.21	0.09
S	0.70	0.28
Ca	0.54	0.17

Table 3.64: Occurrence of various elements (in weight% and atomic%) in spores of in *Leptobryum pyriforme*. No silicon was detected.

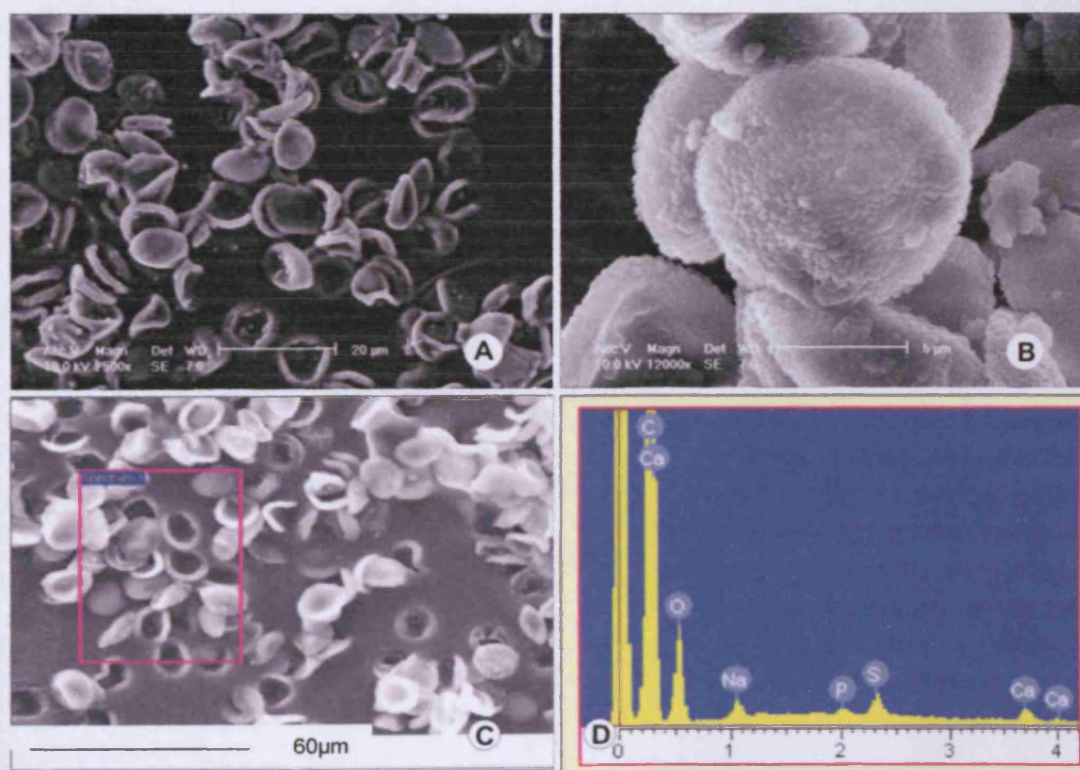


Figure 3.45: **A** SEM of spore clusters of *Leptobryum pyriforme* and **B** a detailed picture of individual spores. **B** note the densely verrucate sculpture. **C** shows the area from where the EDX analysis was taken and **D** the spectrum obtained. No silicon was detected.

3.5.1.3 Bryaceae

Spore clusters of *Bryum capillare* Hedw. contain silicon as well as some other elements such as carbon, oxygen, magnesium, phosphorus, potassium, calcium and molybdenum.

Element	Weight%	Atomic%
C	73.13	79.78
O	23.06	18.88
Mg	0.28	0.15
Si	0.16	0.08
P	0.85	0.36
K	0.49	0.16
Ca	1.62	0.53
Mo	0.40	0.05

Table 3.65: Occurrence of silicon and other elements (in weight % and atomic %) in the spore clusters of *Bryum capillare*.



Figure 3.65: A 3D plot of spore clusters of *Bryum capillare* and Si deposited spores. It shows the spore clusters and spores. The spore clusters are the large, irregular, multi-layered structures. The spores are the small, spherical particles. The plot shows the spore clusters and spores in a 3D space. Note the silicon peak at 1.2.

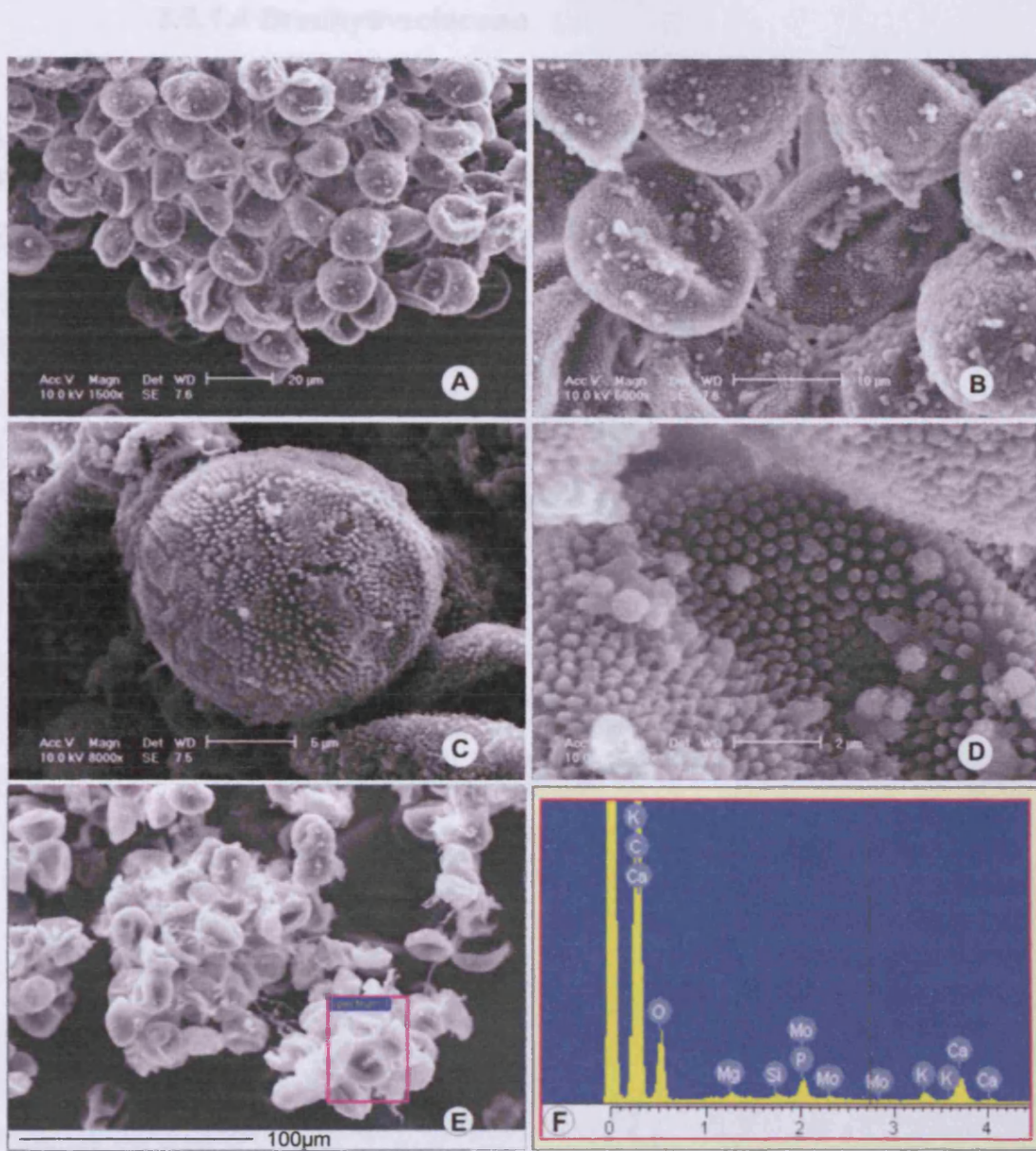


Figure 3.46: **A** SEM of spore clusters of *Bryum capillare* and **B** individual spores. **B** and **C** no aperture was observed. The spore sculpture is densely verrucate **D**. **E** shows the area from where the EDX analysis was taken (spore clusters) and **F** the spectrum obtained. Note the silicon peak at 1.8.

Figure 3.47: A SEM of individual spores of Bryum capillare and B a detailed picture of the densely verrucate sculpture. C shows that individual verrucae are made from quarters of spiral granules. C shows the area from where the EDX analysis was taken (spore clusters) and D the spectrum obtained. Note the silicon peak at 1.8.

3.5.1.4 Brachytheciaceae

The analysis of spore clusters of *Brachythecium velutinum* (Hedw.) B.S.G. showed the presence of silicon as well as the following elements: carbon, oxygen, sodium, magnesium, phosphorus, sulphur, potassium and calcium.

Element	Weight%	Atomic%
C	73.92	80.39
O	22.20	18.13
Na	0.23	0.13
Mg	0.23	0.12
Si	0.20	0.09
P	0.60	0.25
S	0.23	0.10
K	1.42	0.47
Ca	0.97	0.32

Table 3.66: Occurrence of silicon and other elements (in weight % and atomic %) in the spore clusters of *Brachythecium velutinum*.

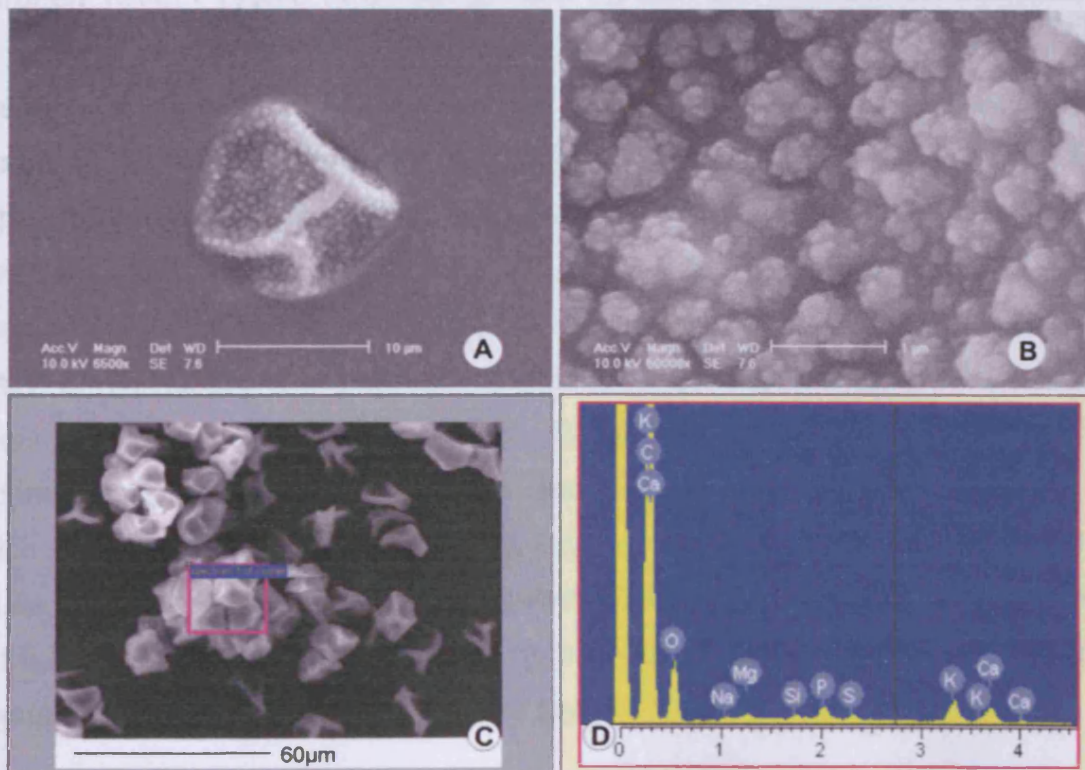


Figure 3.47: **A** SEM of individual spore of *Brachythecium velutinum* and **B** a detailed picture of the densely verrucate sculpture. **B** note that individual verrucae are made from clusters of small granules. **C** shows the area from where the EDX analysis was taken (spore clusters) and **D** the spectrum obtained. Note the silicon peak at 1.8.

3.5.2 Discussion

The literature on general bryophyte biochemistry is comprehensive (for a review see Mues 2000). Recently, the moss *Physcomitrella patens* was shown to release volatile oxylipins, oxygen-containing lipids, upon tissue damage (Wichard *et al.* 2004). Their findings suggest that mosses use different chemical pathways to synthesise the same products that many higher organisms use to conduct chemical signalling and defences. This is only one example, which serves to demonstrate a highly complex secondary metabolism in mosses. Fewer than 10% of all bryophyte species were studied in greater detail and investigations were limited to the gametophyte generation (Mues 2000). Hence, there is very little literature on the chemical composition of bryophyte spores.

Cullmann and Becker (1998) are, to my knowledge, among the few authors to publish on the sporophyte generation of mosses and to study their spores. They cited two other papers focusing on spore chemistry in mosses (Karunen 1972; Pyysalo *et al.* 1978, cited therein) but they did not elaborate on these investigations. Cullmann and Becker's own work revealed the presence of terpenoid and phenolic constituents in sporophytes and terpenoids in spores from *Pellia epiphylla* L. Corda (liverwort). They used a large amount of spores (24.8g) from which several main compounds were extracted: isoafricanol, 1,8-humuladien-5-ol and phytol. Isoafricanol and 1,8-humuladien-5-ol are both classified as sesquiterpenoids, which are a large family of C₁₅-isoprenoid products naturally occurring in higher and lower plants (Peñuelas and Munné-Bosch 2005) and are the largest class of secondary metabolites in bryophytes (Mues 2000). Phytol is a diterpenoid, which belongs to the second largest terpene class detected in bryophytes (Mues 2000), and, as a diterpene alcohol, phytol is part of the chlorophyll a and b complex in its esterified form (Hänsel and Hölzl 1996; Mues 2000). For a summary of terpenoids in bryophytes see the following table 3.67.

Compound class	Liverworts	Hornworts	Mosses
Terpenoids	+++	+	++
Aromatic compounds	+++	++	+++
Nitrogen-containing comp.	++	+	+
Sulphur-containing comp.	+	-	-
Chlorine-containing comp.	++	-	-
Terpenoid class	Liverworts	Hornworts	Mosses
Monoterpenes	60	-	3
Sesquiterpenes	~600	5	9
Diterpenes	~300	-	4
Triterpenes	18	2	25

Table 3.67: Secondary compounds in bryophytes, focusing on terpenoids. +++ indicates >100 compounds, ++ 10-100 compounds and + <10 compounds. This table was modified from Mues (2000, p.154).

The presence of phytol in the spore extracts is not surprising since bryophyte spores are often rich in chlorophyll and hence are green in appearance, an observation that was also noted by Cullmann and Becker (1998) and Mues (2000). Cullmann and Becker (1998) conclude that the sporophyte seems to have its own secondary metabolism, due to the high variety and amount of constituents found therein. There are also differences in metabolites of the gametophyte and the sporophyte generation, which strengthens the hypothesis that these two generations have separate secondary metabolisms. One can merely speculate on the pathway of sporophyte constituents such as phytol or isoafiranol into the spores but it is suspected that during sporogenesis metabolites are transported into the spore capules and eventually become incorporated into the spores, which would explain their presence in spore extracts. Cullmann and Becker do not elaborate on possible functions of the sesquiterpenes and diterpenes in the sporophyte or spores. Sesquiterpenoids as well as dipterpenoids are both synthesised by plants from isoprenoids, of which over 30000 have so far been characterised (Peñuelas and Munné-Bosch 2005). In plants, isoprenoids function, for example, as visual pigments, reproductive hormones, defensive agents, constituents of membranes, components of signal transduction networks, mating pheromones, and photoprotective agents (Sacchetti and Poulter 1997). Strasburger (1998) provides a comprehensive overview on the biosynthesis of isoprenoids, and gives various examples for the occurrence of terpenoids in plants. Monoterpenes, for instance, can be synthesised into

menthol, thymol, menthon and cineol, sesquiterpenes occur as farnesole or abscisic acid, diterpenes as phytol or gibberelins, triterpenes such as steroids and tetraterpenes as carotenoids. Some products of the isoprene synthesis in plants are shown in figure 3.48, demonstrating the variety of secondary plant metabolites.

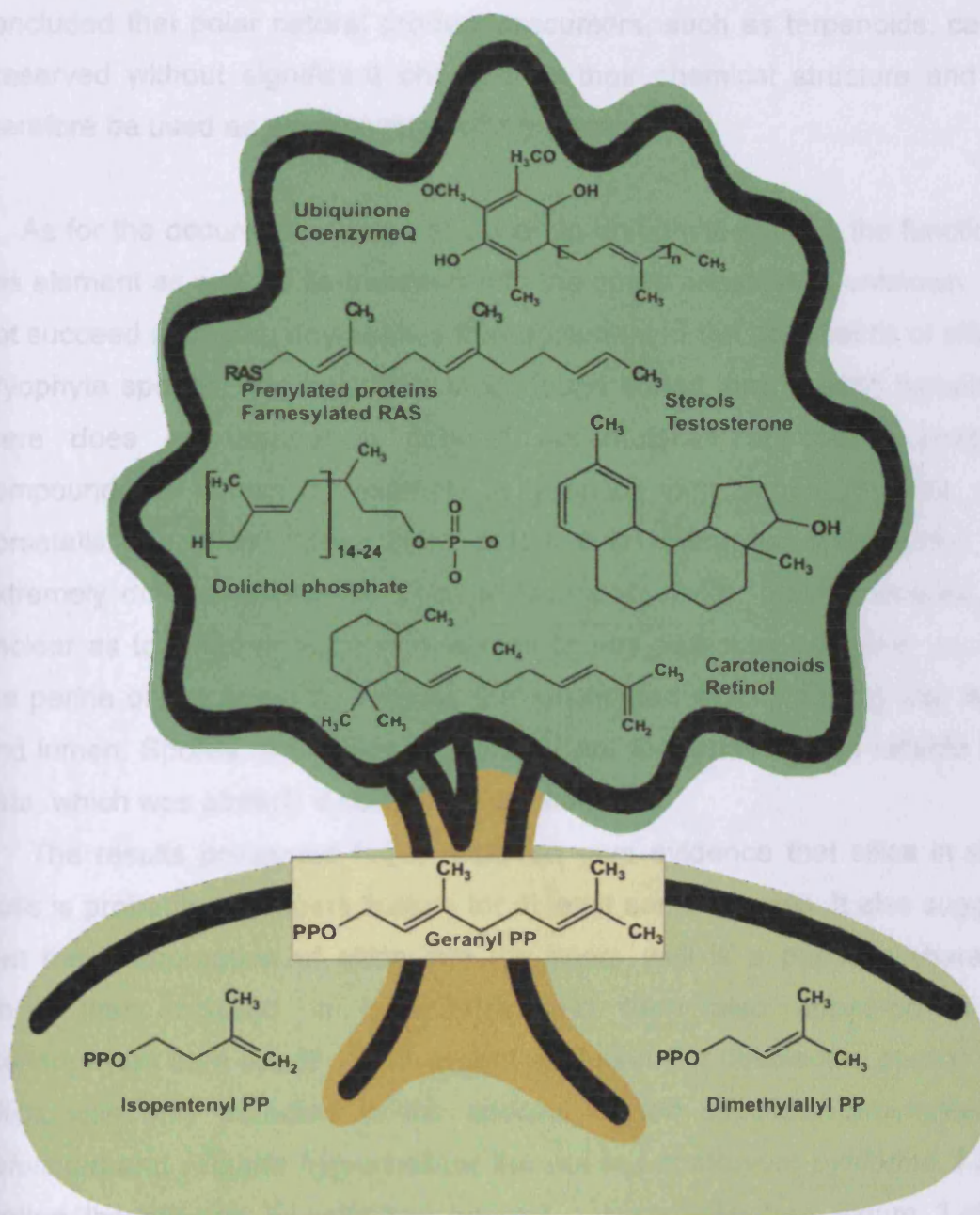


Figure 3.48: Isoprenoid synthesis in plants, starting with the two precursors isopentenyl PP and dimethylallyl PP. The tree gives various examples of secondary metabolites such as carotenoids, sterols, phosphates, proteins or co-enzymes - all of which are derived from the two precursors. The figure is redrawn from Sacchettini and Poulter (1997).

Terpenoids can also be utilised as valuable markers for (paleo-) chemosystematics and phylogeny, as shown for two fossil conifer cones from *Taxodium balticum* (Eocene) and *Glyptostrobus oregonensis* (Miocene) (Otto *et al.* 2002). The authors demonstrated that terpenoids isolated from the fossil cones matched those from the extant conifer *Taxodium distichum* and concluded that polar natural product precursors, such as terpenoids, can be preserved without significant changes to their chemical structure and can therefore be used as chemosystematic markers.

As for the occurrence traces of silicon in bryophyte spores, the function of this element as well as its transport into the spore capsules is unknown. I did not succeed in tracing any studies that documented the occurrence of silica in bryophyte spores. The only reference found stated that “among bryophytes there does not appear a general accumulation of special inorganic compounds as known for example in lycopods with aluminium oxide, or in horsetails with silica” (Mues 2000, p.151, 5.1.1 Inorganic compounds). It is extremely difficult to localise silica in the spore walls, mainly because it is unclear as to whether silica is restricted to any particular wall layer such as the perine or the exine or whether it is distributed evenly among wall layers and lumen. Spores of 8-18 μ m in diameter are too small to gain reliable EDX data, which was already discussed in *section 3.3*.

The results presented here, however, give evidence that silica in spore walls is probably a genuine feature for at least some species. It also suggests that the incorporation of silica into the spore wall is a primitive character, which first occurred in bryophytes and then also appeared in the pteridophytes as a result of convergent evolution (for details see *section 3.3*). Silica was only detected in the species *Bryum capillare*, *Brachythecium velutinum* and *Funaria hygrometrica* but not in *Leptobryum pyriforme*. I have plotted the species investigated against a systematic tree (figure 3.49) in order to see how closely the species are related and whether there is any correlation between their systematic position and the presence of silica in the spore clusters. *Funaria hygrometrica* is in the out-group, whereas *Leptobryum*

pyriforme, *Bryum* and *Brachythecium* form separate clades, of which none of the above is placed sister to the other.

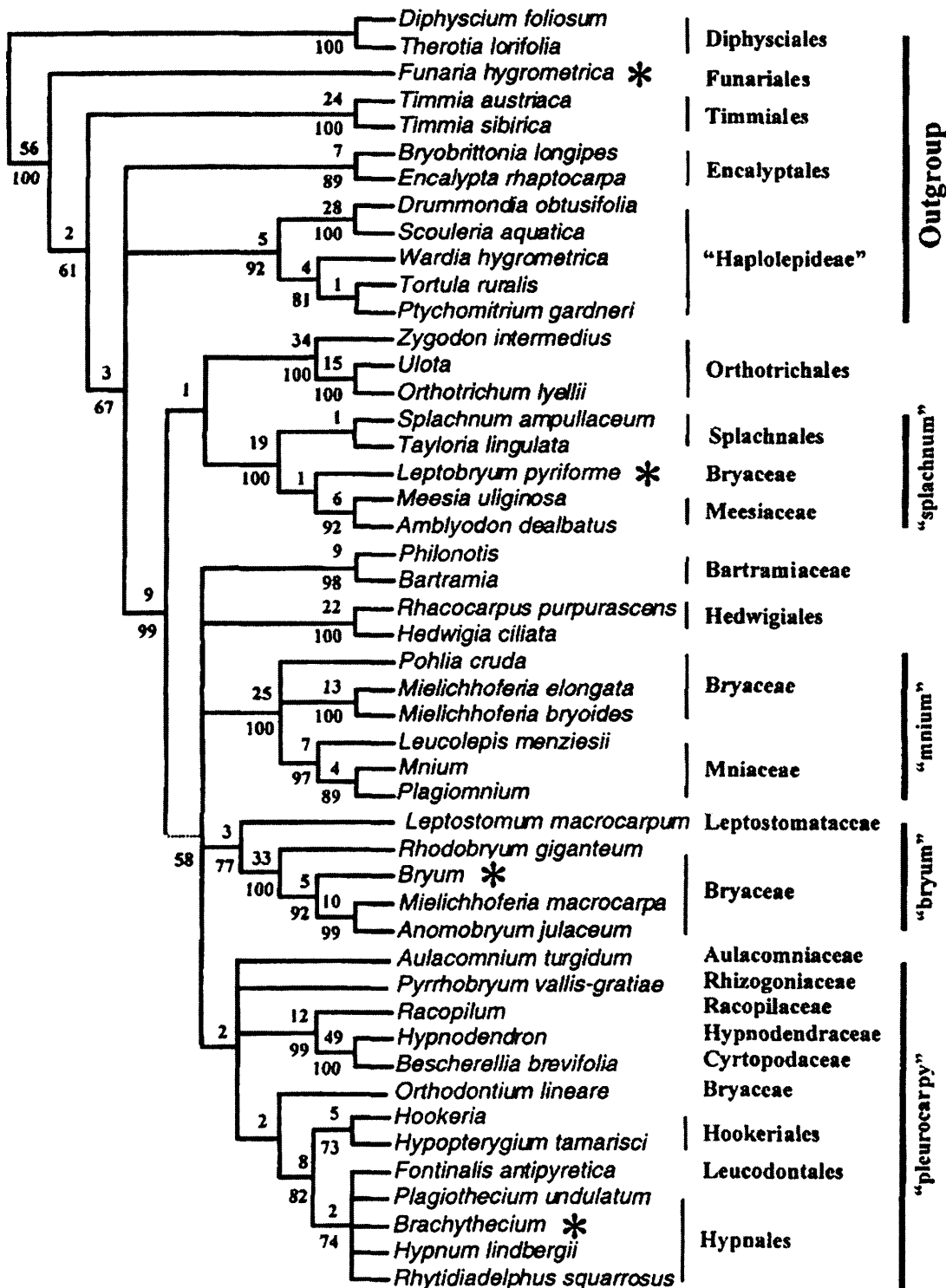


Figure 3.49: Summary tree of equally-weighted parsimony analyses of combined *rps4*, *trnL-F*, *rbcL* and 18s rDNA sequences for 48 taxa of the diploleptideous-alternate mosses. The species investigated in this study are highlighted with an asterisk. Systematic tree from Cox *et al.* (2000).

Although *Leptobryum pyriforme* is often placed among the Bryaceae (Cox *et al.* 2000), some authors place them into the Meesiaceae (Bruck and Goffinet 2000). This does not have any implications for this study as Meesiaceae and Bryaceae form a clade with *Leptobryum pyriforme* being placed sister to *Meesia uliginosa* and *Amblyodon dealbatus*.

In the light of the present results it seems that silica in spore walls could be as randomly distributed among bryophytes as it is among pteridophytes. As for all the other elements detected in bryophyte spore clusters such as carbon, phosphorus sulphur, potassium, calcium, oxygen, sodium, chlorine, magnesium or molybdenum, the same considerations apply to bryophytes and pteridophytes, see *sections 3.3 and 3.4* where plant nutrients are discussed in more detail. I can only reiterate the statement that “there is not a single element that has not been detected in plants” (Strasburger 1998).

4 New Insights from MALDI-ToF MS, NMR, GC-MS and chemical treatments: analytical chemistry techniques applied to palynology

The following table (4.1) summarises this chapter providing methods, protocols, species investigated and their morphological descriptions with references to other chapters. Analytical chemistry was carried out in order to find out more about the chemical nature of spore walls and of sporopollenin in particular. Chemical treatments were aimed at removing and analysing the perispore of certain pteridophytes. In both cases *Pinus sylvestris* pollen served as a control.

Results	Species investigated	References
Analytical Chemistry		
MALDI - ToF MS	<i>Selaginella pallescens</i> and <i>Lycopodium clavatum</i>	Protocols: <i>Material and Methods 2.6.2</i>
¹ H NMR and GC-MS	<i>Selaginella pallescens</i> and <i>Pinus sylvestris</i>	Protocols: <i>Material and Methods 2.6.1</i>
Chemical Treatments		
Treatment with 1% potassium permanganate solution	<i>Pellaea calomelanos</i> , <i>P. rotundifolia</i> , <i>Blechnum gibbum</i> , <i>Lycopodium clavatum</i>	Protocols: <i>Material and Methods 2.5.1</i>
Treatment with MMNO (plus ¹ H NMR)	<i>Lycopodium clavatum</i> , <i>Selaginella pallescens</i> , <i>Pinus sylvestris</i>	Protocols: <i>Material and Methods 2.5.2</i>
Soxhlet Extractions with DCM (plus ¹ H + ¹³ C NMR)	<i>Lycopodium clavatum</i> , <i>Selaginella pallescens</i>	Protocols: <i>Material and Methods 2.5.3</i>

Table 4.1: Summary of results, methods and references for *chapter 4*.

4.1 Results

4.1.1 MALDI - ToF MS

The spectra obtained from analysis of *Selaginella pallescens* and *Lycopodium clavatum* are shown in figure 4.1. The MALDI-ToF mass spectra obtained from spores extracted with a base, acid and solvent treatment might represent pure sporopollenin. As the structure of sporopollenin is unknown, any possible reactions of sporopollenin with either the base, acid or solvent are difficult to anticipate but should not be ignored. This harsh treatment was

chosen as it is supposed to remove lipids, polysaccharides, proteins and callose, which are all part of the spore wall (Pettitt 1974, 1979b; Schneider and Pryer 2002).

The spectra indicate ions at approximately m/z 8000 and 4400 to 4800 with the *Lycopodium clavatum* analysis also generating ions between m/z 6936 and 7588 (in positive ionisation mode) and at m/z 17654. The differences in mass between these ions suggest that they are not related purely by simple dimerisation of the smallest suspected sporopollenin monomer molecule (*p*-coumaric acid). They must therefore arise from complex arrangements possibly between different subunits or between subunits representing *p*-coumaric acid and co-complexing moieties of differing masses.

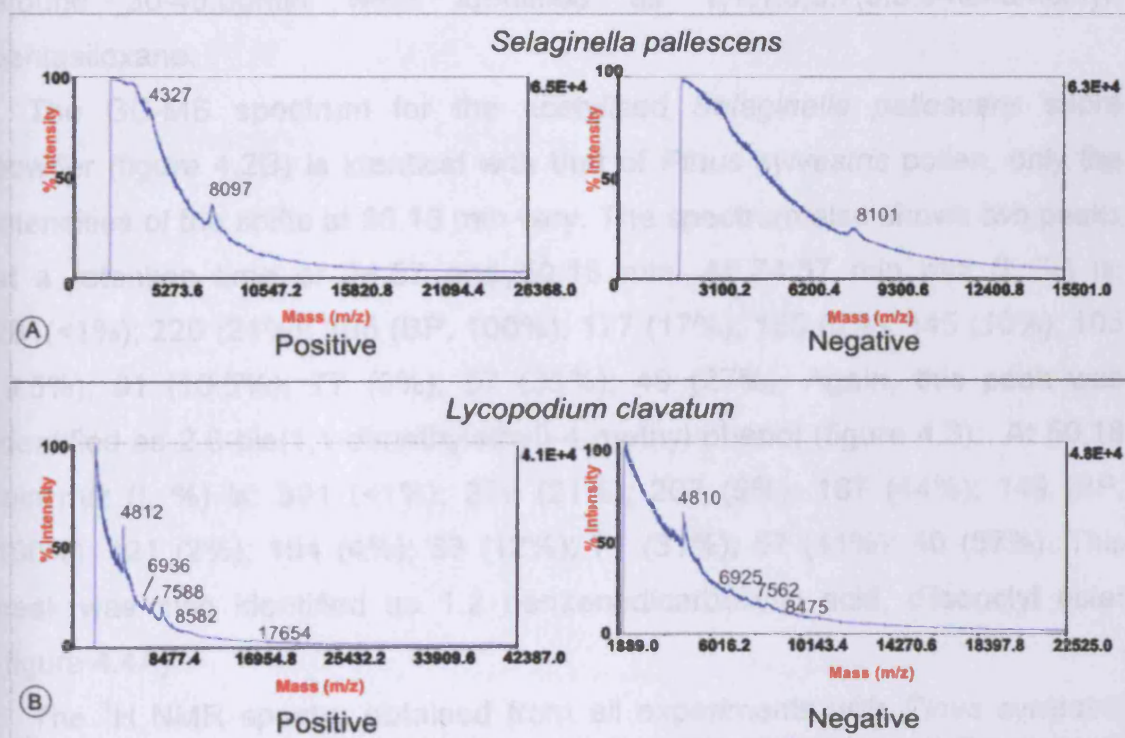


Figure 4.1: MALDI-ToF MS spectra of spore powder of **A** *Selaginella pallescens* and **B** *Lycopodium clavatum* prepared for this analysis (see *Material and Methods* 2.6.2). Both show ions at approximately m/z 8000 and 4400 to 4800 with *Lycopodium clavatum* also generating ions between m/z 6936 and 7588 (in positive ionisation mode) and above m/z 17654.

4.1.2 GC-MS and ^1H NMR

The GC-MS spectrum (figure 4.2A) for *Pinus sylvestris* pollen shows two components at retention times of 24.54min and 50.10min, respectively, as well as a range of smaller peaks between 30–45.00. At 24.54 min mass peaks (I, %) of: 281 (<1%); 220 (21%); 205 (BP, 100%); 177 (17%); 155 (5%); 145 (10%); 105 (9.5%); 91 (10.5%); 77 (9%); 57 (35%); 40 (27%) are presented. The GC-MS' internal library identified this peak as 2,6-bis(1,1-dimethylethyl)-4-methyl phenol (figure 4.3). At 50.10 min mass peaks m/z (I, %) are: 391 (2%); 279 (11%); 207 (1%); 167 (44%); 149 (BP, 100%); 121 (2%); 104 (4%); 83 (9.5%); 71 (27%); 57 (41%); 40 (52%). This peak was identified as 1,2 benzenedicarboxylic acid, diisooctyl ester (figure 4.4A). Several small peaks around 30–45.00min were identified as 1,1,1,3,5,7,9,9,9-nonamethyl-pentasiloxane.

The GC-MS spectrum for the acetylated *Selaginella pallescens* spore powder (figure 4.2B) is identical with that of *Pinus sylvestris* pollen, only the intensities of the shifts at 50.18 min vary. The spectrum also shows two peaks at a retention time of 24.57 and 50.18 min. At 24.57 min m/z (I, %) is: 281(<1%); 220 (21%); 205 (BP, 100%); 177 (17%); 155 (5%); 145 (10%); 105 (9.5%); 91 (10.5%); 77 (9%); 57 (35%); 40 (27%). Again, this peak was identified as 2,6-bis(1,1-dimethylethyl)-4-methyl phenol (figure 4.3). At 50.18 min m/z (I, %) is: 391 (<1%); 279 (21%); 207 (5%); 167 (44%); 149 (BP, 100%); 121 (2%); 104 (4%); 83 (12%); 71 (31%); 57 (41%); 40 (57%). This peak was also identified as 1,2 benzenedicarboxylic acid, diisooctyl ester (figure 4.4A).

The ^1H NMR spectra obtained from all experiments with *Pinus sylvestris* pollen, including the blank, are identical (figure 4.5A-C). They differ only in shift intensity. Shifts can be found in the range of ppm: 0.7-0.9, 1.1-1.25, 1.4, 1.5-1.7, 1.9, 2.1, 2.2, 3.3-3.4, 3.7, 4.1-4.2, 4.9, 6.9, 7.2 (*d*-chloroform), 7.55 and 7.64.

The ^1H NMR spectrum obtained from acetylated *Selaginella pallescens* megaspore powder (figure 4.5C) is almost identical to that of *Pinus sylvestris* pollen. The only difference found is in the area of 3.7ppm, which is not present in the spectrum of the acetylated *Selaginella pallescens* megaspore powder.

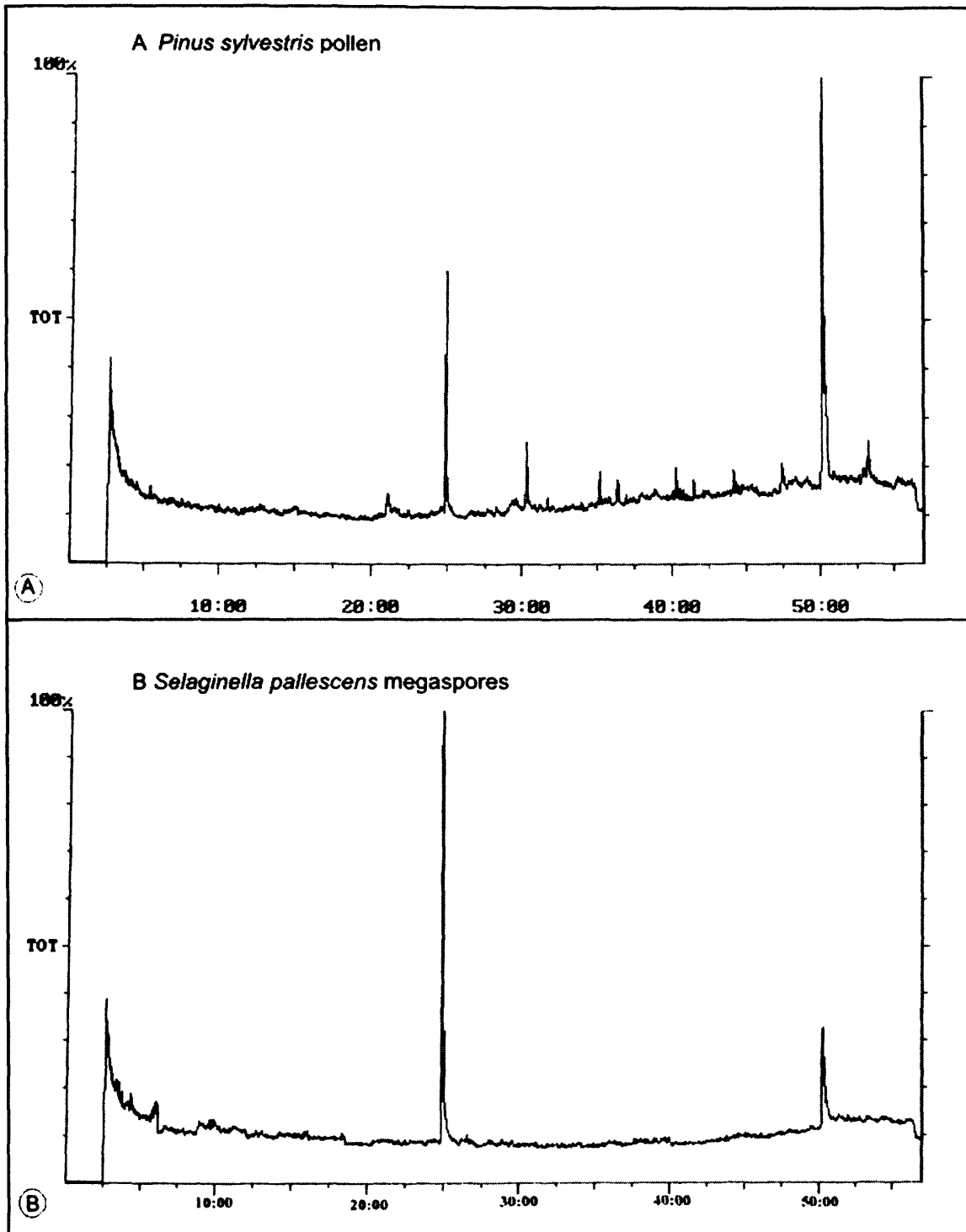


Figure 4.2: GC MS spectra of *Pinus sylvestris* and *Selaginella pallescens*. **A** *Pinus sylvestris* pollen showing two peaks at a retention time of 24.54 and 50.10 minutes, as well as various smaller shift between 30-45 minutes. The peaks were identified as 2,6-bis(1,1-dimethylethyl)-4-methyl phenol (BHT) and 1,2 benzenedicarboxylic acid, diisooctyl ester (Phthalic acid-diisooctyl ester). **B** *Selaginella pallescens* megaspore powder showing two shifts at a retention time of 24.7 and 50.18 minutes. The peaks were identified as 2,6-bis(1,1-dimethylethyl)-4-methyl phenol (BHT) and 1,2 benzenedicarboxylic acid, diisooctyl ester (Phthalic acid-diisooctyl ester).

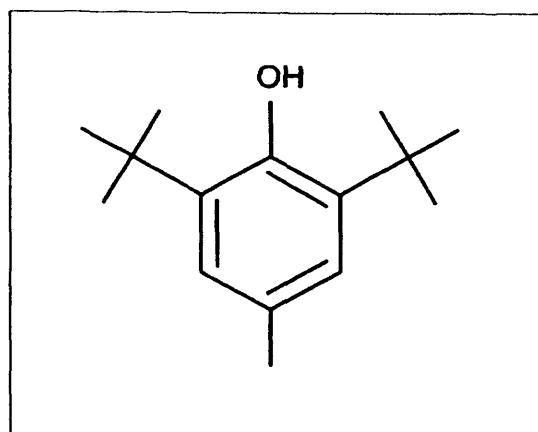


Figure 4.3: Chemical structure of 2,6-bis(1,1-dimethylethyl)-4-methyl phenol (BHT) found in the present study.

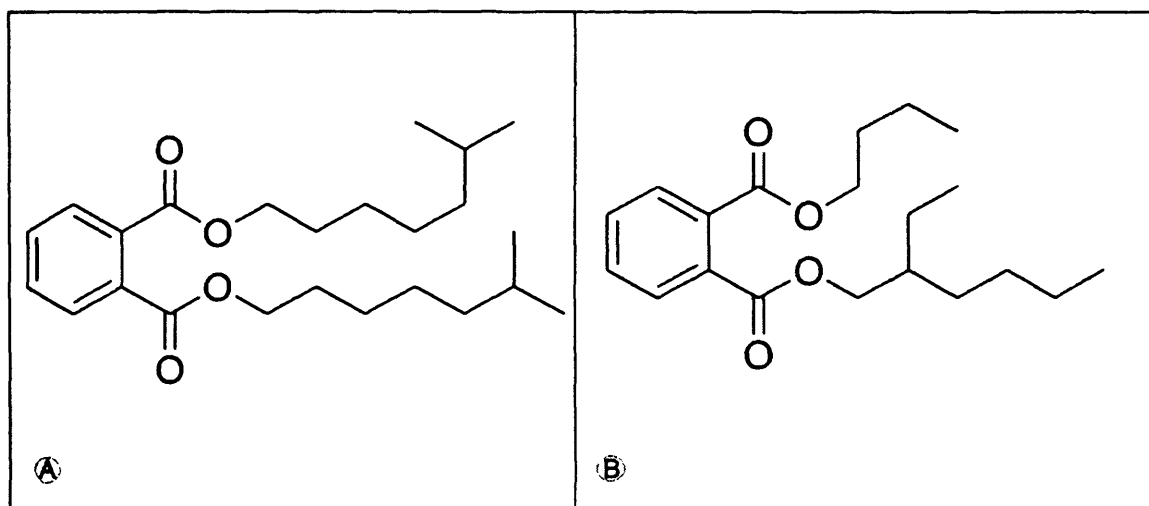


Figure 4.4: Chemical structure of **A** 1,2 benzenedicarboxylic acid, diisooctyl ester (Phthalic acid-diisooctyl ester) and **B** 1,2 benzenedicarboxylic acid, butyl 2-ethylhexyl ester. 1,2 benzenedicarboxylic acid, diisooctyl ester ($C_{24}H_{38}O_4$) has an exact mass of 390.28 and a molecular weight of 390.65. 1,2 benzenedicarboxylic acid, butyl 2-ethylhexyl ester ($C_{20}H_{30}O_4$) has an exact mass of 334.21 and a molecular weight of 334.45.

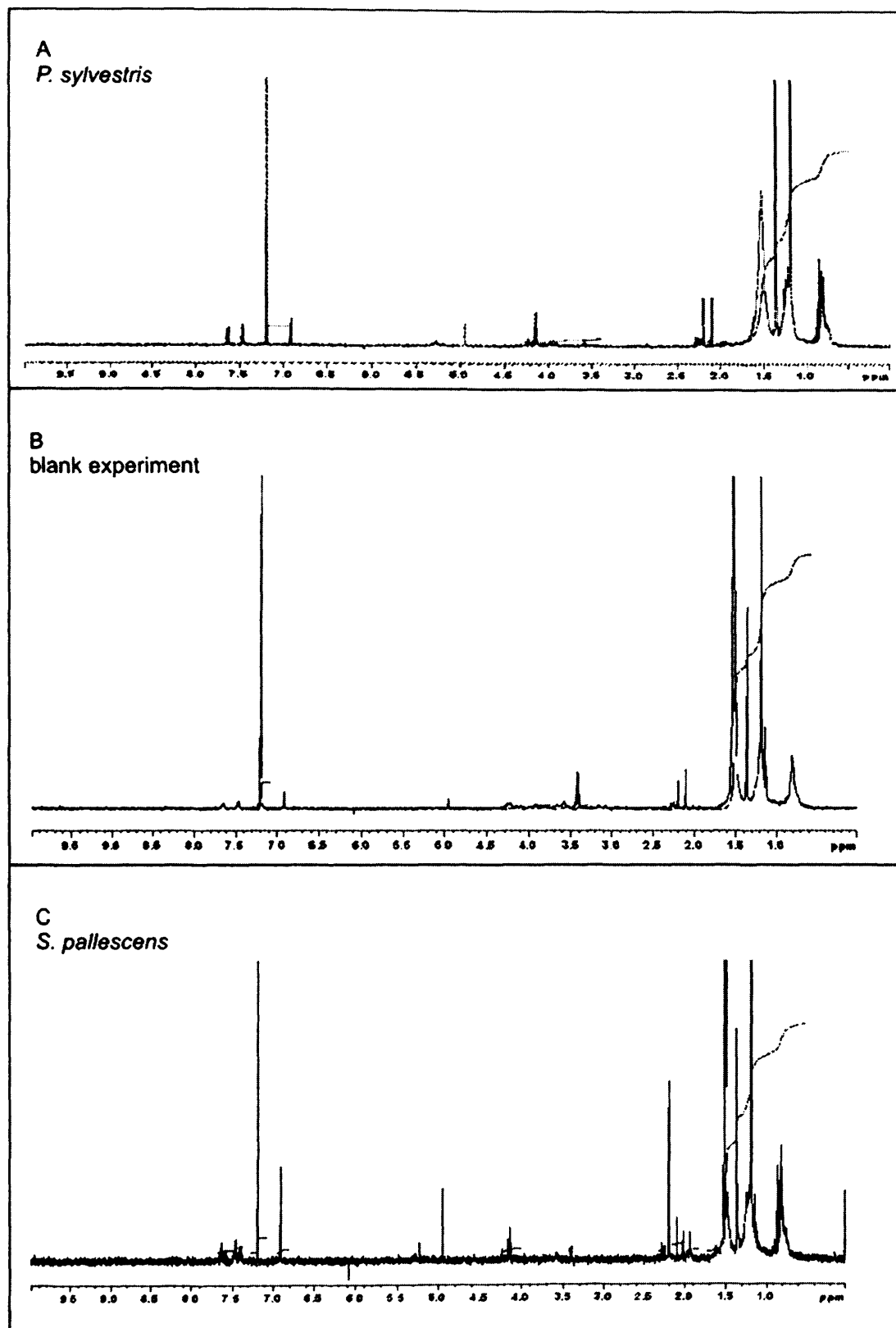


Figure 4.5: Three identical ^1H NMR spectra obtained from experiments using **A** *Pinus sylvestris* pollen, **B** a blank experiment and **C** *Selaginella pallescens* megaspore powder. The reference at 0ppm is TMS.

4.1.3 Chemical Treatments

Treatment with 1% KMnO₄ solution Potassium permanganate solution did not have any effects on the perispore of the spores investigated. It was only in *Pellaea calomelanos* that the true perispore broke away (compare figure 4.6A and B) partly revealing the finely granulate exospore (compare figure 4.6C and D). Although the potassium permanganate solution left a thin, granulate crust on all treated spores it is still obvious that the sculpture was not affected. The spores of *Pellaea rotundifolia* (figure 4.6E-H), *Blechnum gibbum* (figure 4.7A and B) and *Lycopodium clavatum* (figure 4.7C-H) remained unchanged in respect to their true perispore.

Treatment with MMNO The hot MMNO treatment had a clear effect on the perispore of *Selaginella pallescens*. The perispore was almost completely abraded, revealing the underlying exospore. In some megaspores the distal, formerly reticulate surface, was completely abraded revealing a laevigate exospore (compare figure 4.8C with D). Proximally, the overall densely granulate face was also abraded revealing a laevigate exospore (compare figure 4.8A with B). At higher magnification it becomes clear that on the distal face the reticulae are covered with a thin, echinulate micro-sculpture (figure 4.8E). This micro-sculpture dissolved entirely after MMNO treatment (figure 4.8F). On the proximal face again the densely verrucate surface is covered by an echinulate micro-sculpture (figure 4.8G). This micro-sculpture also becomes abraded but some debris can still be seen after 30min of MMNO treatment (figure 4.8H).

Pinus sylestris pollen as well as *Lycopodium clavatum* isospores were not affected by MMNO treatment (figure 4.9A-F). Although the sculpture of *Lycopodium clavatum* shows holes of <1.5nm in diameter, this is a feature that can also be observed in untreated spores (compare figure 4.9A with B). There are also no signs of changes in the ectexine of *Pinus sylvestris* (compare figure 4.9C, E with D, F). The ¹H NMR spectra obtained from *Pinus sylvestris* pollen, *Selaginella pallescens* megaspores and *Lycopodium clavatum* isospores after MMNO treatment are identical. ¹H : Shifts can be

found in the range of ppm: 0.7-0.9, 1.1-1.25, 1.4, 1.5-1.7, 1.9, 2.1, 2.2, 4.1-4.2, 4.9, 6.9, 7.2 (*d*-chloroform), 7.55 and 7.64 (figure 4.10A-C).

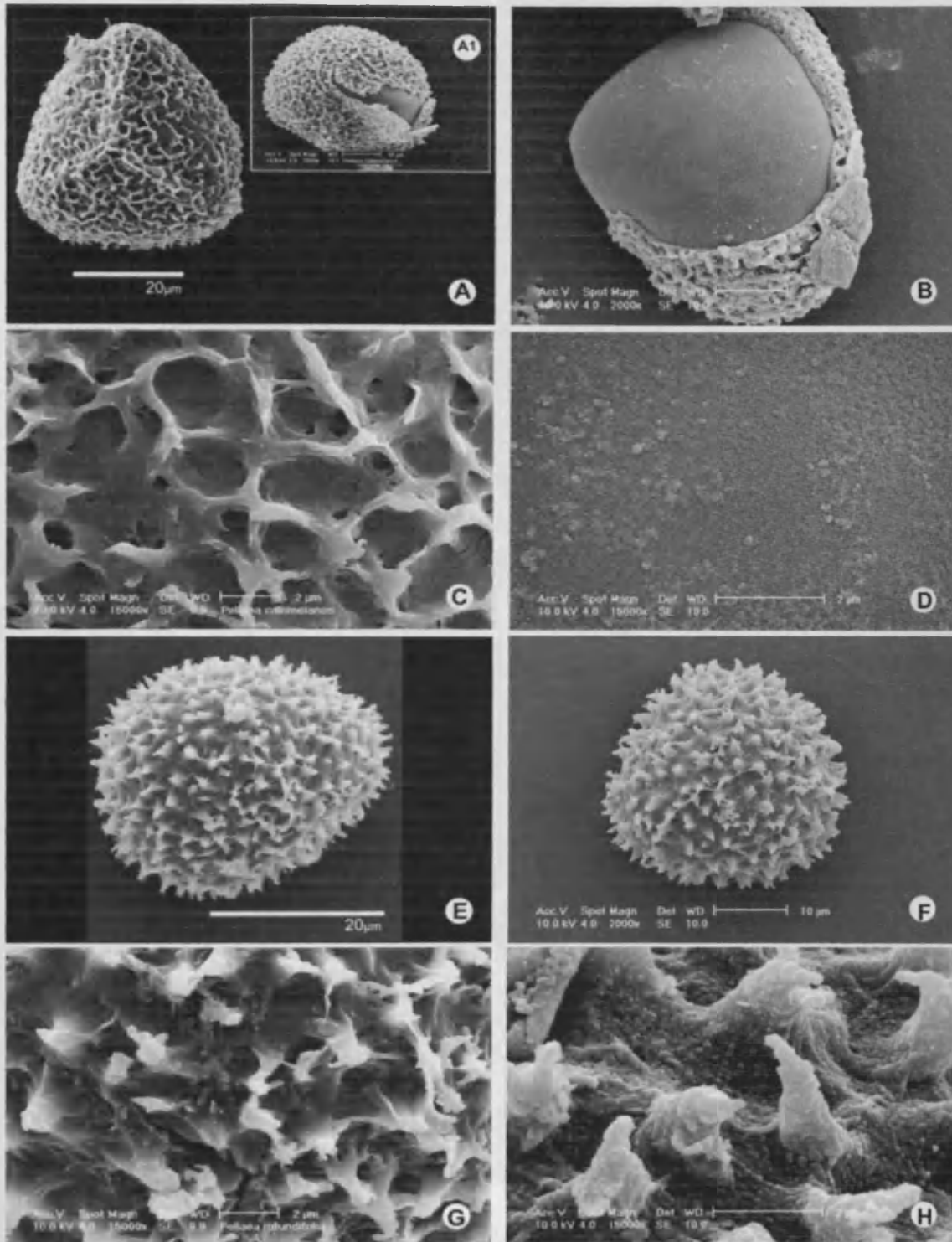


Figure 4.6: SEM pictures of *Pellaea calomelanos* (A-D) and *Pellaea rotundifolia* (E-H) before (A+C, E+G) and after (B+D, F+H) treatment with 1% potassium permanganate solution. For scale bars see individual pictures. Figs A, A1 and C show the untreated spore of *Pellaea calomelanos* in polar view A and the reticulate surface sculpture C. The potassium permanganate treatment did not change the overall sculpture but triggered the shedding of the true perispore B so that the exospore D is fully exposed. The echinate sculpture of *Pellaea rotundifolia* (E+G) remained unaffected by potassium permanganate (F+H).

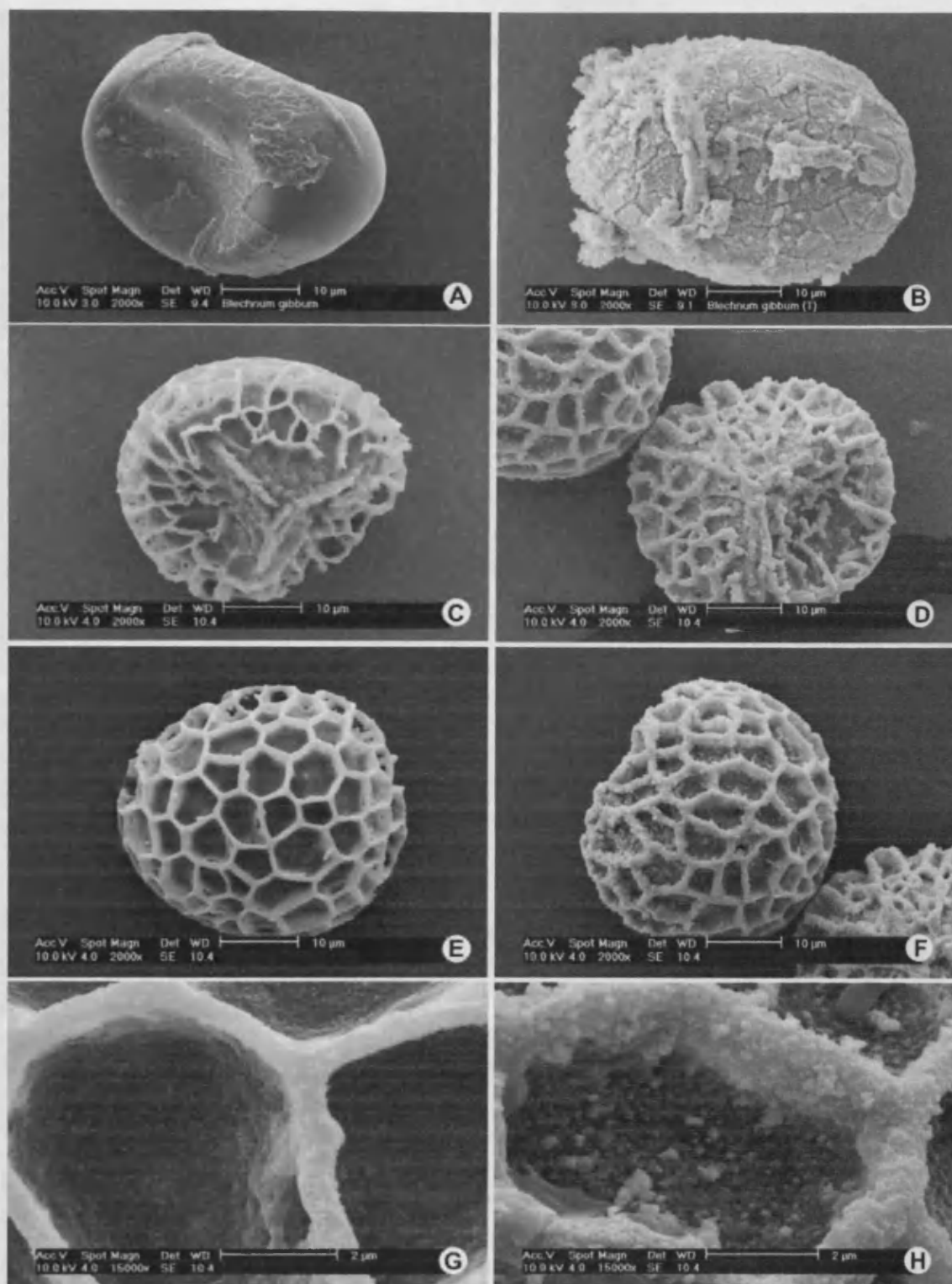


Figure 4.7: SEM pictures of *Blechnum gibbum* (A+B) and *Lycopodium clavatum* (C-H) before (C,E,G) and after (D,F,H) treatment with 1% potassium permanganate solution. All treated spores show no change in sculpture. In *Lycopodium clavatum* neither the proximal face D nor the distal face F are affected. The potassium permanganate access deposits in form of a thin, granulate crust (C+H in particular).

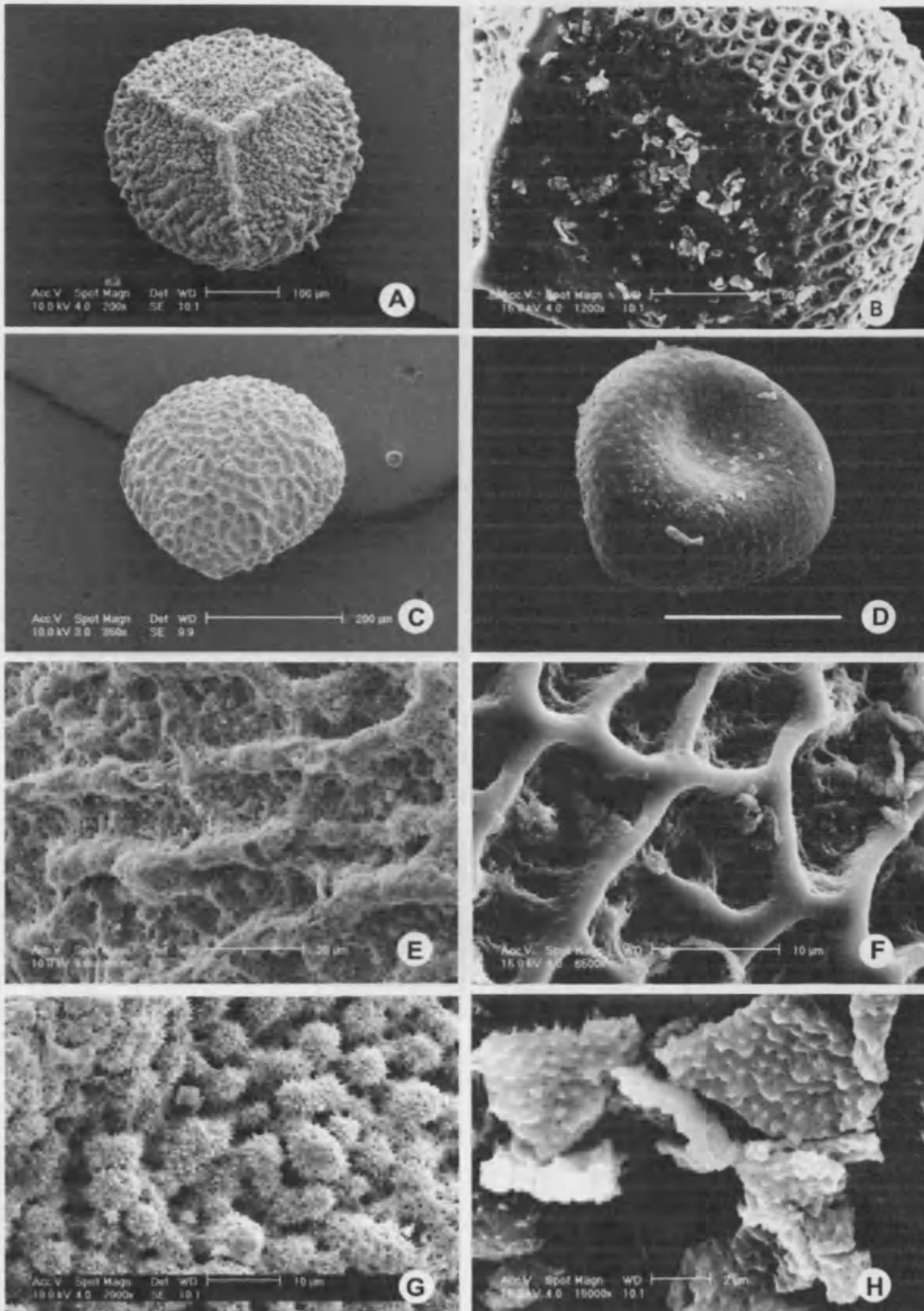


Figure 4.8: SEM pictures of *Selaginella pallescens* before (A,C,E,G) and after (B,D,F,H) treatment with MMNO. The untreated megaspore A shows a closely verrucate proximal and a reticulate distal C surface. The micro-sculpture (for a definition of this term see Moore *et al.* in press a) is echinate (E+G). After MMNO treatment the proximal surface is almost completely abraded B. In some megaspores even the reticulate distal surface is entirely abraded D. Figs E and F show the untreated distal sculpture E and the exposed ridges after treatment F. A more detailed view of the untreated echinate proximal face is given in G. MMNO has a visible effect on the micro-sculpture H, which is partially dissolved.

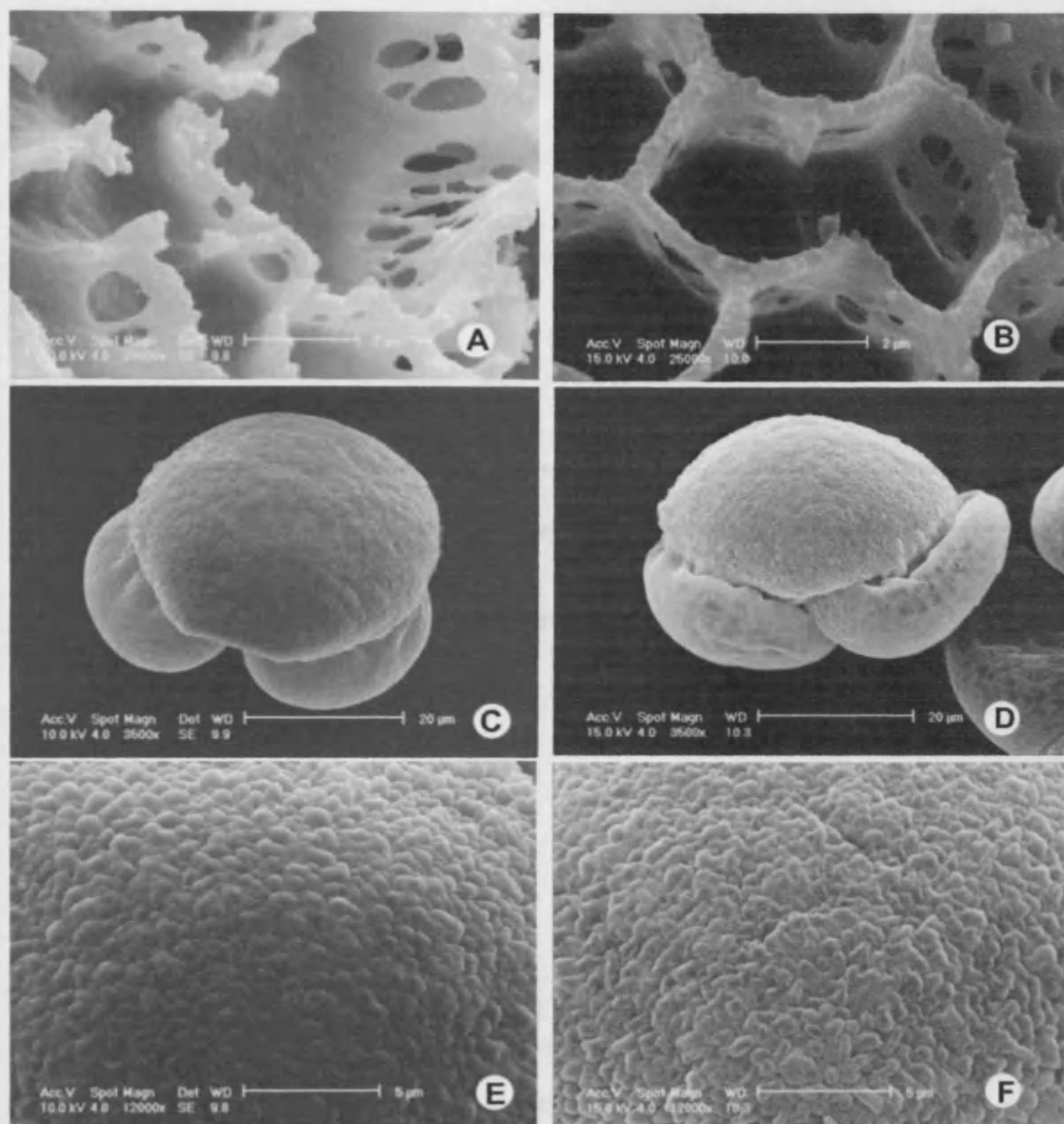


Figure 4.9: SEM of *Lycopodium clavatum* A + B and *Pinus sylvestris* C-F before (A, C+E) and after (B, D+F) treatment with MMNO.

Scientific extractions with CH_2Cl_2 . The ^{13}C and ^{15}N NMR spectra were obtained from the stems, needles, cones, and leaf material (Seymour's procedure) and assigned to corresponding structures and chemical figure 4-11A-F. ^{13}C shifts can be found in the region of ppm: 0-119, 11-125, 14, 13-17, 18, 21-22, 27, 28, 34, 33, 41-43, 59, 72 (aromatics), 73 and 76. ^{15}N 10-17, 22, 23-24, 25, 26, 27, 28, 29, 30, 31, 32, 33, 34, 35, 36, 37, 38, 39, 40, 41, 42, 43, 44, 45, 46, 47, 48, 49, 50, 51, 52, 53, 54, 55, 56, 57, 58, 59, 60, 61, 62, 63, 64, 65, 66, 67, 68, 69, 70, 71, 72, 73, 74, 75, 76, 77, 78, 79, 80, 81, 82, 83, 84, 85, 86, 87, 88, 89, 90, 91, 92, 93, 94, 95, 96, 97, 98, 99, 100. The ^{13}C NMR spectrum generated by a Bruker Avance 400 is shown in appendix number 3) as only the organic cone was available, it could not be processed digitally.

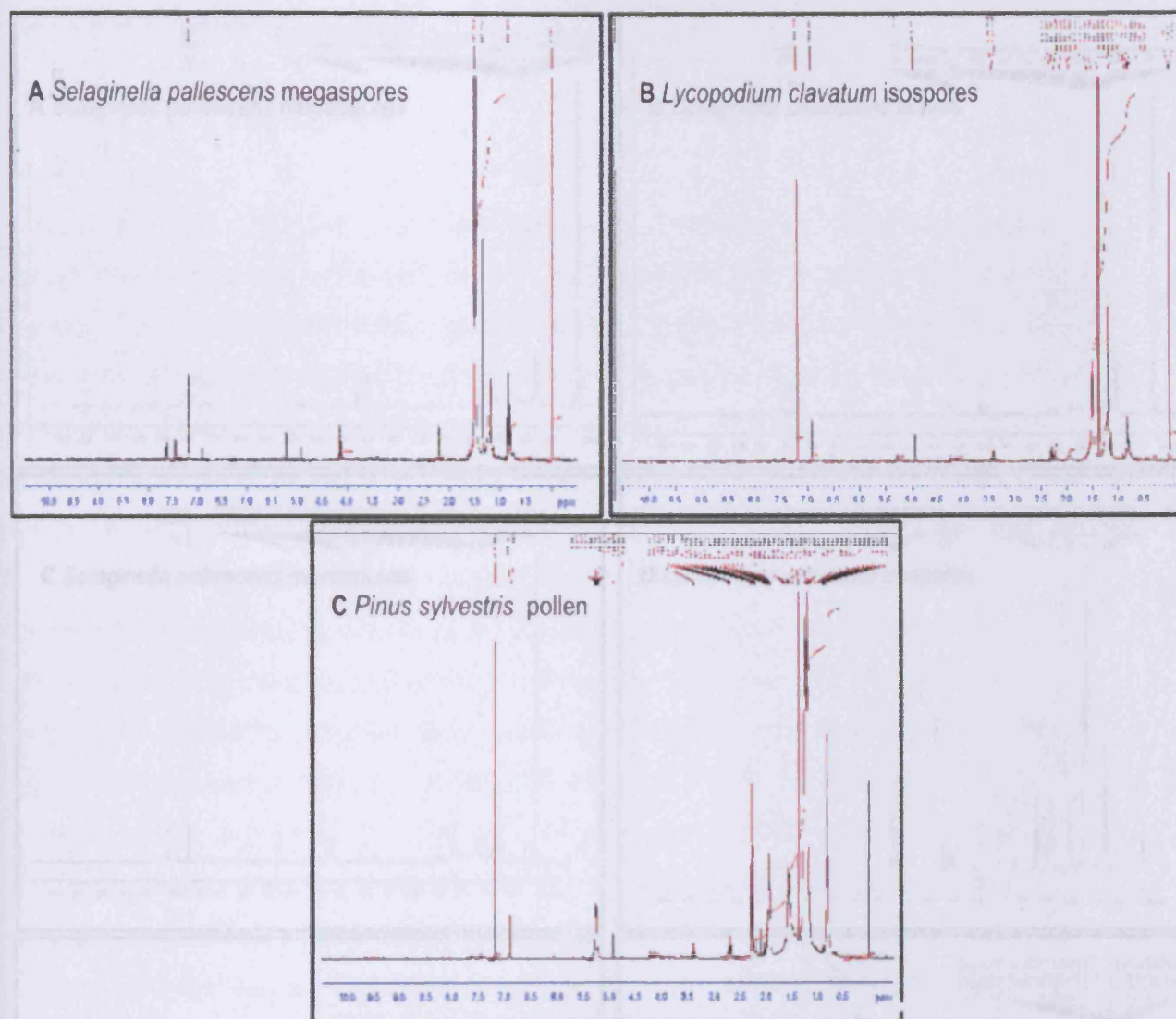


Figure 4.10: ^1H NMR data: Spectra of MMNO treated *Selaginella pallescens* megaspores **A**, *Lycopodium clavatum* isospores **B** and *Pinus sylvestris* pollen **C**. The spectra show a correlation of shifts, which leads to the hypothesis that they all characterise the same product.

Soxhlet extractions with DCM The ^1H and ^{13}C NMR spectra obtained from extractions of mega-, microspore and leaf material (*Selaginella pallescens*) and isospores (*Lycopodium clavatum*) are identical (figure 4.11A-F). ^1H : Shifts can be found in the range of ppm: 0.7-0.9, 1.1-1.25, 1.4, 1.5-1.7, 1.9, 2.1, 2.2, 2.7, 3.3-3.4, 3.7, 4.1-4.2, 6.9, 7.2 (*d*-chloroform), 7.55 and 7.64. ^{13}C : 10-37, 60-79 (75-79 *d*-chloroform), 125-131, 172-174, 178. The ^{13}C NMR spectrum generated at a scan rate of 5000 is attached as appendix (number 3) as only the original data set was available, it could not be processed digitally.

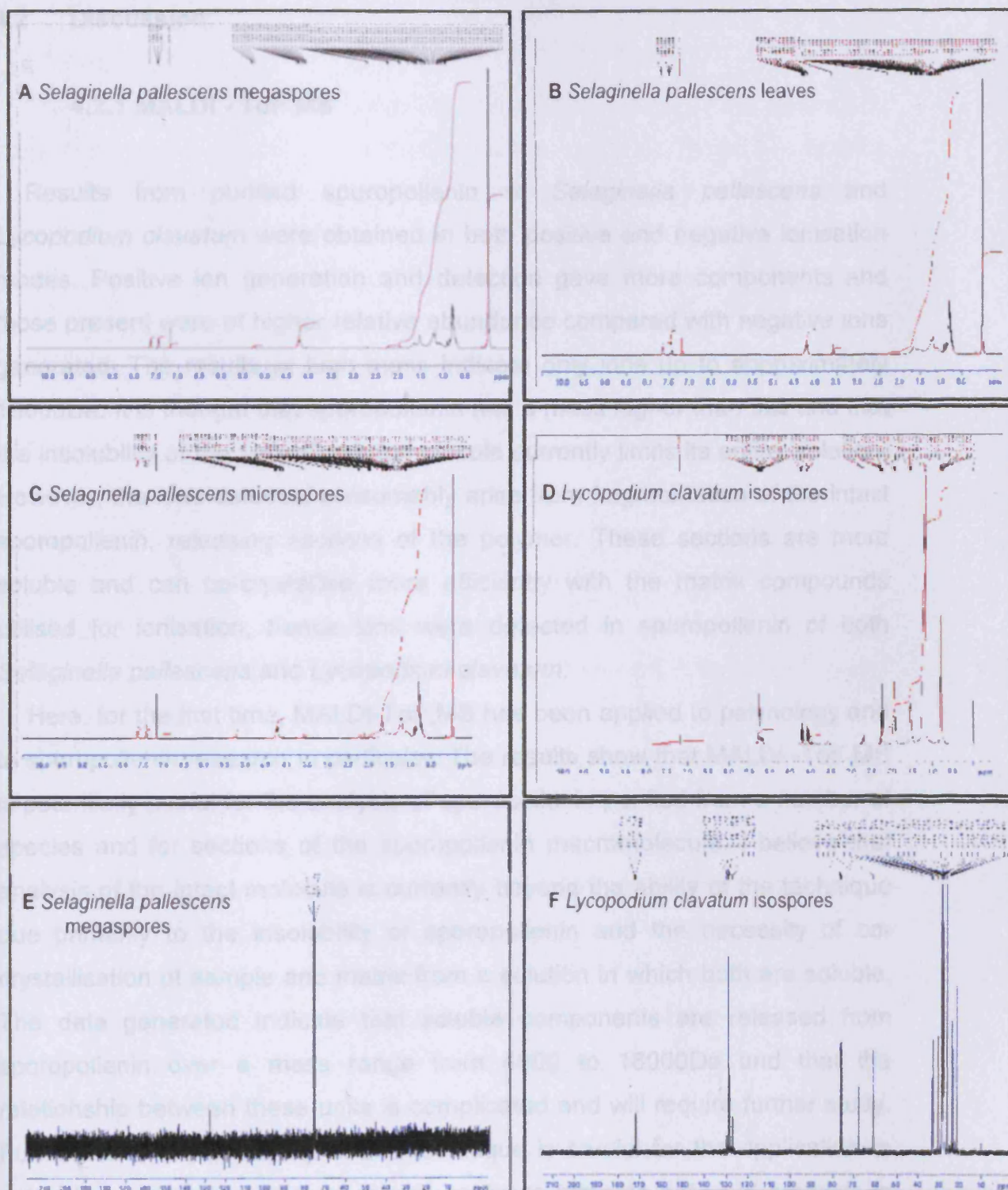


Figure 4.11: ^1H and ^{13}C MR data: ^1H NMR spectra of DCM extracted *Selaginella pallescens* megaspores **A**, leaves **B** and microspores **C** as well as *Lycopodium clavatum* isospores **D**. Although the peak intensities differ in each spectrum, they all show the same chemical shifts. A comparison with Fig 10 shows that all ^1H NMR spectra are identical. ^{13}C NMR spectra of *Selaginella pallescens* megaspores **E** and *Lycopodium clavatum* isospores **F**. *Lycopodium clavatum* isospores have a greater shift intensity and variety, probably because more starting material was used. Both spectra, however, agree showing two shifts at around 130 and 75ppm.

4.2 Discussion

4.2.1 MALDI - ToF MS

Results from purified sporopollenin of *Selaginella pallescens* and *Lycopodium clavatum* were obtained in both positive and negative ionisation modes. Positive ion generation and detection gave more components and those present were of higher relative abundance compared with negative ions generated. The results at high mass indicate only ions up to approximately 18000Da. It is thought that sporopollenin has a mass higher than this and that the insolubility of the "intact" macromolecule currently limits its entire isolation. However, the ions detected presumably arise from fragmentation of the intact sporopollenin, releasing sections of the polymer. These sections are more soluble and can co-crystallise more efficiently with the matrix compounds utilised for ionisation, hence ions were detected in sporopollenin of both *Selaginella pallescens* and *Lycopodium clavatum*.

Here, for the first time, MALDI-ToF MS has been applied to palynology and to sporopollenin research in particular. The results show that MALDI -ToF MS is potentially useful for the analysis of sporopollenin purified from a number of species and for sections of the sporopollenin macromolecule. I believe that analysis of the intact molecule is currently beyond the ability of the technique due primarily to the insolubility of sporopollenin and the necessity of co-crystallisation of sample and matrix from a solution in which both are soluble. The data generated indicate that soluble components are released from sporopollenin over a mass range from 4000 to 18000Da and that the relationship between these units is complicated and will require further study. Furthermore, the sensitivity of this technique is crucial for the application to palynology, as pollen- and spore wall analyses often do not yield products in high quantities.

4.2.2 GC-MS and ^1H NMR

The GC-MS from *Pinus sylvestris* pollen and *Selaginella pallescens* megaspore powder show that both spectra are identical. These two spectra were obtained using two completely different methodologies with different chemicals (see *Material and methods 2.6.1*). The two peaks in each spectrum were identified as 1,2 benzenedicarboxylic acid-diisooctyl ester, better known as a phthalic acid ester. Phthalic acid and their esters are common plasticizers, rubber polymerisation activators and retardants as well as a preservative. The second peak, 2,6-bis(1,1-dimethylethyl)-4-methyl phenol, with the synonym BHT, is also a common plasticizer. The results presented here agree with those of Kawase and Takahashi (1996), as they described the finding of 1,2 benzenedicarboxylic acid butyl 2-ethylhexyl ester (figure 4.4B). Although the chemical structure of the two products (figure 4.4) is not identical, they both classify as phthalates. Kawase and Takahashi (1996) furthermore mentioned the presence of various (trimethylsiloxy)tetrasiloxanes in their spectra. This investigation found 1,1,1,3,5,7,9,9,9-nonamethylpentasiloxane, which actually derives from the GC-MS column used for the experiments. The column is specified as 5%-phenylmethylpolysiloxane, non-polar, which, depending on its age, is known to leach siloxane contaminants. It would therefore seem that what Kawase and Takahashi (1996) described as silicon cross-linked with sporopollenin is more likely to be a contaminant coming from their GC-MS column. Moreover, the data are comparable, as the column they used (Supelco SPB-1) is a poly(dimethylsiloxane) column, which is very similar to the one used here.

From the ^1H NMR results it is clear that the spectra of *Pinus sylvestris* pollen and *Selaginella pallescens* megaspore powder as well as that of the blank experiment are identical. This implies that all results obtained from ^1H NMR and GC-MS analyses are contaminants. None of the spectra indicated sporopollenin or a compound of this macromolecule. The ^1H NMR spectrum of BHT is characterised by shifts at 6.97, 4.99, 2.27 and 1.4ppm (Integrated Spectral Data Base System for Organic Compounds No.1196, SDBSWeb: <http://www.aist.go.jp/RIODB/SDBS/>). The corresponding ^1H NMR spectrum of phthalic acid is characterised by shifts at 13, 7.698 and 7.601ppm

(Integrated Spectral Data Base System for Organic Compounds No. 3002, SDBSWeb: <http://www.aist.go.jp/RIODB/SDBS/>). All ^1H NMR spectra obtained from this study show shifts in the aromatic region (6-9) at 6.9, 7.55 and 7.64ppm as well as a number of other shifts correlating with those of either BHT and phthalic acid. It is assumed that other shifts not deriving from the plasticizers either come from the acetylation of *Selaginella pallescens* (shifts at around 2.0-2.2ppm) or from other products formed during isolation or acetylation procedures. Although it should not be ignored that, in the case of the *Pinus sylvestris* pollen experiment, MMNO might have reacted during the experiments to form BHT, the occurrence of BHT in the spectrum of *Selaginella pallescens*, where no MMNO was used, remains unclear. Possible explanations are that traces of plasticizers might have contaminated various chemicals as they are often stored in bottles with plastic caps or in plastic bottles. In conclusion, GC-MS as well as ^1H NMR data agree in characterising common plasticizers.

From this work it is clear that the MADLI -ToF spectra presented above are genuine sections of the macromolecule sporopollenin and no contaminants since the specific mass of the sections seen in MALDI-ToF analysis are more than an order of magnitude higher in mass (minimum of 4000 m/z) than the phenolic compounds characterised by GC-MS (maximum of 391 m/z).

4.2.3 Chemical Treatments

Treatment with 1% KMnO_4 solution KMnO_4 solution is a strong oxidiser, which gave interesting results when applied to *Quercus coccifera* pollen (Rowley and Claugher 1991; Rowley and Skvarla 1993; Rowley 1996). Similar experiments but with different oxidisers and solvents, were carried out by Southworth (1974) and Kress (1986). Potassium permanganate solution fully removed from the pollen what the authors define as "receptor-independent sporopollenin" (Rowley and Claugher 1991). They describe that *Quercus* pollen exhibits an intra-specific variability of rod-shaped substructures, which are masked by sporopollenin in some species or remain unmasked in others. Potassium permanganate solution removes this masking

sporopollenin from between the substructures. Hence, the authors propose that the rods include sporopollenin receptors and that the sporopollenin between these rods is defined as "receptor-independent sporopollenin". There is no proof that what the authors interpret as sporopollenin is indeed the bio-macromolecule. It is acknowledged that the overall chemical structure of sporopollenin is still unknown but energy dispersive x-ray analysis (EDX) combined with either TEM or SEM would have possibly revealed any elements, which are normally not associated with sporopollenin and which could have given clues as to whether this coating material might consist of elements other than C, O and H. Furthermore, it has recently been demonstrated for non-sporopolleninous Araceae pollen (Weber 1999, 2004) that lipids form an ectexine-like layer that proved acetolysis resistance. A resilient, oily surface coating was also reported for *Lycopodium* spores, making them resistant to wetting and highly flammable (Balick and Beitel 1988, and literature cited therein). Though the effects of potassium permanganate treatment on the lipid coating of Araceae pollen have not yet been tested, it is important to note that other forms of coating materials exist and that presumably further non-sporopolleninous coatings may be described for pollen and spores. Another example for this variability is the perispore of *Selaginella* megaspores, which shows a tendency to resist potassium permanganate treatment as described in a study investigating correlations of morphology and ultrastructure patterns in *Selaginella* megaspores (Moore 2001). It is known that silica is an important component of the perispore of *Isoetes* megaspores (Taylor 1989, 1992, 1993). For further discussions on the occurrence of silica in *Selaginella* megaspores, please refer to Moore *et al.* (in press a) (appendix 1) and *chapter 3* herein. More insights into the composition of the perispore of *Selaginella* and *Isoetes* are needed to fully understand the diversity in sculpture material. It is suggested that further studies concentrate on the variability of these non-sporopolleninous coatings in pollen and spores.

In the present study potassium permanganate solution leaves a finely granulate encrustation on the spores' perispore. The SEM pictures, however, clearly demonstrate that the overall sculpture of the treated spores was not affected (figures 4.6E-H and 4.7A-H). The shedding of the true perispore as seen in *Pellaea calomelanos* (figure 4.6A and B) was likely to be triggered by

the potassium permanganate solution. Some very few untreated *Pellaea calomelanos* spores, however, also showed this pattern, as documented in figure 4.6A1. This observation leads to the assumption that *Pellaea calomelanos* spores are capable of naturally shedding their perispore, which also occurs in many other ferns. With a finely granulate exospore (figure 4.6D) and a relatively thick true perispore coating (1-2 μm , figure 4.6B) it is not surprising that the adhesion between perispore and exospore is somewhat looser than in spores with a thin perispore conforming to an echinate or verrucate exospore, for example. Any chemical analyses with the perispore of this species are probably extremely difficult. Although the perispore could be extracted even from untreated spores, one has to bear in mind that the spores are not bigger than 40 μm in diameter. It would need a great amount of spores to yield 1g or more of perispore material, in order to get reliable data from chemical analyses. This matter is also discussed below.

Treatment with MMNO There were two aims for this study. Firstly, to combine the solvent MMNO with a species that has a perispore and produces a large amount of spores which are over >100 μm in diameter. The greater the quantity of spores used would yield more perispore material. Based on observations made during several years of research with different *Selaginella* species, *Selaginella pallescens* produces a vast number of megaspores all year round in a greenhouse (pers. comm. Lyndon Tuck 2003), which provides enough material for a set of experiments and was therefore chosen. Secondly, this study aimed to contribute to the understanding of the effect of MMNO on pollen and spore morphology, complementary to the ultrastructural data published by Rowley *et al.* (2001). Hence, the two species were chosen (*Lycopodium clavatum*, *Pinus sylvestris*), for which the effects of this solvent on the ultrastructure were already documented.

Rowley *et al.* (2001) conducted a comprehensive study on the effects of MMNO on pollen and spore exines based on earlier findings by Loewus *et al.* (1985) on *Lilium longiflorum* exines. Both studies agree that MMNO is a potent solvent for the polysaccharide rich exines of various pollen and spore species. Loewus *et al.* reported the quick and effective dissolution of *Lilium longiflorum* sporoplasts and sporoplast outer membranes. The authors define

the term *sporoplast* as “a pollen grain that has been stripped of its exine encasement” (p. 652, final paragraph of their Introduction). Rowley’s SEM and TEM studies covered pollen of *Betula pendula*, *Borago officinalis*, *Calluna vulgaris*, *Fagus sylvatica*, *Lilium longiflorum* and *Pinus sylvestris* as well as *Lycopodium clavatum* isospores. In *Lycopodium clavatum* isospores, the treatment with MMNO revealed closely spaced (about 10nm) helical lamellae which form linear structures. In *Pinus sylvestris* exposure to MMNO made SAPs (Sporopollenin Acceptor Particles, term coined by the authors) visible, which are normally only seen in immature pollen of *Pinus sylvestris*. The authors interpret the subtle changes in the exine/exospore of *Pinus sylvestris* and *Lycopodium clavatum* as exposure to water, solvents and fixatives during TEM preparation. MMNO penetrates the exine/exospore through micro-channels, which then expand and allow any further chemicals to enter and eventually affect the ultrastructure. There have been no reports that the ectexine in *Pinus sylvestris* or the true perispore in *Lycopodium clavatum* were affected by MMNO. These observations agree with the SEM findings of this study in which no changes in the ectexine or the perispore were detected (compare figure 4.9A,C,E with B,D,F). The only reservation towards the results of Rowley *et al.* (2001) is that those few SEM pictures shown in the publication, which served as a control, have actually been acetolyzed. It has recently been shown (Calderón *et al.* 2004) that standard techniques of pollen analysis such as acetolysis or Schulze solution have greater effects on pollen and spore morphology and ultrastructure than previously thought. The two techniques mentioned, proved to be harsh treatments resulting in degradation and a significant loss of pollen and spore material. It is therefore questionable that the results are comparable. Furthermore, Rowley *et al.* (2001) do not provide TEM data of untreated pollen and spores, which makes it difficult to judge the results presented therein. Although the text refers to previous studies in which untreated material was used, it is still not clear whether this material was also acetolyzed and might therefore have given misleading results.

As for *Selaginella pallescens* it is noteworthy that the perispore was eliminated successfully after treatment with MMNO. Unfortunately, chemical analysis with a conventional technique such as NMR did not reveal the nature

of the perispore. The ^1H NMR data generated after MMNO treatment of *Pinus sylvestris* pollen, *Selaginella pallescens* megaspores and *Lycopodium clavatum* isospores are almost identical except shifts between 4.1 and 4.25 are missing in *Selaginella pallescens*. The three spectra also agree with all other ^1H NMR data presented in this chapter. This supports the idea that the product characterised by NMR is a contaminant.

Soxhlet extractions with DCM There are not many reports in the literature about conventional Soxhlet extraction methods of pollen or spores with solvents. It is in the research of sporopollenin that various authors have tried Soxhlet extractions with organic solvents, methanolic KOH and phosphoric acid (Zetzsche and Huggler 1928; Zetzsche and Vicari 1931; Guilford *et al.* 1988).

The aim of this extraction procedure was to document any products that can be obtained from spore material (*Selaginella pallescens* and *Lycopodium clavatum*) and to compare them to products extracted from leaf material (*Selaginella pallescens*). All NMR data generated from Soxhlet extraction are not only identical within this study but also agree with all other NMR data presented herein. It is of particular interest that the extractions of *Selaginella* leaves as well as those of mega- and microspores document the same product. The spectra all show a highly aromatic product (^1H : peak region of 7.5ppm and ^{13}C NMR: peak region of 130ppm) as further described in the results herein. Although a greater amount of starting material was used for *Lycopodium clavatum* (1g in comparison to 6mg of *Selaginella pallescens* megaspore material), the products extracted are still the same. The minor differences in the ^{13}C NMR data (figure 4.11E and F) can be explained by varying amounts of starting material. A higher scan rate for the leaf extract of *Selaginella pallescens*, however, increased from the usual 256 to 5000, resulted in exactly the same spectrum as that of *Lycopodium clavatum* isospores. The original spectrum is attached to the appendix (number 3) as no digital copy could be generated. The results are consistent with the view that the spectra presented in this chapter represent an as yet unknown contaminant.

5 *Osmunda regalis* L. spores: a modern analogue for certain Lower Devonian spores?

This study arises from an apparent similarity between fossil spore clusters seen by SEM in specimen HD 437 and in clusters from extant, immature *Osmunda regalis* L. spores (figure 5.6).

The following table 5.1 provides a synopsis of methods applied and results obtained.

	HD 437	<i>Osmunda regalis</i> L.
LM documentation	specimen not translucent enough to give results	true perispore and chloroplasts visible
SEM documentation	sporangium (complete and broken open), spores and spore sculpture	spore sculpture, inner wall of sporangium
TEM documentation	not available	TEM of immature spores, TEM of mature spore taken from Tryon and Lugardon (1990)

Table 5.1: Summary of methods applied to the fossil spore cluster and extant *Osmunda regalis* spores.

Fossil Osmundaceae The fossil record of fertile osmundaceous specimens with *in situ* spores dates back to the Late Triassic although the family Osmundaceae was first described from the Upper Permian where some preserved stem genera share typical osmundaceous anatomical features (van Konijnenburg van Cittert 2000). Many spores have also been recorded from the Jurassic and Lower Cretaceous (van Konijnenburg van Cittert 2000) - for a review see van Konijnenburg van Cittert (1978). All fossil osmundaceous spores are globose and trilete but none of them is known to have a perispore - it is thought that this thin layer is lost during sample preparation (van Konijnenburg van Cittert 2000).

Extant *Osmunda regalis* L. Extant Osmundaceae comprises three genera: *Osmunda*, *Todea* and *Leptopteris* which are well documented by Tryon and Lugardon (1990) by the means of SEM and TEM. This family, as well as the families Marattiaceae and Ophioglossaceae, are classified as "primitive" by the authors in regard to the evolutionary level of spore wall structure (figure 3.35 in section 3.3). This view is shared by other scientists

(van Konijnenburg van Cittert 2000, more references cited therein). The latter provides a general review of osmundaceous spores throughout time (from the Triassic to today), describing the family as homogenous and stable in respect to spore characters. It was also observed that in extant *Osmunda* occasionally monolete or incomplete trilete spores occur and very rarely double laesurae ("bipolar apertures", terminology *sensu* van Konijnenburg van Cittert). A definite study documenting different developmental stages of extant *Osmunda* spores was published by Lugardon (1972). This was carried out by the means of TEM: a similar SEM study is lacking but has been attempted herein.

Fossil specimen HD 437 The fossil specimen containing *in situ* spores is as yet unidentified but falls under the general heading "rhyniophytoid". Several authors have described *in situ* spores for the same locality (Edwards *et al.* 1995a; Edwards 1996; Wellman *et al.* 1998a and b; Habgood 2000). Since this study compares general features between fossil and extant spores, the derivation of the specimen is not relevant.

Self-assembly experiments In recent years self-assembly experiments have provided a unique insight into the pattern formation processes involved in pollen and spore wall formation. The spore mimics obtained from the latest experiments very much resemble the living organism so that it allows comparisons with both the fossil and the extant spores described above. A brief review of previous self-assembly studies is given in 1.7.4 *Colloidal structures*. For experimental details see 2.8 *Self-assembly experiments*.

5.1 Results

The fossil spore cluster (figure 5.5C and D) has a striking similarity to that of immature *O. regalis* (figures 5.1A and 5.2B). Spore wall mimics derived from self-assembly experiments (figure 5.6D) also share common features with both spore clusters, which will be discussed later.

5.1.1 *Osmunda regalis* L. spores

Spores from three developmental stages were collected: the first stage comprised immature spores from a light green sporangium, the second almost mature spores from a dark green sporangium and the third, spores from a brown sporangium.

Spores from the first developmental stage Isolation of individual spores from immature sporangia is difficult, mainly because the spores form large clusters (figure 5.1A and B). Spores documented below are about 50 μ m in diameter and seem to be glued together by a discrete layer; their sculpture is clearly covered by this layer, masking the tuberculate sculpture (figure 5.1C and D). Quite a number of spores in these clusters are broken, probably resulting from preparation. Those spores that are broken appear to be thinly walled and hollow (figure 5.1A). There are also numerous signs of cracks on the sculpture (figure 5.1D). TEM documentation of an immature spore, possibly isolated during the embedding process, shows a thick, tuberculate exospore (figure 5.1E). Exospore thickness ranges between 2-3 μ m. The latter measurement includes tubercles (figure 5.1E and F). True perispore formation seems to have taken place (figure 5.1D, arrows). The perispore material appears slightly more electron dense than the surrounding resin and less dark than the exospore. It consists of fibrous material and is scattered around the spore, probably due to the embedding process. There was possibly not enough perispore material deposited on top of the exospore to form a continuous layer, which would withstand embedding.

The layer surrounding the spore clusters cannot be observed using TEM as it would have been removed during the embedding process. It is also noteworthy that none of the spores appear to have a visible trilete mark. This is also the case for the individual spore that was sectioned for TEM, where no clear aperture region can be observed (figure 5.1D).

The inner wall of the sporangium is ribbed and has a smooth surface (figure 5.1G), on which spheric bodies of about 1 μ m in diameter are randomly scattered (figure 5.1G and H). Similar structures of comparable size are observed on the inner wall of the fossil sporangium (figure 5.5F). This phenomenon has previously been interpreted as tapetal residue and both the terms granules and globules have been applied (Shute and Edwards 1989; Edwards 1996: *granules*; Lugardon 1981; Tryon and Lugardon 1990: *globules*). I will use the term *globules*.

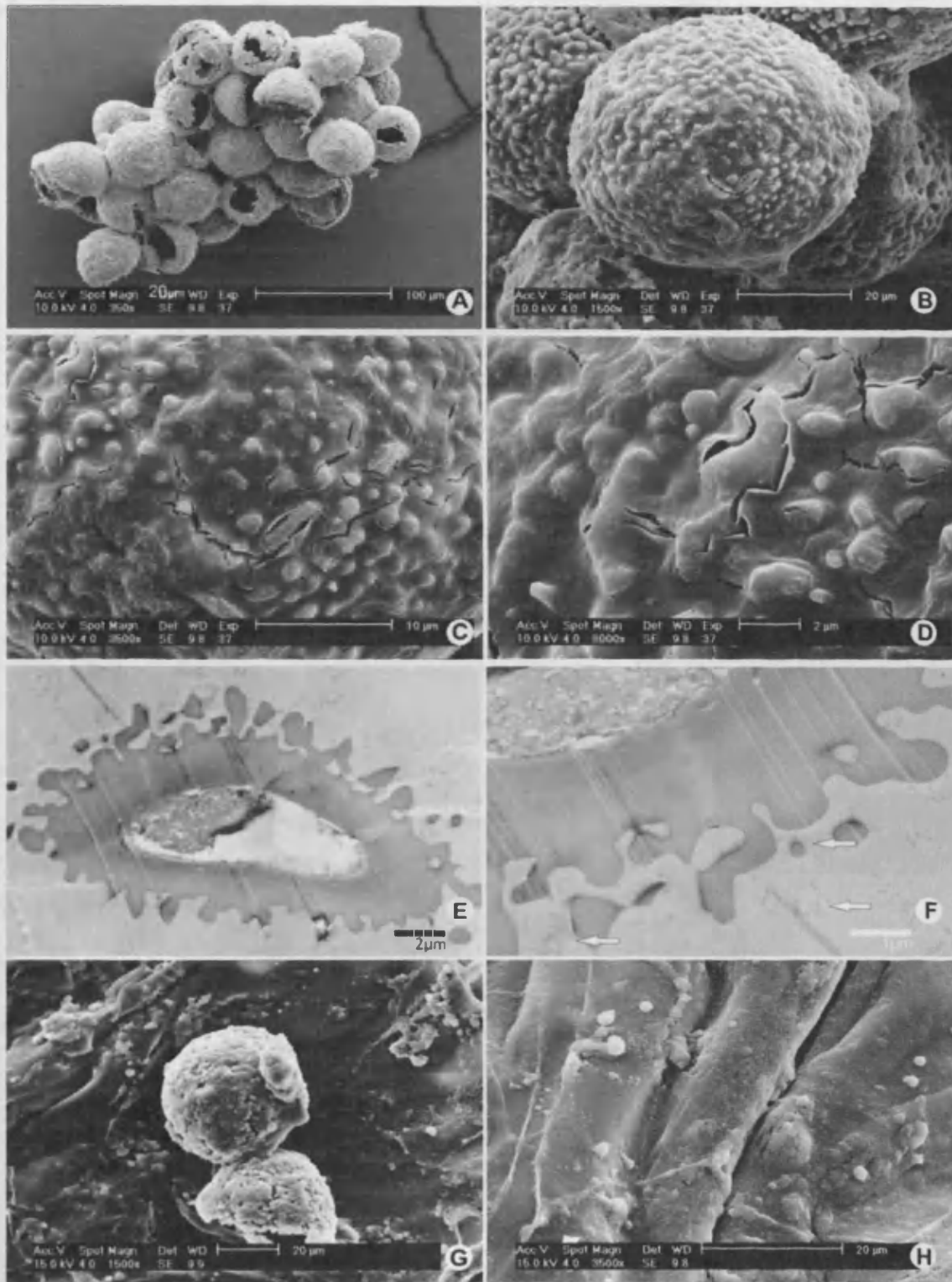


Figure 5.1: SEM documentation of immature spores and a sporangium (first stage of development) of *Osmunda regalis*. **A** spores appear in clusters after removal from a light green sporangium. **B** individual spores retain a cover of discrete layer. **C** and **D** the spore sculpture is tuberculate and porous, showing cracks. **E** TEM work revealed a thick exospore with tubercles. True perispore formation seems incomplete. Finely fibrous material has accumulated towards the exospore **F** (see arrows). **G** and **H** show the inner wall of an immature sporangium. In **G** two immature spores are still attached to the wall. The sporangium wall has small spherical bodies on its surface, which can also be seen in **H** at a higher magnification.

Spores from the second developmental stage Some spores are isolated but the majority still forms large clusters. Average spore size in the pictures below is about 50µm in diameter. The layer covering the cluster as well as the sculpture of individual spores is still visible (figure 5.2A and B).

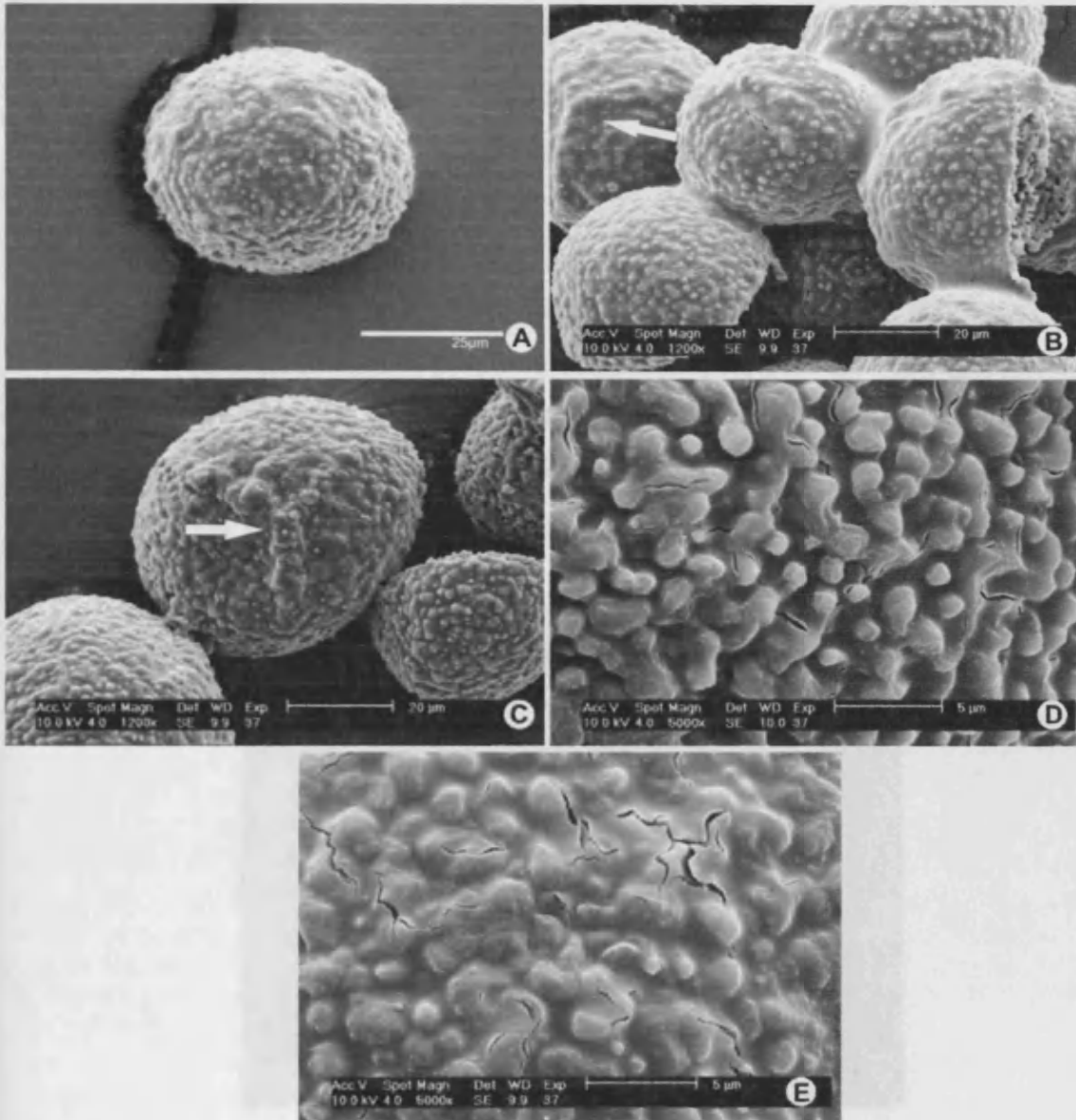


Figure 5.2: SEM documentation of almost mature spores (second stage of development) of *Osmunda regalis*. **B** some spores still appear in clusters after they were removed from a dark green sporangium, whereas **A** and **C** other spores are isolated. **B** and **E** a discrete layer still seems to glue the clusters together and covers the tuberculate sculpture. Note trilete marks in **B** (arrow) and in **C** (arrow). **D** shows the sculpture of a nearly mature spore, where tubercles are almost free from this layer. **D** and **E** note cracks in the sculpture in.

Two trilete marks are documented in figure 5.2B and C. The tuberculate spore sculpture is more pronounced in some of the spores (figure 5.2D), whereas others still seem to be covered by locular fluid (figure 5.2E). A number of cracks are scattered around the spore sculpture (figure 5.2D and E).

Staining with aniline blue Staining of callose with aniline blue was attempted in order to determine the nature of the discrete layer surrounding the immature spores. Positive staining for callose is auto-fluorescent blue under a fluorescent microscope (Baker *et al.* 1994; Dong *et al.* 2005). Before staining, some untreated immature spores were viewed under a fluorescent microscope as a control. They appeared blue, without staining (figure 5.3). Staining did not seem to affect the spores, no difference was found between stained and unstained spores. Light microscopy did not reveal positive staining in the spores, either.

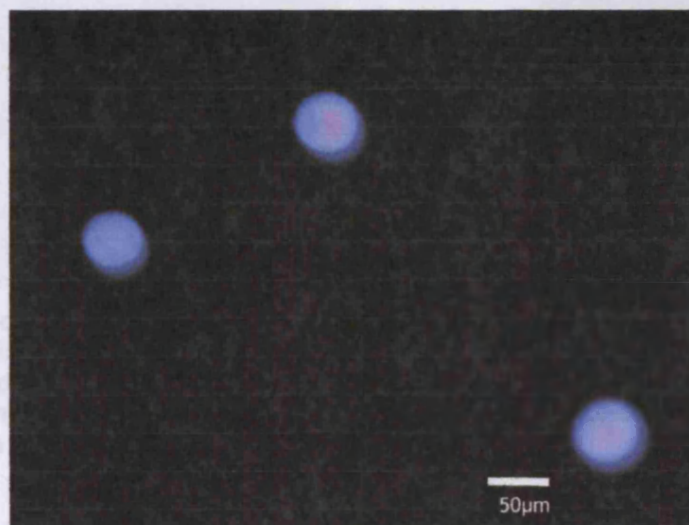


Figure 5.3: Blue auto-fluorescent immature *O. regalis* spores, unstained.

Spores from the third developmental stage Mature spores are all isolated and do not form clusters (figure 5.4A). Spore size ranges from 50-69µm in diameter in the spores documented below. The sculpture is completely free of a discrete layer and the tubercles are fully pronounced as seen both by SEM and LM (figure 5.4B and C). The TEM picture clearly

shows the aperture region (figure 5.4D, central white line). True perispore formation is also complete, forming a very thin, continuous electron dense layer with the occasional echinate spine forming on tubercles (figure 5.4D). Some of the spines grow as long as $1\mu\text{m}$. Exospore wall thickness ranges, in that particular picture, between $2\mu\text{m}$ over the tubercles and up to $3.5\mu\text{m}$ near the aperture region.

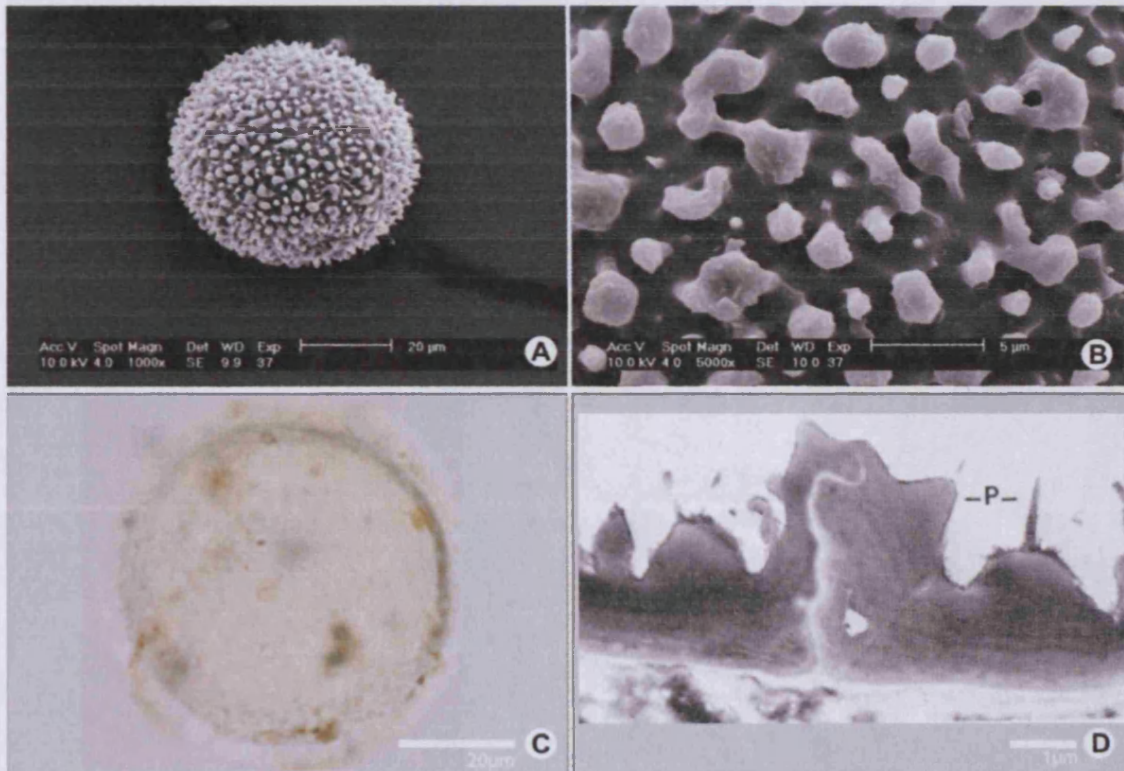


Figure 5.4: SEM documentation of mature spores (third stage of development) of *Osmunda regalis*. **A** and **C** individual spores, **B** tuberculate sculpture. True perispore formation in mature spores is complete. The aperture can clearly be seen in the centre of the picture. **D** the ultrastructure shows sparsely echinate spines (-P-) formed on top of exospore tubercles. The picture is taken from Tryon and Lugardon (1990), page 54.

5.1.2 Fossil spores

Light microscopy of this specimen did not give any results. Isolated spore clusters and parts of the sporangium were not sufficiently translucent to obtain interpretable LM images. Unfortunately, TEM sections through the sporangium wall or the spore mass were unobtainable, therefore the documentation of this specimen was carried out by SEM. The fossil spores

studied were isolated from two ellipsoidal sporangia (figure 5.5A) borne terminally and singly on a dichotomising smooth axis.

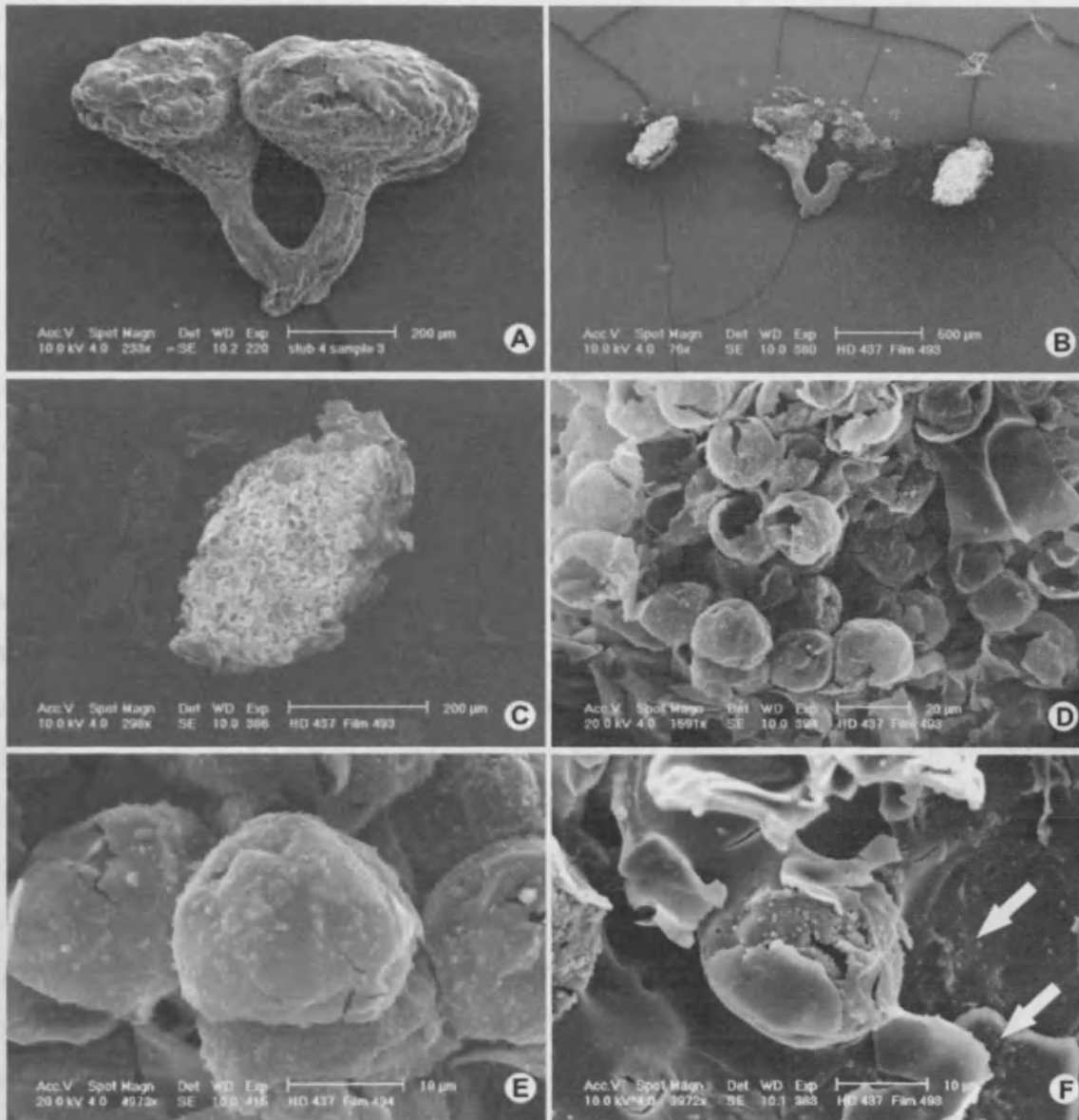


Figure 5.5: C and D SEM documentation of an Early Devonian spore cluster, isolated from an ellipsoidal sporangium A and B. E the spores appear thinly layered, some of them are cracked open. Their sculpture is finely granulate. F the inner wall of the sporangium shows small globules, probably tapetal residue (arrows).

The sporangium on the left has a width of about 360µm and a height of 160µm. This stands in contrast to the sporangium on the right, which is larger, about 427µm wide and 267µm high. The dichotomising axes are each about 80µm thick (figure 5.5A).

The broken sporangia are documented in figure 5.5B and the spore clusters isolated from that particular sporangia can be seen in figure 5.5C and

D. Spores appear thinly walled and hollow, about 20 μ m in diameter, some spores are broken. Their sculpture is finely granulate, there is no sign of a trilete mark. Figure 5.5F shows the inner sporangium wall with a spore attached. The lining appears smooth with few scattered spherical bodies under 1 μ m in diameter. The same bodies seem to form the finely granulate sculpture of the spores.

5.2 Discussion

Spore development Both extant and fossil spore clusters appear to be covered by a layer which might consist of locular fluid. It is unclear as to whether this is a condensed or actual layer. Environmental SEM (ESEM) was attempted to address this question but did not give any results due to either bad image quality at low chamber vacuum in the ESEM or loss of this layer due to increased chamber pressure. The cracks documented on the sculpture of the immature spores (figures 5.1 and 5.2) by SEM might reflect the drying locular fluid, suggesting that this is a condensed layer. The layer seems to contain certain components which hold the spores together as a cluster. In plant cells, callose (β -1,3- glucan) is usually utilised as a sealant for plasmodesmata or sieve-plate pores (Strasburger 1998). Secreted by the tapetum, callose also separates growing pollen (microspores) (Parre and Geitmann 2005). The latter is known for angiosperm, gnetopsid, conifer and cycad pollen as well as for bryophyte spores (Gabarayeva and Hemsley in press).

Callose can be broken down enzymatically by callase (β -1,3- glucanase), a process which takes place in pollen towards the end of microspore development, when they become fully separated from each other (Steiglitz 1977). The timing of callase secretion is critical for normal pollen development - prematurely induced it will result in the collapse of the microspores (Bedinger 1992). Although the occurrence of callose and callase in pteridophytes is poorly understood, it is suggested that the locular fluid seen

around the extant spores illustrated herein contains callose, thus forming a cluster. With the secretion of callase, this cluster could be separated towards spore maturation resulting in isolated spores that are ready to be dispersed. More importantly, due to the similarity between these two spore clusters, it is suggested that the fossil spore represents an immature stage of development.

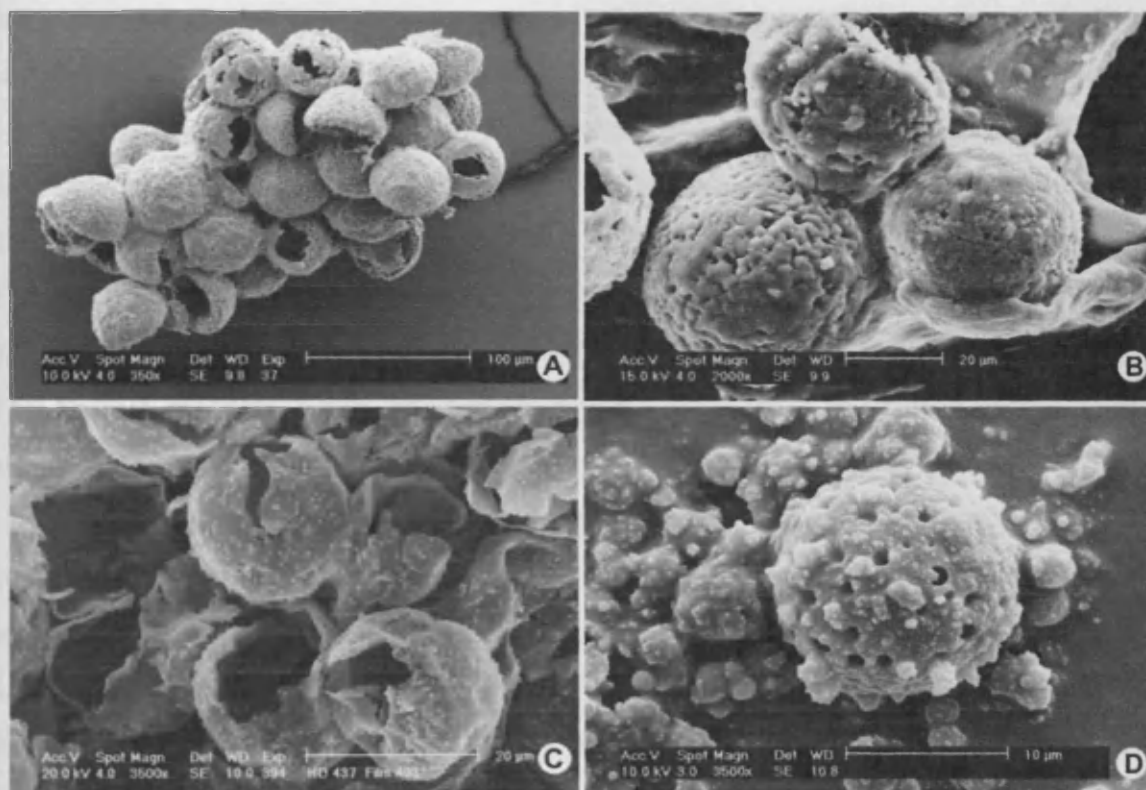


Figure 5.6: A and B SEM documentation of *Osmunda regalis* clusters, C the Early Devonian fossil spore cluster and D a spore mimic made from self-assembly experiments. Note the striking similarity of shape and sculpture in the extant species, the fossil and the spore mimic.

Granules/Globules

Derived from the tapetum, globules are defined as “small, usually spheroidal, compact bodies of sporopollenin formed within the sporangium at the same time as the exospore either “free” (...) or within the perispore (...).” (Tryon and Lugardon 1990, p. 633). Sporopolleninous globules have been shown to resist diagenesis and HF preparation and were found in sporangia produced by both plasmodial and secretory types in extant plants (Lugardon 1981). These globules are believed to be similar to Ubisch bodies (also called *orbicules*) of spermatophytes (Lugardon 1981; Gensel 1982). I concur with the common view that the tapetum is responsible for the globules seen in figures 5.1 and 5.5. In *Osmunda* this is a plasmodial tapetum (Parkinson 1988), probably providing material for perispore formation. During the early stages of development fibrous material is accumulated near the exospore (figure 5.1F). Tryon and Lugardon (1990) describe, for mature spores, a continuous true perispore with echinate elements formed by fascicles of fibrils (p. 52, therein). The fibrous material seen around the immature spore will probably, at a later stage of development, give rise to the echinate ornamentation.

In fossil specimens, two forms of globules have previously been found to cover the inner non-cellular sporangium wall of Lower Devonian *Resilitheca salopensis* (Edwards *et al.* 1995a) and *Uskiella spargens* (Shute and Edwards 1989). It can only be speculated which kind of tapetum was present in the fossil species and as to whether a perispore was developed (Edwards 1996; for a review on the perispore in the fossil record see *chapter 6*, herein). The occurrence of globules on the inner sporangium wall, as seen in both the extant and the fossil specimen, might suggest that the fossil specimen was not yet ready for dehiscence. In pollen, globules become impregnated with sporopollenin towards the end of pollen development preventing water-logging and probably also aiding efficient dispersal (Heslop-Harrison and Dickinson 1969). Whereas the globules on the inner side of the sporangium in the fossil seem to add to a (micro-) granulate spore sculpture (figure 5.5E), the tuberculate sculpture of the immature extant spores originates from the exospore, as suggested by the TEM sections (figures 5.1E and F, 5.4D). Although small globules under 1 μm in diameter can be observed in the vicinity of the spore (figure 5.1F), I believe these globules can be regarded as tapetal

residue from the sporangium wall, probably dislocated by the embedding process.

Spores size, ornament and apertures Spore size differs by about 30µm between the immature extant spores (~50µm) and the fossil spores (~20µm). Since spore size is species specific and there is no suggestion that the fossil spores have osmundaceous affinity, this characteristic can be neglected. This also holds true for the ornament, which happens to be similar in both cases: fossil and extant spores show a granulate to tuberculate sculpture. It is of greater importance that both clusters contain spores without visible aperture regions. SEM documentation only showed trilete marks in some spores of the second developmental stage and in mature spores. Although TEM did not reveal an aperture in the immature spore, it is possible that it was sectioned without cutting through the aperture region.

In *O. regalis* monolete apertures sometimes occur (van Konijnenburg van Cittert 2000), a phenomenon which is not restricted to *Osmunda*, but was also observed in "specialised" families (*sensu* Tryon and Lugardon 1990) like *Pteris* (Kremp 1967; Tryon and Lugardon 1990). Trilete apertures in ferns are believed to be more primitive than monolete apertures, mainly because they are widely spread among fern families like Osmundaceae, Marattiaceae and Ophioglossaceae (van Konijnenburg van Cittert 2000). Trilete marks also occur very early in the fossil record. I suspect that mutations in *Pteris* or *Osmunda* could be responsible for occasional aberrant spore development. The exine pattern formation in pollen, for example, is governed by a protein, which, when inactivated, leads to defective pollen wall formation (Paxon-Sawders *et al.* 2001). This suggests that aperture formation and expression might also be genetically driven rather than resulting from the contact areas within the tetrad. On the basis of the observations made herein it is hypothesised that the fossil spores are immature.

Staining for callose with aniline blue Staining for callose with aniline blue did not answer the question as to whether the discrete layer seen around immature spore clusters of *O. regalis* is made from callose. There might be several reasons for this. Firstly, the discrete layer does not contain callose and therefore no positive staining was achieved. Secondly, the unstained spores are already blue auto-fluorescent, masking any positive staining. I would have expected to observe a positive stain by the means of light microscopy but could not find any difference in the spores before and after aniline blue treatment. Two different staining techniques were attempted (*Material and Methods 2.3.1.1*) and I would have anticipated that at least the first protocol, where fresh material was directly dyed with aniline blue, to give a positive result for the presence of callose. The second protocol involved a fixation with ethanol and glacial acid. I am apprehensive about this protocol as I would expect a chemical reaction between callose and the acid, probably affecting the staining process. The results, however, suggest that this discrete layer does not contain callose. Alternative protocols comprising a pre-fixation in paraformaldehyde, for example, followed by the staining procedure (Jensen 1962), might lead to a different result. The blue auto-fluorescence of the spores could be explained with the presence of phenolic compounds in the spore walls, which was already demonstrated for *Equisetum arvense* L. spores (Roshchina *et al.* 2002). No evidence was found in the literature for comprehensive research on the meaning of auto-fluorescence in spores or pollen, and hence think that not much is known about this aspect. The role of phenolic compounds in plants is discussed in 7.1.

Self-assembly of spore walls It is proposed that similarities in wall morphology of the mimic, extant *Osmunda* spores and those from the fossil specimen (figure 5.6) justify the consideration of mimics. One might argue that similarities such as sculpture and size between the mimic and living/fossil spores are superficial but the importance of this resemblance, however, lies in the achievement of self-assembly experiments. Spore replicas have recently become almost indistinguishable from the living organism. With parallels also seen in fossil spores, this suggests that the mechanisms that underlie spore

wall formation could well be based on fundamental colloidal principles as outlined in Hemsley *et al.* (2004).

6 The perispore of fossil spores – a review

6.1 Introduction

Ever since the perispore was discovered in the 19th century, researchers have studied this sporoderm layer in great detail, dedicating their time to many different aspects such as definition, development, function, evolution and chemical composition. To the present no clear overall picture of the perispore has been drawn resulting in a striking non-conformity of terminology and definitions. This review chapter brings together the very first evidence of a perispore from the Silurian to fossil records into the Tertiary (for references, please refer to the individual sections). Present day definitions and their derivations and modifications through time can be found in the *Introduction* 1.4.

So far, no study has been published summarising the evidence of a perispore in the fossil record. The imprecise use of terminology for perispore has not contributed much to its understanding and hence leaves palynologists with many open questions. This review does not include Mesozoic megaspores although the following is worthy of investigation. Kempf (1971b) studied the megaspores *Banksisporites pinguis*, *Nathorstisporites hopliticus*, *Margaritatisporites turbanaeformis*, *Horstisporites kendalli* and *Istisporites murrayi* and described them with a thick perispore. His view on sporoderm terminology, however, is controversial. What he calls a perispore is often considered as exospore by other authors, especially in extant *Selaginella* (Taylor 1989; Tryon and Lugardon 1990; Morbelli and Rowley 1993, 1999; Rowley and Morbelli 1995; Morbelli *et al.* 2003) to which *Banksisporites pinguis* has a clear affinity (Dettmann 1961). For the above reasons Mesozoic megaspores were omitted.

This current work is not intended to cover all literature published on fossil spore ultrastructure but rather to provide a synopsis of those articles which give evidence for a perispore in the fossil record by the means of SEM and, more importantly, TEM documentation.

6.2 Perispore and the fossil record

Several problems regarding fossil perispores remain. Firstly, it is very difficult to recognise and determine the presence of a perispore, which was previously stressed by Erdtman (1952). Perispore interpretations have so far been achieved by comparisons to extant representatives. It is not known to what extent preparation techniques might limit the recognition of a perispore in fossil spores. The process of fossil spore preparation for ultrastructural analysis sometimes requires a harsh chemical treatment, which may affect ultrastructure in particular (Hemsley *et al.* 1996). Only recently has the perispore of extant spore material been more closely investigated, showing that the chemical nature of this outer wall is highly complex, variable (*chapter 3*) and extremely difficult to analyse (*chapter 4*). Sporopollenin constitutes a major wall component in extant and fossil spores and pollen, but since its chemical nature is still not fully understood, one has to suspect that in case fossil spore material is treated with techniques such as Schulze's solution or acetolysis, major structural damage to sporopolleninous pollen and spore wall layers can be expected (Havinga 1964; Calderón 2004). Possible reactions of this macromolecule with reagents used in spore analysis are hard to predict and any non-sporopollenin components of spore walls are unlikely to withstand taphonomic processes and sample preparation techniques. How do we know whether the outer layer we see in TEM studies of fossil spores is indeed a perispore? In fact, we do not, as we cannot fully exclude the possibility that the perispore was abraded by the harsh treatment necessary to extract the spores from rocks. However, decades of ultrastructural studies on extant and fossil spore material provide a vast, and most of all valuable, documentation and interpretation of wall layers.

Another hurdle in recognising a perispore in fossil spores is that comparisons with extant representatives are often problematic, especially for Silurian and Devonian candidates such as the extinct group of rhyniopsids. Even in extant pteridophytes it is often unclear which sporoderm layers are homologous in different genera or even between micro- and megaspores within heterosporous genera. Until today, no standard test has been established to answer these questions. The number of different terminologies

now used for pteridophyte sporoderm layers mirrors this lack of methodology. This holds true for extant as well as fossil pteridophytes.

A further difficulty is the fact that the definition of the perispore is based on a developmental aspect. The tapetum as a source for the perispore could only be studied in fossil spores if a sufficient number of spores of the same species were preserved, representing various stages of maturation. This is very rare and has so far been published for Lower Carboniferous megaspores, describing exine and not perispore development (Taylor (1974) in *Cystosporites giganteus*; Hemsley (1997) in *Lagenicula crassiaculeata*).

The case for recent pteridophyte spores might be different, since in the future a reliable test for the lack or presence of a perispore might be found making developmental stages much easier to monitor. Until then we can only rely on the data that have so far been generated and published.

6.2.1 Silurian (Přídolí)

Probably the earliest record of perispore occurrence dates back to the Silurian. Comprehensive TEM studies on *in situ* spores of a Silurian *Cooksonia pertoni* from the Welsh Borderland (Long Mountain) have revealed a so-called *peripheral layer* flanking the proximal aperture region (Rogerson *et al.* 1993). The material of this layer was described as highly electron dense and compressed. Comparisons with ultrastructural data of pteridophyte spores launched the discussion as to whether this layer is homologous with perispore (Rogerson *et al.* 1993).

6.2.2 Devonian (Lochkovian/Pragian)

Sporangia from the Lower Old Red Sandstone strata (Lower Devonian) on North Brown Clee Hill have been placed in *Resilitheca salopensis*. Ultrastructure of *in situ* spores was described by way of scanning- and transmission electron microscopy (Edwards *et al.* 1995a). TEM of the spores revealed faint traces of lamellae as well as discrete spherical particles adhering to the distal ornament of the spores. The spheres were also documented for the inner lining of the sporangium. The authors discuss

parallels with the globules of pteridophytes and Ubisch bodies of angiosperms. As in *Sporathylacium salopense* (see below) it remains uncertain whether or not some of the non-particulate extraspore material is perispore or not.

Two cryptospore taxa from the Lower Devonian (Lochkovian) from the Welsh Borderland were investigated by the means of SEM and TEM (Habgood 2000). The *in situ* dyads, *?Cymbohilates cf. horridus*, show a three layered sporoderm, of which the thin, porous outer exospore layer is referred to as an envelope. *Velatiteras* sp. contains tetrads with bi-layered spores featuring a complex and ornamented outer layer. A reticulate envelope surrounds the tetrads and its heterogeneous appearance is well documented by TEM. The author discusses only the envelope of the tetrads of *Velatiteras* sp. as being tapetum derived and therefore concludes that they are likely to represent a true perispore. This is based on a hypothesis by Gray (1985) who suggests that the envelope surrounding individual tetrads is a tapetum-derived perispore.

The dyads of *?Cymbohilates cf. horridus* do not show affinity to any previously described material and one might speculate as to whether the dyads would have separated on maturity as two hilate cryptospores, with or without an envelope. It is also considered that the dyads might remain intact at the time of dispersal.

Published by Edwards *et al.* (2001), the new taxon *Sporathylacium salopense*, based on coalified sporangia from the Lower Devonian from the Welsh Borderland, revealed trilete crassitate isospores with microgranular ornamentation. At the ultrastructural level, the spores showed ornamentation separated from the distal wall by a narrow, less electron dense layer. Spherical particles were found to adhere to the lining of the sporangium as well as to the distal spore surface. Some scattered particles were also found on the proximal ornament. The particles resemble those found in zosterophylls and *Resilitheca* (Edwards *et al.* 1995a; Edwards 1996). Similar structures also occur in extant homosporous Lycopsidea and in some ferns and are probably homologous to the Ubisch bodies of seed plants. Since Ubisch bodies become coated with sporopollenin at the end of tapetal activity it would

be interesting to find out what role these structures play in the Lycopside and ferns and if there is a link with perispore formation. The authors (Edwards *et al.* 1995a) suspect that the ornamented outer layer was a closely adhering perispore. They further interpret that the less electron dense layer marks the disintegration of the innermost perispore layer, where it was attached to the exospore. The layers would eventually become separated, but there was no evidence for this in the fossil taxon.

A study on *Uskiella spargens* with *in situ* spores from the Lower Devonian of South Wales (Shute and Edwards 1989) showed a bi-layered spore wall, of which the outer was interpreted as a perispore. Furthermore, isolated and clustered small spheres on sheets and on the inner sporangium wall were documented. Due to the presence of certain layers on the inside of the sporangium wall with characteristic spherical particles, it was suggested that they refer to tapetal activity and that the perispore was formed by a secretorial tapetum in particular (Gensel 1980; Edwards 1996). Further investigations on Devonian spores on the one hand, and living material on the other will be necessary to gain a deeper insight into the role of the tapetum and these spherical structures in perispore formation.

Spores from sporangia of four Lower Devonian species of the homosporous trimerophyte *Psilophyton* (Dawson) Hueber and Banks were described (Gensel and White 1983). The spores are generally similar in morphology but slightly vary interspecificly in sculpture. The spores correspond to the dispersed spore genera *Apiculiretusispora* (Streel) Streel and/or *Calamospora* Schopf, Wilson and Bentall. It is in the species *Psilophyton forbesii* that ultrastructural studies revealed a perispore. The homogenous sporoderm consists of two electron dense layers: an inner and an outer, thinner layer, the latter giving rise to the sculpture. The authors noted that in some spores the outer layer, which they presume is a perispore, detaches from the inner layer, which is interpreted as the exospore. They assumed that the perispore might be immature due to amorphous material found between individual spores, probably representing tapetal membranes. They further reported that they had tried to reveal the presence of the

perispore with a test devised by Gastony (1974). In his original paper he described a swelling of the perispore in extant Cyatheaceae after treating the spores with an acetolysis mixture, in which sodium hydroxide (NaOH) was substituted for the standard acetolysis mix. Gensel and White, however, mention KOH (potassium hydroxide) as the chemical responsible for the swelling. A personal communication in March 2005 with Pat Gensel revealed that she had tried both chemicals. Since no difference was observed, Gensel might have confused KOH with NaOH in the publication. Whatever chemical Gensel and White used, they did not achieve swelling in the fossil material, correctly concluding that this might be due to chemical changes in the sporoderm during fossilisation and diagenesis.

I am sceptical about the use of NaOH as a standard test for the perispore in fossil as well as in extant pteridophyte spores. NaOH is commonly used in the paper industry mainly to produce pulp (cellulose) and paper (Biermann 1996). NaOH breaks down the lignin in the wood, which normally holds the cellulose fibres together. Once the lignin is removed, the freed cellulose fibres can be processed into paper (Bernd Dirks, pers. comm. 2004).

Pollen and spores both contain callose and sporopollenin (Barnes and Blackmore 1986; Hemsley *et al.* 2004), two compounds which are related to cellulose and lignin (de Leeuw and Largeau 1993). It is therefore not surprising that NaOH affects all of these compounds.

6.2.3 Carboniferous

The outer spore wall layer in lepidodendrid megaspores might be considered more closely related to that of the Isoetaleans (e.g. Kenrick and Crane 1997) but it is clear from the modern literature that the perispore in the latter group is largely siliceous and would therefore be very unlikely to be preserved in Carboniferous specimens. Consideration of the true perispore in Carboniferous lepidodendrid megaspores can hence only be speculative, being based on inferences derived from what ultrastructure is preserved. For this reason, Carboniferous megaspores were omitted.

A number of sphenophyllalean spores have been described with "some form of extra-exinous wall layer (perispore)", which is only detectable at the ultrastructural level (Taylor 1986). Interestingly, a lamellated structure was reported in the perispore for about half of the samples examined, a feature which can also be found in extant *Christensenia* (Marattiaceae), *Asplenium* (Aspleniaceae), *Pteridoblechnum* (Blechnaceae) and *Davallia* (Davalliaceae). In some sphenophyllalean spores, e.g. *Peltastrobus reedae*, the perispore is subdivided into two strata of different electron density, a pattern which is quite commonly distributed among extant pteridophytes. Taylor's observations on sphenophyllalean spores strongly indicate perispore features present as early as the Pennsylvanian that can still be seen in extant spores. This suggests that further investigations on this material with regard to the evolution of perispore might be valuable.

A perispore was also described in the sphenophyllalean elater-bearing specimen of *Elaterites trifernes* Wilson by comparing its ultrastructure with that of extant *Equisetum* (Kurmann and Taylor 1984). Spores of *Elaterites* were macerated from the microsporangia of a *Calamocarpon insignis* cone from a Saharan coal ball locality, of Middle Pennsylvanian age. The perispore is bi-layered with the inner spongy layer, consisting of disorganised, granular sporopollenin units (orbicules) and the outer, homogenous layer, forming a series of ridges. The authors argue that with the occurrence of orbicules the inner layer is consequently composed of sporopollenin. No further chemical analyses have been made, which would strengthen this hypothesis. The article comprehensively discusses the development, evolution and function of the elaters in connection with perispore. Since several spores of different developmental stages, from immature to mature, were preserved, a sequence of sporoderm development could be reconstructed. The exospore is the first layer to be deposited, on which the perispore is then produced. Both layers are homogenous and together form the earliest stage in spore wall development. In a later stage, an additional external layer forms, which gives rise to the elaters. In a mature spore the elaters further subdivide into at least three layers and perispore differentiation is completed with the separation of the elaters. This entire formation process gives rise to a multi-layered

sporoderm consisting of (from the inner to the outer): exospore, a thick two-layered perispore, and elaters made up from three different layers. As far as the formation process of these layers is concerned, it is suggested that they form by the stretching and additional deposition of more sporopolleninous material. However, the article does not provide information on the precise origin of the perispore e.g. superimposed by the tapetum or formed by an internal process through self-assembly.

There is no doubt that *Equisetum* is related to the extinct genus *Calamites*. This is based on the similarity of several morphological and anatomical features (e.g. Stewart and Rothwell 1997 and literature cited therein). The variability in sporoderm ultrastructure suggests that evolutionary modifications in wall structure took place from the Pennsylvanian onwards. Kurmann and Taylor (1984) suggested that the perispore in *Elaterites* is fairly thick and two layered, whereas that of *Equisetum* is thin and consists of only one layer. Sporoderm terminology of *Equisetum* has not been treated consistently in the literature. The outermost layer of the exospore is referred to as *middle layer* (Uehara and Kurita 1989) and *epispore* (Tryon and Lugardon 1990) or as *perispore* (Lugardon 1969; Kurmann and Taylor 1984). For the moment these terms are treated as synonyms. Kurmann and Taylor (1984) describe several evolutionary modifications in the wall structure which must have occurred since the Pennsylvanian. Whereas the thick perispore in the Carboniferous spores might have functioned to insulate and protect the underlying thin exospore, the elaboration of the exospore in *Equisetum*, somewhat replaces the function of the perispore and therefore the latter has perhaps become simplified. Alternatively, the expansion of the perispore in *Elaterites* might have increased the surface area of spores which in turn might affect dispersal. Since *Elaterites* and *Equisetum* are both elater-bearing it is highly likely that elaters have been functioning as dispersal aids since the Pennsylvanian. To see whether there is a connection with biomechanics, in other words, if the perispore has a direct impact on the formation and mechanics of elaters, fundamental experimental studies would be needed.

The fine structure of spores of *Botryopteris* from the Lower to the Upper Pennsylvanian were examined by SEM and TEM (Millay and Taylor 1982).

The sporoderm layers of this fern have been described as (from the inner to the outer) *nexine*, *sexine* and *sculptine*. Since a sculptine was found only in one of the four investigated species (*B. cratis*), the authors comprehensively discuss the homologous aspects of the perispore in homo- and heterosporous ferns. In addition to this, the authors admit that in the case of *B. cratis* it is difficult to decide if the outermost electron dense layer should be called perispore. They also consider that in the three other species such a layer might be lacking due to immaturity, since extra-exinous layers are often deposited at a very late stage in spore development (Millay and Taylor 1982).

Nine species of the marattialean fern *Scolecopteris* were examined at the ultrastructure level (Millay and Taylor 1984). The material was obtained from localities of either Middle or Late Pennsylvanian age. All species described possessed an extraexinous layer carrying the ornamentation (sculptine) (terminology *sensu* Millay and Taylor 1984), which morphologically resembles the perine (their terminology) known in many fern groups. The authors chose the descriptive term *sculptine* to highlight that in *Scolecopteris* this layer is responsible for ornamentation.

6.2.4 Permian

Morphological and ultrastructural studies of *in situ* spores of *Oligocarpia kepingensis* from the Lower Permian showed that despite variations in leaf morphology, a suggested affinity with the Gleicheniaceae can be justified (Wang *et al.* 1999). Whereas extant Gleicheniaceae have a homogenous and thin, one-layered perispore, this is absent in the spores of *O. kepingensis*. Gleicheniacean spores are characterised by a three-layered exospore, divided into a thin inner layer, a complex and elaborate middle layer and a homogenous outer layer. This pattern can still be found in extant Gleicheniaceae (Tryon and Lugardon 1990). The fact that a perispore is missing in the species investigated could well be due to the treatment of the spores by hydrofluoric acid, hydrochloric acid and maceration with Schulze's solution, followed by incubation in ammonia. This method might have dissolved the perispore completely. Further studies on the chemical composition of perispore in extant as well as fossil gleichenian species might

help to explain why a perispore may not have been preserved in the first place or why it was affected by chemical treatment.

Recently Wang *et al.* (2004) proposed a perispore for microspores of *Discinispora* from a Lower Permian, petrified Noeggerathialean stobilus (*Discinites sinensis* Wang). Whereas the Carboniferous *Discinites* microspores of the *Vestispora* type have an operculum and trilete mark on two different spore wall layers (Bek and Opustil 1998), e.g. the trilete mark on the exospore and the operculum on the perispore, the newly described Permian microspores *Discinispora sinensis* show a trilete mark, labrum and operculum on one spore wall layer. The authors argue that following the *Vestispora* type concept, the inner body with a trilete mark is located on the exospore and the middle layer with trilete mark and operculum is found on the perispore. The outer layer, which does not resist maceration, would then be unnamed. This means that the *Vestispora* concept does not fit into the spore wall succession suggested for *Discinispora sinensis* microspores (Wang *et al.* 2004). I concur with their (*ebid.*) hypothesis that in *Discinispora sinensis* the middle layer with trilete mark and operculum can be interpreted as exospore and the outermost layer, which is not maceration resistant, as perispore. The authors acknowledge that TEM studies of the ultrastructure of spores of *Vestispora* and *Discinispora* are vital in order to adequately name sporoderm layers.

6.2.5 Jurassic

The ultrastructure of *in situ* *Marattia asiatica* spores from the Lower Jurassic revealed that no perispore elements were present (Wang *et al.* 2001), although extant *Marattia* has a perispore (Tryon and Lugardon 1990, p. 45f). Exospore pattern, however, shows close affinities to that of extant *Marattia*. Wang *et al.* (2001) explain the absence of a perispore in the investigated material by invoking a bad preservation of an immature stage of development with the assumption that *M. asiatica* spores normally have a perispore. Since the spores were initially treated with hydrofluoric acid, hydrochloric acid and then macerated with Schulze's solution, it is possible that if the perispore is not resistant to oxidation, it would have simply

disintegrated. The fact that extant Marattiaceae all possess a perispore (Tryon and Lugardon 1990) and that the Pennsylvanian marattialean fern spores of *Scolecopteris* were described with an extraexinous layer carrying the ornamentation (Millay and Taylor 1984) adds weight to the hypothesis that the perispore in the case of *M. asiatica* has been lost.

6.2.6 Cretaceous/Tertiary

Smith *et al.* (2003) reported on *Cyathea cranhamii*, the first anatomically preserved tree fern sori of an extant group in the fossil record, showing the presence of the Cyatheaceae as early as the Mesozoic. The permineralised cyatheaceous sori occur in calcareous concretions from the Early Cretaceous (Barremian) of western North America. *Cyathea cranhamii* produced about 35 sporangia per sorus with about 64 spores per sporangium. The spores are about 40-70µm in diameter, triangular with round corners and a trilete mark. The exospore is about 650nm thick, followed by a continuous perispore, which was documented by SEM (structure and sculpture). The sculpturing ranges from granulate/echinate to distinct rodlets. These results clearly show that "specialised" wall structures (*sensu* Tryon and Lugardon 1990) also seen in extant *Cyathea* spores, often comprising a two layered perispore and elaborate ornamentation, can now be traced back to the Mesozoic.

A study carried out in 1987 compared the ultrastructure of extant *Lophosoria quadripinnata* spores with those of fossil *Cyatheacidites tectifera* from the Cretaceous of Argentina and *Cyatheacidites annulata* from the Tertiary of the Kerguelen Archipelago (Antarctica) (Kurmann and Taylor 1987). The specimens were chosen for their similar morphological and ultrastructural characters. The perispore of *Lophosoria quadripinnata* is described as not fully acetolysis resistant, thin and tightly attached to the outer exospore layer. Its very high electron density can be attributed to staining techniques with uranyl acetate (UA) and/or lead citrate (LC). This is supported by the observation that in *Cyatheacidites tectifera* the perispore only became apparent after treatment with UA and LC, attempts of staining with KMnO₄ had no effect on the perispore at all. Therefore UA and LC are postulated to

be more effective stains for the differentiation of spore layers in fossil spores. For *Cyatheacidites annulata* a badly preserved perispore was reported.

All three specimens are very similar in spore morphology and ultrastructure, just varying slightly in spore size, which might well be related to geographic distribution, since extant *Lophosoria* also show variation in spore sizes. Whereas southern populations coming from Argentina or the Juan Fernandez Islands have small spores, the spores of the Jamaican and Costa Rican populations are bigger. A morphological stasis of sporoderm features was observed in *Lophosoria* and *Cyatheacidites* over an extensive geological period, with the oldest fossil record from the Cretaceous of Argentina (*C. tectifera*) and the youngest from the Cenozoic (Pliocene) of Australia (*C. annulata*) with parallels of spore morphology linking these specimens to extant *Lophosoria*.

6.2.6.1 Salviniaceae

This family, comprising the genera *Salvinia* and *Azolla* will be summarised separately due to their extensive fossil record from the Cretaceous to the Upper Tertiary and the link to extant Salviniaceae.

Ariadnaesporites and *Glomerisporites* from the Upper Cretaceous (Cenomanian Stage) are megaspores. Ultrastructural studies of both genera clearly show a perispore (Hall 1975). The perispore of *Ariadnaesporites* megaspores is characterised by a hairy layer whereas *Glomerisporites* resembles that of *Salvinia*. Concerning extant Salviniaceae, their ultrastructure comprises the layers exospore and episporium, the latter is described as vacuolate below a compact surface in *Salvinia* and vacuolate forming massulae and glochidia in *Azolla*. *Ariadnaesporites* is assumed to be the oldest spore genus of the Salviniaceae.

A detailed study of the ultrastructure of *Glomerisporites pupus*, also from the Late Cretaceous, revealed a four-layered perispore (Batten *et al.* 1998). The two inner layers are either loose or dense filamentous, the outer layers vacuolate and largely columnar, all layers merge into each other. These

findings show similarities in ultrastructure patterns with *Ariadnaesporites pilifer* Batten, Collinson and Knobloch, *Capulisporites klikovenssis* Batten, Collinson and Knobloch (Batten *et al.* 1998), *Azolla barbata* Snead and *A. distincta* Snead (Hall and Bergad 1971). All megaspores share a multi-layered, complex perispore. These findings seem to support the idea of an evolutionary progression within the Salviniaceae from the oldest geological genus *Ariadnaesporites* via *Glomerisporites* and *Azolla* (Hall 1975).

Investigations of the ultrastructure of *Paleoazolla patagonia* gen. et sp. nov. from the Upper Cretaceous of Argentina, reveal a two layered perispore with a spongy, densely packed endoperine and a loosely organised exoperine (terminology *sensu* Archangelsky *et al.* 1999). Concerning evolutionary trends, the authors describe a basic structural organization of the megaspore wall in Azollaceae, noting that among all hydropteridinean genera it is the perispore that shows the highest variability. Nevertheless, the authors believe in a taxonomic significance of this structure, if uniformity in preparation techniques is guaranteed.

A revision of species of *Minerisporites* and *Azolla* from the Upper Palaeocene and Palaeocene/Eocene transition of the Netherlands, Belgium and the US was published recently (Batten and Collinson 2001). The ultrastructure of the three species of *Minerisporites* clearly shows similarities with extant *Isoetes*, describing an exospore and an outer exospore but no perispore. For a discussion on the homology of the perispore and outer exospore see Moore *et al.* (in press a) (appendix number 1).

In *Azolla*, on the other hand, a perispore was seen, which is further subdivided into two layers, which the authors call endo-, and exoperine. In all three *Azolla* species the distinct perispore forms rugulae without columnar components, closely packed verrucae or cavate surface sculpture. Especially it seems heterosporous aquatic or semi-aquatic genera, as *Salvinia*, *Marsilea*, *Isoetes* and some species of *Selaginella* as well as *Azolla* are characterised by a very thick, multi-layered, complex perispore, a fact which might correlate with adaptations to humid or wet habitats.

Two publications concentrate on Miocene Salviniaceae megaspores, (Middle Miocene of Denmark; Friis 1977), (Late Miocene Flora of Poland; Collinson *et al.* 2001). Those *Azolla* species investigated show a two-layered perispore of approximately 10µm, the thickness of the perispore in *Salvinia* megaspores varies between 15 and 80µm, and is yellowish in appearance (Friis 1977). Collinson *et al.* (2001) also examined the ultrastructure of *Salvinia* spores describing an endo- and exoperine in *S. intermedia* and *S. cerebrata*. Both spores differ in shape, ornament, surface structure and perine ultrastructure. Whereas in *S. cerebrata* the exoperine is characterised by vacuoles with continuous boundaries, the same layer in *S. intermedia* shows perforated, discontinuous vacuoles. Collinson and co-authors emphasises that the differing characters for both megaspores have potential systematic value.

6.3 Considerations

- Although the effects of chemical treatments on fossil spore morphology and ultrastructure may not be underestimated, a genuine absence of the perispore in certain spore genera should always be considered.
- The spherical particles found in the ultrastructure of *Resilitheca* (Edwards *et al.* 1995) and also on the inner sporangium wall of *Zosterophyllum* (Edwards 1996) might be similar to structures that occur in extant homosporous Lycopsidea and ferns. It is conjectural as to whether these spherical particles are also homologous with Ubisch Bodies of seed plants.
- A consistent use of spore wall terminology is desirable. It is suggested that the same terminology is used for fossil and extant spores, once sporoderm layers have been identified.

	Series or Stage	Author(s)	Specimen(s) investigated	Comment on the perispore
Silurian	Přidoli	Rogerson <i>et al.</i> 1993	<i>Cooksonia pertoni</i>	peripheral layer flanking the proximal aperture region
		Edwards <i>et al.</i> 1995	<i>Resilitheca salopensis</i>	unclear whether the non-particulate extrasporal material is a perispore or not
Devonian	Lochkovian	Habgood 2000	<i>Velatiteras</i> sp.	cryptospore surrounded by envelope which is interpreted as perispore
		Edwards <i>et al.</i> 2001	<i>Sporathylacium salopense</i>	microgranular ornamentation probably deriving from tapetal activity
		Shute and Edwards 1989	<i>Uskiella spargens</i>	bi-layered spore wall of which the outer was interpreted as a perispore
Carboniferous	Pennsylvanian	Taylor 1996	sphenophyllalean spores	described with extra-exenious layer wall layer (perine)
		Millay and Taylor 1982	<i>Botryopteris cratis</i>	extra-exinous layer described as sculptine – discussing homology of perispore in homo- and heterosporous ferns
	Middle Pennsylvanian	Kurmann and Taylor 1984	<i>Elaterites trifernes</i>	bi-layered perispore, the inner spongy, consisting of disorganised, granular sporopollenin units and the outer, homogenous, forming ridges
	Lower Permian of Xinjiang	Wang <i>et al.</i> 1999	<i>Oligocarpia kepingensis</i>	perispore missing probably due to harsh treatment of fossil material
Permian	Lower Permian	Wang <i>et al.</i> 2004	<i>Discinispora</i>	inner layer with trilete mark can be interpreted as an endospore, middle layer with trilete mark and operculum exospore and outermost layer, which is not maceration resistant, as perispore
Jurassic	Lower Jurassic	Wang <i>et al.</i> 2001	<i>Marattia asiatica</i>	perispore missing probably due to harsh treatment of fossil material

Table 6.1: Summarising the occurrence of the perispore in the fossil record (Silurian-Jurassic)

System	Series	Stage	Author(s)	Specimen(s) investigated	Comment on the perispore
Cretaceous	Gallic		Kurmann and Taylor 1987	<i>Cyatheacidites tectifera</i>	perispore only becomes apparent after staining with UA and LC
		Barremian	Smith <i>et al.</i> 2003	<i>Cyathea cranhamii</i>	described with a continuous perispore with sculpture elements (granules, echinae, rodlets)
		Cenomanian	Hall 1975	<i>Ariadnaesporites</i> , <i>Glomerisporites</i>	perispore reported in both species
	Senonian	Santonian	Batten <i>et al.</i> 1998	<i>Glomerisporites pupus</i>	four-layered perispore: two inner layers either loose or dense filamentous, the outer layers vacuolate and largely columnar, all layers merge into each other
		Maastrichtian	Archangelsky 1999	<i>Paleoazolla patagonia</i>	two layered perispore: spongy, densely packed endoperine and a loosely organized exoperine
Tertiary	Palaeocene/ Eocene		Kurmann and Taylor 1987	<i>Cyatheacidites annulata</i>	a badly preserved perispore was reported
			Batten and Collinson 2001	<i>Minerisporites</i>	<i>Minerisporites</i> : outer exospore, which shows similarity with extant <i>Isoetes</i> (homology discussion: outer exospore-perispore see Moore <i>et al.</i> in press a appendix 1)
	Miocene			<i>Azolla</i>	<i>Azolla</i> : bi-layered perispore (endo- and exoperine)
			Friis 1977	<i>Salvinia</i> sp., <i>Salvinia cerebrate</i> , <i>Azolla nikkitinii</i> , <i>Azolla ventricosa</i>	perispore thick and yellowish in both <i>Salvinia</i> sp. and <i>Salvinia cerebrate</i> perispore present in both <i>Azolla</i> species
			Collinson <i>et al.</i> 2001	<i>Salvinia cerebrata</i> , <i>Salvinia intermedia</i> <i>Limnobiophyllum expansum</i>	perispore in both <i>Salvinia</i> species bi-layered (exo- and endoperine)

Table 6.2: Summarising the occurrence of the perispore in the fossil record (Cretaceous/Tertiary).



INTERNATIONAL STRATIGRAPHIC CHART

International Commission on Stratigraphy



Eonothem Eon	Erathem Era	System Period	Series Epoch	Stage Age	Age Ma	GSSP
Phanerozoic	Cenozoic	Neogene	Holocene			
			Pleistocene	Upper	0 0115	
				Middle	0 126	
				Lower	0 781	
			Pliocene	Gelasian	1 806	▶
		Zanclean		2 588	▶	
		Miocene	Messinian	3 600	▶	
			Tortonian	5 332	▶	
			Serravallian	7 246	▶	
			Langhian	11 608	▶	
			Burdigalian	13 65	▶	
			Aquitanian	15 97	▶	
				20 43	▶	
				23 03	▶	
		Paleogene	Oligocene	Chattian	28 4 ± 0.1	▶
	Rupelian			33 9 ± 0.1	▶	
	Priabonian			37 2 ± 0.1	▶	
	Eocene		Bartonian	40 4 ± 0.2	▶	
			Lutetian	48 6 ± 0.2	▶	
			Ypresian	55 8 ± 0.2	▶	
			Thanetian	58 7 ± 0.2	▶	
	Paleocene		Selandian	61 7 ± 0.2	▶	
			Danian	65 5 ± 0.3	▶	
				70 6 ± 0.6	▶	
	Cretaceous		Upper	Maastrichtian	70 6 ± 0.6	▶
				Campanian	83 5 ± 0.7	▶
				Santonian	85 8 ± 0.7	▶
				Coniacian	89 3 ± 1.0	▶
				Turonian	93 5 ± 0.8	▶
				Cenomanian	99 6 ± 0.9	▶
			Lower	Albian	112 0 ± 1.0	▶
		Aptian		125 0 ± 1.0	▶	
Barremian		130 0 ± 1.5		▶		
Hauterivian		136 4 ± 2.0		▶		
Valanginian		140 2 ± 3.0		▶		
Berriasian		145 5 ± 4.0		▶		

Eonothem Eon	Erathem Era	System Period	Series Epoch	Stage Age	Age Ma	GSSP
Phanerozoic	Mesozoic	Jurassic	Upper	Tithonian	145.5 ± 4.0	
				Kimmeridgian	150.8 ± 4.0	
				Oxfordian	155.0 ± 4.0	
			Middle	Callovian	161.2 ± 4.0	
				Bathonian	164.7 ± 4.0	
		Lower	Bajocian	167.7 ± 3.5	▶	
			Aalenian	171.6 ± 3.0	▶	
			Toarcian	175.6 ± 2.0	▶	
			Plesensbachian	183.0 ± 1.5	▶	
		Triassic	Upper	Sinemurian	189.6 ± 1.5	▶
				Hettangian	196.5 ± 1.0	▶
				Rhaetian	199.6 ± 0.6	▶
			Middle	Norian	203.6 ± 1.5	▶
				Carnian	216.5 ± 2.0	▶
			Lower	Ladinian	228.0 ± 2.0	▶
	Anisian			237.0 ± 2.0	▶	
			Anisian	245.0 ± 1.5	▶	
			Givetian	249.7 ± 0.7	▶	
			Induan	251.0 ± 0.4	▶	
	Permian		Lopingian	Changhsingian	253.8 ± 0.7	▶
				Wuchiapingian	260.4 ± 0.7	▶
			Guadalupian	Capitanian	265.8 ± 0.7	▶
				Wordian	268.0 ± 0.7	▶
			Roadian	Roadian	270.6 ± 0.7	▶
				Kungurian	275.6 ± 0.7	▶
			Cisuralian	Artinskian	284.4 ± 0.7	▶
		Sakmarian		294.6 ± 0.8	▶	
		Asselian		299.0 ± 0.8	▶	
		Gzhelian		303.9 ± 0.9	▶	
	Carboniferous	Pennsylvanian	Upper	Kasimovian	306.5 ± 1.0	▶
			Middle	Moscovian	311.7 ± 1.1	▶
		Lower	Bashkirian	318.1 ± 1.3	▶	
Serpukhovian			326.4 ± 1.6	▶		
Mississippian		Upper	Visean	345.3 ± 2.1	▶	
		Lower	Tournaisian	359.2 ± 2.5	▶	

Eonothem Eon	Erathem Era	System Period	Series Epoch	Stage Age	Age Ma	GSSP
Phanerozoic	Paleozoic	Devonian	Upper	Famennian	359.2 ± 2.5	▶
				Frasnian	374.5 ± 2.6	▶
			Middle	Givetian	385.3 ± 2.6	▶
				Eifelian	391.8 ± 2.7	▶
				Emsian	397.5 ± 2.7	▶
				Pragian	407.0 ± 2.8	▶
		Lower	Lochkovian	411.2 ± 2.8	▶	
				416.0 ± 2.8	▶	
		Silurian	Pridoli	418.7 ± 2.7	▶	
			Ludlow	421.3 ± 2.6	▶	
			Wenlock	422.9 ± 2.5	▶	
			Homerian	426.2 ± 2.4	▶	
	Sheinwoodian		428.2 ± 2.3	▶		
	Telychian		436.0 ± 1.9	▶		
	Ordovician	Llandovery	Aeronian	439.0 ± 1.8	▶	
			Rhuddanian	443.7 ± 1.5	▶	
		Upper	Hirnantian	445.6 ± 1.5	▶	
				455.8 ± 1.6	▶	
		Middle	Darrawilian	460.9 ± 1.8	▶	
				468.1 ± 1.6	▶	
	Lower		471.8 ± 1.6	▶		
			478.6 ± 1.7	▶		
	Cambrian	Furongian	Tremadocian	488.3 ± 1.7	▶	
				488.3 ± 1.7	▶	
Middle		Paibian	501.0 ± 2.0	▶		
			513.0 ± 2.0	▶		
Lower			513.0 ± 2.0	▶		
			542.0 ± 1.0	▶		

Eonothem Eon	Erathem Era	System Period	Age Ma	GSSP GSSA	
Precambrian	Proterozoic	Ediacaran	542	▶	
				542	▶
		Neo-proterozoic	Cryogenian	~630	▶
			Tonian	850	▶
			Stenian	1000	▶
		Meso-proterozoic	Ectasian	1200	▶
			Calymnian	1400	▶
			Statherian	1600	▶
		Paleo-proterozoic	Orosirian	1800	▶
			Rhyacian	2050	▶
	Archean	Siderian	2300	▶	
			2500	▶	
		Neoarchean	2800	▶	
		Mesoarchean	3200	▶	
		Paleoarchean	3600	▶	
Lower limit is not defined					

Subdivisions of the global geologic record are formally defined by their lower boundary. Each unit of the Phanerozoic interval (~542 Ma to Present) and the base of the Ediacaran is defined by a Global Standard Section and Point (GSSP) at its base, whereas the Precambrian Interval is formally subdivided by absolute age, Global Standard Stratigraphic Age (GSSA).

This chart gives an overview of the international chronostratigraphic units, their rank, their names and formal status. These units are approved by the International Commission on Stratigraphy (ICS) and ratified by the International Union of Geological Sciences (IUGS).

The Guidelines of the ICS (Remane et al., 1996, Episodes, 19: 77-81) regulate the selection and

definition of the international units of geologic time. Many GSSP's actually have a 'golden' spike (▶) and Stage and/or System name plaque mounted at the boundary level in the boundary stratotype section, whereas a GSSA is an abstract age without reference to a specific level in a rock section on Earth. Updated descriptions of each GSSP and GSSA are posted on the ICS website (www.stratigraphy.org).

Some stages within the Ordovician and Cambrian will be formally named upon international agreement on their GSSP limits. Most intra-stage boundaries (e.g., Middle and Upper Aptian) are not formally defined. Numerical ages of the unit boundaries in the Phanerozoic are subject to revision. Colors are according to the Commission for the Geological Map of the World (www.cgmw.org). The listed numerical ages are from 'A Geologic Time Scale 2004' by F.M. Gradstein, J.G. Ogg, A.G. Smith, et al. (2004; Cambridge University Press).

This chart was drafted and printed with funding generously provided for the GTS Project 2004 by ExxonMobil, Statoil Norway, ChevronTexaco and BP. The chart was produced by Gabi Ogg.

Table 6.3 International Stratigraphic Chart ®. With kind permission for reproduction from the International Commission on Stratigraphy. <http://www.stratigraphy.org/>
The chart serves as a reference for this chapter.

7 Discussion – lower embryophyte spore walls in perspective with particular focus on the perispore

7.1 Evolutionary aspects of spore wall layers

7.1.1 Bryophyta

The earliest record of fragments of land plants comes from dispersed spore masses from the mid Ordovician (Llanvirn) (Wellman *et al.* 2003). These spores with presumed marchantiopsid affinity confirmed that the earliest spores developed in tetrads in large numbers within sporangia. The authors also note that claims for marchantiopsid affinity conform to land plant phylogenies that place the Marchantiopsida as basal (Kenrick and Crane 1997; Kenrick 2000). Although no parent plant could be assigned and elaters, interspersed with spores (a character of extant marchantiopsids and anthocerotopsids), seem to be lacking, the data gained from spore wall ultrastructure analysis seem to support a marchantiopsid affinity. No perine or perine-like layer was found, suggesting that a perine might be absent or was not preserved. The authors provide several reasons for the absence of elaters, such as low preservation potential, present but not discernable or a post-Caradoc adaptation. There are marchantiopsids such as the Sphaerocarpaceae, which lack elaters (Hemsley 1989), but as to whether this is due to a loss of this feature at a later stage in evolution, as suggested by Wellman *et al.* (2003), is unknown.

The perisporeal envelope surrounding cryptospores was interpreted to be homologous with a perispore (Habgood 2000). Although various authors have previously studied cryptospores and discussed the origin of the envelope (e.g. Strother 1991; Hemsley 1994; Taylor 1997) it was Habgood (2000) who mentioned a perisporeal affinity for this envelope. As discussed by Taylor (2003), Strother (1991) considered the envelope to be derived from the spore mother cell wall, and suggested an algal affinity for the enclosed cryptospores and Hemsley (1994) suggested that changes in sporopollenin deposition and timing of the start of meiosis resulted in the wide range of different types of

cryptospores. If Habgood's (2000) hypothesis is correct that the envelope surrounding cryptospores has a perispore affinity, this outer layer would therefore date to the Lower Devonian (Lochkovian) and even later into the Ordovician (Wellman *et al.* 2003) and could hence be considered as an ancestral feature.

I am sceptical about the documentation of a perine-like layer in the spore of the liverwort *Naiadita lanceolata* (Upper Rhaetic) by Hemsley (1989). Spore wall terminology, which was adapted from Harris (1938, 1939 cited in Hemsley 1989), refers to an exine and a perine-like layer. The author admits that the comparison with extant liverworts shows certain similarities with different spore walls in various other species (e.g. *Geothallus*, Sphaerocarpaceae and *Riccia*, Marchantiales) but that not one extant genus shares all exine features found in *Naiadita lanceolata*. Moreover, none of the extant species compared possess a perine. Secondly, what Hemsley (1989) interprets as a perine-like layer is much thicker (between 800nm and 2.4µm) than the perine found in mosses (400nm in *Sphagnum lescurii* Sull. and *Andreaea rothii* Web. & Mohr., 300nm in *Amblystegium riparium* (Hedw.) BSG, see Brown and Lemmon 1990). Since extant liverworts have not been described to possess a perine layer (Crum 2001), the outmost, thick layer seen in *Naiadita lanceolata* is not a perine and is more likely to be an outer part of the exine that for some reason separates from the inner part of the wall.

As far as extant Bryophyta are concerned, neither marchantiopsids (Crandall-Stotler and Stotler 2000) nor anthocerotopsids (Crum 2001) are thought to have a true perine. Renzaglia and Vaughn (2000), however, described a "perine-like layer" seen in *Notothylas temperata* which is derived from the deposition of the residue of the sporocyte wall and the intrasporal septum. This "perine like layer" has not been further studied by the authors and the question remains as to whether this layer is acetolysis resistant. Renzaglia and Vaughn (2000) admit that in anthocerotopsids spore wall development is poorly understood and has so far only been studied by Brown and Lemmon (1990).

Research on the phylogeny and diversification of bryophytes is currently focussing on the resolution of relationships between bryopsids, marchantiopsids and anthocerotopsids (Shaw and Renzaglia 2004). Their work supports the idea that they are paraphyletic with respect to vascular plants, with a bryopsid/vascular plant sister group relationship, which was also previously proposed by Kenrick and Crane (1997), Kenrick (2000) and Nickrent *et al.* (2000). It is also unknown as to whether the marchantiopsids or anthocerotopsids are the most primitive, early divergent, extant land plants (Wellman *et al.* 2003). The absence of a true perine in marchantiopsids and anthocerotopsids suggests that the origin of this layer might not be found in these classes but in the bryopsids. As the perine in extant bryopsids is not acetolysis resistant (Brown and Lemmon 1990), it seems unlikely that fossil bryopsid perine would be preserved and further, harsh treatment during sample preparation might finally destroy all evidence of this layer. Charman (1992) showed that fossil *Sphagnum* spores were badly damaged by prolonged acetylation, which supports the above hypothesis. With a potential lack of the perine in marchantiopsids and anthocerotopsids and a non-acetolysis resistant perine in true mosses (Brown and Lemmon 1990), it will be extremely difficult to determine the inception of this layer in bryophytes.

7.1.2 Pteridophytina

The inception of the perispore in the Pteridophytina seems as difficult to determine as it is for the Bryophyta. This is mainly due to the vast fossil record of fern and fern-related groups, in which very often spores have not been comprehensively studied. Especially, TEM studies are needed in order to comment on perispore occurrence or on qualitative aspects such as its composition. There are several publications which provide sufficient data to allow speculation on possible occurrences of the perispore in ferns and fern-related groups as well as among seed plant ancestors. Refer, for example, to *chapter 6*, here, where information is gathered on the occurrence of the perispore in the fossil record, detailed cladistic studies such as that of Rothwell (1999) on fossils and ferns in the resolution of land plant phylogeny and that by Hammond (2004) on progymnosperms.

Rhyniopsida The first occurrence of the perispore in the earliest vascular plants remains equivocal as discussed previously by Edwards *et al.* (1995) and Edwards (1996) as well as in *chapter 6* herein. Peripheral layers documented in both *Cooksonia pertoni* (Rogerson *et al.* 1993; Edwards *et al.* 1995) and *Uskiella spargens* (Shute and Edwards 1998) might be homologous with a perispore.

Trimerophytopsida The Trimerophytopsida were first proposed by Banks (1968) as a subdivision for those Devonian vascular plants with a main axis that branched pseudomonopodially and had laterals that again branched dichotomously or trichotonously. Sporangia were terminal and all known species were homosporous. The Trimerophytopsida, now recognised as a paraphyletic group, became extinct by the end of the Devonian and are believed to have been ancestral to all megaphyllous vascular plants (Kenrick and Crane 1997). The presence of the perispore in spores of *Psilophyton forbesii* was documented by Gensel and White (1983) and this seems the only reference to a perispore within the Trimerophytopsida. Balme (1995) states that it is usual for trimerophytalean spores to lose their sculptural layer and that it is often not clear as to whether the outer layer, if preserved, is derived from the tapetum or the exine. Gensel and White (1983) suggest the presence of a perispore and I therefore suspect that this layer is probably also present in other genera of the Trimerophytopsida. On the basis of the studies herein it is assumed that not all perispores are preserved in this class owing to differing chemical compositions. The more sporopollenin a perispore contains, the more likely it will be preserved and withstand sample preparation techniques with harsh chemicals. If other components such as cellulose or proteins were the main components, the loss of this layer is not surprising. It would need a comprehensive review of the Trimerophytopsida in order to establish why a perispore has so far only been documented for *Psilophyton forbesii*. Its presence in *Psilophyton forbesii* indicates that this layer could also be present in the Equisetopsida, Cladoxylopsida, and Polypodiopsida as well as in seed plants ancestors such as the progymnosperms. Since the Trimerophytopsida are presumed ancestral to all megaphyllous vascular

plants there is the possibility that this layer was also present in derived plant lineages.

Equisetopsida As previously reviewed (*chapter 6*) a perispore was reported for the Calamitales (e.g. Hemsley *et al.* 1994), for the Equisetales (e.g. Kurmann and Taylor 1984) and the Sphenophyllales (e.g. Taylor 1986). The presence of a perispore in genera of the Equisetopsida is well known, as noted by Stewart and Rothwell (1993). Balme (1995) previously revised fossil *in situ* spores, also giving a comprehensive account of equisetopsid spores and their wall layers. It is clear from the literature that this class has a wide-ranging fossil spore record of extinct as well as of extant plant lineages, of which most possess a perispore. The Iridopteridales are most likely to be ancestral to the Equisetopsida (Berry and Edwards 1996; Kenrick and Crane 1997) but since no spores have been recovered from iridopteridalean specimens, nothing can be said about the occurrence of a perispore in this group. Should spores be recovered in the future, TEM and SEM studies might shed light onto the question, as to whether iridopteridalean spore had a perispore or not. In this case, the character might have been lost in the Iridopteridales and regained in the Equisetopsida, but it is also possible that a perispore was already present in the spores of the Iridopteridales.

The adaptive significance of the perispore (if any) may be protection or inferring advantages in dispersal and germination. The question of its function will be discussed below in *section 7.2*.

Cladoxylopsida The Cladoxylopsida first appeared in the Lower Devonian and extended into the Lower Carboniferous, where they became extinct (Stein and Hueber 1989). Spores of the following two species were described: *Calamophyton bicephalum* (e.g. Bonamo and Banks 1966) and *Foozia minuta* (Gerrienne 1992). No spores have yet been recovered from *Pseudosporochnus* or *Cladoxylon*. Both Bonamo and Banks (1966, *Calamophyton bicephalum*) and Gerrienne (1992, *Foozia minuta*) describe the spore sculpture on the basis of SEM observations. A comprehensive summary of the spore descriptions by Bonamo and Banks (1966) and Gerrienne (1992) is also provided by Balme (1995). The trilete spores of

Calamophyton bicephalum are covered with variable, closely aggregated ornamentations (Bonamo and Banks 1966, based on LM), which I would describe as finely granulate/verrucate and echinate. The spores of *Foozia minuta* are very similar to those of *Calamophyton bicephalum* and covered with coni, pila and verrucae (Gerrienne 1992, based on SEM). I agree with the occurrence of verrucae but prefer to describe the overall sculpture as finely verrucate and echinate as the term pila is usually assigned to pollen walls (Punt *et al.* 1994). Since no TEM sections were taken from either *Calamophyton bicephalum* or *Foozia minuta* spores, the occurrence of a perispore is conjectural. On the basis of the SEM and LM pictures available in the above publications, I suspect that a perispore could well be present. A comparison of these fossil spores with morphologically similar trilete extant spores such as those of *Osmunda* (Tryon and Lugardon 1990, page 53f) allow the assumption that the finely granulate / echinate elements seen in the fossil species might be of perisporeal origin. Unless TEM sections of the fossil spores are taken, no definite interpretations of the wall layers can be made. Since the Cladoxylopsida are regarded by some authors as “preferens” or putative ferns (Stewart and Rothwell 1993) any perispore occurrence would not be surprising, however, a loss of this character in this group should also be considered (see figure 7.2).

Polypodiopsida Within the Polypodiopsida, those orders with living representatives (e.g. Marattiales, Ophioglossales, Psilotales, Osmundales, Polypodiales as well as the two heterosporous orders Salviniiales and Marsileales) include many genera that are shown to possess a perispore (Tryon and Lugardon 1990). The occurrence of a perispore was also documented for some of these orders with a well studied fossil record, which was previously reviewed in *chapter 6*. A perispore was also described for *Rhacophyton ceratangium* (Andrews and Phillips 1968), belonging to the extinct order Zygopteridales that was mostly confined to the Carboniferous and may have been represented in the Devonian by *Rhacophyton* (Bell and Hemsley 2000). *Rhacophyton* is probably the earliest representative of the zygopterids (Stewart and Rothwell 1993). The plant is believed to have been homosporous (Andrews and Phillips 1968). The same authors describe the

perispore as thin and transparent, often folded and wrinkled, varying between 3 to 6µm in thickness. Within the Zygopteridales, it seems that the only known occurrence of a perispore is in *R. ceratangium*. This is probably related to the fact that the fossil record of Devonian species is very sporadic, except for the Upper Devonian *Rhacophyton* (Stewart and Rothwell 1993). As for the Carboniferous and Permian genera such as *Zygopteris* (*Corynepteris*: Galtier 2004), maceration of spores proved unsuccessful and, to my knowledge, TEM studies have not been conducted on this genus.

Balme (1995) describes zygopterid spores as trilete, frequently bearing spines, grana or larger elements such as verrucae and bacula. This elaborate spore ornamentation suggests that a perispore might be present, as seen in extant Polypodiopsida (Tryon and Lugardon 1990). With a perispore in the Upper Devonian *Rhacophyton*, it is possible that this feature is also present in some other genera which evolved later. I suspect that *Rhacophyton* might be the first zygopterid to possess a true perispore and that a review of the Zygopteridales, including more comprehensive TEM analysis of the spores, might possibly reveal a perispore in at least some of the Carboniferous and Permian genera.

7.1.3 Progymnospermopsida

These plants first appeared in the Middle Devonian and became extinct by the Lower Carboniferous (Beck and White 1988). They are believed to be direct seed plant ancestors, representing the transition between ferns (free sporing reproduction) and seed plants (Hammond 2004). Within the three main orders of the Progymnospermopsida (Aneurophytales, Archaeopteridales and Protopytales) the literature describes a perispore only for *Protopytales* (Walton 1957; Balme 1995). Walton (1957) mentions a considerable quantity of granular matter between and on the surface of the spores, which he interprets as tapetal residue. If indeed this granular matter is tapetal residue it might represent globules and any outer layer that might subsequently form is likely to be a perispore of tapetal origin (cf. *chapter 5*).

It is important to point out that the Protopytales evolved later (Lower Carboniferous) than the Aneurophytales (Middle to Upper Devonian) and the

Archaeopteridales (Upper Devonian to Mississippian), suggesting that the character of a perispore might have been lost in the latter two groups but reappeared in at least *Protopitys*. It was noted that the Protopityales have aneurophytalan fertile structures, but that other anatomical features such as the structure of the leaf traces and the endarch primary xylem, differ from those of the Aneurophytales and the Archaeopteridales (Walton 1957). Should *Protopitys* not have evolved from these groups, the occurrence of a perispore in this genus must be seen in a different light (see figure 7.2).

7.1.4 Mesozoic megaspores

The review on the occurrence of the perispore in the fossil record (*chapter 6*) did not include Mesozoic megaspores as explained therein. Kempf's (1971) misconception of spore wall interpretation (calling the broad exospore in *Banksisporites pinguis*, *Nathorstisporites hopliticus*, *Margaritatisporites turbanaeformis*, *Horstisporites kendalli* and *Istisporites murrayi* a perispore) arises from the loss (or lack) of the perispore, which either did not preserve or was removed during sample preparation. Consequently Kempf mistook the exospore as the perispore. These megaspores might have lacked a perispore in the first place but this is impossible to test, unless preservation is exceptional and allows clear spore wall layer assignment. A perispore might have been present, particularly in *Banksisporites pinguis*, due to its presumed affinity to extant *Selaginella* megaspores. There are problems with *Selaginella* megaspore wall terminology that have been discussed elsewhere (Moore *et al.* in press a and *Introduction 1.4*). I call the siliceous coating in *Selaginella* megaspores a perispore (*Introduction 1.4.1.10*). If *Banksisporites pinguis* had a siliceous perispore, I would expect this to be lost during sample treatment with HF and probably also with Schulze's solution (KClO₃ and HNO₃), the latter used by Kempf (1971). He admits that this treatment had damaged some of the sporoderm layers. Schulze's solution also proved particularly damaging for pollen walls (Calderón *et al.* 2004). Moreover, most silica coatings on megaspores consist of nano-particles, as seen in *Selaginella* (Moore *et al.* in press a, TEM documentation therein; figure 3.37B, herein). It is well established that nano-particles have greater solubility properties,

sometimes an order of a magnitude, than their bulk crystalline counterparts (pers. comm. Ian Butler 2005), which supports the idea that the loss of a discrete silica coating, if it existed in Mesozoic megaspores, could be caused by harsh sample preparation techniques.

7.1.5 Synthesis

Although the fossil record of the major groups of tracheophytes is comprehensive, detailed palynological studies including TEM analyses are limited and hence restrict interpretations of spore wall layers. From previous work by various authors cited herein and in *chapter 6* it is clear that the fossil record of the perispore nevertheless allows some speculation on its very first appearance. In figure 7.1 I have summarised the occurrence of the perispore in certain tracheophytes by plotting it on to their phylogeny and taxonomic hierarchy. As discussed above and in *chapter 6*, it shows that the presence of the perispore in the Rhyniopsida is conjectural, which also holds true for the Cladoxylopsida and the Zosterophyllopsida. In the latter, however, the occurrence of tapetal granules were described for the inner sporangium wall of certain *Zosterophyllum* species (Edwards 1996), which indicates that by the end of tapetal activity, a perispore might have been deposited on the spores.

For the Trimerophytopsida and the Progymnospermopsida, only one genus respectively was found to possess a perispore. It is not known if *Protopitys*, for which a perispore was recorded, is more similar to the Archaeopteridales or the Aneurophytales and it is also considered that *Protopitys* represents a male seed plant for which ovulate organs have not yet been identified (Hammond 2004). With many questions unanswered concerning the reproductive strategy and the taxonomic position of *Protopitys*, the identification of a perispore in some of its spores should be treated cautiously. The occurrence of a perispore in other genera within the Trimerophytopsida and the Progymnospermopsida cannot be excluded, or confirmed. This suggests that an assured occurrence of the perispore either dates back to the origin of the Lycopodiopsida, Equisetopsida and/or the Polypodiopsida.

I am inclined to focus on the Polypodiopsida, mainly because different outer spore wall layers are present in the extant representatives of the Lycopodiopsida and the Equisetopsida. In the Lycopodiopsida, extant *Lycopodium*, for example, has a perispore, whereas in the heterosporous genera *Selaginella* and *Isoetes* only the microspores have a true perispore (e.g. Tryon and Lugardon 1990; Moore *et al.* in press a; *chapter 1*, herein). As for the Equisetopsida, extant *Equisetum*, however, possesses an epispore (Tryon and Lugardon 1990) although some authors would call it a perispore (Lugardon 1969; Kurmann and Taylor 1984). Even if extinct orders such as the Sphenophyllales or the Calamitales are taken into consideration, for which a perispore was reported, they did not emerge until the uppermost Upper Devonian and Lower Carboniferous (Stewart and Rothwell 1993). Looking at the Polypodiales reveals that a perispore was reported for the zygopteridalean representative *Rhacophyton ceratangium*, whose fossil record dates back to the early Upper Devonian (Andrews and Phillips 1968; Stewart and Rothwell 1993; Bell and Hemsley 2000). I suggest that this is the earliest record of a true perispore, identified in a fern-like representative. It is, however, possible that the peripheral layer in *Cooksonia* and the envelope around cryptospores already denote perispore-like layers. This means that the first occurrence of this layer might date back as far as the Ordovician and that peripheral layers such as in *Cooksonia* and *Uskiella* and perisporal envelopes surrounding cryptospores could well be an ancestral feature that was later lost in certain plant groups and was retained as a true perispore in *Rhacophyton ceratangium* (Upper Devonian). Hence, I suspect that the outer spore layer in the latter species might be the first true perispore.

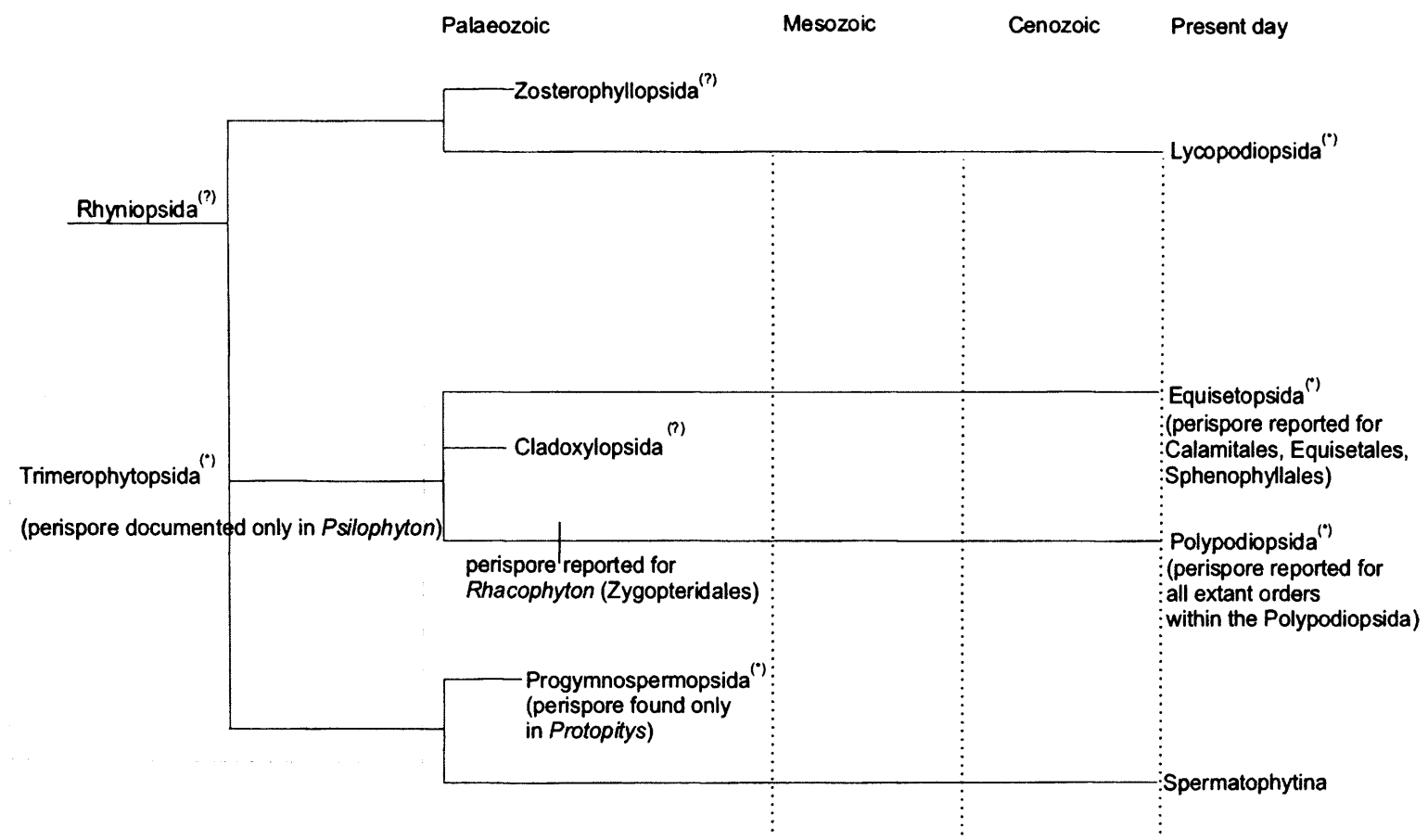


Figure 7.1 A phylogeny of the major groups of tracheophytes and their taxonomic hierarchy, modified after Bell and Hemsley (2000), figure 6.5, p. 141. Asterisks indicate the occurrence of a perispore for certain taxonomic groups. A question mark indicates that the presence of a perispore is conjectural. In some cases (e.g. Trimerophytopsida and Progymnospermopsida), a perispore was only documented in certain genera but it is assumed (e.g. Balme 1995 and chapters 6 and 7, herein) that a perispore could also be present in other genera.

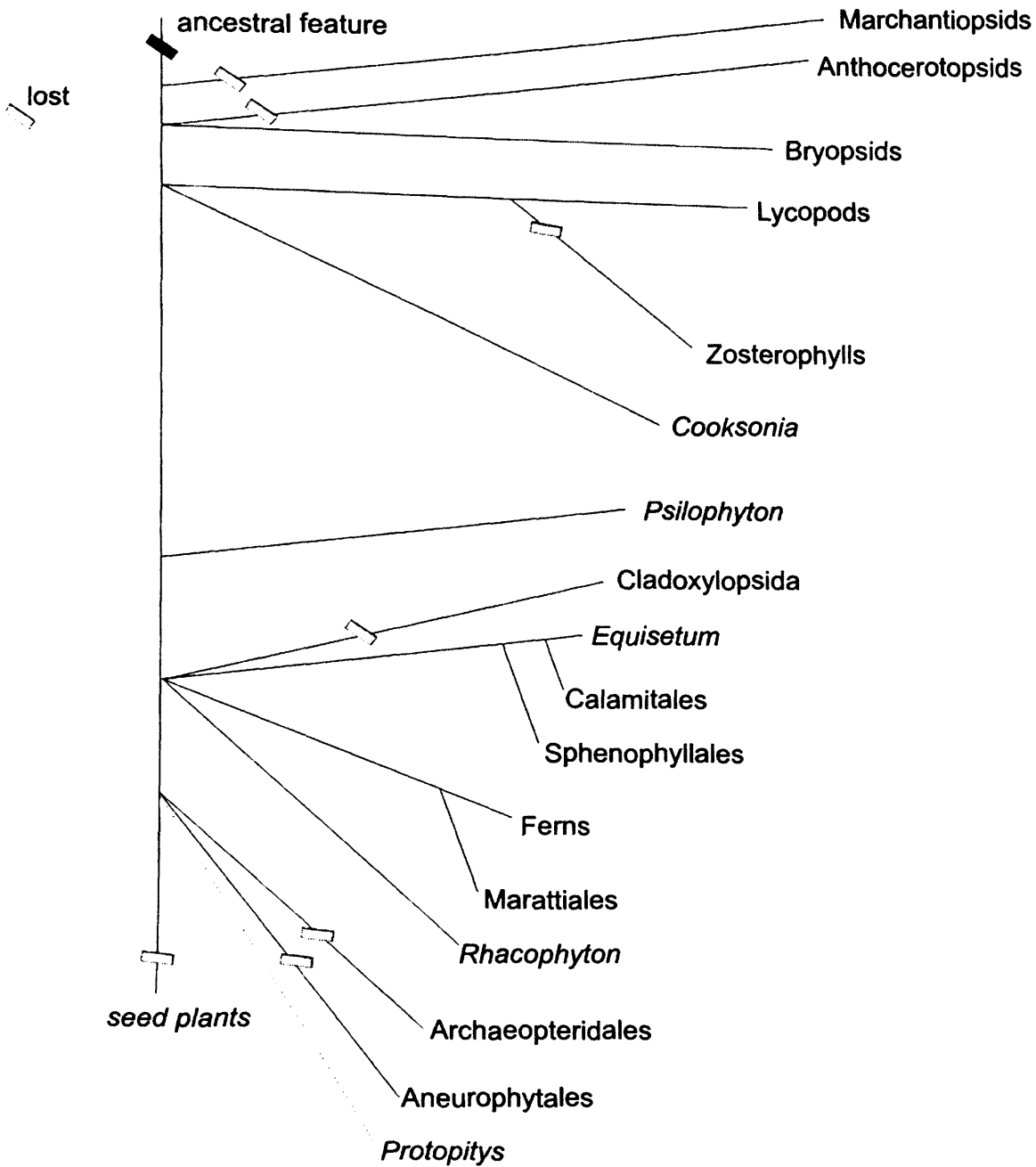


Figure 7.2 Preliminary cladistic hypothesis of phylogenetic relationships among embryophytes, modified after Crane (1990), figure 2 (p. 19), showing the loss of the perispore in various groups. It is believed that the perispore is an ancestral feature that was lost in some groups but retained in the majority of lower embryophytes.

7.2 Functions and Chemistry

Plant cuticles and lower embryophyte perispores/perines are both boundaries between the plant/spore and the environment. At first glance this seems like the only parallel but a more detailed review of aspects such as their first occurrence, ultrastructure, chemical composition and function reveals that cuticle and perispore share far more features than expected. This will be discussed below.

The question of function of the perispore in pteridophytes and the perine in bryophytes is probably very difficult to answer. It is clear from *chapter 1* that the literature has so far not offered many suggestions. I believe that probably its most important function is the protection of the spore and its genetic material from desiccation or pathogenic attack. Other functions will also be considered. Since the chemistry and the function of the perispore are interlinked by the fact that most compounds associated with function (and protection) are chemical compounds, these two aspects will be considered together. Table 7.1 provides a summary of this section, highlighting common aspects of the cuticle and the perispore.

A COMPARISON	CUTICLE	PERISPORE
Fossil evidence (selected examples)	- sporangial cuticle: <i>Cooksonia pertoni</i> (Silurian) described with a heavy cuticle (Edwards <i>et al.</i> 1996)	- possibly in cryptospores in form of an envelope (Silurian/Ordovician) - possibly in <i>Cooksonia pertoni</i> in form of a peripheral layer (Silurian)
Ultrastructure	- lamellate cuticle proper (Jeffree 1996) - self-assembly processes proposed for the formation of cuticle waxes (Koch <i>et al.</i> 2004) and for globules in the cuticle proper (Jeffree 1996)	- commonly considered to be of tapetal origin (e.g. Tryon and Lugardon 1990), other mechanisms possible due to high variability of this layer - lamellate perispore common (Tryon and Lugardon 1990) - self-assembly (e.g. Heslop-Harrison 1972; Hemsley <i>et al.</i> 1996, 1998, 2000, 2003; Gabarayeva and Grigorjeva 2002, 2004) proposed as underlying wall formation process

		Function	
Chemical composition	<ul style="list-style-type: none"> - cutin, an insoluble polymer built mainly from esterified aliphatic C₁₆ and C₁₈ hydroxy and epoxy acids (Fauth <i>et al.</i> 1998), related to suberin / lignin and sporopollenin family (Cooper-Driver 2001) 	<ul style="list-style-type: none"> - sporopollenin, a macromolecule of yet unknown composition (<i>chapters 1 and 4</i>, herein) related to the cutin / suberin and lignin family (Cooper-Driver 2001) - mineral content (e.g. silica), often incorporated into the perispore 	
Permeability	<ul style="list-style-type: none"> - water regulation / transpiration - transpiration proposed as mechanism for wax transport and regeneration (Neinhuis <i>et al.</i> 2001) - import of lipids into cuticle (Samuels <i>et al.</i> 2005) 	<ul style="list-style-type: none"> - prevention of water loss and desiccation (harmomegathic mechanisms) (Blackmore and Barnes 1986) - transport of substances such as proteins demonstrated for the exine but potentially also occurring in the perispore (Pettitt 1976) - lipids shown to be present in the perispore (Schneider and Pryer 2002) 	
Strengthening	<ul style="list-style-type: none"> - mechanical support (cutin) 	<ul style="list-style-type: none"> - mechanical support (sporopollenin / silica) 	
Defence mechanism	<p style="text-align: center;">Structural</p> <ul style="list-style-type: none"> - cutin against bacterial growth, penetration of fungal hyphae or micro-herbivores <p style="text-align: center;">Chemical</p> <ul style="list-style-type: none"> - phenolics - cuticular degradation products (Chassot and Métraux 2005) - phenolics and flavonoids 	<p style="text-align: center;">Structural</p> <ul style="list-style-type: none"> - sporopollenin against bacterial growth, penetration of fungal hyphae or micro-herbivores - silica incorporations might act as additional pathogenic attack deterrents <p style="text-align: center;">Chemical</p> <ul style="list-style-type: none"> - phenolics (Cooper-Driver 2001; Graham <i>et al.</i> 2004) - lectins - phenolics - flavonoids? 	
UV protection	<ul style="list-style-type: none"> - signalling for plant defence , especially aimed at fungi (Chassot and Métraux 2005) 	<ul style="list-style-type: none"> - signalling for plant defence unknown - potential biological signalling between mega- and microspores (discussed herein) 	

Table 7.1 Cuticle and perispore both form a physical barrier between the plant/spore and the environment. Various properties of these boundaries are compared, including chemical, mechanical and functional, evolutionary and developmental aspects.

7.2.1 Fossil evidence

As discussed above in section 7.1, the first true perispore might not have occurred until the Upper Devonian in *Rhacophyton*, but it is also considered that the peripheral layer of *Cooksiona pertoni* (Silurian) constitutes a perispore-like layer. Perhaps significantly, early records of fossil cuticles were also found in *Cooksiona pertoni*, surrounding their sporangia (Edwards *et al.* 1996). This suggests that barriers to the environment or additional protective features such as the sporangial lining, might have evolved at about the same time (e.g. in the Silurian). The preservation of cuticle and peripheral layer/perispore is due to their high fossilization potential (de Leeuw and Largeau 1993; Edwards *et al.* 1996). Both layers are made from related compounds, cutin (cuticle) and sporopollenin (e.g.: perispore).

In *Resilitheca* (Lower Devonian) and *Sporathylacium salopense* (Lower Devonian) a presumed sporopollenin-impregnated lining of the sporangial cavity was documented (Edwards *et al.* 1995c; Edwards *et al.* 2001), which indicates that in addition to cuticle and spores, other anatomical features, such as the inner sporangium wall, for example, became impregnated and/or strengthened.

7.2.2 Composition

In land plants phenolic compounds form a family of biosynthetically related biopolymers and are believed to hold vital structural, mechanical and protective roles. For a review see de Leeuw and Largeau (1993) and Cooper-Driver (2001). The most common compounds are cutin, suberin, sporopollenin and lignin, synthesised from fatty acids and phenyl propanoids. All of these compounds possess a high preservation potential (de Leeuw and Largeau 1993) with evidence for the evolution of the first vascular plants coming from the fossil record (microfossils) of cuticles, tracheids, lignified tubes or spores. Cutin in the cuticle, lignin in the tracheids and sporopollenin in spore walls are structurally homologous polymers (Cooper-Driver 2001). As discussed in *chapter 4*, the chemical structure of sporopollenin is not yet fully understood, almost all other biopolymers have been elucidated (de Leeuw and Largeau

1993). Cutin is an insoluble polymer mainly built from esterified aliphatic C₁₆ and C₁₈ hydroxy and epoxy fatty acids (Fauth *et al.* 1998). Jeffree (1996) points out that some cuticles additionally contain a second compound, cutan, or consist of a mixture of both. He also noted that the chemical structure of cutan has yet to be confirmed by conventional chemical analysis. Its biosynthetic origin, too, awaits elucidation. Sporopollenin is a macromolecule of yet unknown composition (*chapters 1 and 4*, herein). Much as the cuticle is a mixture of at least two closely related polymer compounds, it seems that different types of sporopollenin exist. The receptor-independent sporopollenin described by Rowley and Claugher (1991), for example, is less resistant to degradation methods such as acetolysis or potassium permanganate solution than the “pure” sporopollenin. Differences in the composition of sporopollenin could explain why, for example, the fossil record of perispores from tracheophytes is so sparse, as discussed above in section 7.1. I assume that any mixture of sporopollenin with other organic compounds such as lipids, protein or polysaccharides, for example, would weaken the robustness of this macromolecule, leading to a lower fossilization potential and hence negatively affect the fossil record as well as to the variability of this layer.

The occurrence of cutin and sporopollenin in *Cooksonia* suggests that two very robust, chemically related compounds were utilised by at least some Lower Devonian plants for the protection of different anatomical features. Another common feature of these outer layers is that the two compounds, cutin and sporopollenin, are responsible for mechanical support and strengthening, which is vital for survival of both plant and spore. Further aspects of spore strengthening will be discussed below.

7.2.3 Ultrastructural aspects

At an ultrastructural level, cuticle and perispore share a lamellate feature, which has previously been documented for example in the perispore of *Christensenia aesculifolia* (Marattiaceae) (Tryon and Lugardon 1990, fig. 6.5) or in the exospore of *Lycopodium clavatum* (Tryon and Lugardon 1990, p. 6, figs. 33ff) and in the cuticle proper of *Hakea suaveolens* (Proteaceae) (Jeffree 1996, fig. 2.8). A very similar lamellate pattern has also been described for

suberin in *Agave americana* (Strasburger 1998, fig. 1-114), which is shown in figure 7.3, below.

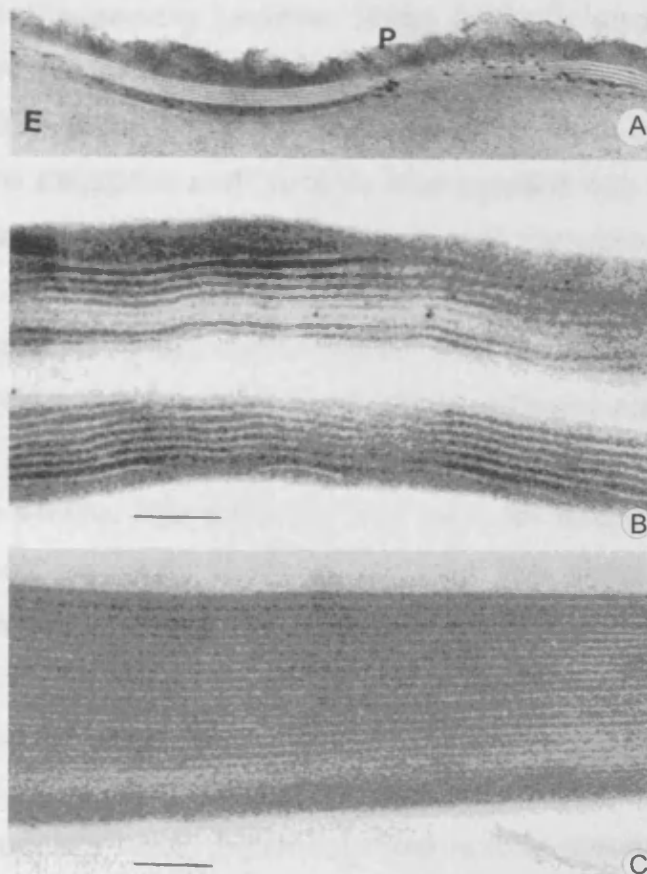


Figure 7.3 **A** lamellate features in the spore wall (P = perispore, E = exospore) of *Christensenia aesculifolia* (sporopollenin), **B** cork cell walls of a potato, separated by lamellate suberin layers, and **C** isolated cuticle of *Agave americana* (cutin). **A** is magnified x 50,000, taken from Tryon and Lugardon (1990), fig. 6.5. Scale bars in **B** and **C** are 0.1 μ m, the picture is taken from Strasburger (1998), fig. 1-114.

These lamellate structures can be part of the outer perispore, the exospore, and the inner part of the cuticle proper and are similar in size and electron density (figure 7.3). In both cases their development and exact chemical composition is unknown (Tryon and Lugardon 1990; Jeffree 1996), although I suspect that sporopollenin, cutin and suberin could be the main components, as they are related, occurring in all these different anatomical features. The similarity of these structures is striking and raises questions as

to whether cuticle and perispore (as well as suberin structures) are comparable at an ultrastructural level. The cuticle proper also contains electron dense globules coated with a translucent shell (Jeffree 1996). It is hypothesised that a possible formation process giving rise to the cuticular globules is via self-assembly (Jeffree 1996), which is also proposed as the underlying pattern formation mechanism in spore walls (Hemsley *et al.* 1996, 1998, 2000, 2003). Globules found on spores (*chapter 5*, herein) normally form on top of the exospore and become impregnated with sporopollenin and perispore material towards the end of spore wall formation (e.g. Tryon and Lugardon 1990). These globules, however, are embedded into the cuticle between the inner part of the cuticle proper and the primary cell wall (figure 7.3). Although these globules can be found in different areas of cuticle and perispore, their size, high electron density and proposed formation mechanisms are similar. The occurrence of globules and lamellate structures in both cuticle and perispore supports the idea that these two layers share common features and presumably also very similar functions.

7.2.4 Permeability

One of the cuticle's most important roles is it to prevent water loss and desiccation by integrating hydrophobic waxes into the outmost layer and hence creating an almost impermeable barrier (Strasburger 1998). The cuticle, however, is capable of minimal transpiration, which is interpreted as the prerequisite for the transport and regeneration of cuticular waxes (Neinhuis *et al.* 2001). The perispore probably also regulates and balances the spore's water relations but instead of being a more or less water impermeable sealant like the cuticle, it might prevent desiccation via harmomegathic mechanisms, as described by Blackmore and Barnes (1986). Harmomegathy is the reaction of the complete pollen and spore wall to the turgor pressure of the cytoplasm by stretching and contraction (*ibid.*). These properties are common for sporopolleninous spore walls, highlighting the robustness and flexibility of this macromolecule. Blackmore and Barnes consider harmomegathy essential for life on land and note that as isolated units, pollen and spores are not permanently attached to a water containing

substrate and a water resistant wall is fundamental to their extended survival. This highlights that the perispore, as part of the sporoderm, is not only a protective layer to avoid desiccation but also prevents spores from taking up too much water, which would result in swelling. Any uptake of water from the environment bears the risk of introducing pathogens such as bacteria or fungi into a closed system, which could harm the spore and its genetic material.

Lipids occur in both cuticles (Neinhuis *et al.* 2001; Koch *et al.* 2004; Samuels *et al.* 2005) and perispores (Tryon and Lugardon 1990, and literature cited therein; Schneider and Pryer 2002) and, incorporated into sporopollenin or cutin/cutan, these lipids impregnate the outer layers. It is not fully elucidated how substances such as lipids are transported into the cuticle but a recent publication (Samuels *et al.* 2005) assumes the presence of a cuticular lipid export system. The transport mechanisms of substances into the perispore are not much studied either. Lipids were found in the perispore of some water ferns (Schneider and Pryer 2002) but so far transport mechanisms have only been documented for the exine (Pettitt 1976) of *Lycopodium*. He suggested that exine channels (terminology *sensu* Pettitt 1976) allow communication between the developing spore wall and the gametophyte. It is not known how widely distributed lipids are in pteridophyte perispores. More work is also needed to fully understand the underlying transport mechanisms in both the exospore and the perispore. It seems that cuticle and perispore are supplied with hydrophobic, impregnating substances such as lipids via almost unknown carrier mechanisms in order to balance the water uptake.

7.2.5 Defence mechanisms

Another vital role of cuticle and perispore is to act as a defence mechanism against pathogenic attack. I will distinguish between structural and chemical defence mechanisms. Structural defence can be achieved by utilising a robust building material, such as the polymer cutin or the macromolecule sporopollenin. The mechanical support of these polymers was also described by de Leeuw and Largeau (1993) and Cooper-Driver (2001). In the case of the perispore (sporopollenin), certain lower embryophytes

additionally incorporate silica into their outer spore wall layer, probably to enhance the structural stability (Tryon and Lugardon 1990; *chapter 3*, herein). The function of silica in spore walls will be discussed in more detail below. The main advantage of having a robust outer layer is that it can prevent attacks from micro-herbivores, but it also decreases the chances of fungal hyphae to penetrate into the epidermis or spore (Edwards *et al.* 1996; Tryon and Lugardon 1978). Bacterial growth is especially difficult on hydrophobic, water repellent and self-cleaning surfaces, as reported by Neinhuis and Barthlott (1997). It is the micro-roughness of the cuticle, caused by cuticular waxes, which gives rise to these water repellent, self-cleaning properties. This phenomenon was first described for the leaf surface of the lotus plant (*Nelumbo nucifera*) and was hence given the name "lotus-effect" (Neinhuis and Barthlott 1997). I do not consider spores to have equally efficient water repellent, self-cleaning properties, although some lipids might be incorporated into the perispore in order to provide at least some protection from wetting. Although some spores have a micro-sculpture (Tryon and Lugardon 1990; Moore *et al.* in press a) comparable in size and coarseness to that of the cuticle, the micro-roughness of the spore sculpture does not seem to enhance water repellence. I suspect that defence mechanisms against bacterial growth are more likely to be based on chemical substances acting as anti pathogens.

Phenolics Common chemical substances used in plant defence are phenolics (Cooper-Driver 2001; Graham *et al.* 2004). Besides being the underlying structure for compounds like sporopollenin, suberin and lignin (see above), phenolics have a proven record of defence against pathogens, influence detritivores and act as light screens against intense irradiation (Cooper-Driver 2001; Graham *et al.* 2004). Biosynthesis and evolution of phenolics are described elsewhere (Cooper-Driver 2001). Phenolics, including flavonoids, occur in both the cuticle and the perispore and I suspect that they have similar functions, as outlined above. Cooper-Driver (2001) notes that the main functions comprise protection from UV radiation, signalling between microbes and disease resistance. I will briefly discuss these aspects.

The effects on UV radiation on plant cells have been reviewed by Hollósy (2002) and were shown to damage DNA, proteins, lipids and membranes. UV

irradiation is also known to cause a more rapid seed germination but subsequent seedling growth was significantly retarded (Noble 2002). Unless spores protect themselves from UV radiation, their metabolism, DNA and the successful development of the gametophyte are at risk. This protection is likely to be similar to that of the cuticle, where flavonoids and cutan / cutin act as natural shields. Sporopollenin, and *p*-coumaric acid in particular, the latter being a compound of the sporopollenin macromolecule (de Leeuw *et al.* in press), has been shown to absorb UV radiation (Rozema *et al.* 2001). Flavonoids are an integral part of the vacuole in pteridophytes and angiosperms (Wallace 1989; Kramer *et al.* 1995) and are also associated with UV protection (Cooper-Driver 2001). The combination of both phenolic compound classes (flavonoids and sporopollenin) is likely to shield spores from harmful UV light. A rough micro-sculpture (e.g. echinate or papillate) might provide additional protection by helping to deflect UV radiation, as proposed for cuticular waxes (Tevini 1988).

Communication between microbes and plant roots in the soil is regulated by phenolics as chemical signals (Cooper-Driver 2001). Of particular interest is the interaction between plants and microbial pathogens, reviewed by Lynn and Chang (2000), which should also be considered for spores and pathogens. I could not find any evidence for biological signalling in spores in the literature, but as spore walls are rich in chemical substances (Pettitt 1976, 1979a and b; Schneider and Pryer 2002; *chapters 3 and 4* herein), a defence mechanism via biochemical signals should not be neglected. Communication via these compounds might occur between mega- and microspores, where megaspores could be in the position to attract gametes for fertilisation. Although this is an unproven hypothesis and some might argue that if that was the case the plant would not need to invest into a large number of microspores, biological signalling in heterosporous genera of lower embryophytes might be an effective way to produce gametophytes. It remains unclear as to whether the substances involved in this communication are also phenolics or pheromone-like substances, synthesised by the secondary plant metabolism.

Phenolics in leaves can act as feeding deterrents to herbivores (Cooper-Driver 2001), but I am not convinced that this might also hold true for spores.

A larger number of spores would have to be consumed in order to deter a herbivore. Based on the discovery of large numbers of different spores in Siluro-Devonian coprolites, Edwards *et al.* (1995b) suggested that detritivorous feeding on litter rich in spore and spore masses or herbivorous feeding on sporangia, were plausible. Both hypotheses, however, indicate that phenolics as feeding deterrents in spores might not be as effective as in leaves.

Lectins It is assumed that lectins are found ubiquitously throughout the plant kingdom (Etzler 1985), including spores (Pettitt 1979a), as previously summarised in *chapter 1*. Lectins seem to be specific within particular taxonomic groups distinguishing them from other closely related taxa. Screening assays revealed that some plants contain more than one lectin gene and therefore more than one type of lectin may be expressed in the plant, indicating that during evolution different types of lectins were adapted for unique functions in various species or tissues (Etzler 1985).

To date, only very few articles have described lectins in pteridophytes. Lectins were characterised in *Azolla* (Mellor *et al.* 1981), *Dryopteris* (Vasheka *et al.* 1999, cited in Tateno *et al.* 2003), *Phlebodium* (Tateno *et al.* 2003) and in the spores of the water ferns *Marsilea* and *Pilularia* (Pettitt 1979a). A study by Southworth (1975) investigated the effect of lectins on pollen germination.

The first evidence for lectin activity in a fern was reported for the *Azolla-Anabaena* symbiosis, by Mellor *et al.* (1981). Proteins recovered from the symbiosis showed haemagglutination activity. Although the water fern *Azolla* lives in symbiosis with the N₂ fixing cyanobacterium *Anabaena azolla*, lectin activity was only present in *Azolla* itself and not in the bacterium.

Tateno *et al.* (2003) are the first to give a detailed and extensive study of a lectin in pteridophytes by describing significant quantities of a mannose/glucose binding protein in the rhizomes of *Phlebodium aureum* (L.) J. Smith. The binding specificity of the lectins discovered are, to jacalin-related lectins (JRL) but differ from legume or monocot lectins. The prototype of JRLs was isolated from the seeds of *Artocarpus integrifolia* (Moraceae – jack fruit), binding and structural properties were reported elsewhere (Sastry *et al.* 1986). Due to a wide distribution of jacalin-related lectins in the plant kingdom, the

authors assume that an ancestral protein of JRLs has evolved with specific functions in each plant family. The identification of a JRL in a fern has contributed to the understanding of the distribution of JRLs in plants and raises questions about the evolution of these lectins in general. From the results obtained by Tateno *et al.* (2003) I assume that although the JRLs were located only in the rhizomes of *Phlebodium*, this does not necessarily exclude the possibility that JRLs or other types of lectins could well be present in the spores of that particular species or in other species. This view is strengthened by the work of Pettitt (1979a) who demonstrated the presence of β -lectins in microspores of the heterosporous water fern *Marsilea*. Specific staining techniques revealed a high lectin concentration near the microspores' germinal site. Pettitt failed to detect β -lectins in the megaspores, for which he does not give any explanation. I suspect that the reason for this phenomenon might be another type of lectin, which is present in *Marsilea* megaspores. The tests used in his study might not have been sensitive for the *Marsilea* megaspore lectin and therefore led to a negative result. It is, however, possible that lectins occur only in microspores. Maybe microspores need a powerful tool to defend themselves chemically, whereas megaspores, bigger in size and with more spore wall volume, can rely on other substances such as larger amounts of sporopollenin, incorporated minerals (e.g. silica) or phenolic compounds (see above).

A study by Southworth (1975) investigated the effect of the lectins concanavalin A and phytohaemagglutinin-M (PHA) on pollen germination. Though the lectins did not increase the maximum percentage of pollen, which eventually germinated, their action might be related to a long-term effect. It is assumed that the stimulation of germination is controlled at the plasma membrane, because lectins are capable of binding cell surfaces. If lectins enhance the permeability of the plasma membrane so that more water and nutrients for germination can be taken up, a long-term effect on germination is plausible. The author speculates that the events mediated by lectins *in vitro* actually might also occur during germination *in vivo*. If lectin activity could be confirmed for lower embryophyte spore walls, this might be another explanation for the occurrence of nutrient elements in spores, besides being providers of energy for gametophyte production.

On the basis of the studies summarised above it is thought that lectins might play an important role in spore germination and also act as defence mechanisms against pathogenic attack. Although their presence in spore walls and in the perispore in particular is not fully understood, their function should not be underestimated.

If the perispore is indeed mainly associated with protection and mechanical support why is it then sometimes brittle or even separates from the exospore as seen in the pteridophyte species of *Pellaea calomelanos* (chapter 4, figure 4.6) or of *Pyrrhosia* (van Uffelen 1986)? A look at the work of Tryon and Lugardon (1990) also reveals that quite a number of pteridophyte spores are described with an abraded perispore. It seems illogical that a protective layer can be lost that easily. This indicates one of the following possibilities: (1) the abraded perispore might have been caused by desiccation before SEM viewing and does not occur in the living species, (2) it occurs in certain species shortly before germination to enhance the process (3) or it is a genuine feature of certain species. The latter would imply that those species that shed their perispore must have defence mechanisms located elsewhere, for example in the exospore. It is also possible that those species are not in need of protection or regulate their defence mechanisms via chemical substances, as described above.

7.2.6 Other functions

The following sections on functions and features of the perispore such as dispersal, mineral content and plasticizer contamination are discussed separately. Since these aspects are unique to the perispore, no comparisons with the cuticle can be made.

Dormancy and dispersal Pteridophyte spores are usually wind distributed and have different times of dormancy and viability in or on soil (Moran 2004). Moran notes that green spores are viable for shorter periods but germinate faster, whereas non-green spores remain viable for many years. In some families (e.g. Ophioglossaceae) or genera (e.g. *Lycopodium*)

spores are capable of germinating in the darkness of the soil. I checked the ultrastructure of these spores in the work of Tryon and Lugardon (1990) and noted a particular thick and often three layered (Ophioglossaceae) exospore and a thin, fibrillous perispore. Since the spore wall needs to be broken down for germination, a thin perispore would be advantageous.

There is a tendency for fibrillous perispore material in green spores of *Osmunda* and spores that germinate in the dark (Ophioglossaceae, *Lycopodium*). The green spores of *Onoclea*, however, have a compact, two layered perispore. Considering a protective, cuticle-like role for the perispore, it is plausible that the perispore, no matter whether it is fibrillous or compact, needs to fulfil two aspects: on the one hand, it needs to contribute to a successful germination by preventing desiccation, decay, microbial and bacterial defence and, on the other hand, the spore wall must be degradable for germination.

As for the dispersal, I suspect that the less spore wall material it is made from, the lighter it is and hence they can be further dispersed. Thus, the thinner the perispore the more this would contribute to better dispersal. Perispore ornamentation can only contribute to a certain extent to this factor: any undulate sculpture will keep spores airborne longer. Many spores, however, are laevigate or have broad ornamentation not necessarily pronounced enough to assist dispersal. I consider the weight of the spore and reduction in spore wall thickness (perispore and exospore) as a more convincing element in dispersal.

Mineral content in spore walls Possible functions of nutrient elements in lower embryophyte spore walls as well as in pteridophyte fronds were already discussed in *chapter 3*. Their occurrence is probably due to metabolic requirements of the plants. The main focus of this discussion is on silica, as it is the only element that forms a discrete spore wall layer (perispore) in *Selaginella* megaspore walls (*Introduction 1.4.1.10*). It is not clear as to whether silica is incorporated into or bound to the sporopollenin macromolecule. It is currently also unknown whether silica forms a discrete outer layer, interconnected with the perispore / perine in lower embryophytes

and how much silica material is also embedded into the underlying exospore / exine. Research on silica in spore walls is in its infancy and has, to date, only been studied in *Selaginella* megaspores (Tryon and Lugardon 1978; Morbelli 1995; Moore 2001; Moore *et al.* in press a; the present study). In this genus, as least for some species, a discrete silica layer seems to lie on top of, and in some cases is integral with, the outer part of the exospore. I can only assume that silica in all other lower embryophytes is integral with the perispore/perine or the outer part of the exospore/exine, as EDX analysis detected silicon signals from the spore surfaces. Comprehensive TEM EDX studies on pteridophyte spore walls would reveal whether silica is also found throughout the exospore, as previously suggested by Tryon and Lugardon (1978, 1990) for *Selaginella* megaspores. Since the chemical nature of sporopollenin remains largely unknown, it is extremely difficult to predict possible chemical bonds between silica and sporopollenin moieties.

Elemental silicon, as a component of pollen exine, was detected by x-ray microanalysis (Crang and May 1974). The same authors suggested that silica compounds enhance the resistance of pollen to diagenesis and microbial decay. Tryon and Lugardon (1978) discussed the presence of silica in *Selaginella* megaspore walls and proposed that silica probably prevents water loss and the penetration of fungal hyphae, but also provides mechanical support. Morbelli (1995) favours the idea that silica as well as the presence of other elements in the spore wall are due to the availability of silicon in the soil and ecological requirements of the plant. The tubular exospore structures, which were only found in *Selaginella convoluta*, out of 10 species investigated, might be related to the resurrection habit of this particular species. Since similar studies have not yet been carried out for *Selaginella lepidophylla* (also a resurrection plant), the correlation between tubular exospore structures and this survival strategy remain a hypothesis. I agree with the above authors that the incorporation of silica into pollen and spore walls is probably related to protection and mechanical support. I assume, however, that this aspect is species specific due to the fact that silica does not occur in all lower embryophytes, as discussed in *chapter 3*. Those species that do not embed additional silica in the spore walls might rely solely on the

robustness of sporopollenin and utilise chemical substances against pathogenic attack.

As far as the transport of silica into the spore walls is concerned, studies on *Selaginella* megaspores suggest that the siliceous coating found in some species (Tryon and Lugardon 1978; Moore *et al.* in press a) is either transferred through the exospore by an as yet unknown mechanism or is a product of a self-assembling pattern formation process giving rise to a vast number of varying sculptures (Hemsley *et al.* 1994; 1996, 1998b, 2000a; 2000b). A combination of both processes is also possible. In *Lycopodium* and *Marsilea* spores, metabolic activity via exine channels between the developing spore wall and the gametophyte was postulated (Pettitt 1976, 1979a and b). If these exine channels also occurred in *Selaginella* megaspores (which I would call *exospore* channels), this communication system could explain the transport of silica into the megaspore walls and also the detection of various other nutrient elements.

Silica content in *Selaginella* megaspores also results in the occurrence of cubic crystals in sporangia and megaspores of *Selaginella myosurus*. Unfortunately, *in vivo* spore wall formation and crystal precipitation could not be studied due to the lack of living material and difficulties in obtaining a specimen from any Botanic Garden. Hence, both processes are subject to speculation. Of special interest are 1) the timing of crystal precipitation in relation to spore wall formation, 2) the occurrence of crystals on the inner wall of the sporangium as well as 3) the presence of few crystals on the ridges.

Initially it was considered that the size of the megaspores might be a contributory factor in the occurrence of these crystals. With a megaspore diameter of around 800 μ m (Moore 2001) those of *S. myosurus* are larger than the spores of other species but not the largest measured. Tryon and Lugardon (1990) cite a general megaspore diameter in *Selaginella* of 200-1033 μ m, unfortunately, without naming the largest species. The only account for crystal growth on megaspores in this genus is for *S. myosurus*, which allows speculation that spore size might not be the reason for the occurrence of these crystals on *S. myosurus*.

With over 50 μm in height, the ridges, seen in *S. myosurus*, are the highest so far documented in the genus (Minaki 1984). They consist of an exospore labyrinthine network, which is not as densely packed as similar regions in other species (Minaki 1984; Moore 2001). This network presumably allows the precipitation of these crystals underneath the ridges as it provides sufficient space for crystal growth. The gap between the exospore and the ridges has a maximum height of 7 μm , which is suitable for the precipitation of these crystals from within the with silica saturated exospore. This is suggested to be the first precipitation process, probably interlinked with the subsequent formation of the ridges. Due to lack of developmental studies it is unknown as to whether the ridges are of tapetal (perispore) or exospore origin. I suspect they are exospore material, as I have not encountered tapetal material deposited on top of the exospore with a thickness in excess of 50 μm . Tapetal deposits normally form a thin, discrete true perispore layer (Tryon and Lugardon 1990). If the ridges were indeed a perispore, then the terminology used by Kempf (1971b) would be adequate, but as previously discussed and explained in *chapter 6*, I do not agree with his terminology and interpretation of spore wall layers.

The silica detected in pteridophytes originates from the soil and is taken up by the plant in the form of monosilicic acid, as described by Epstein (1999). A reason for the presence of these crystals might be the metabolism of the plant, as they may take more silica from the soil than other species. I assume silica is then distributed throughout the plant and any excess will preferably be incorporated into the megaspores and the sporangial fluid. At this stage any silica deposition will be amorphous (e.g. in the form of silica gel). The crystalline form as seen in the cubes is unique to *S. myosurus*.

The second precipitation process of silica probably occurs during desiccation of the sporangia shortly before dehiscence and the release of the mature megaspores. I believe that the (amorphous) silica present in the sporangial fluid will result in the precipitation of crystals on the inner side of the sporangium. The fact that some crystals are also scattered over the ridges means that they must have originated from this process. An indication for this is that their size is similar to that of the crystals on the inner wall of the

sporangium (up to 10µm) and not to the crystals underneath the ridges (2-7µm).

It is noteworthy that a similar phenomenon has not yet been documented for any other species although silica is widely distributed in spores of this genus. I suspect that in other *Selaginella* megaspore species, silica is precipitated, present but not in this cubic, crystalline form. To date these crystals are species-specific to *Selaginella myosurus*. The function of the crystals is unknown. They probably have no specific function and are the "waste product" of excess silica uptake by the plant. I do not believe that they give this species any advantage in terms of germination, defence, or prevention of water loss or structural stability, because a large number of other species survive in apparently similar habitats and do not show these crystals on their spore surface.

Silicon also occurs in pteridophyte leaves and it is suggested that it primarily provides mechanical support in cell walls (Kaufman *et al.* 1971; Crang and May 1974; Parry *et al.* 1985; Perry and Fraser 1991) and functions as protection from pathogenic attack or penetration of fungal hyphae (Tryon and Lugardon 1978; Morbelli 1995), aspects which also apply to the perispore (see above). Studies on the epidermal cells of *Oryz sativa* L. (rice) also support the idea that deposition of hydrated silica gel may provide water to leaf and stem during dry periods or when transpiration causes a loss in turgor (Epstein 1999). There seems no indication of a correlation between silica accumulation and the xerophytic habit of some *Selaginella* species. Silica accumulation, for example, occurs in both species *S. emmiliiana* and *S. lepidophylla*, of which only the latter is a resurrection plant (Dengler and Lin 1980). The same authors note that the function of silicon in the genus *Selaginella* is not known.

Contamination with plastizisers It has also been postulated herein, that previous interpretations of phenolic compounds wrongly described common plasticizers as sporopollenin compounds. Although spore walls contain phenolic compounds in the form of sporopollenin, it is likely that in the past plasticizer contamination has lead to errors regarding spore- and pollen

wall compositions (see *chapter 4*). Comparisons of NMR spectra of plasticizers with organic phenolics such as cinnamic-, *p*-coumaric-, ferulic and sinapic acid show clear differences in essential chemical shifts, which leaves little room for speculation (Integrated Spectral Data Base System for Organic Compounds, SDBSWeb).

8 Conclusions

8.1 Evolutionary aspects of lower embryophyte spore wall layers

- ❖ Within bryophytes, a potential lack of the perine in marchantiopsids and anthocerotopsids and a non-acetolysis resistant perine in the bryopsids, it is possible that this layer was lost in both the marchantiopsids and anthocerotopsids and retained in the lineage leading to the bryopsids.
- ❖ The presence of the perispore in all Rhyniopsida is conjectural, which is also the case for the Cladoxylopsida and the Zosterophyllopsida. For the Trimerophytopsida and the Progymnospermopsida, only one genus respectively was found to possess a perispore. There is not enough evidence to assume that the perispore is a consistent feature in the Trimerophytopsida and the Progymnospermopsida.
- ❖ As addressed by the review chapter, the documentation of perisporal envelopes surrounding cryptospores might constitute the first occurrence of the perispore, dating back as far as the Ordovician.
- ❖ Peripheral layers, as in *Cooksonia* and *Uskiella*, were previously considered as perispore-like. They might be an ancestral feature that was lost in certain plant groups but retained in the basal Upper Devonian species *Rhacophyton ceratangium* in the form of a true perispore.

8.2 Functions and Chemistry

- ❖ The perispore shares many common features and functions with the cuticle. Both outer layers are the physical boundary between the spore/plant and the environment. Aspects such as ultrastructure, chemical composition and function are comparable and lead to the conclusion that the perispore is an important, protective outer layer for lower embryophyte spores.
- ❖ The function of silica in at least some lower embryophyte spore walls is likely to add to mechanical stability, either in the form of a discrete layer or as an integral part of the sporopollenin macromolecule. No correlation between the occurrence of silica and phylogenetic relationships, ecology or habitat could be established; hence silica incorporation into spore walls is probably the result of metabolic activity, derived from silica in the soil. It is suggested that the integration of silica into spore walls has evolved independently in different lower embryophyte lineages. A separate study revealed that there is no obvious distribution pattern for the occurrence of nutrient elements or silica in selected pteridophyte fronds. No apparent link between the occurrence of silica in fronds and spores was found.
- ❖ Evidence from the literature and comparisons with the plant cuticle, made herein, support the view that phenolic compounds such as sporopollenin or flavonoids contribute to the stability and defence mechanisms of the spore. The role of phenolic compounds in spores has not yet been studied comprehensively enough to allow definite conclusions.
- ❖ The chemical and crystalline nature of cubes occurring on *Selaginella myosurus* Sw. Alston megaspores and the inner wall of their sporangia remains enigmatic. Neither partial chemical analyses nor diffractometry match any records of minerals described so far. The interpretation of some of this work is still ongoing. It is hypothesised that this is not only

a new mineral but also an unknown bio-mineralization process occurring in plants. The function and formation process of these structures on the megaspores remains unsolved but the possibilities have been explored with the following conclusions:

- The occurrence of cubic crystals in this genus might be species specific for *Selaginella myosurus* Sw. Alston and it is thought that these crystals do not have any particular function. They are presumably the result of incorporation of excessive silica into the sporangium and the megaspore walls.
 - It is proposed that the crystals precipitate in two, probably separate processes, shortly before dehiscence and drying of the sporangium. The first precipitation occurs from within the silica enriched exospore, giving rise to crystals underneath the ridges. In a secondary process, slightly bigger crystals form on the inner wall of the sporangium and also on the ridges of the megaspores. The precipitation is initiated by the drying of the sporangium shortly before its dehiscence and can be explained with a silica saturated sporangial fluid, which is larger in volume than what can be precipitated from the exospore.
 - The cubic habit and deviation from pure SiO_2 composition suggest a loose silica framework structure stabilised by additional elements. Substantial carbon but lack of cationic species indicates a clathrate rather than a zeolite.
- ❖ Plasticizer contamination in GC-MS and ^1H NMR analyses of pollen and spores was documented not only in this study but also in those of others. From comparisons between this study and published material it is evident that some of the contaminants are plasticizers such as BHT and 1,2 benzenedicarboxylic acid. Although no new compounds could be described from an analysis of *Pinus sylvestris* pollen and *Selaginella pallescens* megaspores, the results presented herein contribute to a better and more careful interpretation of data obtained from analytical chemistry. It was shown that standard analytical

chemistry techniques such as NMR and GC-MS can only generate reliable and interpretable data, if much higher quantities of starting material (> 1g) are used. MALDI-ToF MS has achieved fragmentation of the intact sporopollenin macromolecule, releasing fractions of the polymer. Fragments are thought to arise from complex arrangements possibly between different subunits or between subunits representing *p*-coumaric acid and co-complexing moieties of differing mass. It is believed that the insolubility of the "intact" molecule currently limits its entire isolation and that solid state MALDI is more suitable for the analysis of the already obtained fragments. It has been shown that this relatively new technique of MALDI-ToF MS is potentially useful for sporopollenin research.

- ❖ Comparisons of Lower Devonian spore clusters, extant immature *Osmunda regalis* L. spores and spore wall mimics have provided insights into the development and formation of certain fossil spores. This study has shown that it is possible to favourably compare spore wall mimics to immature fossil *in situ* spores, implying that self-assembly mechanisms probably date back to the Palaeozoic.

8.3 Non specific conclusions

- ❖ Although the view that the perispore is of tapetal origin is commonly accepted, it should also be considered that it might be the last vestige of exospore production and can sometimes be indistinguishable from tapetal origin.
- ❖ Spore wall terminology with respect to the outer wall layers, is inconsistent, especially for *Selaginella* and *Isoetes* megaspores and is in need of a thorough revision, including developmental aspects. The discrepancy lies in the naming and origin of the silica coating. To date this coating is not considered to be a perispore by the majority in this field of study, no matter whether it is a discrete layer or interconnected

with the outer part of the exospore. Although there is no evidence, owing to lack of studies, that this siliceous coating is derived from the tapetum, I would nonetheless call it a perispore, assuming that the source of this material might well be tapetal.

- ❖ For over 50 years palynologists have carried out pollen and spore analysis, utilising harsh treatments with strong acids, bases or solvents. Few authors have studied this problem previously but their calls for more comprehensive research have not yet been sufficiently addressed. Unless this issue is resolved in a comprehensive study, many might risk misinterpreting spore wall layers, simply by the loss of precious morphological and ultrastructural information.

- Adams M, Dogic Z, Keller SL, and Fraden S. 1998.** Entropically driven microphase transitions in mixtures of colloidal rods and spheres. *Nature* **393**: 349-352.
- Ahlers F, Bubert H, Steuernagel S, and Wiermann R. 2000.** The nature of oxygen in sporopollenin from the pollen of *Typha angustifolia* L. *Verlag der Zeitschrift für Naturforschung* **55**: 129-136.
- Ahlers F, Lambert J, and Wiermann R. 1999a.** Structural elements of sporopollenin from pollen of *Toreya californica* Torr. (Gymnospermae): using the ¹H-NMR technique. *Verlag der Zeitschrift für Naturforschung* **54**: 492-495.
- Ahlers F, Lambert J, and Wiermann R. 2003.** Acetylation and silylation of piperidine solubilized sporopollenin from pollen of *Typha angustifolia* L. *Verlag der Zeitschrift für Naturforschung*. **58**: 807-811.
- Ahlers F, Thom I, Lambert J, Kuckuk R, and Wiermann R. 1999b.** ¹H NMR analysis of sporopollenin from *Typha angustifolia*. *Phytochemistry* **50**: 1095-1098.
- Andrews HN, and Phillips TL. 1968.** *Rhacophyton* from the Upper Devonian of West Virginia. *Journal of the Linnean Society (Botanical)* **61**: 37-64.
- Archangelsky A, Phipps CJ, Taylor TN, and Taylor EL. 1999.** *Paleoazolla*, a new heterosporous fern from the Upper Cretaceous of Argentina. *American Journal of Botany* **86**: 1200-1206.
- Baker RP, Hasenstein KH, and Zavada ML. 1994.** Self-incompatibility in *Theobroma cacao*: Hormonal changes associated with the incompatibility response. In: Stephenson AG and Kao TH, eds. *Pollen-Pistil Interactions and pollen tube growth*: American Society of Plant Physiologists. 273-275.
- Balick MJ, and Beitel JM. 1988.** *Lycopodium* spores found in condom dusting agent. *Nature* **332**: 591.
- Balme BE. 1995.** Fossil *in situ* spores and pollen grains: an annotated catalogue. *Review of Palaeobotany and Palynology* **87**: 81-323.
- Banks HP. 1968.** The early history of land plants. In: Drake ET. ed. *Evolution and Environment*. New Haven, Yale University Academic Press. 73-107.
- Barnes SH, and Blackmore S. 1986.** Some functional features in pollen development. In: Blackmore S and Ferguson IK, eds. *Pollen and Spores: Form and Function*. London, Academic Press. 71-80.

- Bateman RM, and DiMichele WA. 1994.** Heterospory: the most iterative key innovation in the evolutionary history of the plant kingdom. *Biological Review* **69**: 345-417.
- Batten DJ, and Collinson ME. 2001.** Revision of species of *Minerisporites*, *Azolla* and associated plant microfossils from deposits of the Upper Palaeocene and Palaeocene/Eocene transition in the Netherlands, Belgium and the USA. *Review of Palaeobotany and Palynology* **115**: 1-32.
- Batten DJ, Collinson ME, and Brain APR. 1998.** Ultrastructural interpretation of the late Cretaceous megaspore *Glomerisporites pupus* and its associated microspores. *American Journal of Botany* **85**: 724-735.
- Batley MH, and Pring A. 1997.** *Mineralogy for students*. Addison Wesley Longman Higher Education, Harlow. 809.
- Bayliss P, Erd DC, Mrose ME, Sabina AP, and Smith DK. 1986a.** *Mineral Powder Diffraction File: Search Manual*. International Centre for Diffraction, Swarthmore, PA, USA.
- Bayliss P, Erd DC, Mrose ME, Sabina AP, and Smith DK. 1986b.** *Mineral Powder Diffraction File: Data Book*. International Centre for Diffraction, Swarthmore, PA, USA.
- Beck CB, and White DC. 1988.** Progymnosperms. In: Beck CB. ed. *Origin and evolution of gymnosperms*. New York, Columbia University Press. 1-84.
- Bedinger P. 1992.** The remarkable biology of pollen. *Plant Cell* **4**: 879-887.
- Bek J, and Opustil S. 1998.** Some lycopsid, sphenopsid and pteropsid frutifications and their microspores from the Upper Carboniferous basins of the Bohemian Massif. *Palaeontographica Abt. B* **248**: 127-161.
- Bell PR, and Hemsley AR. 2000.** *Green Plants: their origin and diversity*. Cambridge, Cambridge University Press. 349.
- Berry CM, and Edwards D. 1996.** *Anapaulia moodyi* gen. et sp. nov.: a probable iridopteridalean compression fossil from the Devonian of western Venezuela. *Review of Palaeobotany and Palynology* **93**: 127-145.
- Biermann CJ. 1996.** *Handbook of Pulping and Papermaking*. London, Academic Press. 782.
- Blackmore S, and Barnes SH. 1986.** Harmomegathic mechanisms in pollen grains. In: Blackmore S and Ferguson IK, eds. *Pollen and Spores: Form and Function*. London: Academic Press. 137-149.

- Blackmore S, and Barnes SH. 1987.** Embryophyte spore walls: origin, development, and homologies. *Cladistics* **3**: 185-195.
- Bonamo PM, and Banks HP. 1966.** *Calamophyton* in the middle Devonian of New York State. *American Journal of Botany* **53**: 778-791.
- Bower FO. 1923.** *The Ferns (Filicales). Treated comparatively with a view to their natural classification*, Volume I, Analytical Examination of the Criteria of Comparison. Cambridge University Press, Cambridge. 359.
- Bower FO. 1935.** *Primitive land plants*. Macmillan & Co. Ltd., London. 658.
- Brooks J, and Shaw G. 1968.** Chemical structure of the exine of pollen walls and a new function for carotenoids in nature. *Nature* **219**: 532-533.
- Brown RC, and Lemmon BE. 1984.** Ultrastructure and sporogenesis in the moss *Amblystegium riparium*. II. Spore wall development. *Journal of Hattori Botanical Laboratory* **57**: 139-152.
- Brown RC, and Lemmon BE. 1985.** Phylogenetic aspects of sporogenesis in *Archidium*. *Monographs of Systematic Botany of the Missouri Botanical Garden* **11**: 25-39.
- Brown RC, and Lemmon BE. 1990.** Sporogenesis in Bryophytes. In: Blackmore S and Knox RB, eds. *Microspores: evolution and ontogeny*. London, Academic Press. 55-93.
- Brown RC, Lemmon BE, and Carothers ZB. 1982.** Spore wall ultrastructure of *Sphagnum lescurii* Sull. *Review of Palaeobotany and Palynology* **38**: 99-107.
- Buchen B, and Sievers A. 1981.** Sporogenesis and pollen grain formation. In: Kiermayer O, ed. *Cytomorphogenesis in plants*. Wien, Springer Verlag. 349-376.
- Buck WR, and Goffinet B. 2000.** Morphology and classification of mosses. In: Shaw AJ and Goffinet B, eds. *Bryophyte Biology*. Cambridge: Cambridge University Press. 71-123.
- Calderón S, Carrasco E, Gómez B, Llergo Y, and Ubera JL. 2004.** Pollen grains transformations after several extraction treatments. XI IPC. Granada: Argos Impresores, **36**. Conference abstract.
- Cernik RJ, Clegg W, Catlow CRA, Bushnell-Wye G, Flaherty JV, Greaves GN, Burrows I, Taylor DJ, Teat SJ, and Hamichi M. 2000.** A new high-flux chemical and materials crystallography station at the SRS Daresbury. 1. Design, construction and test results. Corrigendum. *Journal of Synchrotron Radiation* **7**: 40.

- Charman DJ. 1992.** The effects of acetylation on fossil *Pinus* pollen and *Sphagnum* spores discovered during routine pollen analysis. *Review of Palaeobotany and Palynology* **72**: 159-164.
- Chassot C, and Métraux J-P. 2005.** The cuticle as source of signals for plant defense. *Plant Biosystems* **139**: 28-31.
- Chatti I, Delahaye A, Fournaison L, and Petitet J-P. 2005.** Benefits and drawbacks of clathrate hydrates: a review of their areas of interest. *Energy Conversion and Management* **46**: 1333-1343.
- Chen CH, and Lewin JC. 1969.** Silicon as a nutrient element for *Equisetum arvense*. *Canadian Journal of Botany* **47**: 125-131.
- Coates J. 2000.** Interpretation of Infrared Spectra, A Practical Approach. In: Meyers RA, ed. *Encyclopaedia of Analytical Chemistry*. Chichester: John Wiley and Sons Ltd. 10815-10837.
- Collinson ME, Hemsley AR, and Taylor WA. 1993.** Sporopollenin exhibiting colloidal organization in spore walls. *Grana Suppl.* **1**: 31-39.
- Collinson ME, Kvacek Z, and Zastawniak E. 2001.** The aquatic plants *Salvinia* (Salviniales) and *Limnobiophyllum* (Arales) from the Late Miocene flora of Sosnica (Poland). *Acta Palaeobotanica* **41**: 253-282.
- Cooper-Driver G. 2001.** Biological roles for phenolic compounds in the evolution of early land plants. In: Gensel PG and Edwards D, eds. *Plants invade the land, evolutionary and environmental perspectives*. New York: Columbia University Press. 159-172.
- Cox CJ, Goffinet B, Newton AE, Shaw AJ, and Hedderson TAJ. 2000.** Phylogenetic relationships among the diplolepideous-alternate mosses (Bryidae) inferred from nuclear and chloroplast DNA sequences. *The Bryologist* **103**: 224-241.
- Crandall-Stotler B, and Stotler RE. 2000.** Morphology and classification of the Marchantiophyta. In: Shaw AJ and Goffinet B, eds. *Bryophyte Biology*. Cambridge: Cambridge University Press. 21-70.
- Crane PR. 1990.** The phylogenetic context of microsporogenesis. In: Blackmore S and Knox RB, eds. *Microspores: evolution and ontogeny*. London, Academic Press Inc. 11-41.
- Crang RE, and May G. 1974.** Evidence for silicon as a prevalent elemental component in pollen wall structure. *Canadian Journal of Botany* **52**: 2171-2174.
- Crum HA. 2001.** *Structural diversity of bryophytes*. Michigan, The University of Michigan Herbarium. 379.

- Cullmann F, and Becker H. 1998.** Terpenoid and phenolic constituents of sporophytes and spores from the liverwort *Pellia epiphylla*. *Journal of Hattori Botanical Laboratory* **84**: 285-295.
- de Leeuw JW, van Bergen PF, van Aarssen BGK, Gatellier J-PLA, Sinninghe Damste JS, and Collinson ME. 1991.** Resistant biomacromolecules as major contributors to kerogen. *Philosophical Transactions of the Royal Society London B.* **333**: 329-337.
- de Leeuw JW, and Largeau C. 1993.** A review of the major classes of organic compounds that comprise living organisms and the pathways for their incorporation into sediments. In: Engel MH and Macko S, eds. *Organic Chemistry*. New York: Plenum Publishing Group. 23-72.
- de Leeuw JW, Versteegh GJM, van Mourik A, Warnaar J, Dammers N, Blokker P, Brinkhuis H, and van Bergen PF. 2004.** Macromolecules in modern and fossil spores, pollen and algae. XI IPC. Granada: Argos Impresores, **36**. Conference abstract.
- Dengler NG, and Lin EY-C. 1980.** Electron microprobe analysis of the distribution of silicon in the leaves of *Selaginella emmeliana*. *Canadian Journal of Botany* **58**: 2459-2466.
- Dettmann ME. 1961.** Lower Mesozoic megaspores from Tasmania and South Australia. *Micropaleontology* **7**: 71-86.
- Devi S. 1980.** The concept of perispore - an assessment. *Grana* **19**: 159-172.
- Dominguez E, Mercado JA, Quesada MA, and Heredia A. 1999.** Pollen sporopollenin: degradation and structural elucidation. *Sexual Plant Reproduction* **12**: 171-178.
- Dong X, Hong Z, Sivaramakrishnan M, Mahfouz M, and Verma DPS. 2005.** Callose synthase (CalS5) is required for exine formation during microgametogenesis and for pollen viability in *Arabidopsis*. *The Plant Journal* **42**: 315-328.
- Edman G. 1932.** Verkieselung und Verholzung der Sporenmembran bei *Lygodium japonicum* Sw. *Svensk Botanisk Tidskrift* **26**: 313-326.
- Edwards D. 1996.** New insights into early land ecosystems: a glimpse of a Lilliputian world. *Review of Palaeobotany and Palynology* **90**: 159-174.
- Edwards D, Abbott GD, and Raven AJ. 1996.** Cuticles and early land plants: a palaeoecophysiological evaluation. In: Kerstiens G, ed. *Plant cuticles: an integrated functional approach*. Herndon: β IOS Scientific Publishers Limited. 1-31.
- Edwards D, Axe L, and Mendez E. 2001.** A new genus for isolated bivalved sporangia with thickened margins from the Lower Devonian of the

Welsh Borderland. *Biological Journal of the Linnean Society* **137**: 297-310.

- Edwards D, Fanning U, Davies KL, Axe L, and Richardson JB. 1995a.** Exceptional preservation in Lower Devonian coalified fossils from the Welsh borderland - a new genus based on reniform sporangia lacking thickened borders. *Botanical Journal of the Linnean Society* **117**: 233-254.
- Edwards D, Selden PA, Richardson JB, and Axe L. 1995b.** Coprolites as evidence for plant-animal interaction in Siluro-Devonian terrestrial ecosystems. *Nature*. **377**: 329-331.
- Edwards D, Davies KJ, Richardson JB, and Axe L. 1995c.** The ultrastructure of spores of *Cooksonia pertoni*. *Palaeontology* **38**: 153-168.
- Epstein E. 1999.** Silicon. *Annual Review of Plant Physiology and Plant Molecular Biology* **50**: 641-664.
- Erdtman G. 1943.** *An introduction to pollen analysis*. Waltham, Mass., Chronica Botanica. 239.
- Erdtman G. 1952.** *An introduction to palynology 1, Pollen morphology and plant taxonomy: angiosperms*. Almqvist & Wiksell, Stockholm. 539.
- Estébanz B, Alfayate C, and Ron E. 1997.** Observations on spore ultrastructure in six species of *Grimmia* (Bryopsida). *Grana* **36**: 347-357.
- Etzler ME. 1985.** Plant lectins: molecular and biological aspects. *Annual Review of Plant Physiology* **36**: 209-34.
- Everett DH. 1988.** *Basic principles of colloid science*. London, The Royal Society of Chemistry. 243.
- Exley C. 1998.** Silicon in life: A bioinorganic solution to bioorganic essentiality. *Journal of Inorganic Biochemistry* **69**: 139-144.
- Fabbri F, and Menicanti F. 1970.** Electron microscope observations on intranuclear paracrystals in some pteridophyta. *Caryologia* **23(4)**: 729-761.
- Fauth M, Schweizer P, Buchala A, Markstadter C, Riederer M, Kato T, and Kauss H. 1998.** Cutin monomers and surface wax constituents elicit H₂O₂ in Conditioned Cucumber Hypocotyl Segments and enhance the Activity of Other H₂O₂ Elicitors. *Plant Physiology* **117**: 1373-1380.
- Friis EM. 1977.** EM-studies on *Salviniaceae* megaspores from the Middle Miocene Fåsterholt Flora, Denmark. *Grana* **16**: 113-128.

- Gabarayeva NI, and Grigorjeva VV. 2002.** Exine development in *Stangeria eriopus* (Stangeriaceae): ultrastructure and substructure, sporopollenin accumulation, the equivocal character of the aperture, and stereology of microspore organelles. *Review of Palaeobotany and Palynology* **122**: 185-218.
- Gabarayeva NI, and Grigorjeva VV. 2004.** Exine development in *Encephalartos altensteinii* (Cycadaceae): ultrastructure, substructure and the modes of sporopollenin accumulation. *Review of Palaeobotany and Palynology* **132**: 175-193.
- Gabarayeva NI, and Hemsley AR. in press.** Merging concepts: the role of self-assembly in the development of pollen wall structure. *Review of Palaeobotany and Palynology*.
- Galtier J. 2004.** A new zygopterid fern from the Early Carboniferous of France and a reconsideration of the *Corynepteris-Alloiopteris* ferns. *Review of Palaeobotany and Palynology* **128**: 195-217.
- Gambardella R, Duckett JG, Alfano F, Gargiulo M, and Squillaciotti C. 1993a.** Studies on the sporogenous lineage in the moss *Timmiella barbulooides*. VII. The microtubule arrays at meiosis. *Botanica Acta* **106**: 350-355.
- Gambardella R, Alfano F, Gargiulo M, and Squillaciotti C. 1993b.** Studies on the sporogenous lineage in the moss *Timmiella barbulooides*. VIII. Sporoderm development. *Botanica Acta* **106**: 356-363.
- Gambardella R, Alfano F, Gargiulo M, and Squillaciotti C. 1994.** Studies on the sporogenous lineage in the moss *Timmiella barbulooides* IX. Development of the taptum. *Annals of Botany* **73**: 369-375.
- Gastony GJ. 1974.** Spore morphology in the *Cyatheaceae*. I. The perine and sporangial capacity: General observations. *American Journal of Botany* **61**: 672-680.
- Gensel PG. 1980.** A new species of *Zosterophyllum* from the Early Devonian of New Brunswick. *American Journal of Botany* **69**: 651-669.
- Gensel PG, and White AR. 1983.** The morphology and ultrastructure of spores of the Early Devonian Trimerophyte *Psilophyton* (Dawson) Hueber & Banks. *Palynology* **7**: 221-233.
- Gerrienne P. 1992.** The Emsian plants from Fooz-Wepion (Belgium). III. *Foozia minuta* gen. et spec. nov., a new taxon with probable cladoxylalean affinities. *Review of Palaeobotany and Palynology* **74**: 139-157.
- Glasspool IJ. 2003.** A review of Permian Godwana megaspores, with particular emphasis on material collected from coals of the Witbank

Basin of South Africa and the Sydney Basin of Australia. *Review of Palaeobotany and Palynology* **124**: 227-296.

Goffinet B, Cox CJ, Shaw AJ, and Hedderson TAJ. 2001. The Bryophyta (Mosses): Systematic and Evolutionary Inferences from an *rps4* Gene (*cpDNA*) Phylogeny. *Annals of Botany* **87**: 191-208.

Goldstein IJ, Hughes RC, Monsigny M, Osawa T, and Sharon N. 1980. What should be called a lectin? *Nature* **285**: 66.

Gould KS, and Lee DW. 1996. Physical and ultrastructural basis of blue leaf iridescence in four malaysian understory plants. *American Journal of Botany* **83**: 45-50.

Graham L, Kodner RB, Fisher MM, Graham JM, Wilcox LW, Hackney JO, Bilkey PC, Hanson DT, and Cook ME. 2004. Early land plant adaptations to terrestrial stress: a focus on phenolics. In: Hemsley AR and Poole I, eds. *The evolution of plant physiology*. Amsterdam: Elsevier. 492.

Graham RM, Lee DW, and Norstog K. 1993. Physical and ultrastructural basis of blue leaf iridescence in two neotropical ferns. *American Journal of Botany*. **80**: 198-203.

Gray J. 1985. The microfossil record of early land plants: advances in understanding of early terrestrialization, 1970-1987. *Philosophical Transactions of the Royal Society London B*. **309**: 167-195.

Griffiths PC, Wellappili C, Hemsley AR, and Stephens R. 2004. Ultra-porous hollow particles. *Colloid Polymer Science* **282**: 1155-1159.

Gross J, and Strupat K. 1998. Matrix-assisted laser desorption/ionisation-mass spectrometry applied to biological macromolecules. *Trends in Analytical Chemistry* **17**: 470-484.

Guilford WJ, Schneider DM, Labovitz J, and Opella SJ. 1988. High resolution solid state ¹³C NMR spectroscopy of sporopollenins from different plant taxa. *Plant Physiology* **86**: 134-136.

Habgood KS. 2000. Two cryptospore-bearing land plants from the Lower Devonian (Lochkovian) of the Welsh Borderland. *Botanical Journal of the Linnean Society* **133**: 203-227.

Hall JW. 1975. *Ariadnaesporites* and *Glomerisporites* in the Late Cretaceous: ancestral Salviniaceae. *American Journal of Botany* **62**: 359-369.

Hall JW, and Bergad RD. 1971. A critical study of three Cretaceous salviniaaceous megaspores. *Micropaleontology* **17**: 345-356.

- Hammond SE. 2004.** *Progymnosperms and the origin of the seed*. Thesis for the degree of PhD. School of Earth, Ocean and Planetary Sciences. Cardiff, Cardiff University. 480 (unpublished).
- Hannig E. 1911.** Über das Vorkommen von Perisporien bei den Filicinen nebst Bemerkungen über die systematische Bedeutung derselben. *Flora (Jena)* **103**: 321-346.
- Hänsel R, and Hölzl J. 1996.** *Lehrbuch der pharmazeutischen Biologie*. Berlin, Springer. 545.
- Havinga AJ. 1964.** Investigation into the differential corrosion susceptibility of pollen and spores. *Pollen et Spores* **6**: 621-635.
- Héban C, and Lee DW. 1984.** Ultrastructural basis and developmental control of blue iridescence in *Selaginella* leaves. *American Journal of Botany* **71**: 216-219.
- Hemsley AR. 1989.** The ultrastructure of the spore wall of the Triassic bryophyte *Naiadita lanceolata*. *Review of Palaeobotany and Palynology* **61**: 89-99.
- Hemsley AR. 1990.** *The ultrastructure of fossil spore exines*. Thesis for the degree of PhD. Departments of Biology and Geology. London, Royal Holloway and Bedford College University of London. 324 (unpublished).
- Hemsley AR. 1994.** The origin of the land plant sporophyte: an interpolational scenario. *Biological Reviews* **69**: 263-273.
- Hemsley AR. 1997.** Teratisms in living and fossil megaspores of the Lycopsidea: tetrad arrangement and exine ontogeny. *Botanical Journal of the Linnean Society* **125**: 1-24.
- Hemsley AR, Collinson ME, and Brain APR. 1992.** Colloidal crystal-like structure of sporopollenin in the megaspore walls of recent *Selaginella* and similar fossil spores. *Botanical Journal of the Linnean Society* **108**: 307-320.
- Hemsley AR, Barrie PJ, Chaloner WG, and Scott AC. 1993.** The composition of sporopollenin and its use in living and fossil plant systematics. *Grana Supp.* **1**: 2-11.
- Hemsley AR, Collinson ME, Kovach WL, Vincent B, and Williams T. 1994.** The role of self-assembly in biological systems: evidence from iridescent colloidal sporopollenin in *Selaginella* megaspore walls. *Philosophical Transactions of the Royal Society London B* **345**: 163-173.

- Hemsley AR, Scott AC, Barrie PJ, and Chaloner WG. 1996.** Studies of fossil and modern spores wall biomacromolecules using ^{13}C solid state NMR. *Annals of Botany* **78**: 83-94.
- Hemsley AR, Vincent B, Collinson ME, and Griffiths PC. 1998.** Simulated self-assembly of spore exines. *Annals of Botany* **82**: 105-109.
- Hemsley AR, Collinson ME, Vincent B, Griffiths PC, and Jenkins PD. 2000.** Self-assembly of colloidal units in exine development. In: Harley MM, Morton CM and Blackmore S, eds. *Pollen et Spores: Morphology and Biology*. Kew, The Royal Botanic Garden. 31-44.
- Hemsley AR, and Griffiths PC. 2000.** Architecture in the microcosm: biocolloids, self-assembly and pattern formation. *Philosophical Transactions of the Royal Society London A* **358**: 547-564.
- Hemsley AR, Griffiths PC, Mathias R, and Moore SEM. 2003.** A model for the role of surfactants in the assembly of exine sculpture. *Grana* **42**: 38-42.
- Hemsley AR, Lewis J, and Griffiths PC. 2004.** Soft and sticky development: some underlying reasons for microarchitectural pattern convergence. *Review of Palaeobotany and Palynology* **130**: 105-119.
- Herminghaus S, Gubatz S, Arendt S, and Wiermann R. 1988.** The occurrence of phenols as degradation products of natural sporopollenin - a comparison with "synthetic sporopollenin". *Verlag der Zeitschrift für Naturforschung*. **43c**: 491-500.
- Heslop-Harrison J. 1972.** Pattern in plant cell walls: morphogenesis in miniature. *Proceedings of the Royal Institution of Great Britain* **45**: 335-352.
- Heslop-Harrison J, and Dickinson HG. 1969.** Time relationships of sporopollenin synthesis associated with tapetum and microspores in *Lilium*. *Planta* **84**: 199-214.
- Higson S. 2003.** *Analytical chemistry*. Oxford, Oxford University Press. 434.
- Hodson MJ, and Evans DE. 1995.** Aluminium-Silicon Interactions in Higher-Plants. *Journal of Experimental Botany* **46**: 161-171.
- Hodson MJ, and Sangster AG. 2002.** X-ray microanalytical studies of mineral localization in the needles of white pine (*Pinus strobus* L.). *Annals of Botany* **89**: 367-374.
- Höhne H, and Richter B. 1981.** Untersuchungen über den Mineralstoff- und Stickstoffgehalt von Frankräutern. *Flora (Jena)* **171**: 1-10.

- Hollósý F. 2002.** Effects of ultraviolet radiation on plant cells. *Micron* **33**: 179-197.
- Jackson BD. 1928.** *A glossary of botanical terms with their derivation and accent.* Duckworth, London. 481.
- Jarvis LR. 1974.** Electron microscope observations of spore wall development in *Funaria hygrometrica*. *Proceedings of Eighth Congress on Electron Microscopy, Canberra* **2**: 620-621.
- Jeffree CE. 1996.** Structure and ontogeny of plant cuticles. In: Kerstiens G, ed. *Plant cuticles: an integrated functional approach.* Herndon: β IOS Scientific Publishers Limited. 337.
- Kaufman PB, W.C. Bigelow, Schmid R, and Ghosheh NS. 1971.** Electron microprobe analysis of silica in epidermal cells of *Equisetum*. *American Journal of Botany* **38**: 309-316.
- Kaufmann R. 1995.** Matrix-assisted laser desorption ionization (MALDI) mass spectrometry: a novel analytical tool in molecular biology and biotechnology. *Journal of Biotechnology* **41**: 155-175.
- Kawase M, and Takahashi M. 1996.** Gas chromatography-mass spectrometric analysis of oxidative degradation products of sporopollenin in *Magnolia grandiflora* (Magnoliaceae) and *Hibiscus syriacus* (Malvaceae). *Journal of Plant Research* **109**: 297-299.
- Kealey D, and Haines PJ. 2002.** *Instant Notes: Analytical Chemistry.* Oxford, β IOS Scientific Publishers Ltd. 342.
- Kempf EK. 1970.** Elektronenmikroskopie der Sporodermis von Megasporen der Gattung *Selaginella* (Pteridophyta). *Review of Palaeobotany and Palynology* **10**: 99-116.
- Kempf EK. 1971a.** Elektronenmikroskopie der Sporodermis von Mega- und Mikrosporen der Pteridophyten-Gattung *Salvinia* aus dem Tertiär und Quartär Deutschlands. *Palaeontographica Abt. B* **136**: 47-70.
- Kempf EK. 1971b.** Electron microscopy of Mesozoic megaspores from Denmark. *Grana* **11**: 151-163.
- Kenrick P. 2000.** The relationships of vascular plants. *Philosophical Transactions of the Royal Society London B.* **355**: 847-855.
- Kenrick P, and Crane PR. 1997.** *The origin and early diversification of land plants.* Washington, Smithsonian Institution. 441.
- Koch K, Neinhuis C, Ensikat H-J, and Barthlott W. 2004.** Self assembly of epicuticular waxes on living plant surfaces imaged by atomic force microscopy (AFM). *Journal of Experimental Botany* **55**: 711-718.

- Kolesov BA, and Geiger CA. 2003.** Molecules in the SiO₂-clathrate melanophlogite: a single crystal Raman study. *American Mineralogist* **88**: 1364-1368.
- Kramer KU, Schneller JJ, and Wollenwber E. 1995.** *Farne und Farnverwandte*. Stuttgart, Thieme. 189.
- Kremp GOW. 1965.** *Morphologic Encyclopedia of Palynology*. Tuscon, The University of Arizona Press. 263.
- Kress WJ. 1986.** The use of ethanolamine in the study of pollen wall stratification. *Grana* **25**: 31-40.
- Kurmann MH, and Taylor TN. 1984.** Comparative ultrastructure of the sphenophte spores *Elaterrites* and *Equisetum*. *Grana* **23**: 109-116.
- Kurmann MH, and Taylor TN. 1987.** Sporoderm ultrastructure of *Lophosoria* and *Cytheacidites* (*Filicopsida*): systematic and evolutionary implications. *Plant Systematics and Evolution* **157**: 85-94.
- Lee DW. 1997.** Iridescent blue plants. *American Scientist* **85**: 56-63.
- Lee DW, and Lowry JB. 1975.** Physical basis and ecological significance of iridescence in blue plants. *Nature* **254**: 50-51.
- Linder H. 1992.** *Linder Biologie*. Hannover, J.B. Metzlersche Verlagsbuchandlung und Carl Ernst Poeschel Verlag GmbH. 528.
- Lis H, and Sharon N. 1973.** The biochemistry of plant lectins (phytohemagglutinins). *Annual Review of Biochemistry* **42**: 541-574.
- Loewus FA, Baldi BG, Franceschi VR, Meinert LD, and McCollum JJ. 1985.** Pollen sporoplasts: dissolution of pollen walls. *Plant Physiology* **78**: 652-654.
- Lovering TS, and Engel C. 1967.** Translocation of silica and other elements from rock into *Equisetum* and three grasses. *US Geol. Surv. Prof. Paper* **594**: 1-16.
- Lugardon B. 1969.** Sur la structure fine des parois sporales D'*Equisetum maximum* Lamk. *Pollen et Spores* **11**: 449-474.
- Lugardon B. 1972.** La structure fine des l'exospore et de la périspore des Filicinées isosporées I. Généralités. Eursporangiées et Osmundales. *Pollen et Spores* **14**: 227-261.
- Lugardon B. 1978.** Comparison between pollen and Pteridophyte spore walls. *IV. International Palynological Conference*. Lucknow. **1**: 199-206.

- Lugardon, B. 1979.** Sur la formation du sporoderme chez *Psilotum triquetrum* Sw. (Psilotaceae). *Grana* **18**: 145-165.
- Lugardon B. 1981.** Les globules des Filicinées, homologues des corps d'Ubisch des Spermaphytes. *Pollen et Spores* **23**: 93-124.
- Lugardon B. 1990.** Pteridophyte sporogenesis: a survey of spore wall ontogeny and fine structure in a polyphyletic plant group. In: Blackmore S and Knox RB, eds. *Microspores: evolution and ontogeny*. London, Academic Press Inc. 95-120.
- Luizi-Ponzo AP, and Barth OM. 1998.** Spore morphology of some Bruchiaceae species (Bryophyta) from Brazil. *Grana* **37**: 222-227.
- Lynn DG, and Chang M. 1990.** Phenolic signals in cohabitation: implications for plant development. *Annual Review of Plant Physiology and Plant Molecular Biology* **41**: 497-526.
- Macluf CC, Morbelli MA, and Giudice GE. 2003.** Morphology and ultrastructure of megaspores and microspores of *Isoetes savatieri* Franchet (Lycophyta). *Review of Palaeobotany and Palynology* **126**: 197-209.
- Mann S, Perry CC, Williams RJP, Fyfe CA, Gobbi GC, and Kennedy GJ. 1983.** The characterisation of the nature of silica in biological systems. *Journal of the Chemical Society, Chemical Communications* **4**: 168-170.
- Marschner H. 1995.** *Mineral nutrition of higher plants*. London, Academic Press. 889.
- Martin FW. 1959.** Staining and observing pollen tubes in the style by means of fluorescence. *Staining Technology* **34**: 125-128.
- Mellor RB, Gadd GM, Rowell P, and Stewart WDP. 1981.** A phytohaemagglutinin from the *Azolla-anabaena* symbiosis. *Biochemical and Biophysical Research Communications* **99**: 1348-1353.
- Millay MA, and Taylor TN. 1982.** The ultrastructure of Palaeozoic fern spores: 1. *Botryopteris*. *American Journal of Botany* **69**: 1148-1155.
- Millay MA, and Taylor TN. 1984.** The ultrastructure of Paleozoic fern spores: II. *Scolecoteris* (Marattiales). *Palaeontographica Abt. B* **194**: 1-13.
- Minaki M. 1984.** Macrospore morphology and taxonomy of *Selaginella* (Selaginellaceae). *Pollen et Spores* **24**: 421-480.
- Moore SEM. 2001.** *Self-assembly of Selaginella megaspore walls: correlation of exine morphology and ultrastructure*. Bonn, Botanisches Institut und Botanischer Garten. 86. (unpublished thesis)

- Moore SEM, Hemsley AR, and Borsch T. in press a.** Micro-morphology of outer exospore coatings in *Selaginella* megaspores. *Grana*.
- Moore SEM, Hemsley AR, French AN, Dudley E, and Newton RP. in press b.** New insights from MALDI-ToF MS, NMR and GC-MS: mass spectrometry techniques applied to palynology. *Protoplasma*.
- Moran RC. 2004.** *A natural history of ferns*. Portland, Timber Press. 301.
- Morbelli MA. 1995.** Megaspore wall in Lycophyta-ultrastructure and function. *Review of Palaeobotany and Palynology* **85**: 1-12.
- Morbelli MA, and Rowley JR. 1993.** Megaspore development in *Selaginella*. I. "Wicks", their presence, ultrastructure and presumed function. *Sexual Plant Reproduction* **6**: 98-107.
- Morbelli MA, and Rowley JR. 1999.** Megaspore development in *Selaginella* The gap and the mesospore. *Plant Systematics and Evolution* **217**: 221-243.
- Morbelli MA, Rowley JR, and El-Ghazaly G. 2003.** Wall structure during stages in development of *Selaginella pulcherrima* and *S. haematodes* megaspores. *Taiwania* **48**: 77-86.
- Morgensen GS. 1978.** Spore development and germination in *Cinclidium* (Mniaceae, Bryophyta), with special reference to spore mortality and false anisospory. *Canadian Journal of Botany* **56**: 1032-1060.
- Morgensen GS. 1983.** Chapter 7 The spore. In: Schuster RM, ed. *New Manual of Bryology*: Hattori Botanical Laboratory. 325-342.
- Mueller DMJ. 1974.** Spore wall formation and chloroplast development during sporogenesis in the moss *Fissidens limbatus*. *American Journal of Botany* **61**: 525-534.
- Mues R. 2000.** Chemical constituents and biochemistry. In: Shaw J and Goffinet B, eds. *Bryophyte Biology*. Cambridge, Cambridge University Press. 150-181.
- Nakagawa T, Kihara K, and Harada K. 2001.** The crystal structure of low melanophlogite. *American Mineralogist* **86**: 1506-1512.
- Nédélec FJ, Surrey T, Maggs AC, and Leibler S. 1997.** Self-organisation of microtubules and motors. *Nature* **389**: 305-308.
- Neinhuis C, and Barthlott W. 1997.** Characterization and distribution of water-repellent, self-cleaning plant surfaces. *Annals of Botany* **79**: 667-677.

- Neinhuis C, Koch K, and Barthlott W. 2001.** Movement and regeneration of epicuticular waxes through plant cuticles. *Planta* **213**: 427-434.
- Nickrent DL, Parkinson CL, Palmer JD, and Duff RJ. 2000.** Multigene phylogeny of land plants with special reference to bryophytes and the earliest land plants. *Molecular Biology and Evolution* **17**: 1885-1895.
- Noble RE. 2002.** Effects of UV-irradiation on seed germination. *The Science of the Total Environment* **299**: 173-176.
- Otto A, White JD, and Simoneit BRT. 2002.** Natural product terpenoids in Eocene and Miocene conifer fossils. *Science* **297**: 1543-1545.
- Pacini E. 1990.** Tapetum and microspore function. In: Blackmore S and Knox RB, eds. *Microspores: evolution and ontogeny*. London, Academic Press. 213-237.
- Pacini E, and Franchi GG. 1991.** Diversification and evolution of the tapetum. In: Blackmore S and Barnes SH, eds. *Pollen and Spores - Patterns of Diversification*. Oxford, Carendon Press. 317-329.
- Pacini E, Franchi GG, and Hesse M. 1985.** The Tapetum: its form, function and possible phylogeny in *Embryophyta*. *Plant Systematics and Evolution* **149**: 155-185.
- Parkinson BM. 1987.** Tapetal organization during sporogenesis in *Psilotum nudum*. *American Journal of Botany* **60**: 353-360.
- Parkinson BM. 1988.** A tapetal membrane in *Psilotum nudum* (L.) Beauv. *American Journal of Botany* **61**: 695-703.
- Parkinson BM. 1991.** An investigation of sporangial development, sporogenesis and tapetal organisation in *Schizaea pectinata* (L.) Sw. (Schizaeaceae) Volume 1 *Faculty of Science*. Johannesburg: University of Witwatersrand. 242.
- Parkinson BM. 1994.** Morphological and ultrastructural variations in *Schizaea pectinata* (Schizaeaceae). *Bothalia* **24**: 203-210.
- Parkinson BM. 1995a.** Spore wall development in *Schizaea pectinata* (Schizaeaceae: Pteridophyta). *Grana* **34**: 217-228.
- Parkinson BM. 1995b.** Development of the sporangia and associated structures in *Schizaea pectinata* (Schizaeaceae: Pteridophyta). *Canadian Journal of Botany* **73**: 1867-1877.
- Parkinson BM. 1995c.** The tapetum in *Schizaea pectinata* (Schizaeaceae) and a comparison with the tapetum in *Psilotum nudum* (Psilotaceae). *Plant Systematics and Evolution* **196**: 161-172.

- Parkinson BM. 1996.** The sporangium wall in *Schizaea* - a source of components for sporogenesis? In: Camus JM, Gibby M and Johns RJ, eds. *Pteridology in Perspective*. Kew: Royal Botanic Gardens. 489-496.
- Parre E, and Geitmann A. 2005.** More than a leak sealant. The mechanical properties of callose in pollen tubes. *Plant Physiology* **137**: 274-286.
- Parry DW, Hodson MJ, and Newman RH. 1985.** The distribution of silicon deposits in the fronds of *Pteridium aquilinum* L. *Annals of Botany* **55**: 77-83.
- Parry DW, Oneill CH, and Hodson MJ. 1986.** Opaline silica deposits in the leaves of *bidens-pilosa* L and their possible significance in cancer. *Annals of Botany* **58**: 641-647.
- Paxson-Sowers D, Dodrill CH, Owen HA, and Makaroff CA. 2001.** DEX1, a novel plant protein, is required for exine pattern formation during pollen wall development in *Arabidopsis*. *Plant Physiology* **127**: 1739-1749.
- Peggs A, and Bowen H. 1984.** Inability to detect organo-silicon compounds in *Equisetum* and *Thuja*. *Phytochemistry* **23**: 1788-1789.
- Penuelas J, and Munne-Bosch S. 2005.** Isoprenoids: an evolutionary pool for photoprotection. *Trends in Plant Science* **10**: 166-169.
- Perry CC, and Fraser MA. 1991.** Silica deposition and ultrastructure in the cell wall of *Equisetum arvense*: the importance of cell wall structures and flow control in biosilification. *Philosophical Transactions of the Royal Society London B* **334**: 149-157.
- Pettitt JM. 1976.** A route for the passage of substances through the developing pteridophyte exine. *Protoplasma* **88**: 117-131.
- Pettitt JM. 1979a.** Ultrastructure and cytochemistry of spore wall morphogenesis. In: Dyer AF, ed. *The experimental biology of ferns*. London: Academic Press. 213-255.
- Pettitt JM. 1979b.** Developmental mechanisms in heterospory: cytochemical demonstration of spore-wall enzymes associated with β -lectins, polysaccharides and lipids in water ferns. *Journal of Cell Sciences* **38**: 61-82.
- Pettitt JM, and Jermy AC. 1974.** The surface coats on spores. *Biological Journal of the Linnean Society* **6**: 245-257.
- Prahl AK, Rittscher M, and Wiermann R. 1986.** New aspects of sporopollenin biosynthesis. In: Strumpf PK, ed. *The biochemistry of plants - a comprehensive treatise*. New York: Springer. 313-318.
- Prahl AK, Springstube H, Grumbach K, and Wiermann R. 1985.** Studies on sporopollenin biosynthesis: the effect of inhibitors of carotenoid

biosynthesis on sporopollenin accumulation. *Zeitschrift für Naturforschung* **40**: 621-626.

Pryer KM, Schneider H, Smith AR, Cranfill R, Wolf PG, Hunt JS, and Sipes SD. 2001. Horsetails and ferns are a monophyletic group and the closest living relatives to seed plants. *Nature* **409**: 618-622.

Pryer KM, Schuettpelz E, Wolf PG, Schneider H, Smith AR, and Cranfill R. 2004. Phylogeny and evolution of ferns (Monilophytes) with a focus on the early leptosporangiate divergences. *American Journal of Botany* **91**: 1582-1598.

Punt W, Blackmore S, Nilsson S, and Le Thomas A. 1994. *Glossary of Pollen and Spore Terminology*. Utrecht, LPP Foundation. 71.

Raven AJ. 1983. The transport and function of silicon in plants. *Biological Review* **58**: 179-207.

Renzaglia KS, and Vaughn KC. 2000. Anatomy, development and classification of hornworts. In: Shaw AJ and Goffinet B, eds. *Bryophyte Biology*. Cambridge: Cambridge University Press 1-20.

Rogerson ECW, Edwards D, Davies KL, and Richardson JB. 1993. Identification of *in situ* spores in a Silurian *Cooksonia* from the Welsh Borderland. *Special Papers in Palaeontology* **49**: 17-30.

Roshchina VV, Mel'nikova EV, Iashin VA, and Karnaukhov VN. 2002. Autofluorescence of intact *Equisetum arvense* L. spores during their development. *Biofizika* **47**: 318-324.

Rothwell GW. 1999. Fossils and ferns in the resolution of land plant phylogeny. *The Botanical Review* **65**: 188-218.

Rowley JR. 1995. Are the endexines of pteridophytes, gymnosperms and angiosperms structurally equivalent? *Review of Palaeobotany and Palynology* **85**: 13-34.

Rowley JR. 1996. Chapter 14D: *In situ* pollen and spores in plant evolution: exine origin, development and structure in Pteridophytes, Gymnosperms and Angiosperms. In: Jansonius J and McGregor DC, eds. *Palynology: Principles*. Salt Lake City: American Association of Stratigraphic Palynologists Foundation. **Volume 1**: 443-462.

Rowley JR, and Claugher D. 1991. Receptor-Independent Sporopollenin. *Botanica Acta* **104**: 316-323.

Rowley JR, Gabarayeva NI, Skvarla JJ, and El-Ghazaly GA. 2001. The effect of 4-methylmorpholine N-oxide monohydrate (MMNO.H₂O) on pollen and spores exines. *Taiwania* **46**: 246-273.

- Rowley JR, and Morbelli MA. 1995.** Megaspore wall growth in *Selaginella* (Lycopodiatae). *Plant Systematics and Evolution* **194**: 133-162.
- Rowley JR, and Skvarla JJ. 1993.** Exine receptors. *Grana Suppl.* **2**: 21-25.
- Rozema J, Broekman RA, Blokker P, Meijkamp BB, de Bakker N, van de Staaij J, van Beem A, Ariese F, and Kars SM. 2001.** UV-B absorbance and UV-B absorbing compounds (para-coumaric acid) in pollen and sporopollenin: the perspective to track historic UV-B levels. *Journal of Photochemistry and Photobiology B: Biology* **62**: 108-117.
- Russow E. 1872.** Vergleichende Untersuchungen betreffend die Histologie (Histographie und Histologie) der vegetativen und sporenbildenden Organe und Entwicklung der Sporen der Leitbündel-Kryptogamen mit Berücksichtigung der Phanerogamen, ausgehend von Betrachtung der Marsiliaceen. *Mém. Acad. Imp. Sci. St.-Petersbourg* **VII**: 1-207.
- Sacchetti JC, and Poulter CD. 1997.** Biochemistry: Creating Isoprenoid Diversity. *Science* **277**: 1788-1789.
- Samuels L, Jetter R, and Kunst L. 2005.** First steps in understanding the export of lipids to the plant cuticle. *Plant Biosystems* **139**: 65-68.
- Sangster AG, and Hodson MJ. 1986.** Silica in higher-plants. *Ciba Foundation Symposia* **121**: 90-111.
- Sastry M, Banarjee P, Patanjali S, Swamy M, Swarnalatha G, and Surolia A. 1986.** Analysis of saccharide binding to *Artocarpus integrifolia* lectin reveals specific recognition of T-antigen (beta-D-Gal(1----3)D-GalNAc). *Journal of Biological Chemistry* **261**: 11726-11733.
- Schneider H, and Pryer KM. 2002.** Structure and function of spores in the aquatic heterosporous fern family Marsileaceae. *International Journal of Plant Sciences* **163**: 485-505.
- Schraudolf H. 1984.** Ultrastructural events during sporogenesis of *Anemia phyllitidis* (L.) Sw. *Beiträge zur Biologie der Pflanzen* **59**: 237-260.
- Schulze-Osthoff K, and Wiermann R. 1987.** Phenols as integrated compounds of sporopollenin from *Pinus* pollen. *Journal of Plant Physiology* **131**: 5-15.
- Shaw J, and Renzaglia KS. 2004.** Phylogeny and disarticulation of Bryophytes. *American Journal of Botany* **91**: 1557-1581.
- Shute CH, and Edwards D. 1989.** A new rhyniopsid with novel sporangium organization from the Lower Devonian of South Wales. *Botanical Journal of the Linnean Society* **100**: 111-137.

- Skoog DA, West DM, Holler FJ, and Crouch SR. 2004.** *Fundamentals of Analytical Chemistry*. Belmont (CA), Thomson, Brooks/Cole. 1051.
- Smith SY, Rothwell GW, and Stockey RA. 2003.** *Cyathea cranhamii* sp. nov. (Cyatheaceae), anatomically preserved tree fern sori from the Lower Cretaceous of Vancouver Island, British Columbia. *American Journal of Botany* **90**: 755-760.
- Southworth D. 1974.** Solubility of pollen exines. *American Journal of Botany* **61**: 36-44.
- Southworth D. 1975.** Lectins stimulate pollen germination. *Nature* **258**: 600-602.
- Southworth D. 1988.** Isolation of exines from gymnosperm pollen. *American Journal of Botany* **75**: 15-21.
- Stainier F. 1965.** Structure et infrastructure des parois sporales chez deux selaginelles (*Selaginella myosurus* et *S. kraussiana*). *Cellule* **65**: 220-224.
- Stainier F. 1967.** Morphological study of the walls of the mega- and microspores of *Selaginella myosurus* (SW.) Alston. *Review of Palaeobotany and Palynology* **3**: 47-50.
- Steiglitz H. 1977.** Role of β -1,3- glucanase in postmeiotic microspore release. *Developmental Biology* **57**: 87-97.
- Stein WE, and Hueber FM. 1989.** The anatomy of *Pseudosporochnus*: *Pseudosporochnus hueberi* from the Devonian of New York. *Review of Palaeobotany and Palynology* **60**: 311-359.
- Stevenson DW, and Loconte H. 1996.** Ordinal and familiar relationships of Pteridophyte genera. In: Camus JM, Gibby M and Johns RJ, eds. *Pteridology in Perspective*. Kew: Royal Botanic Gardens. 435-467.
- Stewart WN, and Rothwell GW. 1993.** *Paleobotany and the evolution of plants*. Cambridge, Cambridge University Press. 521.
- Strasburger E. 1976.** *Strasburger's textbook of botany*. New York, Longman Inc. 581.
- Strasburger E. 1998.** *Lehrbuch der Botanik für Hochschulen*. Stuttgart, Gustav Fischer Verlag. 1003.
- Strother PK. 1991.** A classification schema for the cryptospores. *Palynology* **15**: 219-236.
- Tanaka H, Waki H, Ido Y, Akita S, Yoshida Y, and Yoshida S. 1988.** Protein and polymer analysis up to m/z 100.00 by laser ionisation time-

of-flight mass spectrometry. *Rapid Communications in Mass Spectrometry* **2**: 151-153.

Tarlyn NM, Franceschi VR, Everard JD, and Loewus FA. 1993. Recovery of exine from mature pollen and spores. *Plant Science* **90**: 219-224.

Tateno H, Winter HC, Petryniak J, and Goldstein IJ. 2003. Purification, characterization, molecular cloning, and expression of novel members of jacalin-related lectins from rhizomes of the true fern *Phlebodium aureum* (L.) J. Smith (Polypodiaceae). *The Journal of Biological Chemistry* **13**: 10891-10899.

Taylor TN. 1974. Scanning electron microscopy of fossil megaspores: wall development. *Scanning Electron Microscopy* **2**: 359-366.

Taylor WA. 1986. Ultrastructure of Spenophyllean spores. *Review of Palaeobotany and Palynology* **47**: 105-128.

Taylor WA. 1988. Developmental and structural aspects of lycopod megaspore ultrastructure. *American Journal of Botany* **76**: 50-51.

Taylor WA. 1989. Megaspore wall ultrastructure in *Selaginella*. *Pollen et Spores* **31**: 251-288.

Taylor WA. 1991. Ultrastructural analysis of sporoderm development in megaspores of *Selaginella galeottii* (Lycophyta). *Plant Systematics and Evolution* **174**: 171-184.

Taylor WA. 1992. Megaspore wall development in *Isoetes melanopoda*: morphogenetic post-initiation changes accompanying spore enlargement. *Review of Palaeobotany and Palynology* **72**: 61-72.

Taylor WA. 1993. Megaspore wall ultrastructure in *Isoetes*. *American Journal of Botany* **80**: 165-171.

Taylor WA. 1997. Ultrastructure of lower Paleozoic dyads from southern Ohio II: *Dyadospora murusattenuata*, functional and evolutionary considerations. *Review of Palaeobotany and Palynology* **97**: 1-8.

Taylor WA. 2003. Ultrastructure of selected Silurian trilete spores and the putative Ordovician trilete spore *Virgatasporites*. *Review of Palaeobotany and Palynology* **126**: 211-223.

Tevini M. 1988. The effects of UV radiation on plants. *Journal of Photochemistry and Photobiology B: Biology* **2**: 401.

Thom I, Grote M, Abraham-Peskir J, and Wiermann R. 1998. Electron and x-ray microscopic analyses of reaggregated material obtained after fractionation of dissolved sporopollenin. *Protoplasma* **204**: 13-21.

- Tryon AF, and Lugardon B. 1978.** Wall structure and mineral content in *Selaginella* spores. *Pollen et Spores* **20**: 316-340.
- Tryon AF, and Lugardon B. 1990.** *Spores of the pteridophyta. Surface, wall, structure and evolution based on electron microscope studies.* New York, Spinger-Verlag. 648.
- Uehara K, and Kurita S. 1989.** An ultrastructural study of spore wall morphogenesis in *Equisetum arvense*. *American Journal of Botany* **76**: 939-951.
- van Bergen PF, Blokker P, Collinson ME, Sinninghe Damste JS, and de Leeuw JW. 2004.** Structural biomacromolecules in plants: what can be learnt from the fossil record? In: Hemsley AR and Poole I, eds. *The Evolution of Plant Physiology. From whole plants to ecosystems.* London: Elsevier. 133-154.
- van Bergen PF, Collinson ME, Briggs DEG, de Leeuw JW, Scott AC, Evershed RP, and Finch P. 1995.** Resistant biomacromolecules in the fossil record. *Acta Botanica Neerlandica* **44**: 319-342.
- van Konijnenburg-van Cittert JHA. 1978.** Osmundaceous spores *in situ* from the Jurassic of Yorkshire, England. *Review of Palaeobotany and Palynology* **26**: 125-141.
- van Konijnenburg-van Cittert JHA. 1993.** A review of the Matoniaceae based on *in situ* spores. *Review of Palaeobotany and Palynology* **78**: 235-267.
- van Konijnenburg-van Cittert JHA. 2000.** Osmundaceous spores throughout time. In: Harley MM, Morton CM and Blackmore S, eds. *Pollen and Spores: Morphology and biology.* London: Royal Botanic Gardens Kew. 435-449.
- van Uffelen GA. 1986.** Some functional aspects of the spore wall in *Pyrrosia* (Polypodiaceae, Filicales). In: Blackmore S and Ferguson IK, eds. *Pollen and Spores: Form and Function.* London: Academic Press. 405-407.
- van Uffelen GA. 1991.** The control of spore wall formation. In: Blackmore S and Barnes SH, eds. *Pollen and Spores: Patterns of Diversification.* Oxford: Clarendon Press. 89-102.
- von Aderkans P, Rogerson A, and de Freitas ASW. 1986.** Silicon accumulation in fronds of the ostrich fern *Matteuccia struthiopteris*. *Canadian Journal of Botany* **64**: 696-699.

- Wallace JW. 1989.** Chemosystematic implications of flavonoids and C-Glycosylxanthenes in ferns. *Biochemical Systematics and Ecology* **17**: 145-153.
- Walton J. 1957.** On *Protopitys* (Göppert): with a description of fertile specimen *Protopitys scotica* sp. nov. from the Calciferous Sandstone series of Durbartonshire. *Transactions of the Royal Society Edinburgh* **63**: 333-343.
- Wang J, Zhang G, Bek J, and Pfefferkorn HW. 2004.** A new morphological type of operculate microspore, *Discinispora* gen. nov., from the Permian petrified Noeggerathialean strobilus *Discinites sinensis* Wang. *Review of Palaeobotany and Palynology* **128**: 229-245.
- Wang YD, Guignard G, and Barale G. 1999.** Morphological and ultrastructural studies on *in situ* spores of *Oligocarpia* (Gleicheniaceae) from the Lower Permian of Xinjiang, China. *International Journal of Plant Sciences* **160**: 1035-1045.
- Wang YD, Guignard G, Lugardon B, and Barale G. 2001.** Ultrastructure of *in situ* *Marattia asiatica* (Marattiaceae) spores from the Lower Jurassic in Hubei, China. *International Journal of Plant Sciences* **162**: 927-936.
- Watt IM. 1997.** *The principles and practice of electron microscopy*. Cambridge, Cambridge University Press. 484.
- Weber M. 1996.** The existence of a special exine coating in *Geranium robertianum* pollen. *International Journal of Plant Sciences* **157**: 195-202.
- Weber M. 2004.** Unique pollen features in Araceae. In Ubera JL, ed. *XI International Palynological Congress*. Granada: Argos Impresores Cordoba, 18. (Conference abstract)
- Wehling K, Niester C, Boon JJ, Willemse MTM, and Wiermann R. 1989.** *p*-Coumaric acid - a monomer in the sporopollenin skeleton. *Planta* **179**: 376-380.
- Weiss A, and Herzog A. 1978.** Isolation and characterization of a silicon-organic complex from plants. In Bendz G and Lindqvist I, eds. *Biochemistry of Silicon and Related Problems*. New York, Plenum Press, 109-128.
- Wellman CH, Edwards D, and Axe L. 1998a.** Ultrastructure in laevigate hilate spores from sporangia and spore masses from the Upper Silurian and Lower Devonian of the Welsh Borderland. *Philosophical Transactions of the Royal Society London B* **153**: 1983-2004.

- Wellman CH, Edwards D, and Axe L. 1998b.** Permanent dyads in sporangia and spore masses from the Lower Devonian of the Welsh Borderland. *Botanical Journal of the Linnean Society* **127**: 117-147.
- Wellman CH, Osterloff PL, and Mohiuddin U. 2003.** Fragments of the earliest land plants. *Nature* **425**: 282-285.
- Wichard T, Gobel C, Feussner I, and Pohnert G. 2004.** Unprecedented lipoxygenase/hydroperoxide lyase pathways in the moss *Physcomitrella patens*. *Angewandte Chemie International Edition English* **44**: 158-161.
- Wiermann R. 2001.** Sporopollenin. In: Steinbuechel H and Hofrichter M, eds. *Biopolymers*. Weinheim: WILEY-VCH. 209-227.
- Williams RJP. 1986.** Introduction to silicon chemistry and biochemistry. In: 121 CFS, ed. *Silicon Biochemistry*. Chichester: John Wiley & Sons. 24-39.
- Yule BL, Roberts S, and Marshall JEA. 2000.** The thermal evolution of sporopollenin. *Organic Geochemistry* **31**: 859-870.
- Zetzsche F, Kalt P, Liecht J, and Zieger E. 1937.** Zur Konstitution des *Lycopodium*-spononins, des tasmanins und des Lange-Sponins. XI Mitteilungen über die Membran der Sporen und Pollen. *Journal der Praktischen Chemie* **148**: 267-286.
- Zetzsche F, and Vicari H. 1928.** Untersuchungen über die Membran der Sporen und Pollen II. *Lycopodium clavatum* L. *Helvetica Chimica Acta* **14**: 58-62.
- Integrated Spectral Data Base System for Organic Compounds S.**
<http://www.aist.go.jp/RIODB/SDBS/>. National Institute of Advanced Industrial Science and Technology (AIST), Tokyo, Japan. Last access date: 27.10.2005
- von Sengbusch P. 2003.** Botany online: P. van Sengbusch Klaus Harms-Str. 85 D-25746 Heide. <http://www.biologie.uni-hamburg.de/b-online/> Last access date: 27.10.2005

Appendix 1

Moore *et al.* in press a (GRANA): UNCORRECTED PROOF

Micro-morphology of outer exospore coatings in *Selaginella* megaspores

SUSANNAH E. M. MOORE, ALAN R. HEMSLEY and THOMAS BORSCH

Micro-morphology of outer exospore coatings in *Selaginella* megaspores

SUSANNAH E. M. MOORE¹, ALAN R. HEMSLEY¹ & THOMAS BORSCH²

¹Laboratory for Experimental Palynology, School of Earth, Ocean and Planetary Sciences, Cardiff University, Cardiff CF10 3YE, Wales, UK, and ²Nees-Institut für Biodiversität der Pflanzen, Meckenheimer Allee 170, 53115 Bonn, Germany

Abstract

Variability of *Selaginella* megaspore microsculpture is defined and illustrated by means of SEM and TEM. Additional EDX analyses demonstrated that micro-sculpture elements in the investigated specimens are mainly formed by silica which may be removed by hydrofluoric acid. Our observations suggest that different proportions of sporopollenin/silica are present in the outer coating of at least some *Selaginella* megaspore walls. Pattern formation mechanisms as well as implications for terminology are discussed. On the basis of this investigation and using data available from the literature, it is argued that the sporoderm layers of *Isoetes* and *Selaginella* megaspores are probably homologous, supporting the consensual view.

With over 750 mostly tropical terrestrial or epiphytic species, *Selaginella* Milde is the largest genus among heterosporous lycopsids. A number of researchers have studied the genus from different viewpoints, ranging from anatomical (Hebant & Lee, 1984) and morphological (Lyon, 1901; Horner & Arnott, 1963; Horner, Beltz, Jagels & Boudreau, 1975; Dengler, 1983; Page, 1989; Webster, 1992) to palaeobotanical (Bek, Oplustil & Drabkova, 2001; Cottnam, Hemsley, Rössler, Collinson & Brain 2000) and most recently to phylogenetic and taxonomic investigations (Korall, Kenrick & Therrien, 1999; Korall & Kenrick, 2002). Phylogenetic analyses of DNA sequence data agree that Lycophytes (including *Selaginella*, *Isoetes* Linnaeus and *Huperzia* Bernardi) form a distinct clade, branching off from other tracheophytes early in land plant evolution (Pryer et al. 2001, Quandt et al. 2004). The majority of publications, however, are from a palynological perspective with some focussing on the origin of heterospory, and discussing this character comprehensively (Duerden, 1929; Pettitt, 1977; Haig & Westoby, 1988; DiMichele, Davis & Olmstead, 1989; Bateman & DiMichele, 1994). A significant proportion of published work has concentrated upon

micro- and megaspore development (Sievers & Buchen, 1970; Morbelli & Rowley, 1993, 1999), spore morphology (Minaki, 1984) and ultrastructure (Kempf, 1970, Buchen & Sievers, 1978a, b; Tryon & Lugardon, 1978, 1990; Taylor, 1989, 1991). Recently a number of articles describing the underlying processes of megaspore wall formation have discussed the role of self-assembly in a completely new light (Hemsley, Collinson & Brain, 1992; Hemsley, Collinson, Kovach, Vincent & Williams, 1994; Hemsley, Griffiths, Mathias & Moore, 2003). Only Kempf (1970), Tryon & Lugardon (1978), Taylor (1989) and Morbelli (1995) have so far mentioned the presence of silica in *Selaginella* megaspore walls. The aim of this study is to highlight the variability of micro-sculpture in *Selaginella* megaspores, revealed by a combined approach of SEM and TEM. Although no TEM data were obtained for *Selaginella helvetica* (L.) Spring, it was included into this study to demonstrate the extent of micro-sculpture patterns. Secondly, it is suggested that silica is a major spore wall component in *Selaginella* that has so far been underestimated. Furthermore, the interrelationship of silica and sporopollenin in spore walls is discussed on the

Correspondence: Susannah E. M. Moore, Laboratory for Experimental Palynology, School of Earth, Ocean and Planetary Sciences, Cardiff University, Cardiff CF10 3YE, Wales, UK. E-mail: MooreS@cf.ac.uk

(Received: 30 July 2004; accepted 30 September 2005)

ISSN 0017-3134 print/ISSN 1651-2049 online © 2006 Taylor & Francis
DOI: 10.1080/00173130500537150

1 basis of novel results with hydrofluoric acid
treatment.

5 Material, methods and terminology

Plant material

The material originated from the living collection of
the Botanical Garden in Bonn and the University
10 Research Gardens at Talybont, Cardiff. Taxa,
voucher specimens, the geographical origin of the
specimen and the place where the plants are
cultivated are listed (see, Specimen Investigated
list included). For all megaspores taken from
15 living plants, herbarium specimens from the original
collector are cited, if these exist and clearly
assigned. If no original voucher existed, herbarium
specimens were newly made from the plants in
cultivation. Where identification was uncertain, the
20 plant was given a working name "*Selaginella* sp."
plus a number, i.e. *S. sp.1*. All new specimens
vouched in this study are deposited in the Bonn
Herbarium (BONN). Herbaria are abbreviated
according to Holmgren, Holmgren & Barnett
25 (1990).

Scanning Electron Microscopy (SEM)

30 Megaspores recently collected from living plants
were mounted onto stubs using carbon adhesive
disks and coated with gold/palladium at a voltage
of 15 mA and later viewed using a Phillips
XL30 ESEM (Environmental Scanning Electron
35 Microscope) with an average working distance of
10 mm and a voltage of 15 Kv.

Transmission Electron Microscopy (TEM) and x-ray diffraction analysis (EDX)

40 All megaspores recently collected from living
plants were rinsed with distilled water and directly
transferred into 100% acetone and later embedded
into Spurr "hard mix" (Glasspool, 2003). The
megaspores were incubated for 24 hours in a
45 mixture of acetone/Spurr (50:50), another 24
hours in 100% Spurr "hard mix" and finally placed
in block moulds and polymerised at 70°C for 12 h.
The megaspores were not stained. Sections were
50 taken on a standard ultramicrotome measuring
between 50 and 100 nm, using a diamond knife,
collected on coated copper grids (200 mesh) and
viewed using a JEOL 1210 TEM at 80 Kv.
Additionally x-ray diffraction analyses (EDX)
55 were carried out for all species in order to docu-
ment major chemical components in the outer
exospore and exospore. The analytical system used

1 for detecting megaspore wall components was a
pentafet detector coupled to Oxford Instruments
(ISIS) software. The megaspore diameters given are
for the individual spores examined. They are
5 maximum diameters.

Treatment with hydrofluoric acid (HF)

10 Megaspores of *S. denticulata* (L.) Spring, *S. per-
uviana* (Milde) Hieron and *S. sp.1* were washed with
distilled water and then soaked into hydrofluoric
acid (40%) for 20 minutes, caught on polypropylene
mesh, rinsed with distilled water, dried and prepared
15 for scanning electron microscopy as described
above.

Terminology

20 In order to describe precisely megaspore morphol-
ogy or ultrastructure a clear terminology is neces-
sary. Concerning morphology, a common and
widely accepted terminology is provided by Grebe
(1971), Tryon & Lugardon (1990), Punt et al.
(1994), and Playford & Dettmann (1996). The
25 morphological descriptions used here follow the
definitions of Tryon & Lugardon (1990) and Punt
et al. (1994). The presentation of our results follows
the format established by Tryon & Lugardon
(1990). In most *Selaginella* megaspores there is
30 rather a coarse sculpture made of sporopollenin
units of the exospore and outer exospore. We refer to
this level of patterning as "sculpture". This is in
contrast to the "micro-sculpture" which is the
patterning caused by elements of the outer wall
35 coating largely composed of silica (see discussion).
In describing the megaspore surface using the SEM
we will employ the terms "sculpture" and "micro-
sculpture" because no qualitative differentiation of
wall components can be achieved by SEM. For the
40 ultrastructure, however, no overall terminology
exists. A summary of the various attempts to find a
general ultrastructure terminology was given by
Minaki (1984). In order to avoid confusion and to
use only one terminology, the description of the
45 ultrastructure follows Taylor (1989) (see, Specimen
Investigated list included). Ideally, this terminology
should reflect concepts of homology for the different
wall layers.

50 Morphological description of unidentified species
Selaginella sp.1: The plant cultivated in BG Bonn
(accession 14599) does not fit the description of *S.
njamnjamensis* Hieron. in the Flora Zambesiaca
(Schelpe, 1970), although it has a similar habit.
Megaspore morphology is deviant from all known
55 megaspores in the Flora Zambesiaca area, so that the
plant might represent a new species; and *S. sp.2*:

cultivated under accession BG Bonn 15014, it is a big, robust plant with a woody stem, stem leaves with a cilium at the leaf apex and rhizophores. These features no longer allow identification as *S. uncinata* (Desv.) Spring to which this plant has previously been assigned.

Results

Selaginella denticulata (L.) Spring

Scanning Electron Microscopy (Fig. 1 A, B)

Size. 318 µm at laesurae.

Shape of spore. Globose.

Aperture. The laesurae are 119.25 µm long extending to $\frac{3}{4}$ of the spore radius in polar view. The ends of the trilete mark gradually shallow, becoming less prominent, the laesurae are triangular in perpendicular cross-section. The ornament on the mark is similar to the sculpture of the proximal face between the laesurae.

Surface. Proximal and distal face are similar and can be described as coarsely granulate. The micro-sculpture is echinulate (Tryon & Lugardon, 1990: p. 632) with spines ranging from 1–1.5 µm (Fig. 1 B).

Transmission Electron Microscopy (TEM) and X-ray diffraction analysis (EDX) (Figs 2 A–C & 5 A, B)

Structure. The exospore consists mostly of laterally fused spherules and rod-like units but also some closed vesicles (Fig. 2 C). Towards the inner separable layer (not shown) the units seem to be more compressed (Fig. 2 C). Silica was detected in the exospore (Fig. 5 B) and the outer exospore (Fig. 5 A). In the latter it is seen as a patchy, electron dense siliceous coating (Fig. 2 B), which spreads into the exospore to a depth of 1 µm (Fig. 2 A).

Treatment with hydrofluoric acid (HF) (Fig. 4 B)

Whereas the overall verrucate sculpture has not been affected by HF, the echinulate micro-sculpture was partially removed (Fig. 4 B in comparison to Fig. 4 A and Fig. 1 B). Higher magnification shows (Fig. 4 B, small quadrant) that the micro-sculpture consists of verrucae, which are no longer covered by spines.

Selaginella helvetica (L.) Spring

Scanning Electron Microscopy (Fig. 1 C, D)

Size. 350 µm at laesurae.

Shape of spore. Globose.

Aperture. The laesurae are 131.25 µm long extending to $\frac{3}{4}$ of the spore radius in polar view. The mark is triangular in perpendicular cross-section with a laevigate sculpture and slightly elevated ends.

Surface. Proximal and distal sculptures are similar, covered with randomly distributed tubercles. The micro-sculpture is granulate with irregular shaped platelets between single grains (Fig. 1 D).

Selaginella peruviana (Milde) Hieron

Scanning Electron Microscopy (Fig. 1 E, F)

Size. 365 µm at laesurae.

Shape of spore. Globose,

Aperture. Laesural length is of 136.9 µm, extending to $\frac{3}{4}$ of the spore radius in polar view. The ends of the mark merge into the ornament characteristic of the distal hemisphere, which extends proximally to the curvature. The mark itself is triangular in perpendicular cross-section and its sculpture is laevigate.

Surface. The sculpture is a network of interrupted muri covered with closely aligned tubercles. Though less pronounced, the proximal face is similar to the distal. The micro-sculpture is densely verrucate (Fig. 1 F) supported on an undulating surface.

Transmission Electron Microscopy (TEM) and x-ray diffraction analysis (EDX) (Figs 2 F–H & 5 C)

Structure. The exospore shows a mixture of spherical units and closed vesicles, which are not highly interconnected and therefore build free-sheet like margins (Fig. 2 G). Towards the inner separable layer (not shown) the exospore (Fig. 2 G) becomes less compact but more electron dense, mainly forming rod-like units. Silica was detected in the outer exospore (Fig. 5 C). The siliceous coating on the outer exospore is patchy, up to 2 µm thick and forms a layer that does not spread into the exospore (Fig. 2 F).

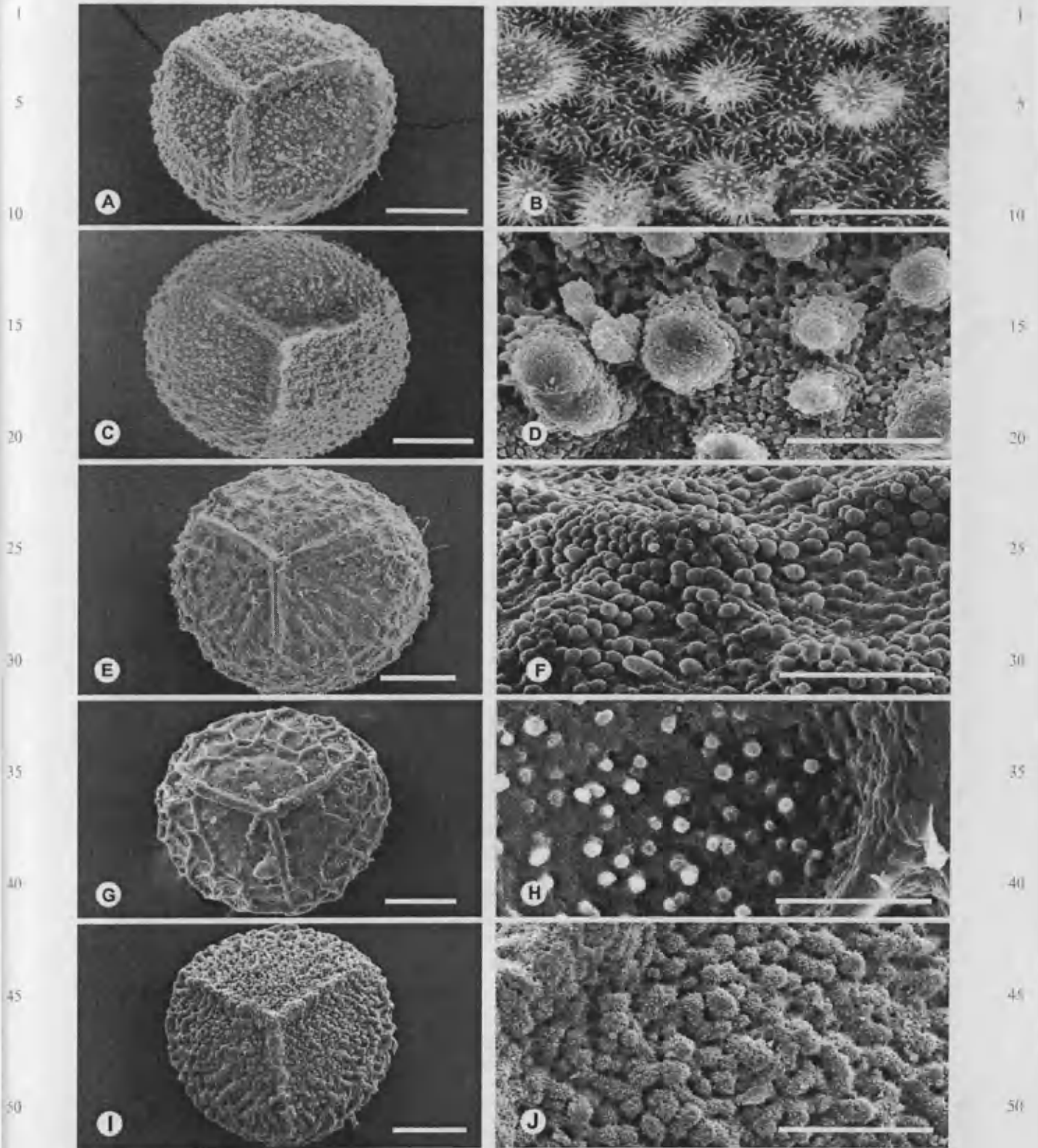


Figure 1. A–J. *Selaginella* megaspores proximal view (left), all scale bars 100 μm . Micro-sculptures (right), all scale bars 20 μm . A and B. *S. denticulata*: (A) proximal view; (B) echinulate micro-sculpture. C and D. *S. helvetica*: (C) proximal view; (D) granulate micro-sculpture with irregular shaped platelets between single grains. E and F. *S. peruviana*: (E) proximal view; (F) undulate and densely verrucate micro-sculpture. G and H. *S. sp. 1*: (G) proximal view; (H) reticulate micro-sculpture with finely granulate lumen and laevigate, retate muri (distal). I and J. *S. sp. 2*: (I) proximal view; (J) verrucate micro-sculpture covered with incipient spines.

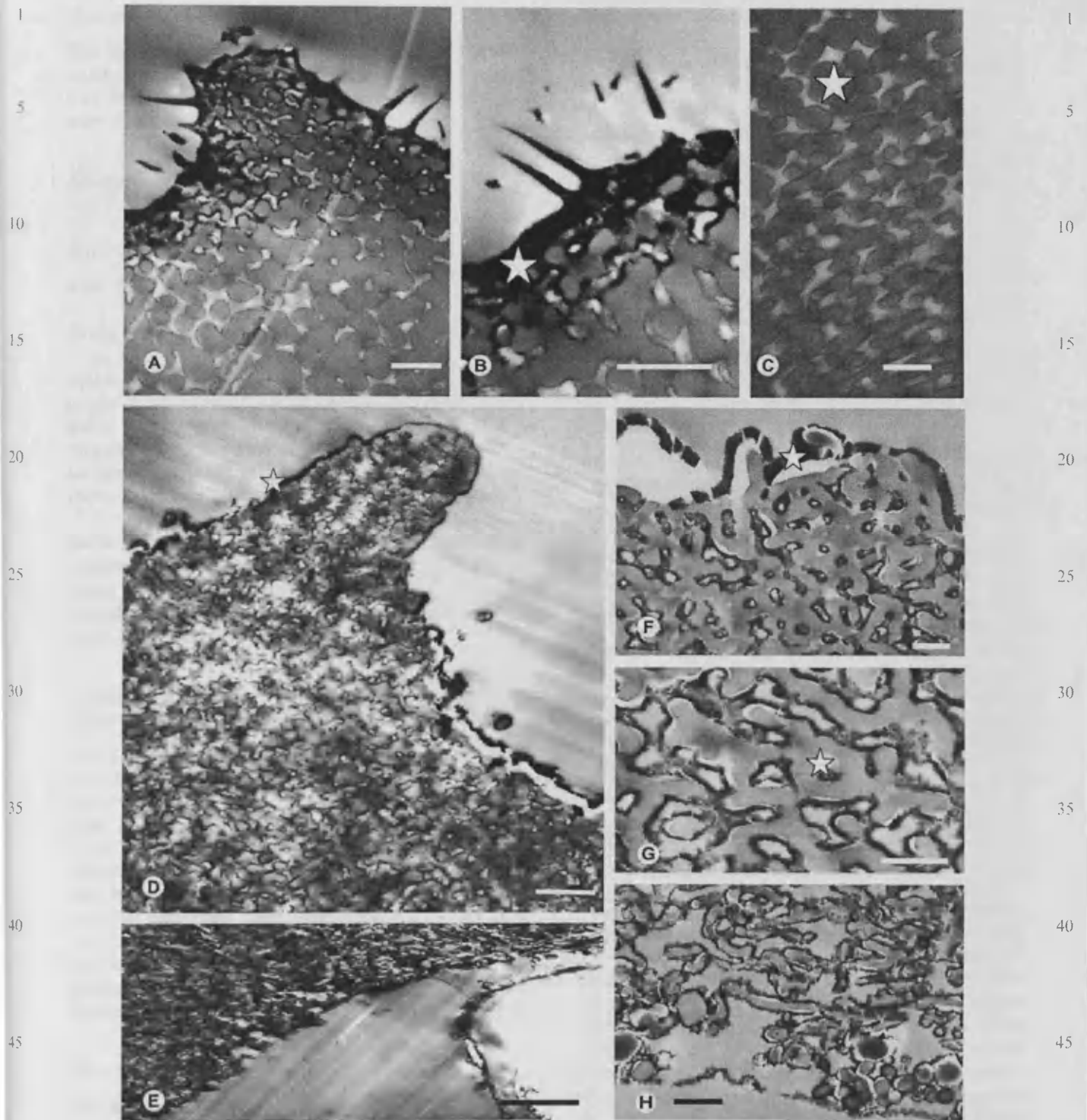


Figure 2. A–H. Wall structure in three different *Selaginella* megaspores. Scale bars A–C 1 μm, D and E 2 μm and F–H 1 μm. Stars mark the areas from which EDX-analyses were taken. A–C. *S. denticulata*: The siliceous outer exospore is very electron dense and penetrates into the exospore (B). The overall granulate sculpture is formed by the exospore, the echinulate micro-sculpture is shaped by the outer exospore (A). The exospore consists of closed vesicles, rod-like units as well as laterally fused spherules and is more compressed towards the inner separable layer (not shown) (C). D and E. *S. sp. 1*: The exospore mainly consists of spherical units and closed vesicles. The thin siliceous outer exospore, seen as a thin electron coating, is deposited on top of the exospore, to which it conforms (D). The inner separable layer (ISL) is detached from the exospore and is extremely thin (E). F–H. *S. peruviana*: The siliceous outer exospore is thick and is deposited on top of the exospore (F). The exospore shows a mixture of spherical units and closed vesicles, which are highly interconnected (G). Towards the inner separable layer (not shown), the exospore becomes less compact but more electron dense (H).

Treatment with hydrofluoric acid (HF) (Fig. 4 D)

The HF treated micro-sculpture (Fig. 4 D) shows much denser granulation than the untreated sculpture (Fig. 4 C), suggesting that parts of the sculpture were dissolved by the acid.

Selaginella sp. 1*Scanning Electron Microscopy (Fig. 1 G, H)*

Size. 310 µm at laesurae.

Shape of spore. Globose.

Aperture. The laesurae are 160 µm, extending to $\frac{3}{4}$ of the spore radius in polar view. The ends of the trilete mark merge into the distal ornament of the megaspore, its laesurae are round in section with a laevigate sculpture. The sculpture bordering the trilete mark is similar to that of the inter-radial area.

Surface. The proximal face of the megaspore is laevigate, the micro-sculpture is finely granulate with grains of less than 1 µm. The distal face shows a reticulum with finely granulate lumen and laevigate muri (Fig. 1 H).

Transmission Electron Microscopy (TEM) and x-ray diffraction analysis (EDX) (Figs 2 D, E & 5 E, D)

Structure. The exospore shows a mixture of spherical units and closed vesicles, which are highly interconnected. No free sheet-like margins are built (Fig. 2 D). Silica was detected in the exospore (Fig. 5 E) as well as in the outer exospore (Fig. 5 D). Its thin electron dense silica coating does not spread into the exospore (Fig. 2 D). The inner separable layer is extremely thin and difficult to measure accurately as it is disconnected from the exospore and a perpendicular angle of section cannot be guaranteed. However, it varies between 0.5–1 µm in thickness (Fig. 2 E).

Treatment with hydrofluoric acid (HF) (Fig. 4 F)

No effects on sculpture or micro-sculpture were observed. The surface remained unchanged (Figs 1 H & 4 E, F).

Selaginella sp. 2*Scanning Electron Microscopy (Fig. 1 I, J)*

Size. 340 µm at laesurae.

Shape of spore. Globose.

Aperture. The laesurae are of 150 µm length extending from $\frac{3}{4}$ of the spore radius in polar view. The ends of the trilete mark merge into the distal ornament of the megaspore; the mark itself is triangular in perpendicular cross-section. Its ornament is similar to the sculpture of the inter-radial areas.

Surface. The proximal face consists of fine, closely aligned verrucae. The distal face is coarser but still highly verrucate. The micro-sculpture of these verrucae, distal as well as proximal, is covered with tiny spines (Fig. 1 J).

Transmission Electron Microscopy (TEM) and x-ray diffraction analysis (EDX) (Figs 3 A–D & 5 F)

Structure. The exospore is a densely packed network of uniformly thick units, consisting of free sheet-like margins and closed vesicles. Along both units small grains of up to 25 nm are accumulated (Fig. 3 C), which are of siliceous material (Fig. 5 F). Silica was also detected on top of the outer exospore, the coating is about 2 µm thick (Fig. 3 A). A greater magnification reveals the patchy ornamentation of this extremely electron dense material (Fig. 3 B). Silica does not spread into the exospore. The inner separable layer is about 2 µm thick and highly compressed. Above the inner separable layer small siliceous grains were observed (Fig. 3 D), which have already been described for the exospore.

Discussion and conclusions*Pattern of variability in outer exospore coatings*

The micro-sculpture of the outer exospore coating, as seen in *Selaginella* megaspores, has only cursorily been described by previous workers (Bajpai & Maheshwari, 1986). Although Minaki (1984) provides a comprehensive account of *Selaginella* megaspore morphology, a detailed characterisation of the micro-sculpture, which often differs from the overall sculpture, is lacking. We refer to “micro-sculpture” (size range: less than 1 µm) of the megaspore as the fine patterning of the outer exospore coating that covers the overall sculpture (size range: 1–10 µm). Hence, during SEM studies the micro-sculpture can usually be observed at a magnification of 2000 × or more.

In this study, we document a variability of megaspore micro-sculpture pattern, which complements that previously known. Micro-sculptures range from undulate and verrucate to echinulate

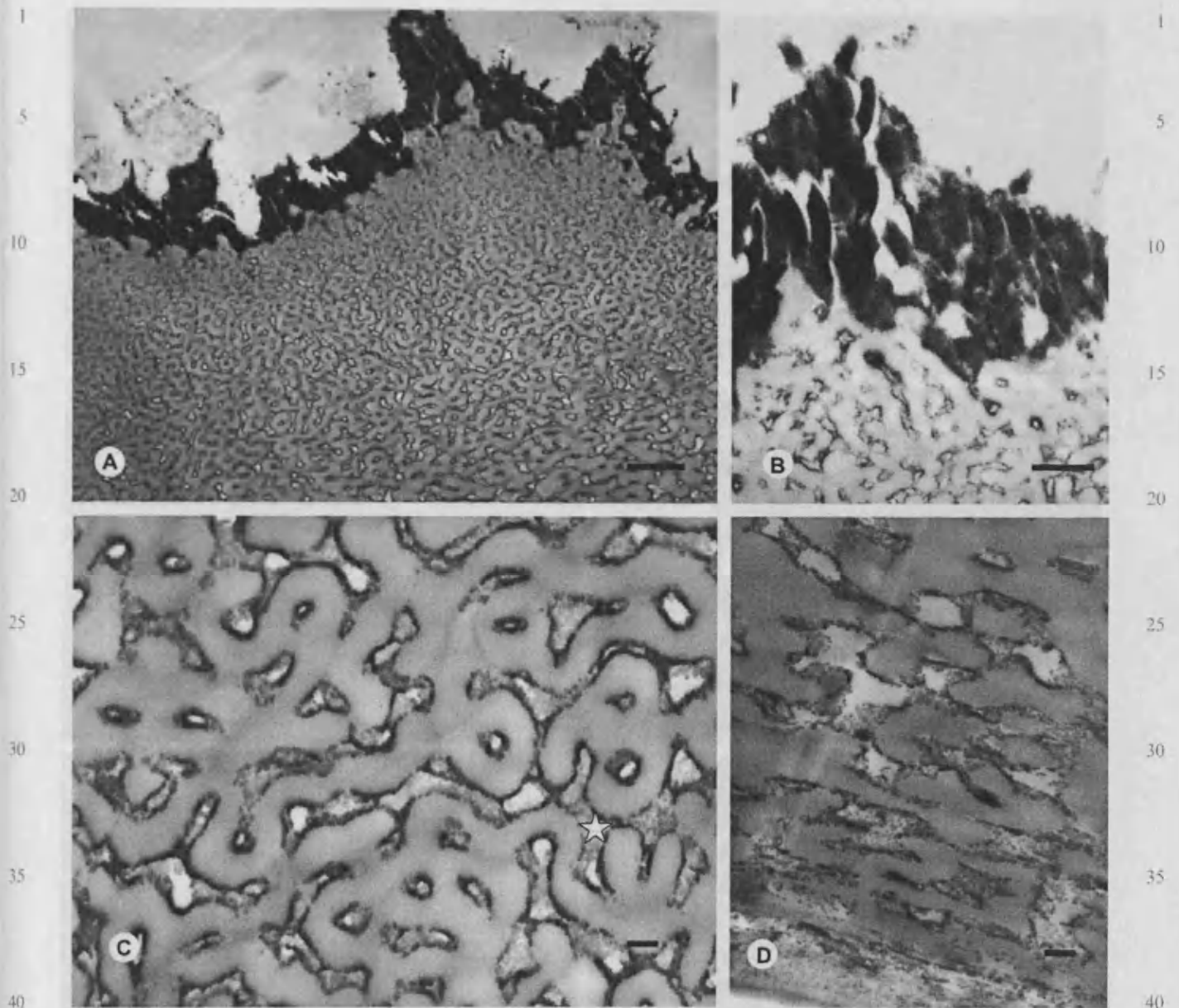


Figure 3. A–D. Wall structure in *Selaginella* sp.2. Scale bars A 1 μ m, B 500 nm, C and D 200 nm. The star marks the area from which an EDX-analysis was taken. The siliceous outer exospore is a thick electron dense coating conforming to the exospore. The latter is a densely packed network of uniformly thick units of free sheet-like margins and closed vesicles (A and B). Both units are surrounded by grains up to 25 nm in diameter (C), which are of siliceous composition (see Fig. 5 F). The inner separable layer is highly compressed; again siliceous grains can be found surrounding the exospore (D).

and granulate (Fig. 1 B, D, F, H, J). Some surface ornaments can be entirely shaped by silica, as seen in *S. denticulata* (Figs 1 B & 2 A, B). Other ornaments, as in *S. sp. 3*, conform to the sporopollenin exospore with silica as a deposit forming an electron dense, surface coating (Fig. 3 A, B). Tests with hydrofluoric acid show that some micro-sculptures are more resistant to HF, as in *S. sp. 1* (Fig. 4 E, F) than others (Fig. 4 B, D). TEM sections of those species treated with HF are in preparation and will

be discussed in a separate study. Our SEM observations suggest that in some species silica is interconnected with another, HF resistant, substance. It has recently been demonstrated for non-sporopollenin Araceae pollen (Weber, Halbritter & Hesse, 1999; Weber, 2004) that lipids form an ectexine-like layer that proved acetolysis resistance. Whether lipids are also responsible for the observed HF resistance in some *Selaginella* megaspores is subject to further studies. In some megaspores the outmost

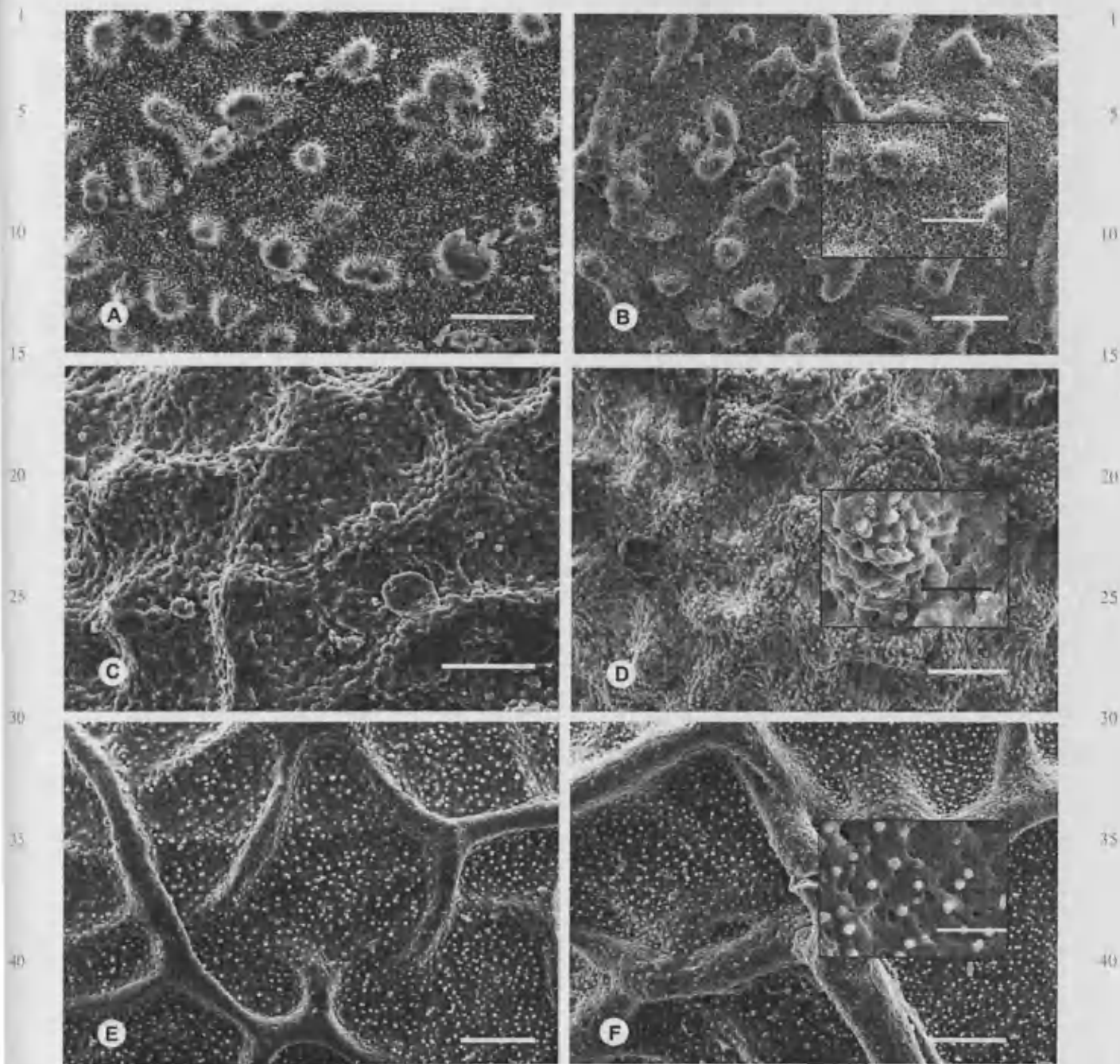


Figure 4. A–F. *Selaginella* megaspore micro-sculptures untreated (left) and after 20 mins of HF treatment (right). All scale bars are 20 μm , except for magnified sections of treated micro-sculptures, in which scale bars are 10 μm . A and B. *S. denticulata*: echinulate micro-sculpture in proximal view (A); HF dissolved siliceous micro-sculpture and left a verrucate surface (B). C and D. *S. peruviana*: Though the micro-sculptures look similar, the treated surface appears more abraded and reveals more grains (D) than seen in the untreated surface (C). E and F. *S. sp. 1*: HF did not effect the micro-sculpture, compare (E) to (F).

layer might consist of a varying degree of sporopollenin/silica mixture, as sporopollenin has HF resistant properties. Whereas in some species silica is loosely deposited on top of the exospore, it is likely that in those species not affected by HF, silica is interconnected with sporopollenin. A macromolecule

like sporopollenin could well incorporate silica into its overall chemical structure, a view that is shared by Crang & May (1974) who stated that silica is likely to be an integrated compound of the pollen wall. Sporopollenin is believed to consist of long saturated aliphatic chains with varying degrees of

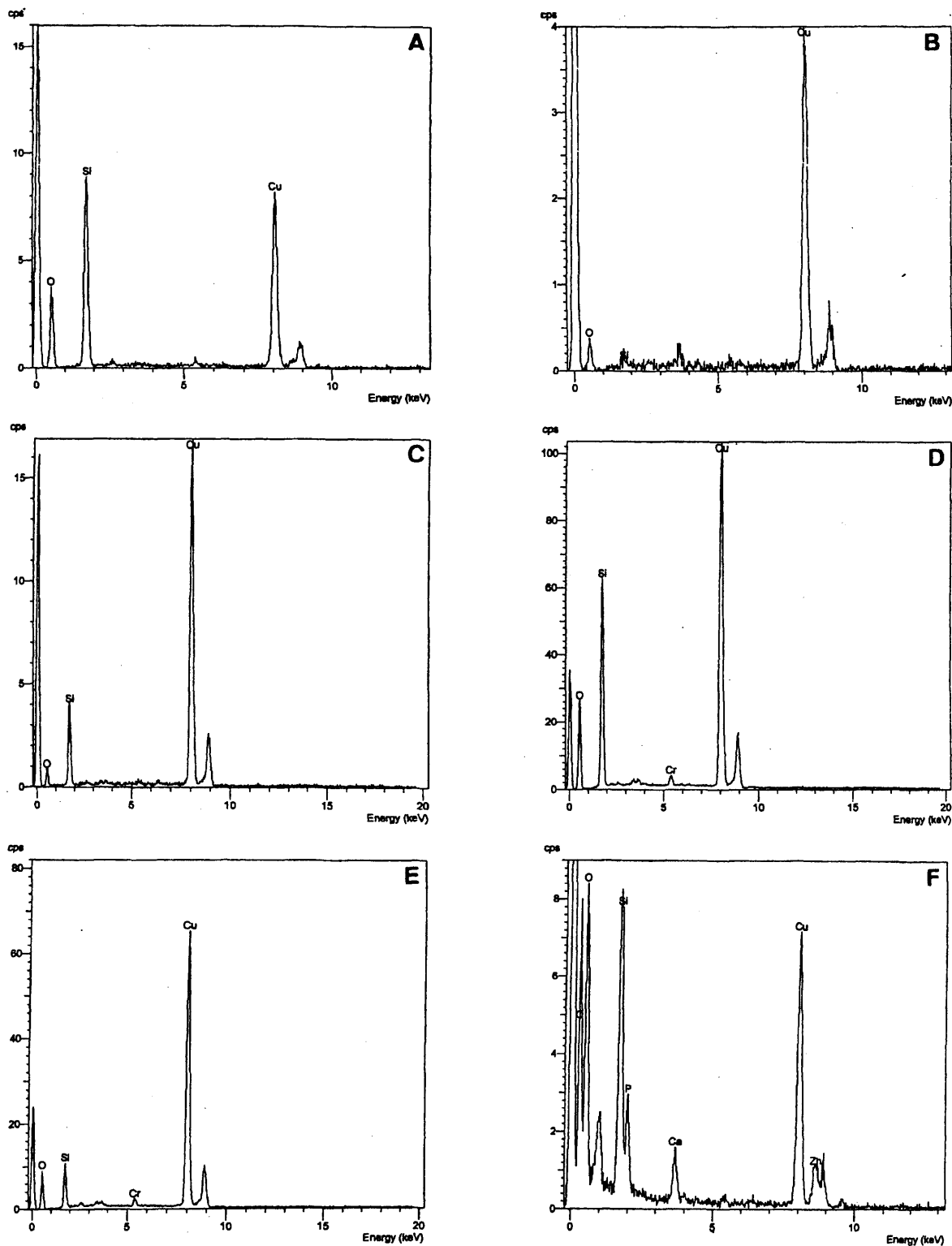


Figure 5. A–F. Spectra of EDX-analysis documenting silica in *Selaginella* megaspore walls. A and B. *S. denticulata*: spectra detecting silica in the outer exospore (A) and a very small amount in the exospore (B). A star in Fig. 2 B and C marks the areas from which these analyses were taken. C. *S. peruviana*: spectrum detecting silica in the outer exospore. A star in Fig. 2 D marks the area from which this analysis was taken. D and E. *S. sp. 1*: spectra detecting silica in the outer exospore (D) and the exospore (E). A star in Fig. 2 F and G marks the areas from which these analyses were taken. F. *S. sp. 2*: spectrum for the fine grains seen around the units of the exospore, which contain silica (see also Fig. 3 C) as well as various other elements such as phosphorus, calcium and zinc. A star in Fig. 3 C marks the area from which this analysis was taken.

1 aromatics (De Leeuw & Largeau, 1993; Bergen
 et al. 1995; Wiermann, 2001, Dominguez,
 Mercado, Quesada & Heredia, 1999). Latest results
 5 suggest that long-chain (C24–28) highly aliphatic
 units form the core of this macromolecule, cross-
 linked with cinnamic acids (Bergen, Blokker,
 Collinson, Sinninghe Damste & De Leeuw,
 2004). The presence of cinnamic acids was also
 shown by Ahlers, Lambert & Wiermann, (2003) in
 10 *Typha angustifolia* L. pollen.

The underlying pattern formation process, giving
 rise to the micro-sculptures described above, has not
 yet been investigated. However, new insights into
 the formation of spore walls have been gained by
 15 experimental approaches, clearly demonstrating that
 spore and pollen walls are subject to self-assembling
 mechanisms (Hemsley et al. 1994; Hemsley,
 Jenkins, Collinson & Vincent, 1996; Hemsley,
 Vincent, Collinson & Griffiths, 1998; Hemsley &
 20 Griffiths, 2000; Hemsley, Collinson, Vincent,
 Griffiths & Jenkins, 2000; Hemsley et al. 2003).
 Patterns of infraspecific and infra-individual varia-
 bility in pollen grains also indicate the involvement
 of self-assembly rather than complete genetic control
 25 of pattern formation (Borsch & Wilde, 2000). It
 would therefore seem that the variability of micro-
 sculpture of the outer exospore coating maybe the
 result of self-assembly processes. In this study no
 correlation between spore (micro-) sculpture and
 30 ultrastructure is found. This could be seen as adding
 weight to a self- assembly hypothesis.

35 *Ontogeny of outer exospore coatings*

Concerning the origin of silica in *Selaginella* spore
 walls, the tapetum is commonly considered as a
 source of peri- and exospore material (Pacini,
 Franchi & Hesse, 1985). In *Selaginella* a periplas-
 40 modal tapetum was described by Pacini & Franchi
 (1991). There is little evidence in the literature that
 the tapetum is the source of silica in *Selaginella*
 megaspores, though Taylor (1992) strongly favours
 this hypothesis for *Isoetes*. Results of the EDX-
 45 analyses clearly demonstrate that in the samples
 studied, silica may be distributed throughout the
 entire exospore, as seen in *S. sp. 3* (Fig. 5 F). This
 distribution pattern was also documented by Kempf
 (1970), Tryon & Lugardon (1978) and Morbelli
 (1995). Hence it is assumed that during spore
 50 development silica moves through the exospore
 and is, at the very final stage of maturation,
 deposited as a more or less thick layer. Some silica
 particles even remain within the exospore after
 maturation. Whether silica is derived from the
 55 tapetum or interconnected with the different spor-
 oderm layers throughout spore wall development

will remain unclear until more results are available. 1
 Even a combination of both is possible but would
 also need verification.

5 *Homology of outer exospore coatings/Terminology*

So far, there has been little consideration of
 homology of outer exospore coatings. Taylor
 (1992) argued that the siliceous coating should not
 be called perispore as it does not follow the
 10 definitions by Erdtman (1952), Kempf (1973) and
 Lugardon (1978). The definition of perispore has
 been discussed controversially since Russow coined
 the word (1872). Further investigations will be
 necessary to elucidate the underlying mechanism
 15 responsible for the distribution of silica throughout
 the exospore and its appearance as an electron dense
 outer layer, which will eventually clarify whether the
 siliceous coating is indeed a perispore.

According to this study, the role of silica in the
 sporoderm has a much greater impact on aspects of
 terminology and homology than might be expected
 (Kempf 1970, Tryon & Lugardon 1978, Taylor
 20 1989). If present throughout *Selaginella*, as it is in
Isoetes (Taylor 1992) then precision is needed in
 describing microsculpture depending on whether
 one is viewing a sporopollenin or silica sculpture.

Inconsistency in *Selaginella* megaspore wall termi-
 25 nology was noted by Minaki (1984), and led to a
 summary of sporoderm terminology from the 1960s
 to the time of his study. An updated overview on the
 terms used for the ultrastructure (after Minaki 1984)
 is presented herein (Table I). Tryon & Lugardon
 (1978) also discussed the non-conformity of termi-
 30 nology and additionally looked at the homology
 aspect of *Selaginella* and *Isoetes* megaspore walls.
 They came to the conclusion that the sporoderm
 layers of both genera are not homologous. From our
 own investigations of *Selaginella* megaspore walls
 and previous publications by Taylor (1993) and
 35 Macluf, Morbelli & Giudice (2003) on *Isoetes*, we
 strongly suggest a homology of the sporoderm
 layers in the megaspores of both genera. If our
 suggestion that silica is widespread in *Selaginella*,
 then both genera share a siliceous outer coating,
 followed by an (outer and inner) exospore, an inner
 40 separable layer and the intine [terminology follow-
 ing Taylor (1989)]. Moreover, habitat is a known
 factor for intraspecific variability, as described for
Schizaea pectinata L. (Sw.) spores by Parkinson
 (1994). Her work demonstrated that *S. pectinata*
 45 species from two very different South African
 habitats show noticeable differences in spore
 morphology and ultrastructure. Therefore, we
 favour the view that the incorporation of more
 50 silica in the exospore of

Table I. *Selaginella* sporoderm terminology, modified after Minaki (1984).

Reference	<i>Selaginella</i> sporoderm layers (from the outer to the inner)			
Morbelli (1995)		outer exospore (oe)	inner exospore (ie)	
Taylor (1989)	siliceous coating	(outer) exospore	inner separable layer (ISL)	intine
Minaki (1984)	outer sclerine (OS)	middle sclerine (MS)	inner sclerine (IS)	endospore (En)
Tryon & Lugardon (1978, 1990)	silica (Si)	outer exospore (Ee)	inner exospore (Ei)	endospore (En)
Kempf (1970)	silification	perine	Exine	intine
Stainier (1965)	perispore	exospore	mesospore	endospore

Isoetes than in *Selaginella* might also be influenced by the habitat, as earlier discussed by (Taylor 1992).

With the contribution of phylogenetic studies in this area of research, *Isoetes* and *Selaginella* have commonly been accepted as sister groups within the Lycophytina (Kenrick & Crane, 1997; Korall et al. 1999; Pryer et al. 2001; Korall & Kenrick, 2004). This reinforces our view that they share similar mechanisms for spore development and ultimately form homologous spore wall layers. *Isoetes* and *Selaginella* sporoderm layers as well as their terminology are summarised (Fig. 6).

The terminology of pollen and spore characters differs in light-, scanning electron- and transmission electron microscopy. A generally accepted nomenclature of pollen and spores is represented by the Glossary of Pollen and Spore Terminology (Punt et al. 1994) defining the term sculpture as "the surface relief, or topography, of a pollen grain or spore". A study on the evolution of primitive angiosperm pollen undermines this definition

(Walker, 1974) pointing out that for the use of pollen wall morphology in an evolutionary context the understanding of the palynological concept of structure versus sculpture must be clear. Both terms are often used interchangeably by various authors. Whereas structure strictly refers to sporoderm layers recognised by TEM, a light microscope or the SEM can generally only characterise sculpture, unless spores are large enough to permit analyses of cross sections. Terminology must reflect homology to be useful in modern evolutionary analyses. Past terminologies have commonly been derived from different sources leading to duplication and potentially misleading overlap. Micro-sculpturing of any particular homologous wall unit will be homologous and should offer potentially useful characters. However, sculpturing at any scale is of no use if there is lack of certainty with respect to the validity and unity of wall layer terminology. It remains to be determined whether micro-sculpturing is uniquely a feature of the outer exospore and not just a feature

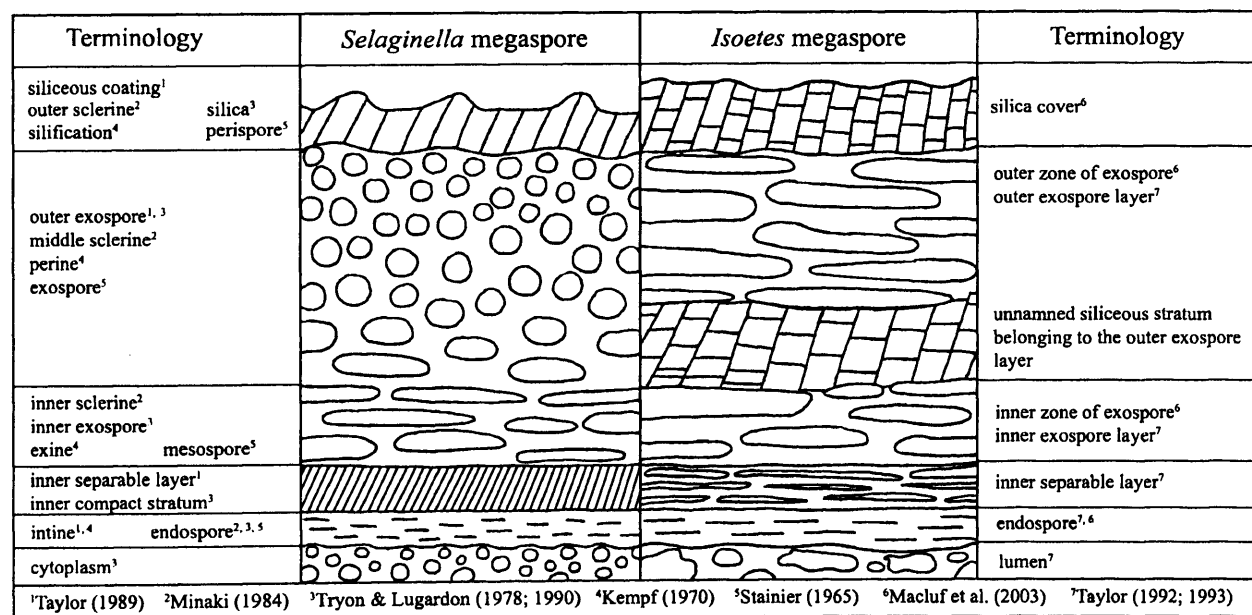


Figure 6. Comparison of *Selaginella* and *Isoetes* megaspore walls suggesting homology, including commonly used terminology by various authors.

common to the outsides of spores from whatever layers they may be composed. Only if micro-sculpturing is consistently associated with outer exospore can this feature be reliably used in detailed systematic studies.

Acknowledgements

The authors would like to thank Prof. W. Barthlott for granting this project and Dr. V. Wilde for helpful discussions as well as two anonymous referees for their valuable comments. The technical assistance of L. Axe and M. Turner was much appreciated.

Specimens Investigated

Selaginella denticulata (L.) Spring. France: Corsica. S. Moore 14 (BONN). BG Bonn 10740

S. helvetica (L.) Spring. *Incertae sedis*. S. Moore 15 (BONN BG). Bonn 00166-90

S. peruviana (Milde) Hieron. Ecuador. S. Moore 7 (BONN). BG Bonn 00737 ex BG Heidelberg

Selaginella sp.1. Rwanda. E. Fischer 6116 (KBL). BG Bonn 14599

Selaginella sp.2. *Incertae sedis*. S. Moore 4 (BONN). BG Bonn 15014 ex BG Osnabrück

References

- Ahlers, F., Lambert, J., & Wiermann, R. (2003). Acetylation and silylation of piperidine solubilized sporopollenin from pollen of *Typha angustifolia* L. *Z. Naturforsch.*, *58*, 807–811.
- Bajpai, U., & Maheshwari, H. K. (1986). SEM study of megaspore sporoderm of some Indian *Selaginellas*. *Phytomorphology*, *36*, 43–51.
- Bateman, R. M., & DiMichele, W. A. (1994). Heterospory: The most iterative key innovation in the evolutionary history of the plant kingdom. *Biol. Rev.*, *69*, 345–417.
- Bek, J., Oplustil, S., & Drabkova, J. (2001). Two species of *Selaginella* cones and their spores from the Bohemian Carboniferous continental basins of the Czech Republic. *Rev. Palaeobot. Palynol.*, *114*, 57–81.
- Bergen, P. F., van, Blokker, P., Collinson, M. E., Sinnighe Damste, J. S., & De Leeuw, J. W. (2004). Structural biomacromolecules in plants: What can be learnt from the fossil record? In A. R. Hemsley, & I. Poole (Eds), *The evolution of plant physiology* (pp. 133–154). London: Acad. Press.
- Bergen, P. F., van, Collinson, M. E., Briggs, D. E. G., De Leeuw, J. W., Scott, A. C., & Evershed, R. P., et al. (1995). Resistant biomacromolecules in the fossil record. *Acta Bot. Neerl.*, *44*, 319–342.
- Borsch, T., & Wilde, V. (2000). Pollen variability within species, populations, and individuals, with particular reference to *Nelumbo nucifera*. In M. Harley, C. Morton, & S. Blackmore (Eds), *Pollen and spores: Morphology and biology* (pp. 285–299). Kew: R. Bot. Gards.
- Buchen, B., & Sievers, A. (1978a). – Megasporogenese von *Selaginella* I. Ultrastrukturelle und zytologische Untersuchungen zur Sekretion von Polysacchariden. *Protoplasma*, *96*, 293–317.
- Buchen, B., & Sievers, A. (1978b). – Megasporogenese von *Selaginella* II. – Ultrastrukturelle und zytologische Untersuchungen zur Sekretion von Lipiden. *Protoplasma*, *96*, 319–328.
- Cottnam, C. F., Hemsley, A. R., Rößler, R., Collinson, M. E., & Brain, A. P. R. (2000). Diversity of exine structure in Upper Carboniferous (Westphalian) Selaginellalean megaspores. *Rev. Palaeobot. Palynol.*, *109*, 33–44.
- Crang, R. E., & May, G. (1974). Evidence for silicon as a prevalent elemental component in pollen wall structure. *Can. J. Bot.*, *52*, 2171–2174.
- De Leeuw, J. W., & Largeau, C. (1993). A review of the macromolecular organic compounds that comprise living organisms and their role in kerogen, coal and petroleum formation. In M. H. Engel, & S. A. Macko (Eds), *Organic geochemistry: Principles and applications* (pp. 23–72). New York: Plenum Press Publ. Group.
- Dengler, N. G. (1983). The developmental basis of anisophyly in *Selaginella martensii* I. – Initiation and morphology of growth. *Am. J. Bot.*, *70*, 181–192.
- DiMichele, W. A., Davis, J. I., & Olmstead, R. G. (1989). Origins of heterospory and the seed habit: The role of heterochrony. *Taxon*, *38*, 1–11.
- Dominguez, E., Mercado, J. A., Quesada, M. A., & Heredia, A. (1999). Pollen sporopollenin: Degradation and structural elucidation. *Sex. Pl. Reprod.*, *12*, 171–178.
- Duerden, H. (1929). Variations in megaspore numbers in *Selaginella*. *Ann. Bot.*, *43*, 451–457.
- Erdtman, G. (1952). *An introduction to palynology. 1 (Pollen morphology and plant taxonomy: Angiosperms)*. Stockholm: Almqvist & Wiksell.
- Glasspool, I. J. (2003). A review of Permian Gondwana megaspores, with particular emphasis on material collected from coals of the Witbank Basin of South Africa and the Sydney Basin of Australia. *Rev. Palaeobot. Palynol.*, *124*, 227–296.
- Grebe, H. (1971). A recommended terminology and descriptive terminology and descriptive methods for spores. In *Microfossils Organiques du Paleozoic* (pp. 7–34). – CIMP Sp.
- Haig, D., & Westoby, M. (1988). A model for the origin of heterospory. *J. Theor. Biol.*, *134*, 257–272.
- Hebant, C., & Lee, D. W. (1984). Ultrastructural basis and developmental control of blue iridescence in *Selaginella* leaves. *Am. J. Bot.*, *71*, 216–219.
- Hemsley, A. R., & Griffiths, P. C. (2000). Architecture in the microcosm: Biocolloids, self-assembly and pattern formation. *Philos. Trans. R. Soc. London A*, *358*, 547–564.
- Hemsley, A. R., Collinson, M. E., & Brain, A. P. R. (1992). Colloidal crystal-like structure of sporopollenin in the megaspore walls of recent *Selaginella* and similar fossil spores. *Bot. J. Linn. Soc.*, *108*, 307–320.
- Hemsley, A. R., Griffiths, P. C., Mathias, R., & Moore, S. E. M. (2003). A model for the role of surfactants in the assembly of exine sculpture. *Grana*, *42*, 38–42.
- Hemsley, A. R., Jenkins, P. D., Collinson, M. E., & Vincent, B. (1996). Experimental modelling of exine self-assembly. *Bot. J. Linn. Soc.*, *121*, 177–187.
- Hemsley, A. R., Vincent, B., Collinson, M. E., & Griffiths, P. C. (1998). Simulated self-assembly of spore exines. *Ann. Bot.*, *82*, 105–109.
- Hemsley, A. R., Collinson, M. E., Kovach, W. L., Vincent, B., & Williams, T. (1994). The role of self-assembly in biological systems: Evidence from iridescent colloidal sporopollenin in *Selaginella* megaspore walls. *Philos. Trans. R. Soc. London B*, *345*, 163–173.
- Hemsley, A. R., Collinson, M. E., Vincent, B., Griffiths, P. C., & Jenkins, P. D. (2000). Self-assembly of colloidal units in exine development. In M. Harley, C. Morton, & S. Blackmore (Eds), *Pollen and spores: Morphology and biology* (pp. 31–44). Kew: R. Bot. Gards.

- Holmgren, P. K., Holmgren, N. H., & Barnett, L. C. (1990). *Index Herbariorum*. 8th ed. Bronx NY: NY Bot. Gard. Press.
- Horner, H. T. J., & Arnott, H. J. (1963). Sporangial arrangement in North American species of *Selaginella*. *Bot. Gaz. (Crawfordsville)*, 124, 371–383.
- Horner, H. T. J., Beltz, K., Jagels, R., & Boudreau, R. E. (1975). Ligule development and fine structure in two heterophyllous species of *Selaginella*. *Can. J. Bot.*, 53, 127–143.
- Kempf, E. K. (1970). Elektronenmikroskopie der Sporodermis von Megasporen der Gattung *Selaginella* (Pteridophyta). *Rev. Palaeobot. Palynol.*, 10, 99–116.
- Kempf, E. K. (1973). Transmission electron microscopy of fossil spores. *Palaeontology*, 16, 787–797.
- Kenrick, P., & Crane, P. R. (1997). The origin and early evolution of plants on land. *Nature*, 389, 33–39.
- Korall, P., & Kenrick, P. (2002). Phylogenetic relationships in Selaginellaceae based on rbcL sequences. *Am. J. Bot.*, 89, 506–517.
- Korall, P., & Kenrick, P. (2004). The phylogenetic history of Selaginellaceae based on DNA sequences from the plastid and nucleus: Extreme substitution rates and rate heterogeneity. *Molec. Phylogen. Evol.*, 31, 852–864.
- Korall, P., Kenrick, P., & Therrien, J. P. (1999). Phylogeny of Selaginellaceae: Evaluation of generic/subgeneric relationships based on rbcL gene sequences. *Int. J. Pl. Sci.*, 160, 585–594.
- Lyon, F. M. (1901). A study of the sporangia and gametophytes of *Selaginella apus* and *Selaginella rupestris*. *Bot. Gaz.*, 32, 124–141.
- Lugardon, B. (1978). Isospore and microspore walls of living Pteridophytes: Identification possibilities with different observation instruments. In D. C. Bharadwaj, K. M. Lele, & R. K. Kar (Eds), 4th Int. Palynol. Conf., Lucknow 1976. *Proc. Vol. I* (pp. 152–163). Lucknow: B. Sahni Inst. Palaeobot.
- Macluf, C. C., Morbelli, M. A., & Giudice, G. E. (2003). Morphology and ultrastructure of megaspores and microspores of *Isoetes savatieri* Franchet (Lycophyta). *Rev. Palaeobot. Palynol.*, 126, 197–209.
- Minaki, M. (1984). Microspore morphology and taxonomy of *Selaginella* (Selaginellaceae). *Pollen Spores*, 24, 421–480.
- Morbelli, M. A. (1995). Megaspore wall in Lycophyta – ultrastructure and function. *Rev. Palaeobot. Palynol.*, 85, 1–12.
- Morbelli, M. A., & Rowley, J. R. (1993). Megaspore development in *Selaginella*. I. “Wicks”, their presence, ultrastructure and presumed function. *Sex. Pl. Reprod.*, 6, 98–107.
- Morbelli, M. A., & Rowley, J. R. (1999). Megaspore development in *Selaginella*: The gap and the megaspore. *Pl. Syst. Evol.*, 217, 221–243.
- Pacini, E., & Franchi, G. G. (1991). Diversification and evolution of the tapetum. In S. Blackmore, & S. H. Barnes (Eds), *Pollen and spores: Pattern of diversification* (pp. 301–316). Oxford: Clarendon Press.
- Pacini, E., Franchi, G. G., & Hesse, M. (1985). The tapetum: Its form, function and possible phylogeny in Embryophyta. *Pl. Syst. Evol.*, 149, 155–185.
- Page, C. N. (1989). Compression and slingshot megaspore ejection in *Selaginella selaginoides* – a new phenomenon in Pteridophytes. *Fern Gazette*, 13, 267–275.
- Parkinson, B. M. (1994). Morphological and ultrastructural variations in *Schizaea pectinata* (Schizaeaceae). *Bothalia*, 24, 203–210.
- Pettitt, J. M. (1977). Developmental mechanisms in heterospory: Features of post-meiotic regression in *Selaginella*. *Ann. Bot.*, 41, 117–125.
- Playford, G., & Dettmann, M. E. (1996). Spores. In J. Jansonius, & D. C. McGregor (Eds), *Palynology: Principles and applications* (pp. 227–260). Salt Lake City CO: AASP Found.
- Pryer, K. M., Schneider, H., Smith, A. R., Cranfill, R., Wolf, P. G., & Hunt, J. S., et al. (2001). Horsetails and ferns are a monophyletic group and the closest living relatives to seed plants. *Nature*, 409, 618–622.
- Punt, W., Blackmore, S., Nilsson, S., & Le Thomas, A. (1994). *Glossary of pollen and spore terminology*. Utrecht: LPP Ser. 1. LPP Found.
- Quandt, D., Müller, K., Stech, M., Hilu, K. W., Frahm, J. P., & Borsch, T. (in press). Molecular evolution of the chloroplast trnL-F region in land plants. *Ann. Mo. Bot. Gard.*
- Quandt, D., Müller, K., Stech, M., Hilu, K. W., Frey, W., Frahm, J.-P., & Borsch, T. (2004). Molecular evolution of the chloroplast trnL-F region in land plants. In B. Goffinet, V. Hollowell, & R. Magill (Eds), *Molecular Systematics of Bryophytes*.
- Russow, E. (1872). Vergleichende Untersuchungen betreffend die Histologie (Histographie und Histologie) der vegetativen und sporenbildenden Organe und Entwicklung der Sporen der Leitbündel- Kryptogamen mit Berücksichtigung der Phanerogamen, ausgehend von Betrachtung der Marsiliaceen. *Méms Acad. Imp. Sci., St. Pétersbourg*, 7, 1–207.
- Schelpé, E. A. C. L. E. (1970). *Flora Zambesiaca*. London: Crown Ag. Overs. Gov. Admin.
- Sievers, A., & Buchen, B. (1970). Über den Feinbau der wachsenden Megaspore in *Selaginella*. *Protoplasma*, 71, 267–279.
- Taylor, W. A. (1989). Megaspore wall ultrastructure in *Selaginella*. *Pollen Spores*, 31, 251–288.
- Taylor, W. A. (1991). Ultrastructural analysis of sporoderm development in megaspores of *Selaginella galeottii* (Lycophyta). *Pl. Syst. Evol.*, 174, 171–182.
- Taylor, W. A. (1992). Megaspore wall development in *Isoetes melanopoda*: Morphogenetic post-initiation changes accompanying spore enlargement. *Rev. Palaeobot. Palynol.*, 72, 61–72.
- Taylor, W. A. (1993). Megaspore wall ultrastructure in *Isoetes*. *Am. J. Bot.*, 80, 165–171.
- Tryon, A. F., & Lugardon, B. (1978). Wall structure and mineral content in *Selaginella* spores. *Pollen Spores*, 20, 316–340.
- Tryon, A. F., & Lugardon, B. (1990). *Spores of the Pteridophyta*. New York: Springer.
- Walker, J. W. (1974). Evolution of exine structure in the pollen of primitive angiosperms. *Am. J. Bot.*, 61, 891–902.
- Weber, M. (2004). Unique pollen features in Araceae. In J. L. Ubera (Ed.), 11th Int. Palynol. Congr., Granada 2004. *Abstracts* (pp. 18). Cordoba: Argos Impres, *Polen* 14.
- Weber, M., Halbritter, H., & Hesse, M. (1999). The basic pollen wall types in Araceae. *Int. J. Pl. Sci.*, 160, 414–423.
- Webster, T. R. (1992). Developmental problems in *Selaginella* (Selaginellaceae) in an evolutionary context. *Ann. Mo. Bot. Gard.*, 79, 632–647.
- Wiermann, R. (2001). Sporopollenin. In H. Steimbuchel, & M. Hofrichter (Eds), *Biopolymers. Vol. I. Lignin, humic substances and coal* (pp. 221–227). Weinheim; Wiley VCH.

Appendix 2

Moore *et al.* in press b (PROTOPLASMA): UNCORRECTED PROOF

New insights from MALDI-ToF MS, NMR and GS-MS: mass spectrometry techniques applied to palynology

SUSANNAH E. M. MOORE, ALAN R. HEMSLEY, ANDREW N. FRENCH, ED
DUDLEY AND RUSSELL P. NEWTON

New insights from MALDI-ToF MS, NMR and GC-MS: mass spectrometry techniques applied to palynology

S.E.M. Moore et al., Mass spectrometry techniques applied to palynology

S.E.M. Moore^{1,*}, A.R. Hemsley¹, A.N. French^{2**}, E. Dudley³, R. P. Newton³

¹Laboratory for Experimental Palynology, School of Earth, Ocean and Planetary Sciences, Cardiff University, Park Place, Cardiff CF10 3YE, UK, ²School of Chemistry, Cardiff University, Park Place, Cardiff CF10 3TB, UK, ³Biomolecular Analysis Mass Spectrometry Centre (BAMS), and Biochemistry Group, School of Biological Sciences, University of Wales Swansea, Singleton Park, Swansea. SA2 8PP. Wales, UK

*Correspondence and reprints: School of Earth, Ocean and Planetary Sciences, Cardiff University, Park Place, Cardiff CF10 3YE, UK. E-mail: MooreS@cf.ac.uk,
Tel.: +44 2920 876213, Fax: +44 2920 874326

** Associate Professor of Chemistry, Albion College, Albion, MI 49224, USA

New insights from MALDI-ToF MS, NMR and GC-MS: mass spectrometry techniques applied to palynology

S.E.M. Moore^{1,*}, A.R. Hemsley¹, A.N. French^{2**}, E. Dudley³, R. P. Newton³

¹Laboratory for Experimental Palynology, School of Earth, Ocean and Planetary Sciences, Cardiff University, Park Place, Cardiff CF10 3YE, UK, ²School of Chemistry, Cardiff University, Park Place, Cardiff CF10 3TB, UK, ³Biomolecular Analysis Mass Spectrometry Centre (BAMS), and Biochemistry Group, School of Biological Sciences, University of Wales Swansea, Singleton Park, Swansea. SA2 8PP. Wales, UK

Received

Accepted

*Correspondence and reprints: School of Earth, Ocean and Planetary Sciences, Cardiff University, Park Place, Cardiff CF10 3YE, UK. E-mail: MooreS@cf.ac.uk

** Associate Professor of Chemistry, Albion College, Albion, MI 49224, USA

Summary. The present study for the first time describes the application of matrix-assisted laser desorption ionisation time-of-flight mass spectrometry (MALDI-ToF MS) to palynology. With an accessible mass range of up to about 350, 000 Da at subpicomolar range, this technique is ideal for the characterisation of bio-macromolecules, such as sporopollenin, found in fossil and extant pollen and spore walls, which often can only be isolated in very low quantities. At this stage the limited solubility of sporopollenin allows for the identification of sections of this biopolymer but with the optimisation of MALDI-ToF matrices, further structure elucidation will become possible. Furthermore, gas chromatography mass spectrometry (GC-MS) and ¹H nuclear magnetic resonance (¹H NMR) spectroscopy data obtained from a number of experiments revealed that some previously reported data were misinterpreted. These results add support to the hypothesis that common plasticizers were wrongly described as sporopollenin compounds.

Keywords: Sporopollenin; *Lycopodium clavatum* L.; *Selaginella laevigata* (Willd.); *Pinus sylvestris* L.;

Abbreviations FT-IR Fourier-transform infrared spectroscopy; GC-MS gas chromatography mass spectrometry; HPLC high performance liquid phase chromatography; MALDI-ToF MS matrix-assisted laser desorption ionisation time of flight mass spectrometry; MMNO N4-methylmorpholine *N*-oxide monohydrate; NMR nuclear magnetic resonance (¹³C carbon, ¹H proton); TLC thin layer chromatography

Introduction

For almost two centuries scientist have tried to elucidate the structure of sporopollenin and numerous chemical and instrumental techniques have been adopted for the analysis of this complex bio-macromolecule. In the past two decades these techniques have ranged from chemical extractions (Southworth 1974, 1988; Loewus et al. 1985; Kress 1986; Tarlyn et al. 1993; Rowley et al. 2001), TLC and HPLC (Schulze-Osthoff and Wiermann 1987; Wehling et al. 1989) to spectroscopy techniques such GC-MS (Kawase and Takahashi 1996), ¹³C- and ¹H- NMR (Hemsley et al. 1992, 1993, 1994, 1996; Ahlers et al. 1999a and b, 2000, 2003) and FT-IR (Domínguez et al. 1999; Yule et al. 2000). Most authors mentioned above combined several of these techniques in their studies of sporopollenin.

Chemical extraction experiments showed that two solvents have significant effects on spore and pollen walls. 2-Aminoethanol (Southworth 1974; Kress 1986) and MMNO (Loewus et al. 1985; Rowley et al. 2001) have been shown to successfully dissolve outer spore and pollen layers. Wiermann (2001) reviewed various methodologies, including chemical extractions and mass spectrometry techniques in sporopollenin research. A general review on organic macromolecules is given by de Leeuw and Largeau (1993) and van Bergen PF – Shell Global Solutions–Amersterdam–NL, Collinson ME, Blokker P, van Moekerken, Barrie PJ, de Leeuw JW (2004), submitted.

Work using solid state ¹³C - and ¹H- NMR revealed the presence of aromatic, aliphatic, and oxygen functionalities (Hemsley et al. 1994, 1996; Ahlers et al. 1999a, 2000, 2003). Recently, pyrolysis and GC-MS analysis have elucidated a number of structural characteristics of sporopollenin (van Bergen et al. 1995, 2004). This GC-MS work proposes that two principal components of sporopollenin are fatty acids (C₂₄-C₂₈) and oxygenated cinnamic acid derivatives. Latest results, however, show that the

sporopollenin of *Isoetes* megaspores, isolated via a mild chemical treatment and subjected to various mass spectrometry techniques, consists mainly of polymerized *p*-coumaric acid (de Leeuw JW – Netherlands Institute for Sea Research –Texel– NL, Versteegh GJM, van Bergen PF 2004, submitted). No aliphatic compound could be found.

Matrix assisted laser desorption ionisation time-of-flight mass spectrometry (MALDI-ToF MS) is a new 'soft' technique used to ionise compounds from low mass up to approximately 350, 000Da (Kaufmann 1995). It is especially valuable in the detection and characterisation of bio-macromolecules present in mixtures, such as peptides, proteins, glycoconjugates, oligonucleotides and synthetic polymers (Gross and Strupat 1998). Moreover, this technique is characterised by a very high sensitivity in the range of subpicomoles and works with a mass accuracy and precision of 0.1-0.01% (Kaufmann 1995). During the MALDI process the sample is mixed with an excess of a "matrix" compound on a plate. A laser is then fired at the mixture and the energy from the laser is passed from the matrix to the analyte. This process causes ions of the analyte to be produced in the gas phase which are accelerated through a Time of Flight (ToF) tube in which they travel at a speed related to their mass and are detected by a mass analyser to generate the mass spectrum. MALDI-ToF was used in the present study primarily as it allows the detection of compounds of high and low mass with improved sensitivity over previous methods of mass spectrometric analysis. The present study investigates the use of MALDI-ToF MS as a method for the elucidation of the structure of sporopollenin and discusses its possible applications in palynology.

In a separate study, ¹H NMR and GC-MS data were generated from experiments with pine tree pollen. The results obtained agree with several compounds described in studies by Kawase and Takahashi (1996) and Ahlers et al. (1999b). These results lead to the hypothesis that in the past ¹H NMR and GC-MS data were misinterpreted, describing impurities as sporopollenin compounds.

Material and methods

MALDI ToF MS

Purification of sporopollenin: 0.025 g *Selaginella laevigata* (Willd.) megaspores and 0.1 g *Lycopodium clavatum* L. isospores were collected at the Talybont Research Gardens, Cardiff. The spore samples were washed five times with distilled water and acetone, followed by a 6 hour treatment of a) 80-90°C 5M NaOH b) 80-90°C 3M HCl c) 80-90°C 2-aminoethanol treatment (all chemicals

purchased from Fisher Scientific, UK). The spore powder obtained from this treatment was subjected to MALDI-ToF MS.

MALDI-ToF MS: all chemicals used were purchased from Sigma Aldrich (Dorset, UK). Purified water was produced in-house using an Elix water purification system (Millipore, UK). A proportion of the sporopollenin samples was dissolved in 5µl of a 10mg/ml solution of 3-indoleacrylic acid in 50/50 acetonitrile/ water. This was vortex mixed and a 1µl aliquot was taken and allowed to dry on the MALDI plate. The plate was introduced into a Voyager DE-STR MALDI mass spectrometer and spectra were obtained in both positive and negative ionisation mode using linear mode analysis, an acceleration voltage of 25000V, an extraction delay time of 750ns, 50 laser shots per spectrum and a mass range of 50-100, 000Da.

¹H NMR and GC-MS

1 g of pollen of *Pinus sylvestris* L., collected at the Talybont Research Gardens, Cardiff, was washed in acetone, incubated in hot (80°C) MMNO for 30 minutes, and cooled to room temperature. Distilled water was added, and the solution was extracted with Et₂O (10ml) and 0.1µl of the product injected into an GC-MS Saturn II, Varian 3400 gas chromatograph. The analysis followed the specifications of Kawase and Takahashi (1996) and was performed on a DB5-MS capillary column (30 m × 0.25 mm, 0.5 µm), 5%-phenyl-methylpolysiloxane, non-polar, (JW Scientific, Folsom, CA). From the same experiment a ¹H NMR spectrum was obtained, performed on a Bruker DPX 400 MHz NMR Spectrometre. All ¹H NMR were recorded at room temperature CDCl₃ (*d*-Chloroform) with tetramethylsilane as internal standard (0ppm). Parallel to this experiment with spores, a blank using exactly the same chemicals and glassware was carried out without spores present. The solution obtained from this control experiment was subjected to ¹H NMR.

In a further experiment a new set of spore powder was prepared (see purification process as described above) with 0.025 g *Selaginella laevigata* megaspores, the powder was then acetylated in a solution of 3:1 acetic anhydride:acetyl chloride for 8 hours at 70-80°C. The product was neutralised with NaCO₃, extracted with Et₂O, concentrated, and both a GC-MS and an ¹H NMR spectrum were obtained.

Results

MALDI ToF MS

The results from *S. laevigata* and *L. clavatum* are shown in Fig. 1. The MALDI-ToF mass spectra obtained from spores extracted with a base, acid and solvent treatment should represent pure sporopollenin. Both indicate ions at approximately m/z 8000 and 4400 to 4800 with the *L. clavatum* analysis also generating ions between m/z 6936 and 7588 (in positive ionisation mode) and at m/z 17654. The differences in mass between these ions suggest that they are not related purely by simple dimerisation of the smallest suspected sporopollenin monomer molecule (*p*-coumaric acid). The must therefore arise from complex arrangements possibly between different subunits or between subunits representing *p*-coumaric acid and co-complexing moieties of differing masses.

¹H NMR and GC-MS

The GC-MS spectrum for *P. sylvestris* pollen shows two components at retention times of 24.54min and 50.10min, respectively, as well as a range of smaller peaks between 30-45.00 (Fig. 2a). At 24.54 min mass peaks (I, %) of: 281 (<1%); 220 (21%); 205 (BP, 100%); 177 (17%); 155 (5%); 145 (10%); 105 (9.5%); 91 (10.5%); 77 (9%); 57 (35%); 40 (27%) are presented. A library search identified this peak as 2,6-bis(1,1-dimethylethyl)-4-methyl phenol (Fig. 5a). At 50.10 min mass peaks m/z (I, %) are: 391 (2%); 279 (11%); 207 (1%); 167 (44%); 149 (BP, 100%); 121 (2%); 104 (4%); 83 (9.5%); 71 (27%); 57 (41%); 40 (52%). This peak was identified as 1,2 benzenedicarboxylic acid, diisooctyl ester (Fig. 4a). Several small peaks around 30-45.00 min were identified as 1,1,1,3,5,7,9,9,9-nonamethylpentasiloxane.

The GC-MS spectrum for the acetylated *S. laevigata* megaspore powder is identical with that of *P. sylvestris* pollen, only the intensities of the shifts at 50.18 min vary (Fig. 2). The spectrum also shows two peaks at a retention time of 24.57 and 50.18 min. At 24.57 min m/z (I, %) is: 281(<1%); 220 (21%); 205 (BP, 100%); 177 (17%); 155 (5%); 145 (10%); 105 (9.5%); 91 (10.5%); 77 (9%); 57 (35%); 40 (27%). Again, this peak was identified as 2,6-bis(1,1-dimethylethyl)-4-methyl phenol (Fig. 5a). At 50.18 min m/z (I, %) is: 391 (<1%); 279 (21%); 207 (5%); 167 (44%); 149 (BP, 100%); 121 (2%); 104 (4%) ; 83 (12%); 71 (31%); 57 (41%); 40 (57%). This peak was also identified as 1,2 benzenedicarboxylic acid, diisooctyl ester (Fig. 4a).

The ^1H NMR spectra obtained from all experiments with *P. sylvestris* pollen, including the blank, are identical (Fig. 3a-c). They only differ in shift intensity. Shifts can be found in the range of ppm: 0.7-0.9, 1.1-1.25, 1.4, 1.5-1.7, 1.9, 2.1, 2.2, 3.3-3.4, 3.7, 4.1-4.2, 4.9, 6.9, 7.2 (*d*-chloroform), 7.55 and 7.64.

The ^1H NMR spectrum obtained from acetylated *S. laevigata* megaspore powder is almost identical to that of *P. sylvestris* pollen. The only difference found is in the area of 3.7ppm, which is not present in the spectrum of the acetylated *S. laevigata* megaspore powder.

Discussion

MALDI ToF MS

Results obtained from purified sporopollenin of *S. laevigata* and *L. clavatum* were reasonable in both positive and negative ionisation modes. Positive ion generation and detection gave more components and those present were of higher relative abundance compared to negative ions generated. The results at high mass indicate only ions up to approximately 18,000 Da. It is thought that sporopollenin has a mass higher than this and that the insolubility of the “intact” macromolecule currently limits its entire isolation. However, the ions detected presumably arise from fragmentation of the intact sporopollenin, releasing sections of the polymer. These sections are more soluble and can co-crystallise more efficiently with the matrix compounds utilised for ionisation, hence ions were detected in sporopollenin of both *S. laevigata* and *L. clavatum*.

In the present study for the first time MALDI-ToF MS has been applied to palynology and to sporopollenin research in particular. The results presented show that MALDI-ToF MS is amenable to the analysis of sporopollenin purified from a number of species and for sections of the sporopollenin macromolecule. It is believed that analysis of the intact molecule is currently beyond the ability of the technique due primarily to the insolubility of sporopollenin and the necessity of co-crystallisation of sample and matrix from a solution in which both are soluble. The data generated indicate that soluble components are released from sporopollenin over a mass range from 4000 to 18000 Da and that the relationship between these units is not straightforward and will require further study. Furthermore, the sensitivity of this technique is crucial for the application to palynology, as pollen- and sporewall analyses often do not yield products in high quantities. With the optimisation of matrixes for insoluble

products, like sporopollenin, alongside with the sensitivity of this technique, MALDI-ToF MS is a challenging and promising technique available to palynology.

¹H NMR and GC-MS

The GC-MS results obtained from *P. sylvestris* pollen and *S. laevigata* megaspores show that both spectra are identical. These two spectra were obtained using two completely different methodologies with different chemicals (see Material and methods). The two peaks in each spectrum were identified as 1,2 benzenedicarboxylic acid-diisooctyl ester, better known as a phthalic acid ester. Phthalic acid and their esters are common plasticizers, rubber polymerisation activators and retardants as well as a preservative. The second peak, 2,6-bis(1,1-dimethylethyl)-4-methyl phenol, with the synonym BHT, is also a common plasticizer. The results presented here agree with those of Kawase and Takahashi (1996), as they described the finding of 1,2 benzenedicarboxylic acid butyl 2-ethylhexyl ester (Fig. 4b). Although the chemical structure of the two products (Fig. 4) is not identical, they both classify as phthalates. Kawase and Takahashi (1996) furthermore mentioned the presence of various (trimethylsiloxy)tetrasiloxanes in their spectra. This investigation found 1,1,1,3,5,7,9,9,9-nonamethylpentasiloxane, which derives from the GC-MS column used for the experiments. The column is specified as 5%-phenyl-methylpolysiloxane, non-polar, which, depending of its age, are known to leach siloxane impurities. It would therefore seem that what Kawase and Takahashi (1996) described as silicon cross-linked with sporopollenin is more likely to be an impurity coming from their GC-MS column. Moreover, the data are comparable, as the column they used (Supelco SPB-1) is a poly(dimethylsiloxane) column, which is very similar to the one used in the present study.

From the ¹H NMR results it is clear that the spectra of *P. sylvestris* pollen and *S. laevigata* megaspores as well as that of the blank experiment are identical. This implies that all results obtained from ¹H NMR and GC-MS analyses are impurities. None of the spectra indicated sporopollenin or a compound of this macromolecule. The ¹H NMR spectrum of BHT is characterised by shifts at 6.97, 4.99, 2.27 and 1.4 ppm (Integrated Spectral Data Base System for Organic Compounds No.1196, SDBSWeb: <http://www.aist.go.jp/RIODB/SDBS/>). The corresponding ¹H NMR spectrum of phthalic acid is characterised by shifts at 13, 7.698 and 7.601ppm (Integrated Spectral Data Base System for Organic Compounds No. 3002, SDBSWeb: <http://www.aist.go.jp/RIODB/SDBS/>). All ¹H NMR spectra obtained from our study show shifts in the aromatic region (6-9) at 6.9, 7.55 and 7.64ppm as

well as a number of other shifts correlating with those of either BHT and phthalic acid. It is assumed that other shifts not deriving from the plastizers either come from the acetylation of *S. laevigata* (shifts at around 2.0-2.2ppm) or from other products formed during isolation or acetylation procedures. Although it should not be ignored that in the case of the *P. sylvestris* pollen experiment MMNO might have reacted during the experiments into BHT, the occurrence of BHT in the spectrum of *S. laevigata*, where no MMNO was used, remains unclear. Possible explanations are that traces of plastizers might have contaminated various chemicals as they are often stored in bottles with plastic caps or in plastic bottles. All in all, GC-MS as well as ¹H NMR data agree in characterising common plastizers.

Another ¹H NMR study analysing the pollen of *Typha angustifolia* L. revealed the presence of two “types” of phenolic compounds differing amounts (Ahlers et al. 1999b). Whereas “type I” is described as a 1,2,3,4-tetrasubstituted benzene ring, “type II” is described as a 1,2,3-trisubstituted benzene ring (Fig. 5b). While it is possible that these characterisations may originate from the pollen samples, it is our suspicion that these two types might, in fact, derive from plasticizers, as their overall structure is similar to the one found in the present study (Fig. 5a). The similarity of “type II” and 2,6-bis(1,1-dimethylethyl)-4-methyl phenol (BHT) is noteworthy (Fig. 5a+b). Furthermore, it is questionable that the quantity of 5 mg ml⁻¹ of concentrated sporopollenin used by Ahlers et al. is sufficient to generate reliable ¹H NMR spectra. Not until their isolation protocol is repeated without pollen as a control and the results compared can one be sure that what they described is sporopollenin based and not indicative of plasticizer contamination.

From our work it is clear that the MADLI -ToF spectra presented above are genuine sections of the macromolecule sporopollenin and no impurities since the specific mass of the sections seen in MALDI-ToF analysis are more than an order of magnitude higher in mass (minimum of 4000 m/z) than the phenolic compounds characterised by GC-MS (maximum of 391 m/z). Further studies will be necessary to fully investigate the contamination in GC-MS and ¹H NMR analyses not only of this study but also in that of others.

Acknowledgements

The authors (SEMM) would like to thank Prof. Thomas Wirth (School of Chemistry, Cardiff University) and his research group (especially Raúl Montoro Rueda and Stewart Bissmire) for their support. A special thanks goes to Dipl. Ing. FH Bernd Dirks for inspiring discussions. ANF would like

to thank The Royal Society for a USA Fellowship to Cardiff University during his sabbatical from Albion College, USA.

References

- Ahlers F, Lambert J, Wiermann R (2003) Acetylation and silylation of piperidine solubilized sporopollenin from pollen of *Typha angustifolia* L. *Z. Naturforsch* 58: 807-811
- Ahlers F, Bubert H, Steuernagel S, Wiermann R (2000) The nature of oxygen in sporopollenin from the pollen of *Typha angustifolia* L. *Z. Naturforsch* 55: 129-136
- Ahlers F, Lambert J, Wiermann R (1999a) Structural elements of sporopollenin from pollen of *Toreya californica* Torr. (Gymnospermae): using the ¹H-NMR technique. *Z. Naturforsch* 54: 492-495
- Ahlers F, Thom I, Lambert J, Kuckuk R, Wiermann R (1999b) ¹H NMR analysis of sporopollenin from *Typha angustifolia*. *Phytochemistry* 50: 1095-1098
- Bergen van PF, Blokker P, Collinson ME, Sinninghe Damste JS, De Leeuw JW (2004) Structural biomacromolecules in plants: what can be learnt from the fossil record? In: Hemsley AR, Poole I (ed) *The Evolution of Plant Physiology. From whole plants to ecosystems*. Elsevier, London, pp 133-154
- Bergen van PF, Collinson ME, Briggs DEG, Leeuw De JW, Scott AC, Evershed RP, Finch P (1995) Resistant biomacromolecules in the fossil record. *Acta Bot Neerl* 44: 319-342
- De Leeuw JW, Largeau C (1993) A review of the major classes of organic compounds that comprise living organisms and the pathways for their incorporation into sediments. In: Engel MH, Macko SA (eds) *Organic Chemistry*. Plenum Publishing Group, New York
- De Leeuw JW, Bergen van PF, Aarssen van BGK, Gatellier J-PLA, Sinninghe Damste JS, Collinson ME (1991) Resistant biomacromolecules as major contributors to kerogen. *Phil Trans R Soc London B* 333: 329-337
- Dominguez E, Mercado JA, Quesada MA, Heredia A (1999) Pollen sporopollenin: degradation and structural elucidation. *Sex Plant Reprod* 12: 171-178
- Gross J, Strupat K (1998) Matrix-assisted laser desorption/ionisation-mass spectrometry applied to biological macromolecules. *Trends in Analytical Chem* 17: 470-484
- Hemsley AR, Chaloner WG, Scott AC, Groombridge CJ (1992) Carbon-13 solid state nuclear magnetic resonance of sporopollenins from modern and fossil plants. *Ann Bot* 69: 545-549
- Hemsley AR, Barrie PJ, Chaloner WG, Scott AC (1993) The composition of sporopollenin and its use in living and fossil plant systematics. *Grana Supp.* 1: 2-11
- Hemsley AR, Collinson ME, Kovach WL, Vincent B, Williams T (1994) The role of self-assembly in biological systems: evidence from iridescent colloidal sporopollenin in *Selaginella* megaspore walls. *Phil Trans R Soc London B* 345: 163-173
- Hemsley AR, Scott AC, Barrie PJ, Chaloner WG (1996) Studies of fossil and modern spores wall biomacromolecules using ¹³C solid state NMR. *Ann Bot* 78: 83-94

- Kaufmann R (1995) Matrix-assisted laser desorption ionization (MALDI) mass spectrometry: a novel analytical tool in molecular biology and biotechnology. *J Biotechnol* 41: 155-175
- Kawase M, Takahashi M (1996) Gas chromatography-mass spectrometric analysis of oxidative degradation products of sporopollenin in *Magnolia grandiflora* (Magnoliaceae) and *Hibiscus syriacus* (Malvaceae). *J Plant Res* 109: 297-299
- Integrated Spectral Data Base System for Organic Compounds, SDBSWeb:
<http://www.aist.go.jp/RIODB/SDBS/>, National Institute of Advanced Industrial Science and Technology (AIST), Tokyo, Japan.
- Kress WJ (1986) The use of ethanolamine in the study of pollen wall stratification. *Grana* 25: 31-40
- Loewus FA, Baldi BG, Franceschi VR, Meinert LD, McCollum JJ (1985) Pollen sporoplasts: dissolution of pollen walls. *Plant Phys* 78: 652-654
- Rowley JR, Gabarayeva NI, Skvarla JJ, El-Ghazaly GA (2001) The effect of 4-methylmorpholine N-oxide monohydrate (MMNO H₂O) on pollen and spore exines. *Taiwania* 46: 246-273
- Schulze-Osthoff K, Wiermann R (1987) Phenols as integrated compounds of sporopollenin from *Pinus* pollen. *Plant Phys* 131: 5-15
- Southworth D (1974) Solubility of pollen exines. *Am J Bot* 61: 36-44
- Southworth D (1988) Isolation of exines from gymnosperm pollen. *Am J Bot* 75: 15-21
- Tarlyn NM, Franceschi VR, Everard JD, Loewus FA (1993) Recovery of exine from mature pollens and spores. *Plant Sci* 90: 219-224
- Wehling K, Niester C, Boon JJ, Willemse MTM, Wiermann R (1989) *p*-Coumaric acid - a monomer in the sporopollenin skeleton. *Planta* 179: 376-380
- Wiermann R (2001) Sporopollenin. In: Steinbuechel H, Hofrichter M (ed) *Biopolymers*. vol 1 Lignin, Humic Substances and Coa. WILEY-VCH, Weinheim, pp 2210-227
- Yule BL, Roberts S, Marshall JEA (2000) The thermal evolution of sporopollenin. *Org Geochem* 31: 859-870

Figure legends

Fig. 1a+b: MALDI-ToF MS spectra of **a** *S. laevigata* megaspores and **b** *L. clavatum* isospores. Both show ions at approximately m/z 8000 and 4400 to 4800 with *L. clavatum* also generating ions between m/z 6936 and 7588 (in positive ionisation mode) and above m/z 17654.

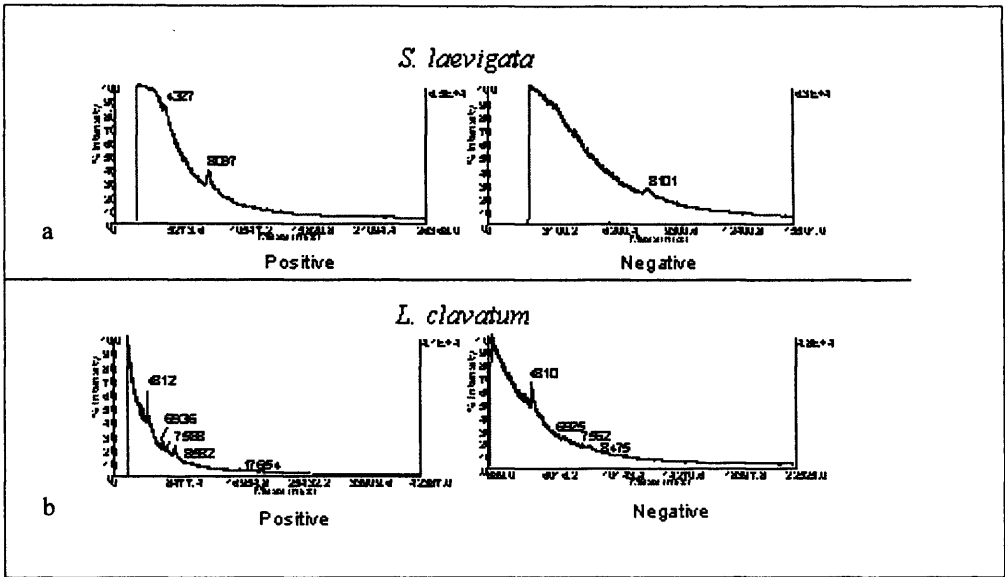
Fig. 2 a+b: **a** GC-MS spectrum of *P. sylvestris* pollen showing two peaks at a retention time of 24.54 and 50.10 minutes, as well as various smaller shift between 30-45 minutes. The peaks were identified as 2,6-bis(1,1-dimethylethyl)-4-methyl phenol (BHT) and 1,2 benzenedicarboxylic acid, diisooctyl ester (Phthalic acid-diisooctyl ester).

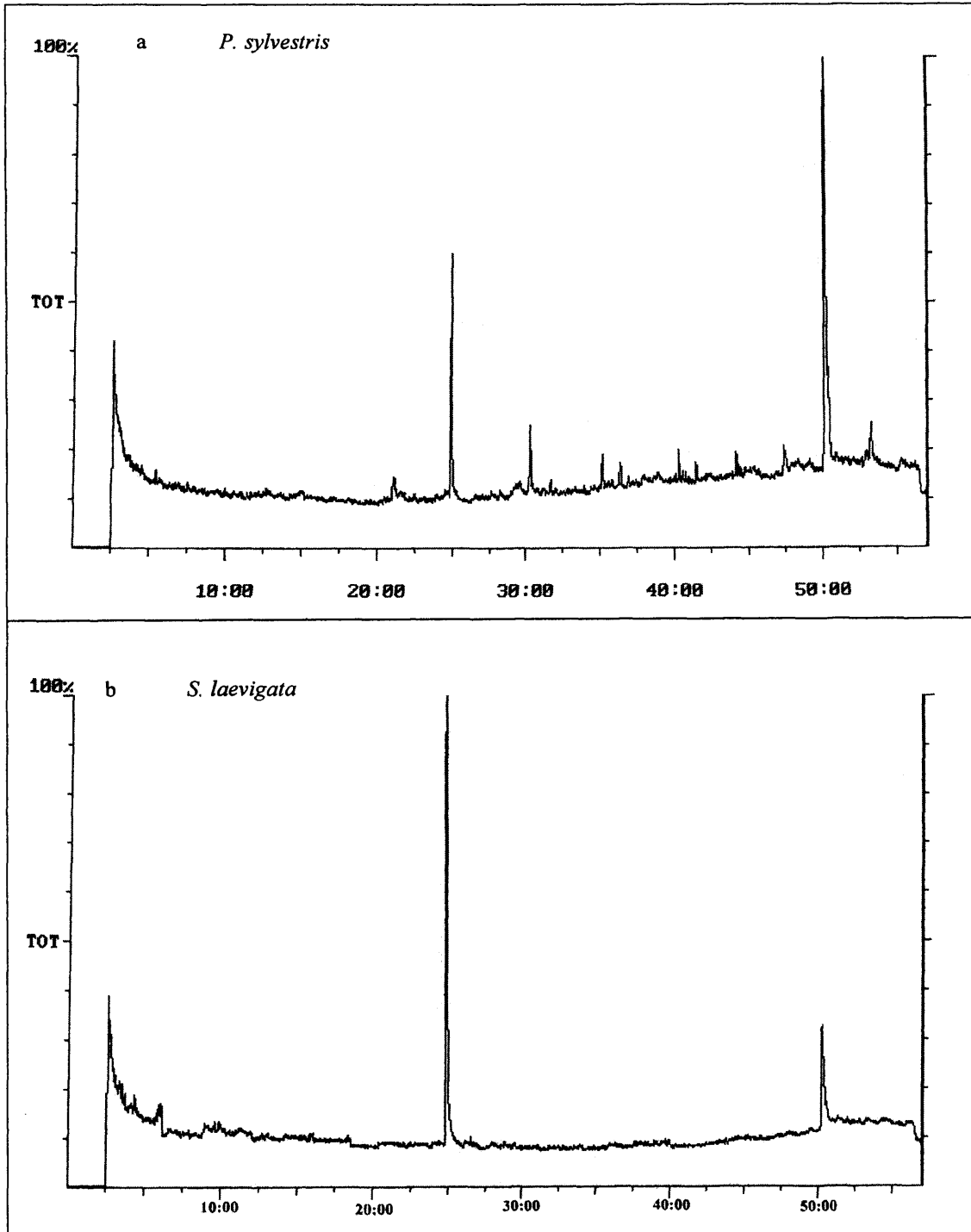
b GC-MS spectrum of *S. laevigata* megaspore powder showing two shifts at a retention time of 24.7 and 50.18 minutes. The peaks were identified as 2,6-bis(1,1-dimethylethyl)-4-methyl phenol (BHT) and 1,2 benzenedicarboxylic acid, diisooctyl ester (Phthalic acid-diisooctyl ester).

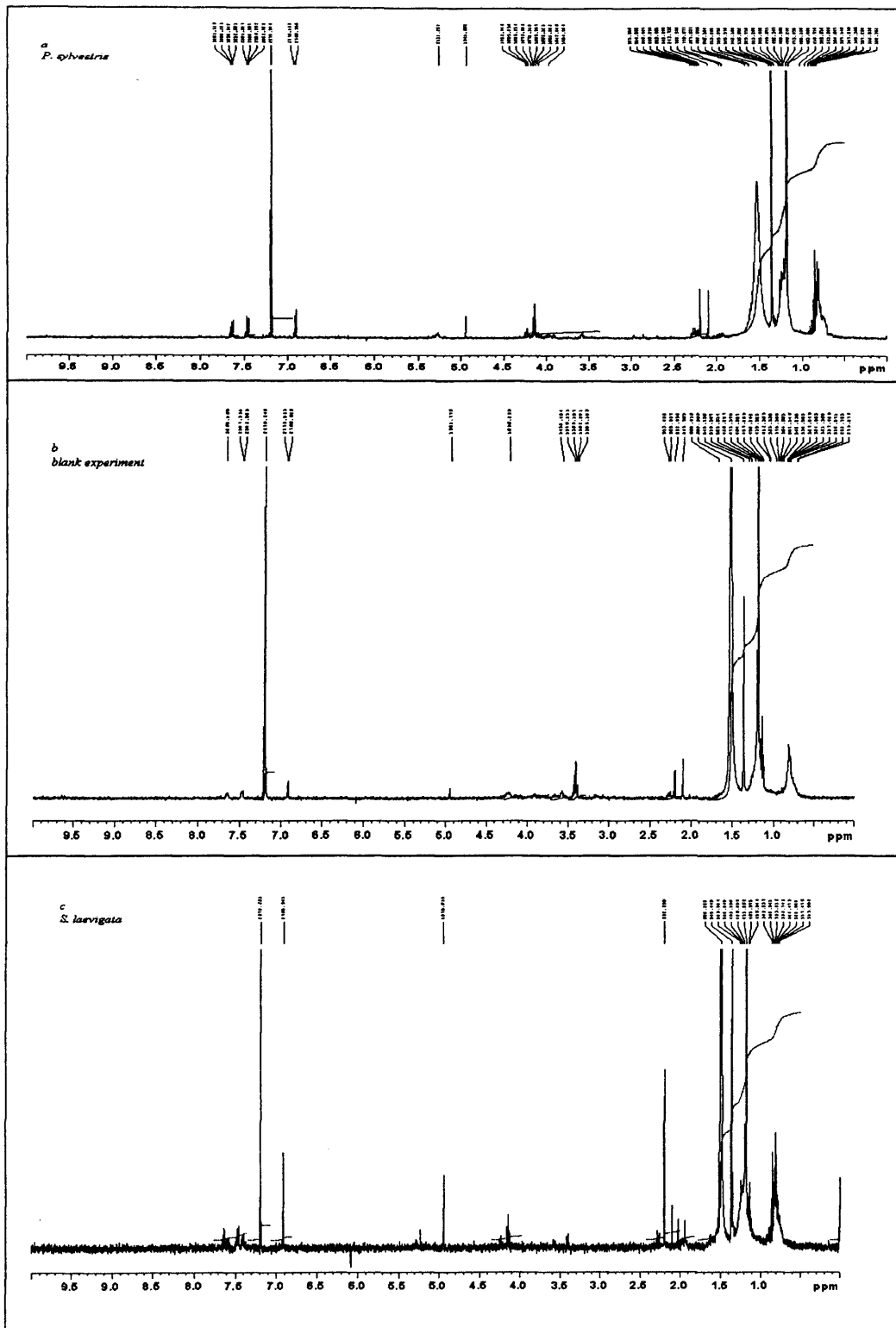
Fig. 3a-c: Three identical ^1H NMR spectra obtained from experiments using **a** *P. sylvestris* pollen, **b** a blank experiment and **c** *S. laevigata* megaspore powder. The reference at 0ppm is TMS.

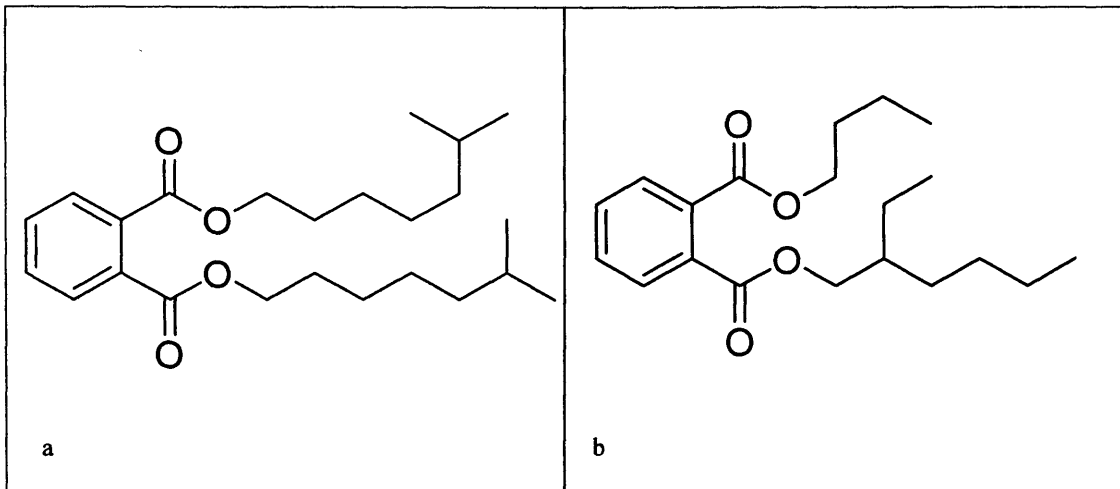
Fig. 4a+b: Chemical structure of **a** 1,2 benzenedicarboxylic acid, diisooctyl ester (Phthalic acid-diisooctyl ester) and **b** 1,2 benzenedicarboxylic acid, butyl 2-ethylhexyl ester. 1,2 benzenedicarboxylic acid, diisooctyl ester ($\text{C}_{24}\text{H}_{38}\text{O}_4$) has an exact mass of 390.28 and a molecular weight of 390.65. 1,2 benzenedicarboxylic acid, butyl 2-ethylhexyl ester ($\text{C}_{20}\text{H}_{30}\text{O}_4$) has an exact mass of 334.21 and a molecular weight of 334.45.

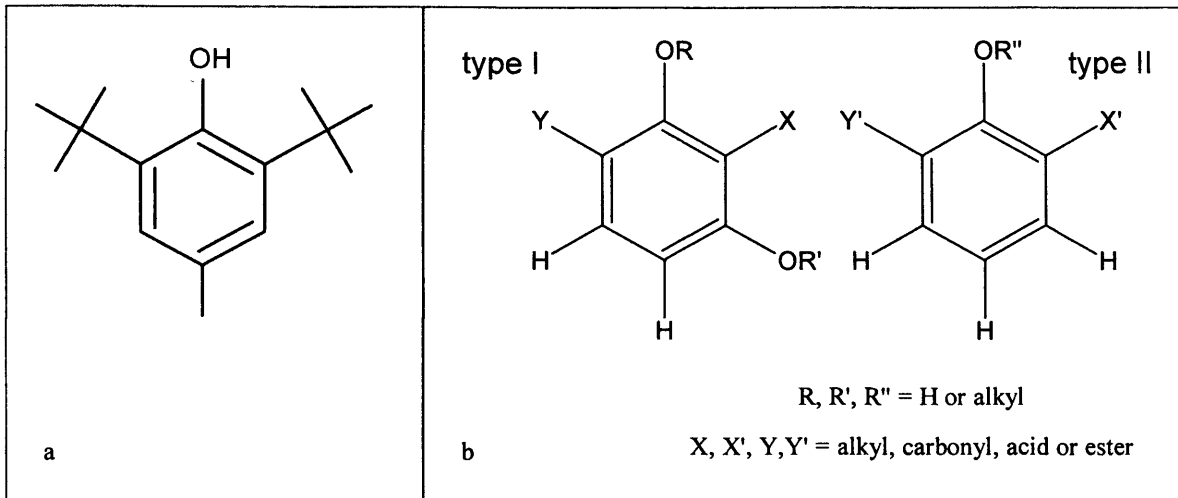
Fig. 5a+b: Chemical structure of **a** 2,6-bis(1,1-dimethylethyl)-4-methyl phenol (BHT) found in the present study and **b** two types of phenolic compounds presented in Ahlers et al. (1999b, reprinted from Fig. 3 therein with permission from Elsevier)











Appendix 3

NMR spectrum *Selaginella pallescens* (leaves):

Scan rate 5000

Current Data Parameters
NAME SEM11.1
XPNO 10
PROCNO 1

2 - Acquisition Parameters
Date_ 20030719
Time 2.02
INSTRUM Dp400
PROBHD 5 mm Dual 13
SOLVENT CDCl3
P1 500
P2 1.028965
P3 300.0 K
P4 0.50000000 sec
P5 0.03000000 sec
P6 0.0002000 sec

166.710

131.235
129.907
127.792

76.315
76.201
75.997
75.679
69.510
65.197
64.888
63.855
63.318
49.959
45.550
42.006
37.379
36.635
35.100
34.363
33.631
32.389
30.890
28.916
28.678
28.350
28.232
27.247
26.249
25.253
25.008
24.136
22.406
21.753
21.597
21.590
21.160
18.561
18.533
13.356
13.124
0.000

----- CHANNEL f1 -----
----- CHANNEL f2 -----

